TREATMENT OF TEXTILE EFFLUENTS BY ELECTROCHEMICAL ADVANCED OXIDATION PROCESSES

Ph.D. THESIS

by

PARMINDER KAUR

DEPARTMENT OF CHEMICAL ENGINEERING
THAPAR INSTITUTE OF ENGINNERING AND TECHNOLOGY
(Deemed to be University)
PATIALA -147004

April, 2018

TREATMENT OF TEXTILE EFFLUENTS BY ELECTROCHEMICAL ADVANCED OXIDATION PROCESSES

A THESIS

Submitted in partial fulfilment of the requirements for the award of the degree

of

DOCTOR OF PHILOSOPHY

in

CHEMICAL ENGINEERING

by

PARMINDER KAUR

DEPARTMENT OF CHEMICAL ENGINEERING
THAPAR INSTITUTE OF ENGINNERING AND TECHNOLOGY
(Deemed to be University)
PATIALA -147004

April, 2018

CANDIDATE'S DECLARATION

I hereby certify that the work which is being presented in the thesis entitled "**TREATMENT OF TEXTILE EFFLUENTS BY ELECTRO CHEMICAL ADVANCED OXIDATION PROCESSES"** in partial fulfillment of the requirements for the award of the degree of Doctor of Philosophy and submitted in the Department of Chemical Engineering of Thapar Institute of Engineering and Technology, Patiala is an authentic record of my own work carried out during a period from January 2015 to April 2018 under the supervision of Dr. V. K. Sangal, Associate Professor, Department of Chemical Engineering and Dr. J. P. Kushwaha, Associate Professor, Department of Chemical Engineering, Thapar Institute of Engineering and Technology, Patiala.

The matter presented in the thesis has not been submitted by me for the award of any other degree of this or any other Institute.

Parminder Kaur

(PARMINDER KAUR)

This is to certify that the above statement made by the candidate is correct to the best of our knowledge.

Dr. V. K. Sangal
Supervisor

Dr. J. P. Kushwaha
Supervisor

ABSTRACT

Textile industries are associated with the generation of large volumes of wastewater containing recalcitrant dyes and other textile processing chemicals. The discharged effluents from these industries have been demonstrated bearing high pollution load (high dissolved solids, COD, color and chloride content) with poor biodegradability. Therefore, untreated textile wastewater causes severe damage to environment, if discharged without treatment. There are various traditional techniques have been used for the treatment of real textile wastewater, including biological processes, adsorption, membrane process and chemical coagulation. Treatment of real textile wastewater, which is of high strength and complex in nature, has become a real challenge with the traditional methods.

Recently, Electro-oxidation (EO) and electro-Fenton (EF) is drawing attentions for the treatment of non-biodegradable wastewater such as textile wastewater. In the present study, the treatment performance of the EO and EF treatment processes for actual textile wastewater in batch and continuous mode of operation using RuO_2 coated Ti electrode (Ti/RuO_2) was studied. The effects of various selected process parameters of EO and EF processes (batch and continuous) parameters on percentage chemical oxygen demand removal (X_1), percentage color removal (X_2) and energy consumed (X_3) were investigated. Parametric study and multiple response optimization for EO and EF (batch and continuous) was performed using RSM. Experimental data were then analyzed by multiple regression analysis of RSM. Simultaneous optimization of process parameters for the responses was performed with the desirability function approach.

Box Behnken Design (BBD) under RSM was used for experimental design, data analysis, optimization, interaction analysis between the various batch EO parameters whereas Central Composite Design (CCD) under RSM was used for continuous EO process parameters and steady state time analysis. Quadratic model was suggested by exploiting sequential F-test and other adequacy measures for EO (batch and continuous). For the responses X_1, X_2 and X_3, the adequate precision for EO (batch and continuous) indicated that model was efficient and significant. The model summary statistics for responses X_1, X_2 and

X_3 showed high value of coefficient of determination. It supports a satisfactory adjustment between the observed and predicted values for the selected responses for EO (batch and continuous) processes. Optimization was successfully performed using BBD for batch EO and CCD for continuous EO under RSM. The most appropriate optimization condition for batch EO was found to be *i*=1.66 A, t= 79.55 min and pH=5.49 with X_1=80.00%, X_2 = 97.25% and X_3 =14.58 kWh/kg of COD removed, which showed highest overall desirability, D = 0.88. On the other hand, for continuous EO process the most appropriate optimization condition was found to be *i*=1.37 A, t= 124 min and pH=5.45 with X_1=81.00%, X_2 = 92.25% and X_3 =10.88 kWh/kg of COD removed, with overall desirability, D = 0.89. Kinetic study of EO (batch and continuous) follows first order of kinetics for COD and color removal. During kinetic study of EO (batch and continuous) processes faster color removal was observed than COD. The revealing rate constant values for X_1 and X_2 were 0.025 min^{-1} and 0.015 min^{-1} respectively for batch EO whereas, for continuous EO with rate constant values to be 0.0127 min^{-1} and 0.0168 min^{-1}, respectively. Furthermore, disposal study of treated wastewater by EO process was examined through spectrophotometric and GC-MS analysis by identifying eliminated organic compounds and transformation products formed during treatment. GC-MS analysis of the batch and continuous EO treated wastewater revealed that most of the organics were completely eliminated during EO process. The presence of chlorinated organic compounds and other transformation products with the already present compounds in untreated textile wastewater were also detected. Therefore, in view of disposal of treated wastewater, toxicity bioassay test was performed. 100% mortality rate approximately in one hr was observed for treated textile effluent. Acute toxicity bioassay proves that the treated textile wastewater is toxic and harmful to the environment. Moreover, operating cost (electrode and electricity cost) analysis was also performed to see the economic feasibility of the process. The total operating cost for batch and continuous EO was estimated as 8.97$/kg of COD removed and 8.66 $/kg of COD removed at optimum operational conditions, respectively.

The parametric study of batch EF was performed by using BBD under RSM whereas CCD under RSM was used for continuous EF process parameters. Quadratic model was suggested by exploiting sequential F-test and other adequacy measures. For the responses X_1, X_2 and X_3, the adequate precision indicated that model was efficient and significant. The

model summary statistics for responses X_1, X_2 and X_3 showed high value of coefficient of determination. It supports a satisfactory adjustment between the observed and predicted values for the selected responses. The EF (batch and continuous) performance of the treatment process was evaluated in terms of X_1, X_2, and X_3 at different EF (batch and continuous) processes parameters.

The most appropriate optimization condition for batch EF was found to be *i*= 0.32 A, t= 89.63 min and catalyst dose (C_{Fe}) =0.53 mM with X_1=89.75, X_2 = 99.49 and X_3 =1.3 kWh/kg of COD removed, which showed highest overall desirability, D = 0.92. On the other hand, for continuous EF process the most appropriate optimization condition was found to be *i*=1.10 A, t= 137 min and C_{Fe}=0.55 mM with X_1=84.16, X_2 = 94.00 and X_3 =15 kWh/kg of COD removed, which showed highest overall desirability, D = 0.80. Second order kinetic model for X_1 and X_2 was best fitted to the experimental data, at optimum conditions for batch and continuous EF processes. The values of rate constant for batch (X_1 and X_2) and continuous (X_1 and X_2) EF of second order reaction kinetics are 0.001 *l*/mg min, 2.756 *l*/mg min and $2x10^{-5}$ *l*/mg min, 9.5 $x10^{-3}$ *l*/mg min, respectively.

GC-MS and UV-visible spectrophotometric analysis of the untreated and treated wastewater were conducted to identify the oxidized and transformed/degraded compounds during the (batch and continuous) EF process. Spectrophotometric and GC-MS analysis showed that all the components of textile wastewater were totally eliminated after EF treatment of textile effluent. In view of disposal of treated wastewater, toxicity bioassay test was performed. 0% mortality rate in 96 hour was observed for treated textile effluent. Acute toxicity bioassay proves that the treated textile wastewater is not toxic and safe to the environment. To determine the economic feasibility of the EF treatment, the total operating cost was estimated. The total operating cost for batch and continuous EF was estimated as 7.86 $/kg of COD removed and 9.00 $/kg of COD removed, respectively.

The comparative study of the EO and EF treatment processes shows that, EF was more effective for the treatment of textile wastewater as compare to the EO treatment. EO treatment process during the treatment of textile effluent generates chloro-compounds. These chloro-compounds are reported to be toxic but in case of EF treatment no chloro-compounds were generated.

ACKNOWLEDGEMENTS

Words are often less to revels one's deep regards. With an understanding that work like this can never be the outcome of a single person, through this acknowledgement I would like to express my special thanks, gratitude and regards to all those who supported, helped and guided me in completing this work.

At first, my heartfelt thanks to the almighty for his abundant blessing showered on me throughout this endeavor to complete this successful work of mine.

I express my deep and sincere gratitude as well as profound regards to **Dr. Vikas K. Sangal and Dr. Jai Prakash Kushwaha** for providing me an opportunity to work under their guidance. Their wide knowledge, expertise, valuable suggestions, encouragement and freedom of independent work provided a platform for learning and performing research. Their enthusiasm and optimism made this experience both rewarding and enjoyable. Their feedback and editorial comments were also valuable for writing of this thesis.

With the deep sense of gratitude I express my sincere thanks to Head of Department of Chemical engineering department **Dr. R. K. Gupta,** who has at all times been very supportive and accommodating.

I would like to thank **Prof. H. Bhunia, Dr. Amit Dhir, Dr. Avinash Chandra, Dr. Neetu Singh** for his traffic guidance and support through the duration of this work.

I would like to thank **all the faculty members** of the Department of Chemical Engineering for encouraging me to write the thesis report. I would like to thank **all the employees** of the Department of Chemical Engineering for their everlasting support. I would like to thank **entire staff** of the **SAI Labs** for their support throughout my thesis work.

I sincerely thank to **University Grant Commission, India and Thapar Institute of Engineering and Technology, Patiala** for providing financial support and conducive environment to undertake the research work.

I express my deep sense of gratitude to my family. I am thankful to my parents for their great support throughout my life. Words cannot express how grateful I am to my mother, father, mother-in law and father-in-law for all of the sacrifices that you have made on my behalf. Your prayer for me was what sustained me thus far. I would cherish every

moment where my parents were so keen and curious to know about the details and progress of my work, which boosted my confidence. I would like express appreciation to my beloved husband **Mr. Tasbir Singh Ghumman**, who was always my support in the moments when there was no one to answer my queries.

I would like to thank all my colleague and friends **(Metali Sarkar, Bharti Thakur, Meenakshi, Sehaspreet Kaur, Bandhana Sharma, Steffi Talwar, Ravneet Kaur)** for their support and encouragement in carrying out my research smoothly.

(PARMINDER KAUR)

CONTENTS

LIST OF TABLES

LIST OF FIGURES

NOMENCLATURE

ABBREVIATIONS

BOD	Biochemical oxygen demand
COD	Chemical oxygen demand
TDS	Total dissolved solids
TSS	Total suspended solids
BOD_5	Five days biochemical oxygen demand
•OH	Hydroxyl radical
EO	Electro-oxidation
EF	Electro Fenton
BDD	Boron doped diamond
R_T	Retntion time
AR	Analytical reagent
DC	Direct current
CCD	Central composite design
ANOVA	Analysis of variance
GC-MS	Gas chromatography and mass spectroscopy
DSA	Dimensionally stable anode
RSM	Response surface methodology
SEM	Scanning Electron Microscopy
EDX	Energy-dispersive X-ray spectroscopy
XRD	X-ray diffraction
SAR	Sodium Absorption Ratio

NOTATIONS

X_1	% COD removal
X_2	% color removal
X_3	Energy consumed (wh)
pH_f	Final pH
t	Time (min)
i	Current (A)
R_T	Retention time (min)
C_{Fe}	Catalyst dose (mM)
C_0	Initial (COD concentration or Color intensity)
C_s	Final (COD concentration or Color intensity)
D	Overall desirability
d_i	Desirability of response *i*
k	Number of responses
Y_i	Response values of response *i*
Y_i-max	Maximum acceptable value of response i
Y_i-min	Minimum acceptable value of response i

Chapter – 1

INTRODUCTION

1.1 GENERAL

Industrial development has an important impact on the economic growth of any country. Textile industries are one of the oldest industries in India and have made a significant contribution in terms of forex earnings in the country. Indian textile industries are one of the largest in the world in terms of textile manufacturing. Textile industries employ 1/3th of the total export value. The witness growth of textile industries increases from 67 billion $ in 2014 to 108 billion $ in 2015 (Bhalla et al., 2017).

The rapid increase in textile industrialization and globalization leads to environmental pollution in India. Environmental pollution leads to lots of diseases and long term impact on health. Textile industries are the largest wastewater producers and approximately consume 125-250 *l* of water for 1kg of textile product (Neill et al., 1999). Common contaminants in textile wastewater include materials containing biochemical oxygen demand (BOD) and chemical oxygen demand (COD), suspended solids, color and other soluble inorganic and organic substances.

Textile industry can be categorized on the bases of the raw materials used. The wet processing consists of various other processes for the fabric to increase its aesthetic value. The wastewater from textile processing and other operations contains processing bath residues. So, the textile effluent is of major concern by the legislation. The legal requirements are defined for the release of textile effluent into the environment. According to global legislation, new standards have allocated for the large international textile industries to release the textile effluent to the environment. These standards are often higher than the local legislation. In India, textile effluents are discharged to the environment according to The Environment (Protection) Rules, 1986 standards.

1.2 DYES AND PIGMENTS USED IN TEXTILE INDUSTRIES

There is a variety of dyes used in the textile industries. Dyes of the textile industries possess certain properties, namely resistance to scrapping, resistance to photolysis and resistance to chemicals and microbial attack, which make them keep an unaltered long time (Mcmullan et al., 2001; Sharma et al., 2017; Zollinger, 1987) and are recalcitrant in nature. Following are the types of dyes used in textile industries.

1.2.1 Cationic or Basic Dyes

The basic dyes are derivative of coal-tar. These are used in discharge printing on paper, wood, straw, acrylics. It contains organic material which is not biodegradable in nature. The basic dyes were originally used on wool, silk, rayon and linen. These dyes give fast and brilliant colors on rayon, nylon, polyester and acrylic. These dyes are very cheap and used in most of the textile industries (Neill et al., 1999).

1.2.2 The Direct Dyes

These dyes are very similar to the cationic dyes. Direct dyes need a mordant or a binder to link the dye molecules to the cloth. The coloring of the direct dyes is not as bright and brilliant as of cationic dyes but color becomes faster after the diazotization of direct dyes. These dyes are stable for washing and lighting. Direct dyes are used to dye rayon, linen, nylon and silk. These dyes contain azo linkage (–N=N-) and have high molecular weight. So, direct dyes are very toxic and nonbiodegradable in nature. These dyes contain sulfonic group, which make them water soluble (Correia et al., 1994).

1.2.3 The Acid Dyes

Acidic dyes consist of a large group of dyes. The coloring salt of the acidic dyes has come from the acidic component. Certain metallic salts are required for dyeing with acidic dyes. These metallic salts increase the color fastness. These dyes cannot be used for woollen stuff but are very common for silk and nylon. Mordant is required for cotton and linen dying (Correia et al., 1994).

1.2.4 The Sulphur Dyes

Sulphur dyes have excellent deep shades. These dyes are fine with washing but faded away in the presence of sunlight. Sulphur dyes are used to the light coloring of cotton, linen and rayon. These dyes have major drawbacks with dark colors. They have weakened the

fabric so, it is necessary to treat fabric with alkalis to neutralize the acid formed during dyeing process (Kulkarni et al., 1985).

1.2.5 Azoic Dyes

Azoic dyes are used for bright shades in dyeing and printing. The industrial name of azoic dyes is Naphthols. These dyes are formed for double shade dyeing. These dyes have poor fastness to hard rubbing and crocking (O'Neill et al., 1999; Clark, 2011).

1.2.6 The Vat Dyes

A wide range of vat dyes is commercially used in textile industries. These dyes have excellent fastness to washing and sunlight. Indigo, anthraquinone and carbazole are constituents of vat dyes. Vat dyes are compatible with cotton, nylon, linen, wool and rayon. The pigment application process is used to impregnation of vat dyes on the fabric. In this process reduction of dye does not occur whereas, it is incorporated into the fabric (Kulkarni et al., 1985; Clark, 2011).

1.2.7 Collective Dyes

These dyestuffs are latest in the market. These dyes react chemically with the fabric i.e silk, wool, cotton, linen and viscose. These dyes are resistant to light and hand washing. Multi-coloring of the fabric can be possible by a single class of collective dyes (Clark, 2011).

1.3 TEXTILE PROCESSES AND EFFLUENT CHARACTERISTICS

A substantial amount of water is consumed during the textile wet processing (Gregory, 1986; Phalakornkule et al., 2010). There are certain wet and dry processes which increase the aesthetic value of the textile product.

1.3.1 Sizing

Sizing is a protective process to apply an adhesive coating to the yarn. The sizing process can improve the weaving ability, remove hairiness of fabric, increase smoothness and absorbency of the yarn. The sizing process is quite complicated, due to interactions of different types of yarns, chemicals used for sizing and the weaving process.

1.3.2 Desizing

This process is necessary after sizing, to increase the effectiveness of the wet processes. Desizing process removes the sizing material from the fabric such as starch and

waxes, it further hinders the wet processing. The most common desizing technique used in textile industries is enzymatic desizing.

1.3.3 Scouring

It is required for the removal of water-insoluble impurities i.e fats and waxes from the fabric. This process provides a greater extent of cleanliness to remove the transformational and storage stains. Scouring process increases the absorbency of the fabric for dyes. There are two types of scouring practice in the textile industries i.e alkali scouring and solvent scouring. Alkali scouring is better for all types of fabric whereas solvent scouring is selective for fabrics.

1.3.4 Bleaching

This process is required to remove the impurities of the fabric. Hydrogen peroxide is used as a bleaching agent. In alkaline medium, H_2O_2 decomposes and form per hydroxy ion (equation 1.3.1), which ultimately bleach the fabric. A huge amount of liquid wastewater is generated during the bleaching process.

$$H_2O_2 + OH^- \rightarrow OOH^- + H_2O \qquad \textbf{(1.3.1)}$$

1.3.5 Mercerization

The textile fabric appears dull due to the bleaching process. A mercerization process is required to impart lustre and dimensional stability to the textile fabric. The textile fabric is impregnated into the cold solution of NaOH without any tension for mercerization.

1.3.6 Dyeing

Dyeing is the process to impart different types of colors to the fabric. Dyes are organic or inorganic compounds which reflect light of specific wavelengths. Basic dyes are used for dying acrylic fibres. Nylon, wool and silk fibres are dyed using acidic dyes. Dispersive dyes perform better on polyesters. A wide range of dyes is used for cotton fibres.

1.3.7 Printing

This process provides a different type of patterns and designs to the fabric. Printing can be done by using wooden blocks, stencils, silkscreens and engraved plates. Printing process makes the textile product attractive and increases the aesthetic appeals.

1.3.8 Finishing

This process includes mechanical and chemical processes. Finishing process converts the fabric into useful materials. It improves the competitiveness of the textile industry in the global market.

These are the major processes of the textile industries used for textile processing. Textile industries generate wastewater at every step of these processes (Fig 1.2.1). The characterization of generated textile wastewater is different for every process. The amount of fresh water used in the processes and nature of the generated wastewater is depending upon the nature of fabric and fabric processing. The characteristics of the textile wastewater depend upon the types of the dyestuff and chemicals used during the processing of a textile. The general characteristic of generated wastewater during the different process has been shown in Fig 1.2.2.

The generated wastewater is rich with bleaching agents, salts, acids, alkalis etc. Therefore, generated wastewater becomes strong and toxic in nature (U.S. Environmental Protection Agency, 1996). The major step in pollution prevention is a characterization of the textile processes wastewater for the strategic development of treatment methods. Textile processing water is contaminated with dyes, chemicals, oils, grease, and waxes. Textile processing water may also be contaminated with heavy metals (Bisschops et al., 2003). The pollution loads of the textile wet operations are depends upon the nature of the textile fabric used for processing. In the case of the woolen industry, sizing and desizing processes are not necessary so, the composite wastewater has different characteristics. Effluent characteristics for certain textile wet processes are given in Table 1.2.1. In textile processing units the pH range of the generated wastewater varies from acidic to the alkaline pH i.e 5 to 11 (Bisschops et al., 2003). The electrical conductivity of the textile wastewater is quite high due to high salt concentration i.e NaCl, Ca and Mg salts. The concentration of NaCl, Ca and Mg salts varies from 980 to 2185 mg/*l*, 13 to 29 and 1 to 29 mg/*l* respectively. The concentration of NaCl, Ca and Mg salts make the wastewater hard in nature with high conductivity values from 4430 to 8710 μS. During the textile dyeing, the dyes are dissolved into the water. The certain amount of dyes is remaining in the water after the dyeing of textile (Divya et al., 2009). Therefore, the composite effluent contains a high concentration of dyes and other auxiliary additives. The

high concentration of dyes and other textile processing chemicals causes a high level of total dissolved solids (TDS) and total suspended solids (TSS). The TDS content of the textile wastewater varies from 3210 to 5290 mg/*l* and it can be more than 5290 mg/*l* depending upon the textile processing (Bisschops et al., 2003). The insoluble component of the dyes, surfactants and other additives leads to the increase in TSS level. The variable range of TSS in textile wastewater is 830 to 1580 mg/*l*. Textile industrial wastewater has high COD ranges 500 to 3200 mg/l, which can be due to a huge amount of industrial wastes such as detergents, softeners, non-biodegradable dyeing chemicals, formaldehyde-based dye fixing agents etc. Higher concentration of COD in water implies toxic conditions and the presence of biologically resistant organic substances. BOD of textile wastewater is due to the organic content of the dyes and fixing agents, which varies from 300 to 1010 mg/*l*. Textile wastewater is also contaminated with the heavy metals like lead (11 to 61 ug/*l*), copper (6 to 311 ug/*l*) and chromium (150 to 189 ug/*l*) (Hussain et al., 2006; Bisschops et al., 2003).

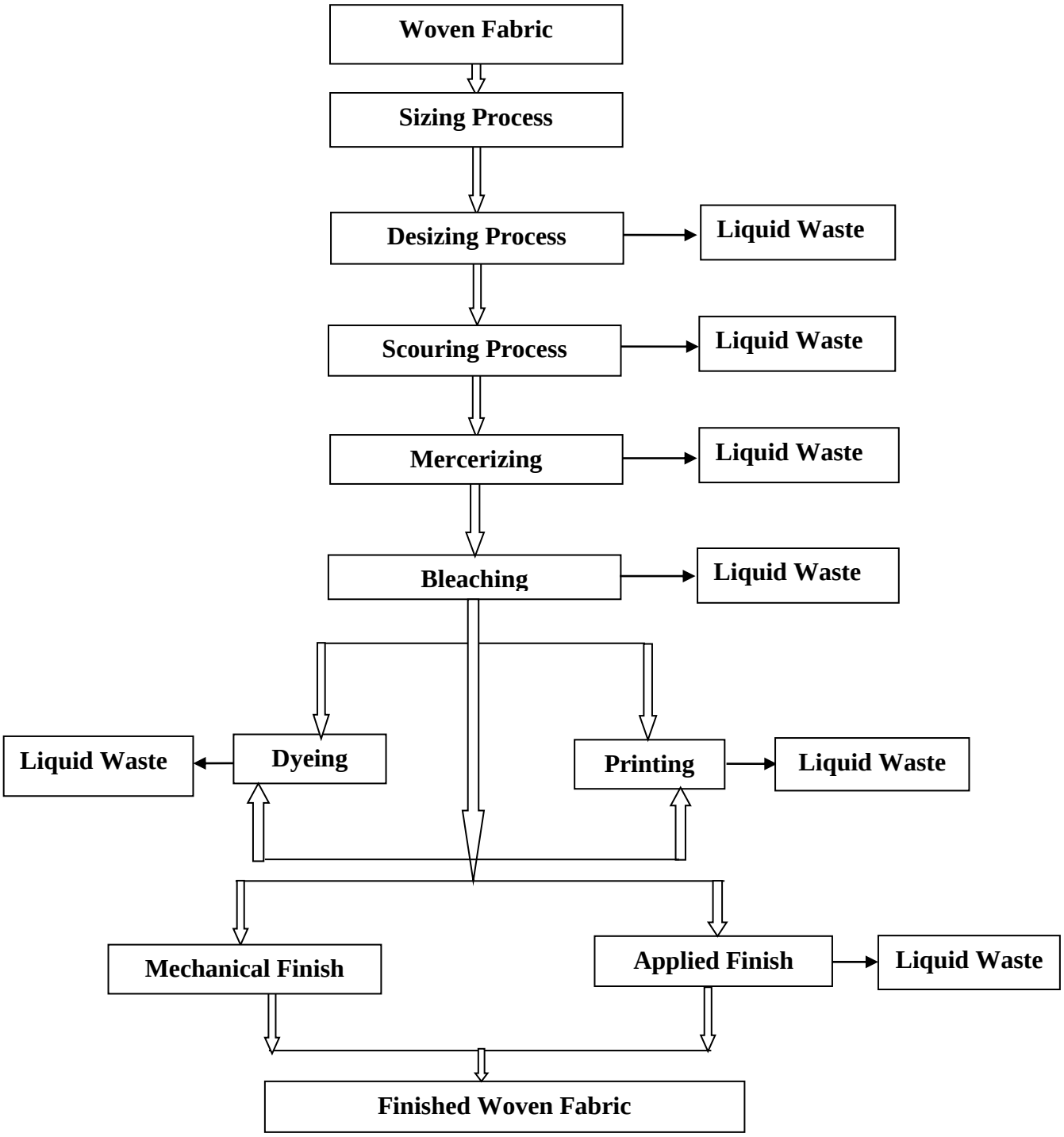

Fig 1.2.1. Manufacturing process of a woven fabric and wastewater generation

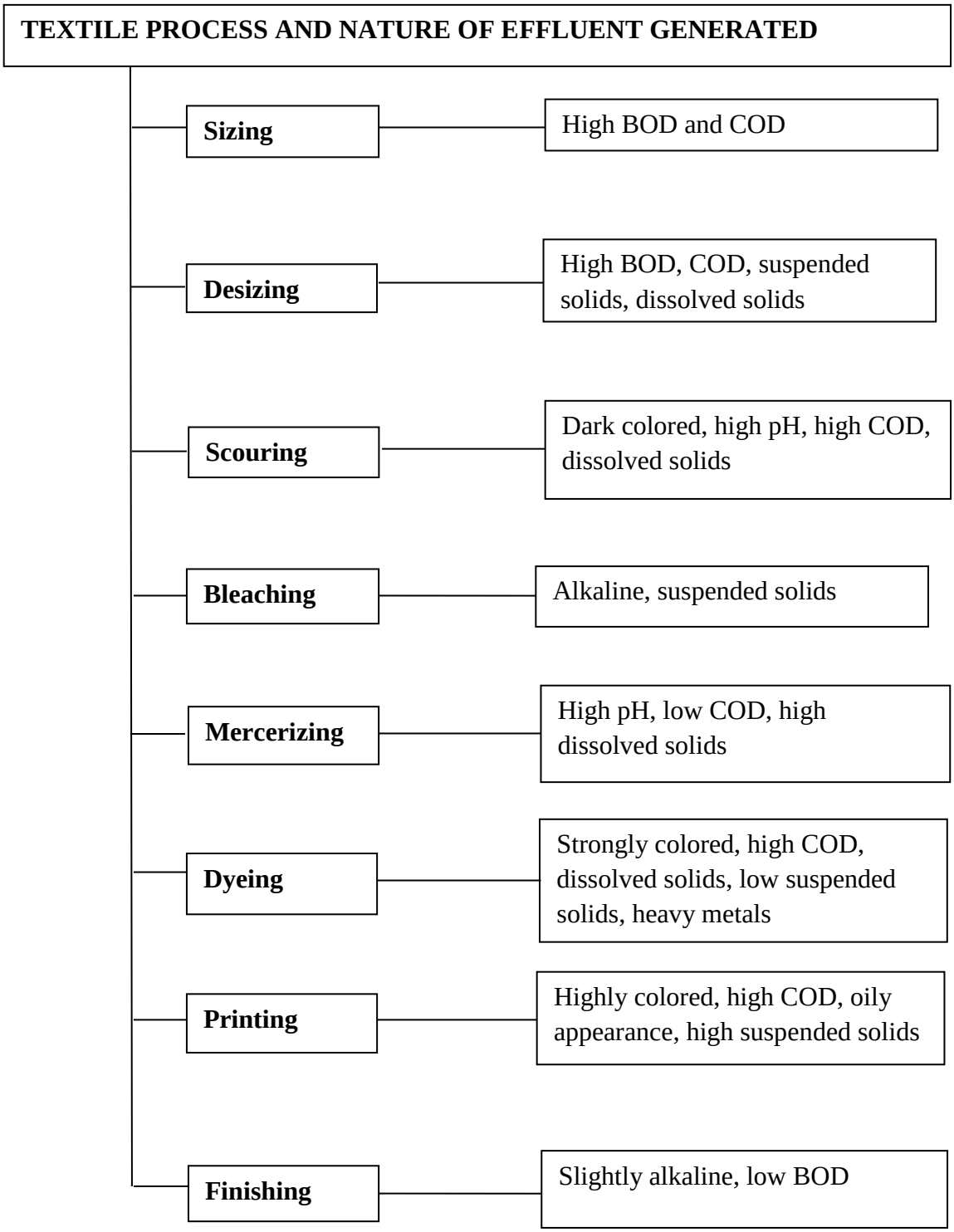

Fig 1.2.2. Characteristics of textile effluent generated from different processes

Table 1.2.1. Characteristics of the textile industry effluent (All terms are in mg/*l* except pH and color (pt.co))

Process	COD	BOD	TSS	TDS	pH	Color	References
Desizing	-	200	400	4029	6.8	-	Correia et al.,(1994)
Scouring	8000	100-2900	7.6-17.4	184-17400	7.3-13	694	Bisschops et al.,(2003)
Bleaching	1099	878	180	7132	8.5-9.6	153	Ranganathan et al., (2007)
Mercerising	1600	50-100	600-1900	4300-4600	5.5-9.5	-	Naveed et al.,(2006)
Dyeing	23	11	37	-	8.35	1450-4750	Van der Bruggen et al.,(2001)

1.4 ENVIRONMENTAL RISK AND STANDARDS FOR TEXTILE EFFLUENT

The effluent discharge from the textile industries causes severe environmental problems. Therefore, a proper channel of legislation is required to control the effluent discharge from the industries to the environment. The untreated effluent discharge from textile industries causes serious issues and has a huge impact on the water bodies. The high ranges of the COD and five days biochemical oxygen demand (BOD_5) of textile generated effluent have a harmful impact on the environment.

Dying and printing involve dangerous chemical and heavy metals like lead, mercury, arsenic etc. The wastewater generated in the textile industries has high strength of color, TDS, TSS, COD, BOD and chloride content (Olmez et al., 2007). These industries use recalcitrant dyes and varieties of chemicals (bleaching agents, salts, acids, alkalis etc.) for better performance of finished textile. Dyes have high molecular weights, complex structure and high solubility in water. These properties of dyes make them persist in a surrounding once discharged to the environment. A high value of COD, BOD and, oil-grease concentration in the textile effluent causes harmful effect on the aquatic life. The depletion of water dissolved

oxygen increases the death rate of water bodies and causes ecological imbalance. Dyes and chemicals used in textile processing make wastewater, turbid and reduce the penetration of light into the water. Therefore, it hinders the photosynthesis process (Sun et al., 2007). Wastewater from textile industries contains heavy metals. These heavy metals accumulate inside the organisms and enter into the food chain. Therefore, textile generated wastewater is toxic in nature (U.S. Environmental Protection Agency, 1996).

In India, the regulatory agencies i.e the Ministry of Environment and Forests (MoEF) and Central Pollution Control Board (CPCB) require textile industries to meet the minimal national standards (MINAS) for the release of the wastewater to the environment. The Environment (Protection) Rules, 1986 prescribes the standards for textile industries specifically under sr. no 6, 7, and 92 of schedule-I. The Environment (Protection) Rules, 1986 standard for wastewater discharge from textile industries has been shown in Table 1.2.2.

1.5 METHODS FOR THE TREATMENT OF TEXTILE EFFLUENT

The real textile effluent contains a huge amount of complex compounds and greatly changing characteristics. In the past several decades, there is a number of treatment methods have been embellished to identify an efficient and economic technique to treat the textile effluent i.e physicochemical treatment methods, biological methods and other technologies.

1.5.1 Physico-Chemical Treatment Process

Physico-chemical treatment methods used for the textile wastewater are chemical coagulation, adsorption processes and membrane filtration. These methods have high efficiency for toxic wastewater but these are not preferable for textile wastewater, because it contains a high concentration of color and TDS. Generally, these treatment methods are expensive for the treatment of textile wastewater. In the case of chemical oxidation, chemicals are of high cost and are not environmental friendly. Adsorption process does not mineralize the pollutant particles. Further, the treatment process is required to treat the desorbed pollutants, which enhance the cost of the adsorption process. In the case of membrane filtration, membranes and membrane fouling are very expensive (Georgiou et al., 2002; Cannizares et al., 2006; Lin and Peng, 1996). Moreover, the generation of secondary pollutants is a major drawback of these physicochemical wastewater treatment processes

(Cannizares et al., 2006). Secondary and tertiary treatments are necessary along with physicochemical treatment methods for disposal of treated wastewater.

1.5.2 Biological Treatment Processes

Biological treatment processes are subdivided into two parts aerobic and anaerobic treatment processes. In both processes, bacteria are the key element of the treatment process. Aerobic biological treatment includes activated sludge process (ASP) and biofilm process. The textile industrial wastewater is of variable COD and BOD loading rate. ASP is very sensitive in case of variable COD and BOD, and sludge bulking is a major problem. The installation of ASP requires a large area and maintenance after installation. The use of ASP is limited for the treatment of textile wastewater, due to non-biodegradability of dyes (Phalakornkule et al., 2010; Chen et al., 2012; Bansal et al., 2013). There are many anaerobic treatment processes used for the treatment of textile effluent. But, anaerobic processes are not effective for the treatment of textile effluent, because the textile effluent degradation under anaerobic conditions generates toxic organic compounds (Meric et al., 2004). These toxic compounds inhibit the growth of bacterial cells.

The shortcomings related to the traditional treatment methods i.e. the generation of secondary pollutants and non-biodegradability of dyes in the effluent can be overcome by the use of advanced electro-chemical methods (Patwa and Viyas, 2012; Jeirani et al., 2015)

1.5.3 Electro-Chemical Treatment Methods

Electrochemical treatment is an emerging water treatment technology. Electro-chemical methods do not require ex-situ addition of chemicals to wastewater, as in the case of chemical oxidation. Electro-chemical methods do not generate secondary pollutants during the treatment process (Chen et al., 2004). In electro-chemical treatment methods, losing and gaining electrons play a vital role in the degradation process. The electrons are an environmentally friendly clean reagent for the treatment of wastewater by electrochemically. The electro-chemical treatment methods are very advantageous for pollution prevention problems, hence it is an environmentally benign technology. The generation of powerful oxidizing agents during electro-chemical treatment leads to the complete mineralization of organics. It is also termed as a green method for wastewater treatment. Other advantages of electrochemical treatment methods include high current efficiency, susceptible to automation,

easy manageable because there is no chemical required for treatment and it operates under mild environmental conditions i.e at room temperature and atmospheric pressure. Electrochemical treatment methods have robustness, the reaction can be start and pause by initiating and terminating, of the power supply. These treatment methods are quite versatile because they can treat the wastewater of variable COD ranges i.e 0.1 to 100 g/l (Sires et al., 2014; Anglada et al., 2009). Hence, electrochemical methods represent a useful solution when the presence of bio-refractory and toxic pollutants inhibits the use of conventional treatment methods. The major screened-off area in the electrochemical treatment is as follows

Table 1.2.2. Standard for Textile Effluent Discharge

Industry	Parameters	Standards
All integrated textile units, units of cotton/ woolen/ carpets / polyester, units having printing / dyeing / bleaching process or manufacturing and garment units.	Color, P.C.U (Platinum Cobalt Units)	150
	pH	6.5 to 8.5
	Suspended Solids (mg/l)	100
	BOD (mg/l)	30
	COD (mg/l)	250
	Total Chromium as (Cr) (mg/l)	2.0
	Sulphide (mg/l)	2.0
	Total residual chlorine (mg/l)	1
	Oil and grease (mg/l)	10
	Phenolic Compounds (mg/l)	1
	Inorganic (TDS) (mg/l)	2100
	Sodium Absorption Ratio (SAR)	26
	Ammonical Nitrogen (as N) (mg/l)	50

Source: Central pollution control board (CPCB), India

1.5.3.1 Electro-flotation: It is a simple separation process which raises pollutants to the surface of a water body with the help of tiny bubbles of hydrogen and oxygen gases generated during the electrolysis of water. The pollutant removal through electro-flotation is achieved by electrically generated air or gas into the wastewater. The released air or gas form bubbles, which cohere to the suspended pollutant particles and float the pollutant particles to the surface of the wastewater. Therefore, the electrochemical cathodic reaction generates hydrogen gas whereas anode evolves oxygen gas. The floated particles can be easily removed by the skimming device or through overflow in a suitable container. The performance of an electro-flotation system is determined by the removal of pollutants and power consumption. The size of the gaseous bubbles has a huge impact on the removal of pollutants.

Power consumption during the electro-flotation process depends upon the design of the reactor, electrode materials, current density and wastewater conductivity, etc (under mild conditions). If the pollutant particles are charged then, the bubbles possess opposite zeta-potential. The electrode material, pH, current density affects the size of the gaseous bubbles during the electro-flotation process (Chen, 2004). At the neutral pH of the electrolyte, the hydrogen bubbles are of smallest size whereas the size of oxygen bubbles becomes larger with the increase in pH. The increase in current density decreases the size of gaseous bubbles. The electro-Flotation method can be successfully used for removing greases, oils, surfactants, petroleum products from the wastewater. It does not convert organic matter into simple compounds. It simply uplifts the suspended solids of the wastewater and reduces the TSS level (Chen, 2004).

1.5.3.2 Electro-coagulation: In this process, the coagulants are generated electro-chemically by using aluminium or iron electrodes. The nature of the generated coagulants depends upon the type of electrode used. The mononuclear complexes of the metal ions formed, which destabilizes the pollutant particles (Kushwaha et al.,2011). These destabilized pollutant particles as flocs are settled down at the bottom of the reactor as sludge (Chen, 2004). At the anode, the metal ions generation takes place whereas, at the cathode hydrogen gas is released. The generation of hydrogen gas at the cathode promotes the raising of pollutants at the surface of the water. This process is called as electro-Flocculation. The arrangement of electrodes in the electro-chemical reactor is either monopolar or bipolar. The electro-Coagulation treatment

method is very advantageous for the removal of high strength pollutants (Cañizares et al., 2006). The electro-Coagulation process does not remove the pollutants from the wastewater itself. It only transforms the pollutants to ease separation by electro-flotation, sedimentation, filtration etc (Chen, 2004). The separation can occur in the reactor or in downstream units. The major drawback of this process is the generation of sludge. The drawbacks of electro-flotation and electro-coagulation electro-chemical treatment methods can be overcome by EO and EF treatment process.

1.5.3.3 Electro-oxidation (EO): EO process is a powerful electro-chemical method, which is based on the generation of powerful oxidants by the electro-chemical reaction under particular conditions. The EO process overcomes the drawbacks of electro-flotation and electro-coagulation process. EO is a versatile process. There is a number of reactions occur simultaneously in an electrochemical cell. The factors which affect the overall degradation efficiency of EO process are a plethora of reactors, electrode materials. The use of chemicals is eliminated in electrochemical technology. Recently, EO is drawing attention for the treatment of non-biodegradable wastewater such as textile effluent.

Recent investigations on the EO treatment methods evident that, EO is a good technique to control the water pollution related problems (Raju et al., 2009; Brillas et al., 2009; Nasr et al., 2005). This treatment method for toxic wastewater is quite effective. The main focus of the researchers is on increasing the oxidation efficiency in oxidizing of various pollutants with different types of electrodes (Sahu et al., 2015). The strong oxidants (•OH radicals and chloro-oxidants, etc) were generated during the electro-chemical treatment of the wastewater (Sandhwar and Prasad, 2017). These oxidants are generated directly during the treatment process by using only water, salt and energy (Sires et al., 2014; Anglada et al., 2009; Panizza and Cerisola, 2009). The •OH radical is a strong oxidant which is able to non-selectively destroy most organic and organo-metallic contaminants to their complete mineralization into CO_2, H_2O and other inorganic ions.

The EO reactions involved in the degradation of organic pollutants is quite complicated. The mechanisms behind the degradation of organic pollutants are not clear yet (Comninellis et al., 2006). The organic pollutants during EO treatment are removing from the wastewater by direct and indirect oxidation. The direct and indirect oxidation method of EO is

discussed in chapter 3 (theory). During the EO treatment process, two types, of oxidation are possible. In one way, toxic and non-biocompatible pollutants are converted into bio-degradable organics, so that further biological treatment can be initiated. On the other way, pollutants are oxidized to water and CO_2. Then, there is no need of further purification is required.

1.5.3.4 Electro-Fenton (EF): EF is very effective advanced oxidation process for the treatment of toxic wastewater. The Fenton reagents are generating in the electrolytic cell by the electrochemical reactions on the cathode, anode and in bulk. EF is a combination of Fenton reaction and electro-oxidation reaction. Fenton reaction and EO reaction are worked together in a single reaction chamber. EF has been demonstrated as an environmentally friendly and promising method that has received great attention for water remediation because of being an efficient, economical, and having a simple configuration. The generation rate of •OH radicals is quite high during the EF process. The oxidation potential of •OH radicals is very high therefore, EF process does not produce secondary pollutants (Lin et al., 2014). EF process allows better control of the process and avoids unnecessary storing and transport handling of the hydrogen peroxide as happens in the case of classical Fenton process. Though various pollutant degradation methods are available, the EF process has indeed advantages of using it at ambient temperature and pressure.

Nowadays, EF process is of interest because it opens up a green approach to electrochemically generated oxidants by utilizing of air as a source of oxygen (Nidheesh et al., 2014; Pajootan et al., 2014). The effective pH of EF process was pH > 4.0, which is the required pH for an efficient E-Fenton reaction (Lin et al., 2014). The organic pollutants get degraded by the gaining and releasing of electrons electro-chemically without the addition of chemicals. EF is efficient for the complete mineralization of wastewater pollutants.

Chapter – 2

LITERATURE REVIEW

2.1 GENERAL

This chapter presents a review of research work for the treatment of textile effluent by EO and EF treatment processes. This chapter includes the review of EO and EF treatment processes and factors which affect the efficiency of these processes.

2.2 TREATMENT OF TEXTILE EFFLUENT BY ELECTRO-OXIDATION

In the EO process, the organic contaminants of the wastewater were oxidized with the generation of oxidants at the surface of electrodes (direct EO) and in the bulk (indirect EO). The oxidants at the surface of electrodes oxidized the organic contaminants of the wastewater by direct oxidation. During direct EO, oxidants such as •OH radicals and H_2O_2 were generated. Direct EO leads to the complete mineralization of the organic contaminants of wastewater. Complete decomposition of organic matter by the oxidation of organic pollutants produces CO_2 and H_2O or other oxides (Chen, 2004).

During indirect oxidation, the organic contaminants of wastewater oxidize in bulk. In the case of indirect EO, oxidants such as Cl_2, HOCl, ClO^- and •OCl radicals etc. were generated. These oxidants oxidize the organic contaminants of wastewater and convert them into transformed compounds. These electrochemically generated oxidants such as Cl_2, HOCl and ClO^-, and •OCl radicals produce chloro-species as intermediate but also helps in the degradation process. As both direct and indirect EO participate in the degradation of the contaminants present in the wastewater. The degradation of contaminants further, pivots on the contaminant's nature and the operational parameters of the EO process. The effect of EO operational parameters i.e electrolyte concentration, pH, current density etc (Table 2.2.1) on the treatment efficiency of the EO was investigated by various authors. The effect of these parameters on the treatment of each category of dyes is different.

Szpyrkowicz et al., (2000) investigated the efficiency of the EO process for the treatment of synthetic wastewater containing sparingly soluble disperses dyes. It was concluded from the investigation of EO for the treatment of synthetic wastewater (soluble disperses dyes) that, it is quite efficient for the treatment of disperse dyes. The

investigation reveals that the overall process efficiency of EO depends upon the supporting electrolyte and the pH of the bulk in the reactor. The degradation efficiency was highly affected by the chloride concentration in the electrolyte and pH of the electrolyte. Under acidic conditions, at high chloride concentration, the EO process has maximum degradation efficiency for the degradation disperse dyes. The degradation of reactive orange 107 contaminated wastewater by the EO treatment process was determined by Rajkumar et al., (2012). It was observed that at a low salt concentration (0.05-0.2 M), as the pH (3-11) increases the % color removal was found to be decreased whereas, the % color removal efficiency increases with increasing pHat high salt concentration. The optimum condition for the degradation of reactive orange 107 contaminated wastewater by the EO treatment process was found pH 9.4, NaCl concentration of 0.08 M, and electrolysis time on 16.0 min. These optimized conditions show maximum color and COD removal of 98.4%, and 90%, respectively. The alkaline pH was highly efficient for the degradation of reactive orange 107 contaminated wastewater by EO as compared to acidic and neutral pH. Dogan and Turkdemir, (2005) investigated the treatment efficiency of EO for CI Vat Blue 1: indigo dye. The experiments were performed at different pH values (1-7) for NaCl concentration of 0.24 mol dm^{-3}. It was observed that the degradation efficiency of EO for CI Vat Blue 1: indigo dye was maximum at pH=1 for salt concentration (NaCl) of 0.24 mol dm^{-3} after 90 min of electrolysis time.

Sakalis et al., (2005) studied the effect of salt or electrolyte concentration on the degradation of azo dyes by EO treatment process. The four azodyes (Reactive Orange 91, Reactive Red 184, Reactive Blue 182 and Reactive Black 5) were used for the preparation of simulated wastewater. The sodium chloride (NaCl) and sodium sulfate (Na_2SO_4) were tested as supporting electrolytes during the EO treatment process of simulated wastewater. It was evaluated that both the electrolyte were effective during EO treatment process. As real wastewater consists of a high concentration of sodium chloride (NaCl) and sodium sulfate (Na_2SO_4). The performance of the EO treatment process was investigated for the degradation of actual textile wastewater at the optimum conditions (elapsed time=60 min, temperature=60^0C, voltage=6V) of simulated wastewater. The degradation of real wastewater by EO yields 94.4% of dye removal at neutral pH. Sakalis et al., 2005 was

determined the degradation efficiency of EO for real textile wastewater. EO has an effective performance in the degradation of real textile wastewater.

Current density is an important operational parameter of the EO treatment process. Current density has a variable effect on the degradation of the different types of dyes wastewater. Raghu et al., (2007) were conducted experiments at different current densities for the treatment of the textile effluent (dye house). The variation of the current density for the treatment of the textile effluent (dye house) was 1 to 2.5 A/dm^2. It was observed that the COD reduction and color removal were maximum at 2.5 A/dm^2. It was concluded that with the increase in current density, there was a significant increase in the % COD removal. Fernandes et al., (2004) investigated the effect on the degradation rates of C.I. Acid Orange 7 by EO process with the variation in the concentration of electrolyte with respect to the change in initial concentration of dye and current density. The influence of electrolyte concentration (sodium sulphate concentration) on the C.I. Acid Orange 7 degradation rate was estimated at three different concentrations (0.01, 0.02 and 0.035 M), on an initial dye concentration of 60 mg/l with the variation of current density (1.25, 2.50, 5 mA/cm^2). It was observed that at higher electrolyte concentration with the increase in current density the % COD removal was more than 90%. Pollutants concentration also affects the efficiency of the electrochemical treatment process. It is also reported that COD reduction is significantly affected by the initial pollutant concentration (Aravind et al., 2016). Zou et al., (2017) studied the effect of applied current density ranges from 20-100 mA/cm^2, electrolyte concentration ranges from 0 - 3 g/l, and pH value ranges from 2.0-10.0 on the % COD removal of the real textile effluent. Under the optimum operational conditions, within 3 hr, there was a complete removal of the COD in the real textile wastewater was observed.

Literature survey concluded that the EO process is quite effective for the degradation of textile dyes wastewater. The EO process parameters have a huge impact on the degradation process. These process parameters must be optimized for each case. Most of the reported studies in the literature are on the optimization of EO process parameters for the treatment of simulated wastewater. Therefore, a vast study is required to study the effect of various EO process parameters on the degradation of real textile wastewater. The

optimization of process parameters for the treatment of real textile wastewater is lacked in the literature. It is also observed from the literature that the higher concentration of electrolyte helps the EO process to perform better during mineralization of contaminants. As real textile wastewater contains a large amount of salt concentration due to textile processing. So, the degradation efficiency of the EO process for real textile wastewater must be high. The high salt concentration affects the electrode material during EO treatment process. So, the selection of electrode material must be pivotal for the EO treatment of real textile wastewater.

The anode materials discussed in literature for the treatment of textile dyes wastewater were of graphite, lead/ lead dioxide, nickel and platinum (Kim et al., 2003; Vlyssides et al, 1999; Dogan et al., 2005; Rajkumar et al., 2006; 2007; Raghu et al., 2007; Saravanathamizhan et al., 2007; Raju et al., 2009; Del Río et al., 2009; Kong et al., 2009; Miled et al., 2010; Zheng et al., 2012; Senthilkumara et al., 2012). The efficiency of different type of electrodes with different dye wastewaters in terms of % COD removal and color removal has been shown in Table 2.2.2. Selection of anode material is very crucial for the EO treatment of the textile wastewater. Various types of electrodes such as Ti/PbO_2, Ti/IrO_2, BDD, Ti/SnO_2, graphite and Ti/RuO_2 have been reported to be used as an anode for the treatment of wastewater using EO process. The oxygen over the potential for both the PbO_2 and SnO_2 anodes is 1.9 V and has been reported to be generally very effective in oxidizing pollutants. However, the electrochemical instability due to electrochemical corrosion and the lower performance in high chloride content wastewater limits their use (Cossu et al., 1998; Chen, 2004; Anglada et al., 2009). Whereas, the IrO_2 and graphite anodes possess low oxygen over potential (1.6 V and 1.7 V, respectively) due to which their performance have been reported to be poor (Rodgers et al., 1999; Pulgarin et al., 1994). In contrast to this, BDD anodes possess very high oxygen over potential (2.7 V) and shown excellent electrochemical stability and performance. However, due to high cost, and limited performance for high chloride content wastewater, the use of BDD anodes is limited. It is reported that the BDD anodes in case of direct anodic oxidation, have good removal efficiencies (Britto-Costa et al., 2012). However, the subsequent amount of anodic material removed during the treatment process, anode instability is a

major drawback. Ti/SnO_2-Sb-Pt electrode as anode show good degradation efficiency for real dyestuff wastewater (Orts et al., 2017). Due to the downside of traditional anode materials (iron, carbon, aluminium etc.) titanium based dimensionally stable anode coated with noble oxides (TiO_2, RuO_2 etc.) were developed (Comninellis et al., 1991). Ti/RuO_2 anodes are dimensionally stable, very efficient in high chloride concentration and possess oxygen evolution potential of 2.0 V (Anglada et al., 2009; Santos et al., 2011). When electrochemical reactor operates at high cell potential, the anodic oxidation becomes dominant and the contaminants destroyed on the surface of the electrode (Simond et al., 1997). On the other hand, if chloride concentration is high in the wastewater, indirect oxidation via active chlorine can be dominant (Szpyrkowicz et al., 2015). Naumczyk et al., (1996) have been investigated the performance of EO for the removal of organic pollutants of wastewater using different types of anode materials, such as graphite and noble metal anodes. It was observed that anodic oxidation of phenol performs with slow degradation rate at a high concentration of NaCl (Comninellis, 1994).

Moreover, if wastewater contains high NaCl concentration as textile wastewater, Ti/ RuO_2 anodes have been reported to show enhanced performance due to the generation of several chlorine-based oxidants (Cl_2, HOCl and ClO^-) via indirect oxidation (Kaur et al., 2017). As a result of electrolysis, hydroxyl radical (•OH) is generated on the anode, which is adsorbed on the surface of the anode (Ti/RuO_2) and degrades pollutants by direct oxidation mechanism (Chen, 2004) However, during the EO process, pollutants are destroyed by indirect EO process also. Electrochemically generated oxidants in bulk such as Cl_2, HOCl and ClO^-, •OH radicals, H_2O_2 and •OCl radicals etc. oxidize pollutants by indirect EO. However, both direct and indirect oxidation processes may be responsible for the degradation of pollutants using Ti/RuO_2.

Senthilkumar et al., (2012) estimated the color removal and COD removal efficiency of Procion Scarlet dye wastewater by using electrochemical oxidation (ECO) and biological oxidation (BO) processes in combined and integrated form using Ti/RuO_2. Integration of ECO and BO processes remove 80% of COD and96.4% of color at an optimum condition whereas a combination of ECO and BO processes showed 90% COD removal and 98.5% of color removal optimum conditions. Aquino et al., (2014)

investigated the degradation of real textile wastewater by electro-oxidation using Ti–Pt/β-PbO_2 and Ti/$Ti_{0.7}Ru_{0.3}O_2$ anodes. Ti/$Ti_{0.7}Ru_{0.3}O_2$ anodes provide better degradation performance as compare to Ti–Pt/β-PbO_2.

Most of the reported studies suggested that Ti/RuO_2 is a stable electrode in the high salt concentration wastewater i.e textile wastewater. But there is limited literature available for the use of Ti/RuO_2 electrodes for the treatment of real textile wastewater in batch and continuous mode of operation of the EO process. Therefore, an appropriate study is required for the treatment of textile wastewater by EO treatment process using Ti/RuO_2 electrodes.

Indirect EO is prominent at high chloride concentration under acidic conditions during the EO process (Szpyrkowicz et al. 2000). Indirect EO generates choro-compounds. It has been reported that chlorine indirectly degrades pollutants but has a drawback of the possibility of generating chlorinated organic compounds (Rajkumar et al. 2006). The anode material has a huge impact on the concentration and generation of oxidants. It is reported in literature the high degradation efficiency electrodes material by EO in higher salt concentration wastewater leads to the generation of chloro- compounds. These chlorinated organic compounds have been reported to be toxic and carcinogenic in nature (Naumczyk et al., 1996; Deborde et al., 2008). The wastewater produced from textile industries has high flow rates and high pollution load (Kim et al., 2003). Therefore, subsequent removal of chlorinated organic compounds from the EO treated wastewater before discharge to water bodies is necessary. There is not a single study in the literature, which shows the generation of chlorinated compounds during the treatment of real textile wastewater by EO process. So, there is a need to study the generation of chlorinated compounds in real textile wastewater whether, there is a need of tertiary treatment after the EO treatment of wastewater.

The available literature shows that EO process has maximum efficiency in terms of COD removal and color removal (Vlyssides et al., 1999; Szpyrkowicz et al., 2000; Dogan et al., 2005). The studies available in the literature have been conducted in batch EO reactor by various authors using various electrodes for simulated wastewater (Kim et al., 2003; Vlyssides et al, 1999; Dogan et al., 2005; Rajkumar et al., 2006; 2007; Raghu et al.,

2007; Saravanathamizhan et al., 2007; Raju et al., 2009; Del Río et al., 2009; Kong et al., 2009; Miled et al., 2010; Zheng et al., 2012; Senthilkumara et al., 2012).

In the literature very few studies have been investigated for the continuous EO operation for simulated textile wastewater treatment (Bahadir et al., 2009; Sakalis et al., 2005). Korbahti et al., 2009 was estimated the effects of the residence time on COD, color and turbidity removal for the treatment of simulated wastewater. The optimum residence time for the continuous process was 3hr. There is limited literature available for continuous EO mode of operation for textile effluent. There is a need to study the treatment efficiency of the EO process for a continuous mode of operation. However, treatment performance for real textile wastewater is hindered by the presence of residue of mixed dyes and chemicals used during the textile processing, and so many other factors such as turbidity, high chloride content, pH, etc. So, treatment performance for real textile wastewater by EO for batch and continuous mode of operation is required to be estimated.

The EO process is electrical power dependent process. The operational cost and energy consumption studies are required for the estimation of cost for the EO treatment process for textile wastewater. In the literature, certain investigators have been estimated the energy consumption and operating cost of the EO process. The effect of different types of electrode materials and wastewater was also investigated (Vlyssides et al., 1997; Kushwaha et al., 2010; Canizares et al., 2009). It was reported in the literature that, the operational cost of EO treatment process for the synthetic textile wastewater was varied from 0.28 to 183\$/m^3 of wastewater(Canizares et al., 2009). The electric energy consumption during the electrochemical process varied from 1.2 to 200 kWh/ kg of COD removal (Vlyssides et al., 1999; Vlyssides et al., 2009). This variation in energy consumption or cost analysis depends upon the nature of wastewater, electrolyte concentration and electrode material. Researchers have been reported that the real textile effluent contains higher salt concentrations than the experimental study. So, the cost of electric power become reduced when real textile effluent treated by EO during the large-scale operations (Rajkumar et al., 2006). It was found that, the increase in the textile dye and salt concentration reduces the energy consumption (Korbahti and Turan, 2016). Zou et al., (2017) estimated that, the specific energy consumption during the treatment of actual

textile wastewater by EO treatment process. The specific energy consumption for the treatment of real textile wastewater by EO was as low as 11.12 kWh/kg of COD removed (Zou et al., 2017). A few investigations were available in the literature for the estimation of the operational cost of EO process in batch and continuous operation. Therefore, more studies are required for the estimation of operation cost of EO process for the treatment of actual textile wastewater in batch and continuous operation. The operational cost of the EO treatment is directly depends upon the number of parameters like electrode material, wastewater nature, electrolyte concentration, generation of oxidants, degradation pathway of oxidation reaction (Maljaei et al., 2009). To understand the relation of all these parameters with degradation and cost, the kinetic study is required. Literature has evident that, the kinetic followed for the COD and color removal of simulated wastewater by EO process follows first order of kinetics (Mohan et al., 2007; Maljaei et al., 2009). There are certain reported investigations in literature claims that the removal of COD and color by EO treatment process follows pseudo-first order kinetics (Rajkumar et al., 2006; Zou et al., 2017). Most of the reported studies on the kinetics of color and COD removal were based on simulated textile wastewater by the treatment of the EO process. The studies of degradation kinetics for real textile wastewater by EO process are limited in the literature. Therefore, the kinetics of the real textile wastewater in batch and continuous mode of operation of the EO process is required to be estimated.

Table 2.2.1. Effect of EO parameters on the % COD removal and % Color removal

Dye	Reactor	Electrode	Current density	Time (min)	%COD removal	%Color removal	pH	References
Disperse Yellow 126	Batch reactor	Ti/Pt-Ir	1.9 Adm^{-3}	40	39%	90%	4.5	Lidia et al., (2000)
CI Vat Blue 1: indigo	Batch reactor	Anode: Pt cage cathode: Pt foil	-	90	60%	100%	1	Dogan et al., (2005)
Reactive dyes	Batch reactor	Anode: Ti/RuO_2 /Ir cathode: stainless-steel	72.2 $mAcm^{-2}$		73.5%	100%	-	Rajkumar et al., (2006)
Procion Black 5B	Continuous reactor; Flow rate: 10 *l*/h	anode: Ti/RuO_2 cathode: stainless-steel	2.5 A dm^{-2}	-	74.05%	100%	-	Raghu et al., (2007)
C.I. Reactive Orange 4	Batch reactor	Ti/SnO_2–Sb–Pt	125 $mAcm^{-2}$	-	94%		-	Del et al., (2009)

Dye	Reactor	Electrode	Current density	Time (min)	%COD removal	%Color removal	pH	References
Rhodamine 6G	Batch reactor	Ti/RuO_2	-	5	-	100%	-	Yu-Ming et al., (2012)
Reactive Orange 107	Batch reactor	Graphite	34.96 mA cm^{-2}	16	90%	98%	9.4	Senthilkumar et al., (2012)
Rhodaine B	Batch reactor	BBD	60-120 mA cm^{-2}	-	100%	-	-	De Araújo et al., (2015)
C.I. Reactive Blue 198	Batch reactor	anode: Graphite	34.96 $mAcm^{-2}$	10.5	98.9%	65.5%	7	Rajkumar et al., (2017)

Table 2.2.2. The EO treatment of various types of textile wastewaters by different electrodes

Waste water	Reactor	Electrode (Anode-Cathode)	%COD removal	%Color removal	Reference
Printing & dyeing	Batch reactor	Graphite - Copper	43.5%	90.6%	Kong et al., (2009)
Simulated dye wastewater	Batch reactor	Iron - Stainless steel	53.5%	99.3%	Korbahti et al., (2009)
Simulated dye wastewater	Batch reactor	Ti/Pt - Stainless steel	-	35%	Seung-HeeCho et al., (2009)
Basic Red 29	Continuous reactor	Boron-doped diamond	91%	97.2%	Koparal et al., (2007)
Reactive Blue 19	Batch reactor	$TiO_2/RuO_2/IrO_2$	55.8%	100%	Rajkumar et al., (2007)
Acid Brown 14	Batch reactor	$Ti/TiO_2/RuO_2$	-	-	Mohan et al., (2007)
Textile effluent	Batch reactor	$RuO_2/IrO_2/TaO_2$/Graphite	$RuO_2/IrO_2/TaO_2$:93 % ; Graphite: 54%	-	Bhaskar et al., (2009)

Waste water	**Reactor**	**Electrode (Anode-Cathode)**	**%COD removal**	**%Color removal**	**Reference**
Simulated dye wastewater	Batch reactor	Iron - Iron	93.9%	99.5%	Korbahti et al., (2008)
Blue Reactive 19 dye	Batch reactor	Nb/BDD and pure Ti–Pt/b-PbO_2	-	90%	Andrade et al., (2007)
Levafix Blue and red CA reactive azo-dyes	Batch reactor	Pt - Reticulated vitreous carbon	90%	100%	El-Desokya et al., (2010)
Levafix Blue (LB), red (LR), yellow CA (LC) reactive dyes	Batch reactor	Iron - Iron	LB=32%; LR=37% and LC=33%	100% for LB,LR and LC	Korbahti et al., (2008)
Dyeing solution from a textile factory	Batch reactor	Aluminum-Iron	63 %	65%	Kobya et al., (2003)
Textile wastewater	Batch reactor	Aluminum	97%	99%	Aouni et al., (2009)
CBSOL LE red wool dye	Batch reactor	Ti/RuO_2 - Aluminum	-	96.71%	Kaur et al., (2015)
Real textile	Batch reactor	_	85%	95%	Aravind et al., (2016)

Waste water	**Reactor**	**Electrode (Anode-Cathode)**	**%COD removal**	**%Color removal**	**Reference**
wastewater					
Real textile wastewater	Batch reactor	BDD electrodes	46%	-	Zou et al., (2017)

2.3 TREATMENT OF WASTEWATER BY ELECTRO-FENTON

EF process is an environmentally benign treatment process. It is very effective for the complete mineralization of toxic wastewater (Oturan et al., 2000; Brillas et al., 2009).

In the EF process, organics are eliminated by the action of Fenton's reaction in the bulk and anodic oxidation at the anode surface. H_2O_2 is continuously generated in an acidic medium during electrolysis in the EF process due to two electron oxygen reduction at the cathode (Brillas et al., 2009; Sires and Brillas, 2012). The acidic medium is favourable for the initiation of Fenton reaction by the formation of •OH radicals. EF process is a very sensitive process for the pH of the wastewater. It is well known that the Fenton reaction is efficient in the pH range of 2.8–3.0 (Sun and Pignatello, 1993) to efficiently produce •OH radicals. There is also a chance of production of HO_2• radicals at a pH of 2.8–3.0 if there is an excess concentration of H_2O_2. HO_2• radicals have lower oxidation power as compared to •OH. The ratio of (H_2O_2/Fe^{2+}) must be optimized for a particular case (Bouafia-Chergui et al., 2010). The ferrous ions are added into the system analogously to generate the ·OH radicals in the classical Fenton's reaction. A couple of Fe^{3+}/Fe^{2+}catalyze the EF treatment process. The excess concentration of ($H_2O_{2/}$ Fe^{2+}) reduces the organic degradation efficiency of the process. In 2009, Hameed and Lee estimated the optimal concentration of H_2O_2 for the toxic wastewater. The •OH radicals are also consumed by the Fenton's reagent during the reaction, it leads to the wasting of the •OH radicals (Bouafia-Chergui et al., 2010).

The standard redox potential of ·OH radicals is very high i.e E^o (·OH /H_2O) = 2.80 V/SHE. So, during the EF process, the organics present in the wastewater are oxidized to simple compounds and inorganic ions. But, the degradation of saturated or aromatic compounds by the attack of •OH generates dehydrogenated and hydroxylated derivatives (Brillas et al., 2009). At the same time, in this process, the ferrous ion is regenerated at the cathode reducing its addition. The regeneration of ferrous ion reduces the cost of the treatment process in comparison to the traditional Fenton process. So, the role of cathode material is crucial, as it also affects the rate of H_2O_2 generation (Salazar et al., 2012). It is reported that the Fenton's reaction in EF process is usually controlled by the H_2O_2 production rate, which pivots on factors such as oxygen solubility, temperature, pH, the

material of cathode and current density (Sun and Pignatello, 1993). Current density controls not only the H_2O_2 generation rate but also the regeneration rate of Fe^{2+}. Nature and concentration of catalyst used significantly affect the process efficiency. Use of Cu^{2+} with Fe^{2+} or Fe^{3+} proved good catalytic characteristics (Brillas et al., 2004; Salazar et al., 2012; Manoli et al., 2017), but it requires a high concentration of the catalyst. Uses of other types of catalysts such as Mn^{2+} (Balci et al., 2009) Co^{3+} and Ag^{+} (Pimentel et al., 2008) have also been reported. But the use of Mn^{2+}, Co^{3+} and Ag^{+} is restricted due to their eco-toxicity. Fe^{2+} has been reported as the best catalyst for the EF process, due to its efficient activity even at lower concentrations. Fe^{2+} is abundant on the crust, low cost and a non-toxic environmentally safe element (Sires et al., 2014). Ozcan et al., (2009b) estimated the 92% of TOC removal from the acid orange 7 synthetic wastewater by EF treatment process.

The selection of electrode material is important to enhance the treatment efficiency of the process. EF treatment technology has been successfully investigated for the dyes degradation using different types of anodes and cathodes (Salazar et al., 2012; Martinez-Huitle and Brillas, 2009; Zhou et al., 2007; Ozcan et al., 2008; Nasr et al., 2005; Brillas and Casado, 2002; Wang et al., 2005; Oturan et al., 2012; Panizza et al., 2011; Pajootan et al., 2014).

Xu et al., (2014) use graphene doped gas diffusion electrode to degrade the simulated wastewater of reactive brilliant blue dye. The study reveals that under the optimum conditions, color removal and TOC removal was 80% and 33% respectively after 180 min. Ghoneim et al., (2011) observed 100% color removal of sunset yellow FCF azo dye contaminated wastewater. The mineralization of the dye was 97% by EF process using carbon as cathode and platinum as an anode. Sirés et al., (2008) reported the comparative study of the color removal efficiency of simulated dyes wastewater by EF treatment process using carbon-felt cathode. Total COD removal was observed of dye mixture containing wastewater with initial COD of 1000 mg/l by EF treatment. Apart from cathodic oxidation, the oxidation of pollutants is achieved by anodic oxidation if dimensionally stable electrodes with O_2 overvoltage anodes such as Pt and BDD anode (Lin et al., 2014; Nidheesh et al., 2013). It has been reported that Ti/RuO_2 anodes are

dimensionally stable, and possess high oxygen evolution potential and stable in high NaCl concentration as textile wastewater (Anglada et al., 2009; Santos et al., 2011; Kaur et al., 2017). Transition metals are the most commonly used a catalyst in the number of chemical reactions. Ruthenium is the only element of the platinum group elements that possesses Fenton-like activity in the existence of hydrogen peroxide. The ruthenium metal has oxidation states from 1 to 8. The most common oxidation states of the ruthenium element are +2, +3 and+4. It has been reported that ruthenium complexes are effective catalyst during the treatment of wastewaters like olefin hydroxylation wastewater, alcohol dehydrogenation wastewater and drinking water oxidation (Brillas et al., 2009). A few investigations have been reported for the EF treatment of toxic wastewater using ruthenium as a catalyst in EF treatment. Ruthenium as an electrode overcomes the traditional drawbacks of the electrode material such as metal leaching to the treated wastewater. It also performs multiple catalytic cycles, which increase the durability of the electrode material (Brillas et al., 2009). It is clear from the literature that Ti/RuO_2 electrodes are effective to treat the textile wastewater. Moreover, Ti/RuO_2 electrodes are stable in high salt concentration wastewater. There are a few investigations for the treatment of textile effluent by EF using Ti/RuO_2 as anodes. There is a need of present to investigate the EF process to treat the real textile effluent using Ti/RuO_2 as anodes. The O_2 overvoltage anodes i.e $TiRuO_2$ electrodes increase the EF process efficiency by the combination of electro-mediated oxidation and Fenton mediated oxidation. The efficiency of the EF process can be increased by combining EO and EF processes by using O_2 overvoltage anodes i.e $TiRuO_2$ electrodes.

EF treatment process effectively treated the different types of wastewater has been shown in Table 2.3.1. However, most of the studies were reported with the synthetic effluent in batch mode, not with the real industrial effluent. In 2009, Hameed and Lee estimated the color removal of the malachite green dye by EF treatment process. The % of color removal of the malachite green dye was maximum at pH 3.4. The optimal conditions of the EF process for the degradation of the malachite green were experimentally determined. At optimum conditions, 99.25% degradation of the malachite green in simulated wastewater was achieved after 60 min of the EF reaction. Fu et al., (2010a, b)

investigated the degradation of C.I. Acid Red 73 by EF process based on zero-valent iron (0_v)and H_2O_2. The results showed that C.I. Acid Red 73 %color removal increased with the increase of 0_v. It was also observed that the residual pH was increasing for C.I. Acid Red 73 degradation. It is clear from the investigation of EF that, it is an extremely effective process for toxic wastewaters treatment. El-Desoky et al., (2010) observed the complete color removal and 85 to 90% of mineralization of simulated wastewater by EF treatment.

Ji et al., 2011 investigated the mineralization of methylene blue dye by EF treatment process. It was estimated that after 90 min of reaction time almost complete mineralization occur. Khataee et al., (2014) treated the C.I acid blue wastewater by the photoelectron-Fenton process. It was observed 98.25% of the dye color removal with in 60 min of electrolysis time. Iglesias et al., (2013a) determined the % color removal from the simulated dye wastewater by EF treatment in an airlift continuous reactor. The decolorization percentages were high at high residence times. The removal of RhB dye from synthetic wastewater by EF process was investigated using a bubble column continuous flow reactor. (Nidheesh and Gandhimathi 2015a, b). The effect of various operational parameters was investigated on the degradation of RhB dye wastewater. 98% of color removal of the RhB solution was observed at optimum conditions. Similarly, the EF process for the degradation of real textile effluent was performed in batch and continuous operation. EF was effective to remove the color from actual textile effluent (Nidheesh and Gandhimathi, 2015b).

Real textile wastewater has a number of factors which hinder the treatment efficiency of the EF process. The chloride concentration is quite high in real textile wastewater. It increases the process efficiency by boosting the electron transfer. The EF process efficiency is affected by the hardness of the wastewater. The presence of ions, which are responsible for the hardness of water reduces the dye degradation efficiency. These cations are divalent in nature so, the breakage of divalent cations and dye complex is quite difficult (Dos Santos et al., 2016). Therefore, to explore the EF process efficiency in batch and continuous operation for real textile wastewater more investigations are required.

Cost analysis and energy consumption are required to be investigated along with the studies of other parameters of the EF process. In the literature available the energy consumption of the EF process for the treatment of direct blue 15 ranged from 23.3 to 41.7 kW h/m3 (Weng et al., 2015). On the bases of energy consumption, cost varies from 1.87 to 3.33 $/m3 of simulated wastewater. Nidheesh and Gandhimathi, 2015b estimated the operational cost to treat the real textile wastewater by EF process. The operational cost was found to be 2.13 $/g of COD removed. It was concluded from the available literature review that, there is a limited literature for the operational cost analysis of EF process for batch and continuous mode of operation. The concept of cost analysis for real textile wastewater requires further research. Therefore, further investigations of cost analysis for EF treatment are necessary for the commercial applications of the EF process.

EF is quite proficient for the mineralization of organic compounds from the aqueous source. There are chances of a generation of toxic organic compounds during EF treatment of organic pollutants due to incomplete mineralization. The partial mineralization of toxic pollutants may lead to environmental issues. Le et al., (2016) investigated the toxicity of simulated wastewater after the degradation of by EF process. During the beginning time of the treatment process, there was an abrupt increase in the toxicity values than the parent compound. Roshini et al., (2017) investigated phytotoxicity and microbial toxicity after the treatment of actual textile effluent by EF treatment process. It was observed that toxicity has been lessening after 1 hr of EF treatment. Moreover, EF treatment process has been demonstrated as eco-friendly, efficient and economical having a simple configuration and controlling. This process does not produce any secondary pollutants. EF process is highly efficient in terms of pollutants removal in comparison traditional process (Brillas et al., 2009; Panizza et al., 2011). Generally, in the Fenton process, the Fenton reagent and H_2O_2 consumption have been reported to be high (Nidheesh et al., 2013). Therefore, in real textile wastewater, due to the very high level of the pollutants concentration, a large amount of chemical reagents (H_2O_2 and Fe^{2+}) are required. Furthermore, iron was used as a catalyst in a minute quantity during EF treatment but there are chances of a generation of $Fe(OH)_3$and it requires suitable disposal, which needs proper investigation (Modenes et al., 2012; Chou et al., 1999; Fu et

al., 2010b). Moreover, this process contributes to water pollution because of the addition of ofFe^{2+}. The disposal study of the treated textile wastewater is also lacked in the available literature. It is required to study the disposability after EF treatment, to identify whether there is a need for tertiary treatment.

A few authors have been investigated the kinetics of degradation of organic contaminants of the wastewater. Khataee et al., (2014) was performed pseudo-first order reaction kinetic modelling of the EF process for the removal of phenol-contaminated wastewater. Ting et al., (2009) investigated the kinetics of 2,6-dimethylaniline degradation by EF process. The pseudo-first order reaction kinetics was followed by degradation of 2,6-dimethylaniline during EF treatment. Liu et al., (2007) investigated the degradation kinetics followed by EF in an aqueous solution. It was demonstrated that in an aqueous solution degradation kinetics of EF process follows the first-order kinetics. Rosales et al., (2009) estimated the kinetics of color removal of the different types of dyes (Lissamine Green B, Methyl Orange, Reactive Black 5 and Fuchsin Acid) by EF process.

A first-order kinetic model was best fitted for the color removal at the optimum operating conditions. There is limited literature available for the kinetic study of the EF process for the degradation study of real textile effluent. Treatment of real textile wastewater and its kinetics study using Ti/RuO_2 as anodes for EF treatment processes is not available in the literature. The individual kinetics of COD and colour removal need to be investigated to predict the cost variation for different wastewaters and for the proposal of a mechanism for the degradation process. Over the last decade, electro-Fenton process based on cathodic electrogeneration of hydrogen peroxide and catalytic regeneration of Fe^{2+} were developed and successfully applied for the treatment of wastewaters containing several families of persistent and or toxic organic pollutants (Oturan, 2000; Oturan et al., 2004; Oturan and Brillas, 2007; Brillas et al., 2009; Martinez-Huitle and Brillas, 2009; Nidheesh and Gandhimathi, 2012; Sires and Brillas, 2012).

Table2.3.1. Reported investigations for the Electro-Fenton process for wastewater treatment

Electrode (Anode-Cathode)	Wastewater	Conditions/Results	Reactor	Time	References
Iron	Formaldehyde	i =8.5 mA/cm^2, pH=10, Fe/H^2O^2 ratio =26 mM/M; 50 mg/l COD removal after 16 day	Batch reactor	-	Gholamreza et al., (2012)
RuO_2/Ti-Activated carbon fiber	Cefalexin	i =6.66 mA/cm^2, pH=3, catalytic dose= 1 mM; Biodegradability increased	-	-	Ledezma et al., (2012)
Cu supported on bamboo charcoal	Organic contaminants	i = 5-50 mA further increase to 100 mA, pH=4	Batch reactor	-	Xiaofeng et al., (2013)
Iron	liquid organic fertilizer plant	i =50 A/cm^2, pH=3, H_2O_2 conc.=25mM%;TOC, %COD and %Color removal: 87, 91 and 99, respectively	Batch reactor	45 min	Abdurrahman et al., (2013)
Ti-based mixed metal oxides	Bisphenol A, triclosan and ibuprofen solutions	i=25mA, pH=4; TOC Partially removed	Batch reactor	20 min	Songhu et al., (2013)

Electrode (Anode-Cathode)	**Wastewater**	**Conditions/Results**	**Reactor**	**Time**	**References**
cathode: Gas diffusion type	brilliant red X-3B	i=0.3 A; H_2O_2 production rate=125 micro mol/*l*, color removal=97% , Mineralization =87% (3 h)	Continuous reactor	Color in 20 min Mineralization 3 h	Yangming et al., (2013)
Graphite	Rhodamine	i=0.03 A; %Color removal = 99.2	Batch reactor	180 min	Nidhesh et al., (2013)
Carbon-Graphite	Dimethyl phalate	Degradation rate was increased 8.8-11.5 times	Batch reactor	-	Wang et al., (2013)
Ti/IrO_2/ Ta_2O_5	RB4	i= 63 A/m^2; %Color removal= 85	Batch reactor	90 min	Yu et al., (2013)
CNT–PTFE electrode	Phenol	pH=4; Photo EF, EF and photocatalysis (UV/TiO_2) removed phenol 32%, 23% and 13%, respectively	-	180 min	Khataee et al., (2013)
Carbon-felt (CF)	Orange II	i=1.78 mA/cm^2, pH=3; TOC-removal =58% - 94.3%	Batch reactor	60 to 90 min	Lin et al., (2014)
Graphite sheets	Reactive Black 5 (RB5)	V=5 V, pH=2; %Color removal =96	Batch reactor	2 h	Bocos et al., (2014)

Electrode (Anode-Cathode)	**Wastewater**	**Conditions/Results**	**Reactor**	**Time**	**References**
Pt and BDD - carbon-PTFE	Acid Red 1	i =100 mA cm^{-2}, pH= 3.0.; BDD showed higher decolorization & mineralization rate	Batch reactor	180 min	Xavier et al., (2014)
Iron-aluminum	Basic Red 29 (BR29) dye	i=20 mA/cm^2 ; Toxicity reduction=80%,%COD removal=71.43, %color removal=>95	Batch reactor	40 min	Yusuf et al., (2014)
Graphite	C.I. Acid Red 14 (AR14) and C.I. Acid Blue 92 (AB92)	pH= 3, i=0.18 A, catalyst dose=0.1 mM Fe^{3+} ; %AR14 removal = 91.22, %AB92 removal = 93.45, %COD removal (AR14) =86.78, %COD removal (AR92) = 83.51	Batch reactor	210 min	Pajootan et al., (2014)
Fe_2O_3/ACF	Methyl orange	i= 600 to 1200 mA/m^3; %Color removal= 86.7	Dual-chamber Biological EF reactor	3 h	Ling et al., (2016)
Iron	Textile wastewater	pH 2.84, i=40.11 mA/cm^2, H_2O_2= 2.3mM; %COD removal=76.33	Batch reactor	71.74 min	Davarnejad et al., (2016)

Electrode (Anode-Cathode)	**Wastewater**	**Conditions/Results**	**Reactor**	**Time**	**References**
Graphite felt mesh	Tartrazine synthetic wastewater	pH =3, V= 4.0V, flow rate = 40 ml/min, catalyst dose = 0.4 mM/l, Aeration rate= 80 m*l*/min.	Continuous reactor	-	Ren et al., (2016)
Coated nickel foam	Poly R-478 and Lissamine Green B (LGB)	pH=3	Batch and Continuous reactor	-	Bocos et al., (2016)
carbon fiber brush	Orange G	pH = 2, i =1.73 A/m^2,	Batch reactor	6 h	Lin et al., (2017)

2.4 OBJECTIVES

On the basis of the literature survey, there is a necessity for investigation of real textile effluent by electro-oxidation and electro-Fenton process. Based on the critical literature review, the following objectives have been set for the present work:

- To characterize the textile effluent collected from the equalization tank.
- To carry out parametric studies (current density, pH, electrolyte concentration, time) for treating textile effluent for electro-oxidation and electro-Fenton process.
- Kinetic study and determination of kinetic parameters for electro-Fenton and electro-oxidation process.
- Treated effluent disposal study by both electro-Fenton and electro-oxidation process.
- To carry out toxicity analysis of the degraded compounds.

Chapter – 3

THEORY

3.1 GENERAL

In this chapter, theories and role of electrons in the degradation processes related to EO and EF have been discussed. The electrochemical cell of EO and EF consist of anodes and cathodes in a parallel arrangement. The oxidants are generated in the bulk and on the surface of the anode. These oxidants help in the degradation of organic pollutants of the wastewater. The generation of oxidants is fully depended upon electric current, as the electric current pass through electrodes in the electrochemical cell, oxidants are generated. The degradation efficiency of the EO and EF is different from each other. The efficiency of the EO and EF process depends upon the conditions applied during the treatment process. In EO only anode material is required for catalytic activity but in the case of EF addition of catalyst is required. So, the theory behind the degradation of EO and EF is a little bit different. But the oxidants generated in EO and EF processes are same. The concentration of the oxidants generated is variable in EO and EF processes. There is various reaction that is involved in the degradation process of EO and EF. The generation of oxidants by the losing and gaining of the electron due to electric current is discussed in detail as follows.

3.2 ELECTRO-OXIDATION

The EO process performed the oxidation reaction at the anode material with the help of electric current. The organic pollutants are transferred into non-toxic substances by decomposition into simpler compounds. EO is mostly used for the degradation of organic substances. In the EO process of wastewater treatment, organic contaminations are oxidizing directly at the surface of the electrode or oxidizing agents are generating electrochemically to perform oxidation. Complete decomposition of organic material by the oxidation of organics produces carbon dioxide and water or other oxides (Chen, 2003). Therefore, no generation of secondary pollutants takes place. EO treatment process oxidizes the organics present in

wastewater by two ways (1) indirect anodic oxidation and (2) direct oxidation, has been shown in Fig 3.2.1 (Angela et al., 2009).

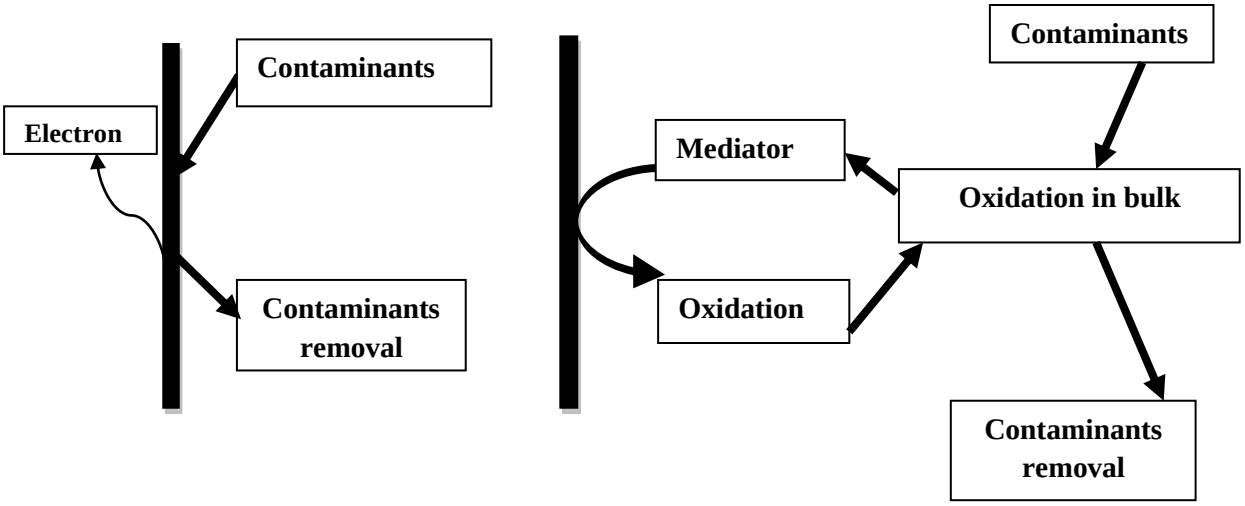

Fig 3.2.1. Direct and indirect oxidation during EO process

Source: Angela et al., 2009

3.2.1 Indirect Anodic Oxidation

Electro-oxidation of pollutants can be performed by the use of chlorine and hypochlorite, which are generating at electrodes. The role of active chlorine in the oxidation is not clear yet. The other oxidants are generating during the indirect anodic oxidation with the oxygen feeding to the electrolyte (equation 3.2.1-3.2.10) i.e hydrogen peroxide (H_2O_2), peroxodisulfuric acid ($H_2S_2O_8$), ozone (O_3) (Sarkka et al., 2015).

$$2Cl^- \rightarrow Cl_2 + 2e^- \quad \textbf{(3.2.1)}$$

$$Cl_2 + OH^- \rightarrow Cl^- + ClO_3^- + ClO^- \quad \textbf{(3.2.2)}$$

$$Cl_2 + H_2O \rightarrow HOCl + H^+ + Cl^- \quad \textbf{(3.2.3)}$$

$$HOCl \rightarrow H^+ + OCl^- \quad \textbf{(3.2.4)}$$

$$H_2O \rightarrow OH^\bullet + H^+ + e^- \quad \textbf{(3.2.5)}$$

$$2OH^\bullet \rightarrow H_2O_2 \quad \textbf{(3.2.6)}$$

$$O_2 + O^{\bullet} \rightarrow O_3 \quad \textbf{(3.2.7)}$$

$$O_2 + 2H^+ + 2e^- \rightarrow H_2O_2 \quad \textbf{(3.2.8)}$$

$$HCl + SO_3 \rightarrow ClSO_3H \quad \textbf{(3.2.9)}$$

$$ClSO_3H + H_2O_2 \rightarrow H_2S_2O_8 + 2HCl \quad \textbf{(3.2.10)}$$

The indirect electro-oxidation is called as mediated electro-oxidation. In indirect EO the metal ions are oxidized on an anode and convert into a reactive species from a stable state. These reactive species attack on the pollutants directly in the bulk. This technique can effectively oxidize many inorganic and organic pollutants at high chloride concentrations. In an indirect oxidation process, strong oxidants such as hypochlorite/chlorine, ozone, and hydrogen peroxide are electrochemically generated. The pollutants are then destroyed in the bulk solution by an oxidation reaction of the generated oxidant. All of the oxidants are generated in-situ and are utilized immediately. Among the oxidants, generation of hypochlorite is cheaper, as most of the effluents have a certain amount of chloride which gets converted to chlorine/hypochlorite. The chlorine/hypochlorite so generated oxidizes the pollutants and gets reduced to a chloride ion as shown in Fig 3.2.2 (Carlos et al., 2006). The pattern of chloro-oxidation species for the degradation of organics in the electrochemical system is purposed by comninellis as shown in Fig 3.2.2. The organic and inorganic pollutants at a high salt concentration (NaC*l*) are destroyed by the anodic generation of hypochlorite. At the same time, a number of side reactions run parallel and reduce the degradation efficiency by the formation of chlorate and chlorine evolution (Carlos et al., 2006).

3.2.2 Direct Anodic Oxidation

In direct anodic oxidation process, the pollutants are adsorbed on the anode surface followed by destruction by means of the anodic electron transfer reaction. Electro-oxidation of pollutants by direct anodic oxidation is due to the generation of physically adsorbed "active oxygen" (adsorbed hydroxyl radicals, •OH) or chemisorbed "active oxygen" (oxygen in the oxide lattice, $MO_{(x+1)}$) (Anglada et al., 2009). Direct oxidation of pollutants takes place in two steps:

- Diffusion of pollutants from the bulk solution to the anode surface
- Oxidation of pollutants at the anode surface.

$$MO_X + H_2O \rightarrow MO_X(OH^{\bullet}) + H^+ + e^- \quad \textbf{(3.2.11)}$$

$$R + MO_X(OH^{\bullet}) \rightarrow CO_2 + H^+ + e^- + MO_X \quad \textbf{(3.2.12)}$$

$$R + MO_{X+1} \rightarrow RO + MO_X \quad \textbf{(3.2.13)}$$

$$MO_X(OH^{\bullet}) \rightarrow \frac{1}{2}O_2 + H^+ + e^- \quad \textbf{(3.2.14)}$$

Direct anodic oxidation converts the toxic organic and inorganic pollutants into biocompatible organics. The feasibility of the treatment process depends upon certain parameters.

- Generation of $OH^{\bullet}$ radicals
- Nature of anode material
- Competition of treatment process with the evolution of O_2

The overall efficiency of the electrochemical process will depend on the relationship between the mass transfer of the substrate and electron transfer at the electrode surface. The rate of electron transfer has been determined by the electrode activity and current density. In the case of active electrodes, there is a strong interaction of metal and metal oxides with $OH^{\bullet}$ radicals. Metal and metal oxides act as mediators for the degradation of pollutants but, in the case of non-active electrodes, there is a weak interaction between the metal and $OH^{\bullet}$ radicals (Carlos et al., 2006). Non-active electrodes do not participate in the degradation reaction. The mechanism of anodic oxidation of organics with simultaneously oxygen evolution on active and non-active electrodes has been shown in Fig 3.2.3 (Carlos et al., 2006).

3.2.3 Operational Parameters and Their Effect on The Performance of EO Process

3.2.3.1 Electrode materials: The electrochemical oxidation of wastewater is strongly influenced by the type of anode material. The electrochemical oxidation with different types of dimensional stable electrodes is used to remove the organic contaminants (Sarkka et al., 2015). There are certain properties of the electrode material such as high over the potential for oxygen and hydrogen evolution, high electrochemical stability under severe conditions, resistance to anodic corrosion, and high current efficiencies required for the optimum performance of EO process (Anglada et al., 2009). Ti-based anodes and BDD (boron doped diamond) found to be promising electro catalytic materials and are suitable for commercial applications. There are two types of electrodes active and inactive electrodes. The inactive

electrodes in an aqueous solution can only transfer electrons rather than exchanging ions with the aqueous solution. These electrodes do not participate in the chemical reaction but serve as a source of electron i.e platinum electrodes. An active electrode is an electrode that oxidizes or reduces during EO reactions. Active electrodes are participated in the chemical reaction during the EO process, for example, BBD electrodes, ruthenium coated electrodes (Anglada et al., 2009). The efficiency and performance of the electrode material to generate oxidants is depending upon the nature of the wastewater as the electrolyte.

3.2.3.2 Current density: The current has a major role in the EO process. The generation of the oxidants is directly depended upon the electric current. The increase in electric current increases the generation of oxidant species (Sires et al., 2014). The extremely high current hindered the performance of the EO process. Because the side reaction becomes prominent as compared to the mineralization process. The electrochemical oxidation treatment is more convenient and cost-effective when the waste-waters to be treated already have high salinity (Anglada et al., 2009). The high salinity reduces energy consumption by increasing the conductivity of the electrolyte.

3.2.3.3 pH: The generation of oxidants is highly dependent on the pH range of the electrolyte. pH of the electrolyte solution has a huge impact on the performance of the EO process. EO has a good performance at acidic and as well as in the basic range of pH (Sarkka et al., 2015). In acidic condition direct anodic oxidation dominant and in case of basic pH indirect EO is dominant. The plot of generation of chloro-oxidant species is divided into three parts with respect to the pH of the electrolyte as shown in Fig 3.2.4 (Anglada et al., 2009).

In the acidic region (up to pH-5) free hypochlorous (HOCl) acid is generated. At acidic pH values hypochlorous acid decomposes and the chlorine gas liberates (equation 3.2.15) (Sires et al., 2014). The liberated chlorine gas has no bleaching action. The wastewater treatment by EO at strongly acidic conditions provides the best degradation as chlorine is the strongest oxidant followed by HClO. The fraction of free hypochlorous (HOCl) acid increases as the pH increases and at pH 5.0, almost all the hypochite exists as free hypochlorous acid (equation 3.2.16). At the pH value of 7.0-7.5, the concentration of hypochlorous acid and hypochrorite ions is almost the same in the electrolyte. In the pH range 9.0-11.5, hypochlorite is dominant in the form of OCl^- ions (Anglada et al., 2009). It is

concluded that chloro-oxidant species are highly dependent on the pH of the wastewater during EO treatment process. As the pH of the wastewater is highly acidic then Cl_2 is dominant. At the neutral pH, HOC*l* is dominant and participate in the indirect oxidation. During highly basic pH range C*l*O$^-$ seems to be dominant (equation 3.2.17). At highly basic pH electrochemical oxidation of wastewaters promotes desorption, which hinders the action of an oxidizing agent. But during desorption, the electro-oxidation of pollutants by HClO and ClO− is on its peak. Because oxidants like HClO and ClO− are not affected by the desorption of gases (Anglada et al., 2009).

$$Cl^- \rightarrow \frac{1}{2}Cl_2 + e^- \quad \textbf{(3.2.15)}$$

$$Cl_2 + H_2O \rightarrow HOCl + Cl^- + H^+ \quad \textbf{(3.2.16)}$$

$$HOCl \rightarrow OCl^- + H^+ \quad \textbf{(3.2.17)}$$

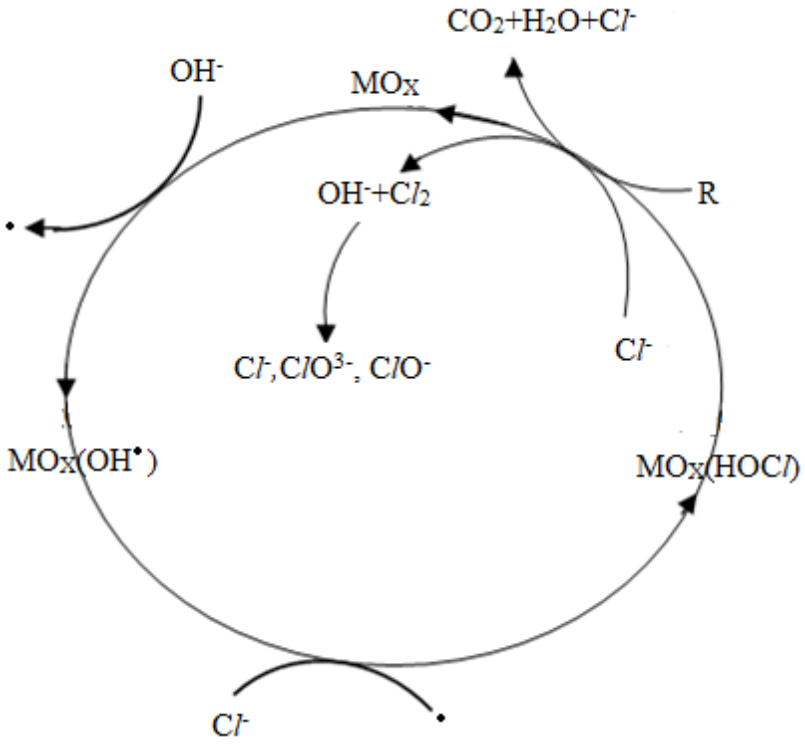

Fig 3.2.2. Extension pattern for indirect oxidation
Source: Carlos et al., 2006

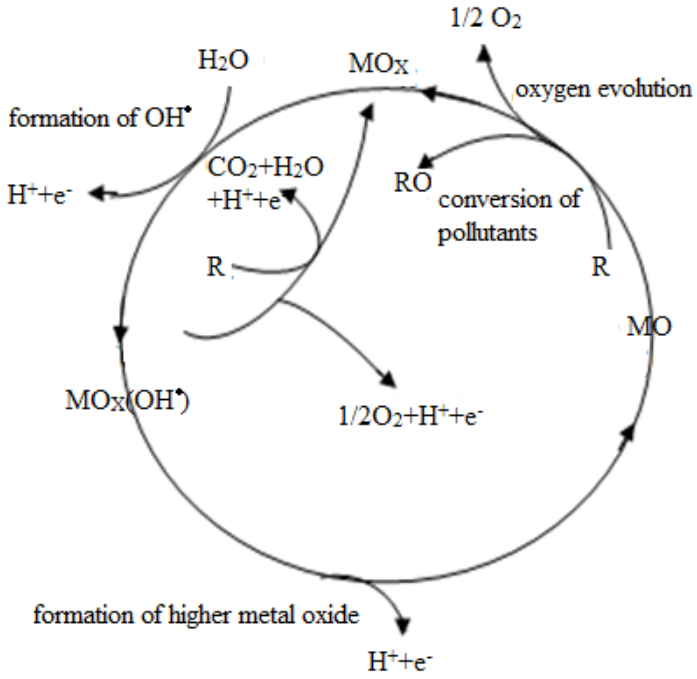

Fig: 3.2.3. Extension pattern for direct oxidation
Source: Carlos et al., 2006

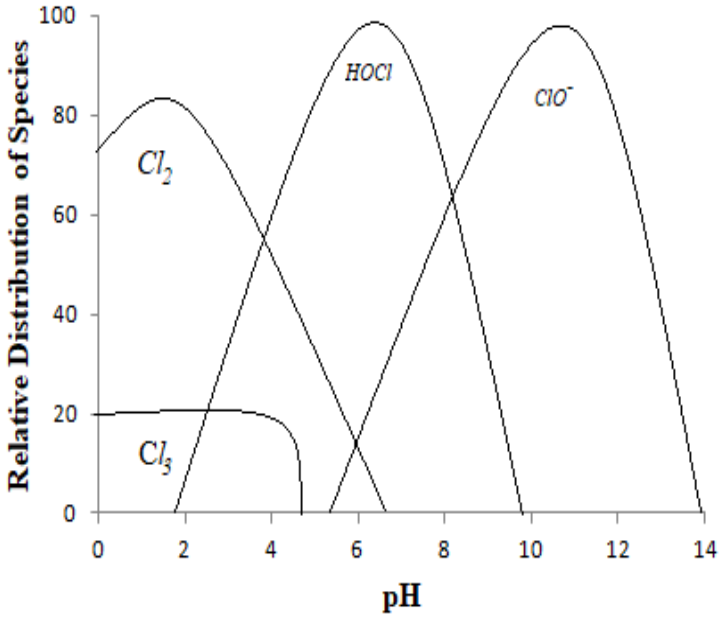

Fig 3.2.4. Generation of chloro-oxidants species with respect to pH

Source: Anglada et al., 2009

3.3 ELECTRO-FENTON

Electro-Fenton treatment process is based on the continuous generation of hydrogen peroxide. This is a promising technology for the treatment of wastewater. H_2O_2 with the combination of catalyst provide high efficiency of mineralization of organics at a low energy cost. During EF process, organics are eliminated by the Fenton mediated reaction in the bulk (Eq. 3.3.2) and on the surface of the anode by anodic oxidation (Eq. 3.3.4). O_2 gas reduces two electrons at the cathode (Brillas et al., 2009; Sirés and Brillas, 2012) in an acidic medium (Eq. 3.3.1) for the generation of H_2O_2. H_2O_2 is continuously generated by consuming O_2 in the solution during electrolysis in the EF process. Ferrous ion is added into the electrolyte, it helps in the analogously generates the ·OH radicals in the classical Fenton's reaction (Eq. 3.3.2). Due to high standard redox potential (E^o (OH/H_2O) = 2.80 V/SHE) of •OH radicals, organics present in the wastewater are oxidized to CO_2, water and inorganic ions (Gupta and Garg, 2018). At the same time, in this process, the ferrous ion is regenerated at the cathode (Eq. 3.3.3), reducing its addition, and hence the cost, in comparison to the traditional Fenton process (Salazar et al., 2012). The oxidation of pollutants shows complete mineralization achieved by anodic oxidation if using high oxygen overvoltage anodes (such as dimensionally stable anode (DSA), Pt and BDD anode (Lin et al., 2014; Nidheesh et al., 2013). Role of cathode material is crucial, as it affects the rate of H_2O_2 generation via equation 3.3.1.

$$O_2 + 2H^+ + 2e^- \rightarrow H_2O_2 \quad \textbf{(3.3.1)}$$

$$Fe^{2+} + H_2O_2 \rightarrow Fe^{3+} + OH^- + \bullet OH \quad \textbf{(3.3.2)}$$

$$Fe^{3+} + e^- \rightarrow Fe^{2+} \quad \textbf{(3.3.3)}$$

$$M(H_2O) \rightarrow M(\bullet OH) + H^+ + e^- \quad \textbf{(3.3.4)}$$

A number of operating parameters, such as anode material, solution pH, current density, catalyst (Fe^{2+}) concentration, O_2 concentration, supporting electrolyte, organic load, etc., influence process efficiency. It is well known that Fenton's reaction can be applied in acidic pH of 2.8–3.0 (Sun and Pignatello, 1993) to efficiently produce •OH radicals. But, at this pH, HO_2• radicals are produced in excess of H_2O_2, which has lower oxidation power as compared to •OH. The rate of Fenton's reaction in the EF process is predominantly controlled by the

H_2O_2 production rate, which depends on factors such as O_2 solubility, temperature, pH, cathode type and current density. The mechanism of electro-Fenton has been shown in Fig 3.4.1 (Nidheesh et al., 2012). Current density controls not only the H_2O_2 generation rate (Eq. 3.3.1) but also controls the regeneration rate of Fe^{2+} (Eq. 3.3.3). At the same time, high current density supports other side reactions leading to reduce the H_2O_2 (Eq. 3.3.5, 3.3.6, 3.3.7) and production of H_2 at the cathode (Eq. 3.3.8) (Sirés et al., 2014).

$$H_2O_2 + 2H^+ + 2e^- \rightarrow 2H_2O \quad \textbf{(3.3.5)}$$

$$H_2O_2 \rightarrow HO_2\bullet + H^+ + e^- \quad \textbf{(3.3.6)}$$

$$HO_2\bullet \rightarrow O_2 + H^+ + e^- \quad \textbf{(3.3.7)}$$

$$2H_2O + 2e^- \rightarrow H_2 + 2OH^- \quad \textbf{(3.3.8)}$$

3.3.1 Operational Conditions and Their Effect on The Performance of EF Process

3.3.1.1 Fe^{+2}/Fe^{+3} and H_2O_2 concentrations: Fe^{+2} acts as a catalyst in the Fenton reaction. The availability of Fe^{+2} is a prerequisite requirement in an electro-Fenton process. In the electro-Fenton system, Fe^{+2} is electro regenerated from Fe^{+3}. Fe^{+2} promote the EF process and enhance the degradation process. The phenomenon of generation of H_2O_2 is also influenced by the concentration of ferrous ion present. The concentration of H_2O_2 plays a vital role in the efficiency of an electro-Fenton reaction. The increase in the dosage of H_2O_2, increases the rate of Fenton reaction. But a higher concentration of H_2O_2 as compare to the Fe^{+2} reduces the process efficiency. The ratio of hydroxyl radicals to ferrous ion must be optimizing. Otherwise higher concentration of H_2O_2 in the presence of a high concentration of H^+ ions to form stable oxonium ion $[H_3O_2]^+$. Oxonium ions make hydrogen peroxide more stable and reduce its reactivity with ferrous ions (Nidheesh et al., 2012). Furthermore, it reduces the overall performance of the EF treatment process.

3.3.1.2 pH: Fenton process is highly pH-dependent process. The optimum pH reported for the electro Fenton process is 3.0 (Sun and Pignatello, 1993). The Fenton reagents at higher pH range form inactive iron oxo-hydroxides which ultimately convert into ferric hydroxide (Nidheesh et al., 2012). It slows down the performance of the EF process. The pH value lower

than 3, generates iron complex species, which further hinder the degradation process by the generation of hydrogen peroxide in higher concentration than other oxidant species. In addition, at pH < 3.0, hydrogen peroxide converts into oxonium ion (equation 3.3.9). At higher pH, the efficiency of the EF process decreases rapidly, especially pH> 5.0. This is due to the fact that H_2O_2 is unstable in a basic solution. Therefore, the overall efficiency of the Fenton process to degrade organic compounds is reduced both at high and low values of pH.

$$H_2O_2 + H^+ \rightarrow H_3O_2^+ \quad \textbf{(3.3.9)}$$

3.3.1.3 Current density: Current is a necessary force for the reduction of oxygen at cathode into hydrogen peroxide. The higher value of applied current leads to the generation of H_2O_2. The higher concentration of H_2O_2 generates highly reactive species, which ultimately helps in the degradation process. The higher current density regenerates ferrous ion from ferric ion which ultimately increases the efficiency of Fenton reaction (Nidheesh et al., 2012). A very high current density shows a negative effect on the efficiency of the Fenton reaction. The O_2 gas discharge at the anode (equation 3.3.10) and hydrogen gas discharge at the cathode (equation 3.3.11) at very high current density. These reactions hinder the efficiency of the EF process.

$$2H_2O \rightarrow 4H^+ + O_2 + 4e^- \quad \textbf{(3.3.10)}$$

$$2H^+ + 2e^- \rightarrow H_2 \quad \textbf{(3.3.11)}$$

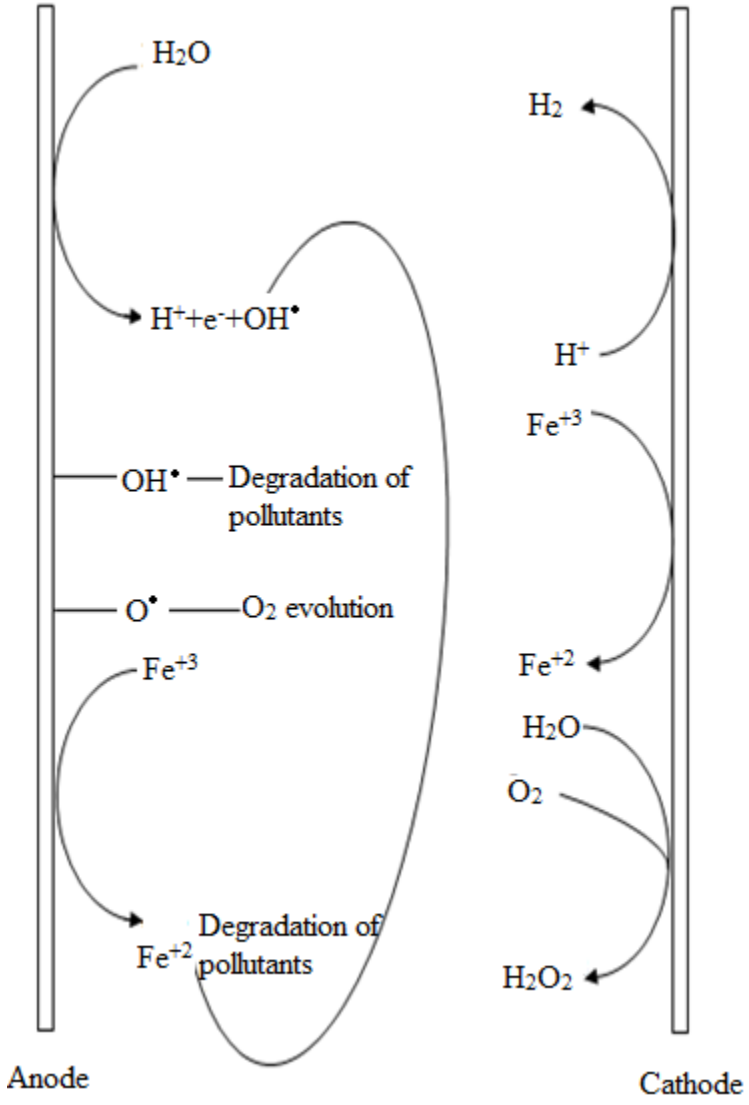

Fig 3.4.1. Degradation mechanism of electro-Fenton

Source: Nidheesh et al., 2012

Chapter – 4

MATERIALS AND METHOD

4.1 GENERAL

This chapter includes a description of the materials and experimental methods used for the treatment of textile effluent by electro-oxidation and electro-Fenton treatment processes. Experimental setup, chemicals and electrodes used for the batch and continuous mode of operation has been discussed in detail.

4.2 MATERIALS AND METHODS

4.2.1 Wastewater

Real textile wastewater was collected from a Mink Blanket industry situated in Ludhiana, Punjab. The real textile wastewater was store in the refrigerator at 4^0C. Textile effluent contains high strength of dyes that were used in mink blanket industry. To precede the study on textile effluent, it was characterized for water quality parameters i.e pH, BOD, COD, TDS, TSS, color, chloride, alkalinity, oil/grease, Nitrogen, conductivity and hardness.

4.2.2 Chemicals and Electrodes

All the chemicals used in the present study were of analytical reagent (AR) grade. 1N sulphuric acid (H_2SO_4), potassium chromate indicator, standard silver nitrate, sodium chloride, methyl orange indicator, phenolphthalein indicator, bromocresol green indicator, boric acid, ethyl alcohol, petroleum ether and erichrome black-T indicator purchased from Merck KGaA Darmstadt, Germany. Ferrous sulphate ($FeSO_4$), mercuric sulphate (Hg_2SO_4), silver sulphate (Ag_2SO_4), potassium dichromate ($K_2Cr_2O_7$), sodium hydroxide (NaOH) and dichloromethane (CH_2Cl_2) purchased from Sigma Aldrich fine chemicals, America.

The Ti/RuO_2 electrodes were used as anodes purchased from Titanium Tantalum Products Limited, Chennai, India. Each electrode has the dimension of 100 mm x 85 mm x 1.5 mm and having the surface area of 85 cm^2. Aluminium (A*l*) plates used as cathode purchased from the local supplier in the form of a sheet with the thickness of 1.5mm. Then,

aluminium sheets were cut into dimensions of 100 mm x 85 mm x 1.5 mm. The cleaning of electrodes was performed by the 15% HCl followed by washing with distilled water. Washed Ti/RuO_2 and Aluminum electrodes were air dry at ambient temperature prior to use for electro-chemical treatment methods.

4.2.3 Analytical Methods

A closed reflux method was used for the COD measurement of the real textile effluent. COD was measured using digestive unit (thermo reactor, model 2025D, Spectra lab) and double beam UV visible spectrophotometer (HACH, DR 5000, USA) at COD program 1500 mg/l was used to observe the COD in mg/the standard methods were used to measure the TDS and TSS of the textile effluent. The turbidity of the textile effluent was measured using turbidity meter (Spectra lab Model NT 4000 Turbidity Meter). Standard titrimetric volhard method was used for the measurement of chloride content. To determine the total nitrogen content of the textile effluent standard Kjeldahl method was used. Oil and grease of textile wastewater were determined by using a standard petroleum ether solvent method. The alkalinity of the textile effluent was measured using the standard titrimetric method. Hach colorimeter (Colorimeter DR900, HACH) was used to measure the color of the textile wastewater in platinum-cobalt units. BOD of the sample was measurement using Oxitop BOD bottles (WTW OxiTop® IS 6, BOD package). A benchtop pH/conductivity meter (Benchtop Water Quality Meter – 860033,) was used for the pH and conductivity measurement.

To study the topographical and elemental information at a huge magnification of anode material SEM and EDX was performed. In the present study, zeiss ultra 55 FE-SEM with oxford EDX system was used for SEM and EDX. XRD was used to know about the structure, phases, crystal orientations and other structural parameters of anode material. X-ray diffraction of electrodes was performed using panalytical's X'pert pro-diffracto-meter with Cu Ka radiation and angular range of 20^0 to 80^0.

4.2.4 Experimental Setup and Methods of Operation

A cubical shaped batch EO and EF reactor were fabricated with plexiglass sheet (Fig 4.2.1). The dimensions of the fabricated reactors were 110mm x 110 mm x 130mm and having a working volume of 1.5 *l*. The Ti/RuO_2 plates and aluminium plates act as an anode and cathode respectively. The arrangement of electrodes for EO and EF treatment processes

were in a parallel and mono-polar mode. The total effective anodic area for two anodes 170 cm^2 (2 x 85 cm^2).The inter-electrode spacing was kept to be 1 cm (Benazzi et al., 2016; Linares-Hernández et al., 2009; Hanay et al., 2011; Sengil et al., 2009). A magnetic stirrer was used to mix the reactor contents (textile wastewater) during the treatment process. In the case of the electro-Fenton process, aeration was necessary therefore, electric spargers were used to aerate the reactor content. A precision DC power supply (DIGITECH, Roorkee, India, Model: 4818A10) was used to supply the current during EO and EF experiments.

The continuous mode of operation for EO and EF was also performed with the same dimensions of reactor and electrodes were adjusted as of batch reactor as shown in Fig 4.2.2. To regulate the flow rate (Q) and retention time (R_T) for a particular run in case of continuous EO and EF, peristaltic pump (Miclins peristaltic pump PP 20 EX) was used.

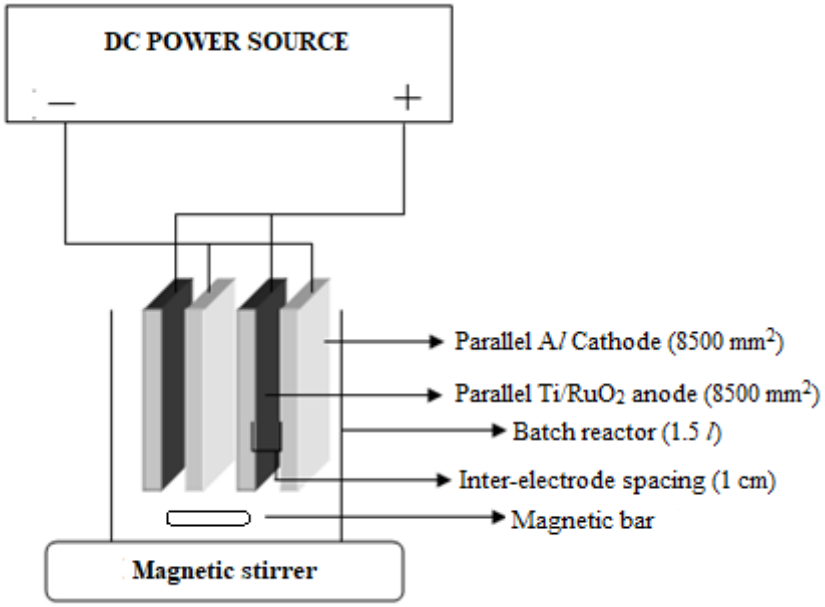

(a)

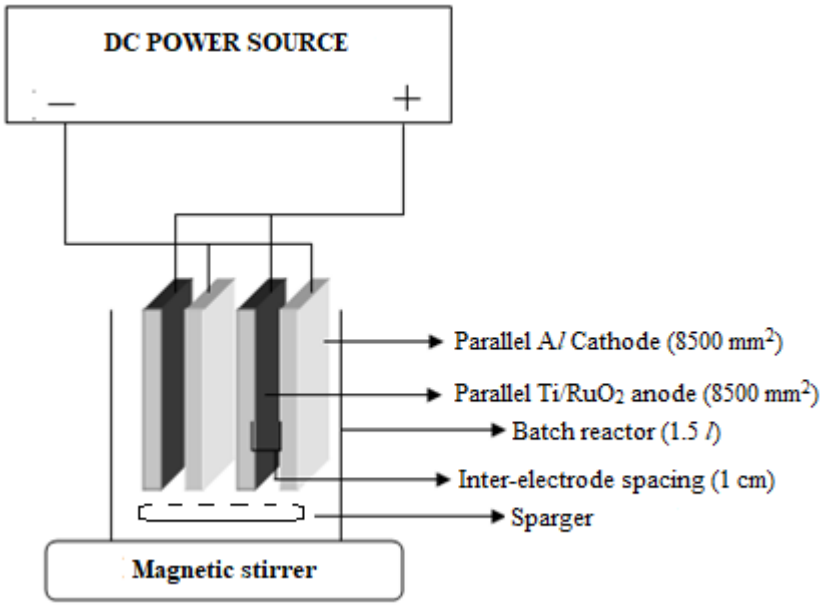

(b)

Fig 4.2.1. Schematic diagram of batch experimental setup (a) EO (b) EF

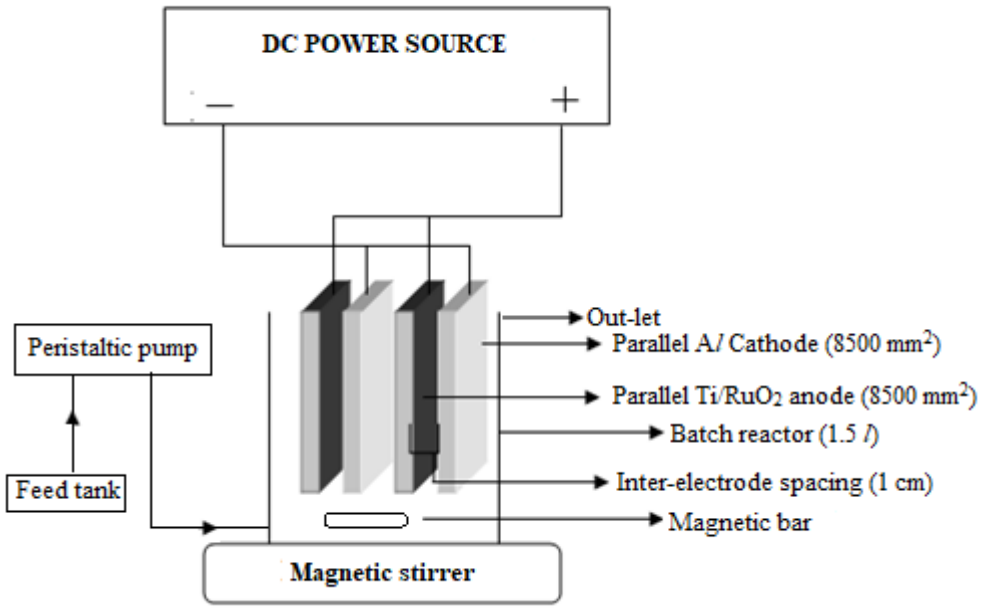

(a)

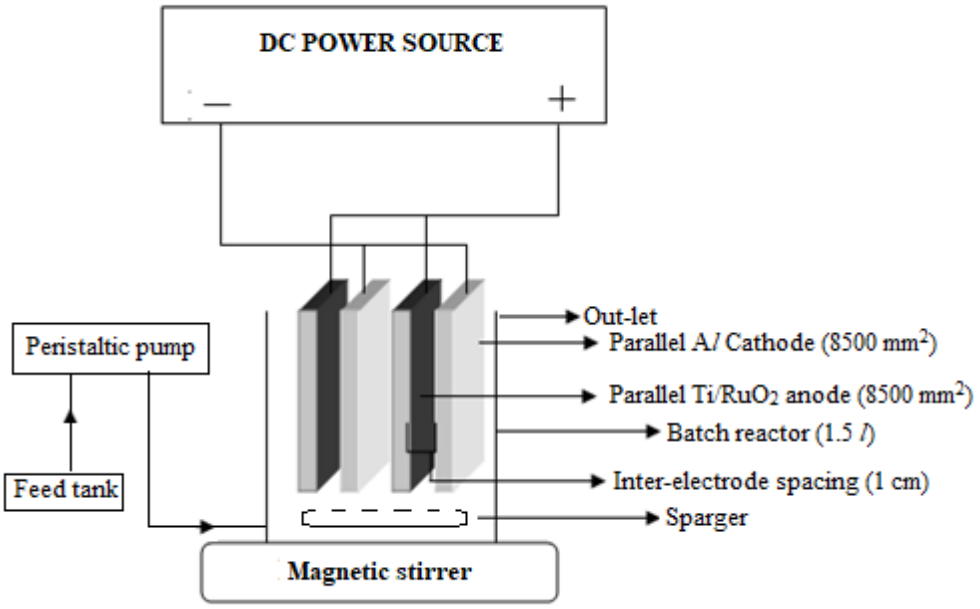

(b)

Fig 4.2.2. Schematic diagram of continuous experimental setup (a) EO (b) EF

4.3 EXPERIMENTAL DESIGN

To design the experiments for the treatment of textile effluent by EO and EF for the continuous and batch mode of operation response surface methodology (RSM) was used. RSM is a factual strategy for outlining experimental runs and assessing the impacts of different parameters on the selected system responses. Response surface methodology (RSM) is a collection of mathematical and statistical techniques for the designing of experiments. The major application of RSM is aimed at reducing the number of experiments and the cost of expensive analysis methods (Bidin et al., 2009)

RSM develop an adequate functional relationship between a response of interest (X) and a number of input variables denoted by a_1, a_2, …. a by using low-degree polynomial model (equation 4.3.1).

$$X = f(a)\beta + £ \quad \textbf{(4.3.1)}$$

Where, a = (a_1, a_2, ….a_n), f(a) is a vector function of p elements, β is a vector of unknown constant coefficients of parameters, and £ is a random experimental error assumed to have a zero mean. There are two low-degree polynomial models used for RSM modelling. It includes the first-degree model (4.3.2) and the second-degree model (4.3.3).

$$X = \beta_0 + \sum_{i=1} \beta_i a_i + £ \quad \textbf{(4.3.2)}$$

$$X = \beta_0 + \sum_{i=1}^{n} \beta_i \ a_i + \sum_{i<j} \sum \beta_{ii} a_i a_j + \sum_{i=1}^{n} \beta_{ij} {a_i}^2 + £ \quad \textbf{(4.3.3)}$$

Where β_0 is the constant coefficient, β_i, β_{ii}, β_{ij} are linear interaction coefficients, of quadratic and second-order terms respectively (equation 4.3.3). The terms a_i and a_j are variables and £ is an error function. The major purpose of considering a model is to establish a relationship between x and a_1, a_2, ..….a_n, and to determine the significant values of the input parameters (a_1, a_2, ….a_n,) by the testing of hypothesis. Which further helps in the determination of the optimum values of a_1, a_2, …….a_n, with respect of maximizing or minimizing the responses desired.

The first order model (equation 4.3.2) and second-order model (equation 4.3.3) are the most commonly used polynomial models for RSM modelling. The first-order designs used for the design of experiments are 2k factorial, Plackett–Burman, and simplex designs. First order model is less rotatable designs so, there is less stability in the prediction of variance in the vicinity of the design centre. A first-order model is suffered from the lack of fit due to the

individual interaction of input parameters to the responses due to the curvature of the surface. Therefore, three-level studies are required to construct a quadratic response surface model. The full factorial design is used in the case of five and fewer input parameters. The most common full factorial designs used are second-order designs i.e Box–Behnken designs and central composite.

4.3.1 Box–Behnken Design

Box -Behnken design was developed by Box and Behnken in 1960. This design provides three levels to each factor and generated subsets of the factorial combination from the 3k factorial design. Box-Behnken design (BBD) is very popular at the industrial scale to optimize the process parameters because it requires only three levels setting for each factor are -1, 0, 1. The BBD is independent of the quadratic design. There are certain Box-Behnken designs that are rotatable but most of the designs are nearly rotatable based on three-level incomplete factorial designs. A BBD in the form of a cube, consider the central point and the middle points of the edges, as shown in Fig 4.3.1 (Ferreira et al., 2007). BBD has three levels per factor, so it avoids the space corners but fills the combinations of centre and extreme levels of the cube. BBD combines a fractional factorial with incomplete block designs and avoids the ex+treme vertices to maintain the rotatability of the design (Hanrahan and Lu, 2006). The number of experiments (N) desired for the optimization of process parameters were designed by BBD using equation 4.3.4

$$N= 2k(k-1) +C_0 \quad \textbf{(4.3.4)}$$

Where k is the number of factors and C_0 is the number of central points

BBD is quite better than other response surface designs for three-level full factorial designs. The efficiency of an experimental design is defined as the number of coefficients in the estimated model divided by the number of experiments (Ferreira et al., 2007).

4.3.2 Central Composite Design

Central composite design (CCD) was developed by Box and Wilson in 1978. CCD is efficient for the construction of the second-order model five-level full factorial designs. It consists of central and axial factorial points. The first order model has lack of fit evidence so, more axial factorial points are added in terms of quadratic. The input parameters are divided into groups that are run in each block. In the case of CCD, the shape of the response surface is

protected by the orthogonal block effect. So, the rotatability of the design does not affect the variance (Hanrahan and Lu, 2006).

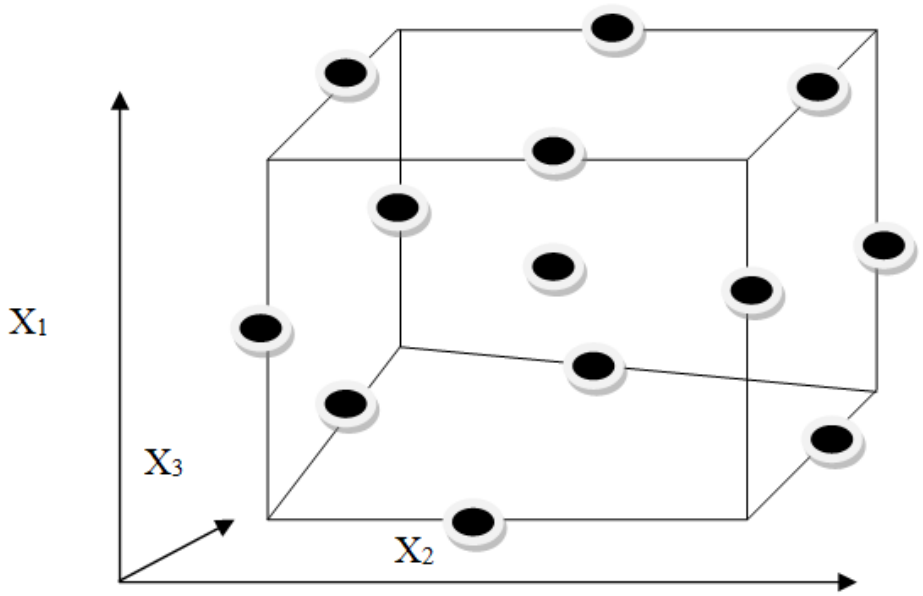

Fig 4.3.1. Three interlocking 2^N factorial design for BBD

Source: Ferreira et al., 2007

Rotatability of the design provides equal precision of the surface in all directions. Central composite designs are a factorial or fractional factorial design with centre points. These centre points augmented with a group of axial points. CCD provides more curvature to the centre and axial points. Data can be divided into multiple blocks in case of CCD. It creates orthogonal blocks with input variables. The effect of model terms on the blocks can be estimated independently during CCD modelling. So, the variation in the regression coefficient becomes minimum. Central composite designs are face centred designs with an alpha of 1. In this design, the axial points are at the centre of each face of the cube or factorial space as shown in Fig 4.3.2 (Ferreira et al., 2007). The CCD is an appropriate alternative to the full factorial three-level design for a large number of input variables with respect to the responses. It helps in the measurement of reproducibility and model lack of fit (Ferreira et al., 2007). It demands less number of experiments and providing comparable results.

The total number of needed design points (N) is determined by the equation 4.3.5.

$$N = 2^k + 2\,k + C_0 \qquad \textbf{(4.3.5)}$$

Where k is the number of factors and C_0 is the replication number of centre points.

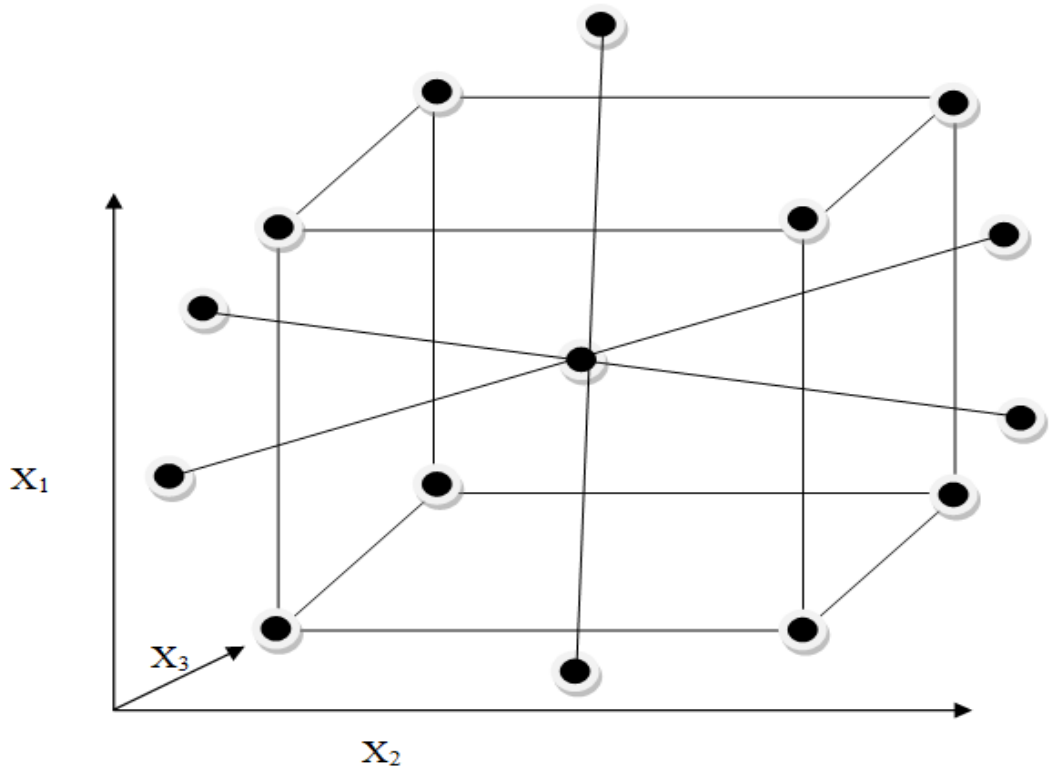

Fig 4.3.2. Three interlocking 2^N factorial design for CCD

Source: Ferreira et al., 2007

In the present study, statistical Design-Expert software version 6.06 (STAT-EASE Inc., Minneapolis, US) was used to design the experiments. A second-order model was constructed efficiently with RSM designs. RSM designs were augmented by the additional centre and axial points to allow estimation of the tuning parameters of a second-order model. In the optimization of process parameters, responses were related to the process parameters linearly or quadratic. The experimental data were processed for a second-order polynomial Eq. (4.3.3) to recognize the relevant model terms. Three levels BBD was used for batch EO and EF whereas five level CCD was used for continuous EO and EF.

A full factorial experiment strategy was used in the present study. In a full factorial experiment strategy, input parameters are varied together, instead of one at a time. The lower and upper ranges of the design input parameters are defined. The defined range of the input parameters is then segregate at different levels. Optimization provides the simultaneous effect of parameters on the responses. Experiments consist of a series of runs, the effect of changes in input parameters (a_1, a_2, ….a_n) on the responses (X) is determined. RSM modelling and optimization reduces the effect of noise by derivative-based algorithms. The interaction of the responses (X) with input parameters (a_1, a_2, ….a_n) can be represented graphically, either in the three-dimensional space or as contour plots. Analysis of variance (ANOVA) was used to study the interaction between the variables and the responses. The adequacy of the model was expressed in the terms of R^2, adjusted R^2 and predicted R^2. Adequate precision ratio (F and P values) shows the statistical significance of the model fitted.

In present the study there were three responses for different operational parameters so, the multi-response processes optimization was used. The multi-response processes optimization is a combined form of overall desirability function approach. In the multi-response processes optimization, desirability function converts each response to a corresponding desirability value between 0 and 1. The desirability function approach is one of the most widely used methods for the optimization of multiple response processes. One-sided desirability *d* is given in equation (4.3.6).

$$d = \begin{cases} 0 & if\ X_i \le X_{i-min} \\ \left[\frac{X_i - X_{i-min}}{X_{i-max} - X_{i-min}}\right]^{\varphi} & if\ X_{i-min} < X_i < X_{i-max} \\ 1 & if\ X_i \ge X_{i-max} \end{cases} \quad \textbf{(4.3.6)}$$

Where X_i is response values, $X_{i\text{-}min}$ and $X_{i\text{-}max}$ is minimum and maximum acceptable values of response *i*, and *r* is weight and a positive constant. Here, weight for all the responses was the same and set to be $\varphi = 1$. These are used to determine the scale of desirability. All the desirability functions are combined to form a composite desirability function, which converts multiple responses into a single response (Sangal et al., 2013). The individual desirability functions are combined in order to obtain the overall desirability, D as in equation (4.3.7)

$$D = (d_1 x\, d_2 x\, d_3 \dots\dots\dots\dots)^{\frac{1}{n}} \quad \textbf{(4.3.7)}$$

Where 0<=D<=1, and n is the number of responses.

4.4 EXPERIMENTAL PROCEDURE

The batch EO and EF experimental runs were designed and examined accordingly BBD under RSM. Whereas, continuous EO and EF were designed and examined by CCD under RSM was used. The ranges of selected variables were determined from preliminary experiments. Anticipated responses (X) were in terms of % chemical oxidation demand (COD) removal (X_1), % color removal (X_2) and energy consumed (X_3). The experimental runs for batch (EO and EF) and continuous (EO and EF) were conducted, as per the design matrixes suggested by RSM. pH of the feed textile wastewater was adjusted for a particular run by 1N NaOH and/or HC*l* for both the processes. Time, t was started by a switch on the current (i), which was maintained constant for an experimental run. Real textile wastewater was continuously stirred for both the process by magnetic stirrer. In the case of EF process, electric spargers were used to agitate the textile effluent. After the desired time, t power supply was switched off and the sample was withdrawn from the (batch and continuous) EO and EF reactor for further analysis. Thereafter, % COD removal (X_1) or % Color removal of the withdrawn samples was measured using a COD digestion unit and UV visible spectrophotometer (equation 4.4.1).

$$X_1 or\ X_2 = \left[\frac{C_0 - C_S}{C_0}\right] X\ 100 \qquad \textbf{(4.4.1)}$$

Where C_0= Initial COD or Initial color intensity; C_S= Final COD or Final color intensity

Energy consumption per kg of COD removed (X_3) during the EO and EF treatment was calculated by the equations (4.4.2) (Batch EO and EF processes) and (4.4.3) (Continuous EO and EF process)

$$\mathrm{X_3} = \frac{[\mathrm{Vti}]}{\mathrm{SVCOD_R}} 10^3 \qquad \textbf{(4.4.2)}$$

Where, *i*= current (A); *V*= voltage (volt); *t*= treatment time (h); SV= sample volume (*l*); COD_R= COD removed (mg/*l*)

$$\mathrm{X_3} = \frac{[\mathrm{Vti}]}{\mathrm{COD_R}} 10^3 \qquad \textbf{(4.4.3)}$$

Where, *i*= current (A); *V*= voltage (volt); *t*= elapsed time (h); COD_R= COD removed (mg/*l*)

RSM permits the analysis of experimental data and optimization of selected parameters for a particular process (EO and EF) in batch and continuous process on % COD removal (X_1), % color removal (X_2) and energy consumed (X_3). Polynomial equation (Eq. 4.3.3) was used to determine the pertinent model terms along the error function. The influence of the process variables on the responses was analyzed from an analysis of variance (ANOVA). Multi-response optimization using the desirability function approach was used to simultaneously maximize the % COD removal, % color removal, and to minimize the energy requirement.

The in-situ chemical analysis of the treated samples by EO and EF was performed by spectrophotometric analysis and GC-MS analysis. Spectrophotometric analysis and GC-MS analysis was performed for treated textile effluent by EO, EF and untreated wastewater. Spectrophotometric analysis was performed to analyze the treated sample by EO and EF under UV range of spectrophotometer with the comparison of the untreated textile effluent sample.

The compounds identified by GC-MS Analysis of the treated textile wastewater by EO and EF were analyzed with the comparison of untreated textile effluent. GC-MS of treated textile wastewater at optimum conditions of EO and EF (batch), EO and EF (continuous) and untreated textile wastewater was carried out to identify various transformation products formed during degradation process for disposal study. The sample for GC-MS analysis was prepared by liquid-liquid extraction method. Perkin−Elmer Clarus 500 MS instrument with fused silica capillary columns (25 m × 0.20 μm internal diameter) coated with a 5% diphenyl/95% dimethyl polysiloxane was used for GC-MS analysis. The split/splitless injector mode was used at injector temperature 350°C. Helium was used as carrier gas with a flow rate of 1 *ml*/min. The temperatures corresponding to the inlet line and ion source were set at 250 °C and 300 °C, respectively. Run time for GC-MS analysis was 30 min.

To evaluate the toxicity of the EO (batch and continuous) and EF (batch and continuous) treated textile wastewater bioassay for acute toxicity was performed using standard procedure IS: 6582. Test organism for the acute toxicity bioassay test was *Aploclzeilus panchax.* The mortality rate of the organisms evaluates the toxicity of the

wastewater before and after the treatment process. Kinetic parameters for the COD and color removal by both the process were evaluated.

The electrodes material was characterized to determine the stability of the electrode material after several experimental runs of EO and EF in both the operational mode. The structural, physical and chemical composition of electrodes before and after treatment processes was investigated by Scanning Electron Microscopy (SEM), Energy-dispersive X-ray spectroscopy (EDX) and X-ray diffraction (XRD) analysis.

Chapter – 5

RESULTS AND DISCUSSION

5.1 GENERAL

This chapter deals with the studies on the de-colorization and oxidation/degradation/transformation of organic matters of real textile effluent by electro-oxidation (EO) and electro-Fenton (EF) treatment processes in batch and continuous reactor. The interactions of various selected process parameters with the responses (% COD removal, % color removal and energy consumption) are discussed in detail. Further, organics oxidation/degradation/transformation pathway and mechanisms involved were explored by identifying transformation/degradation products after the treatment. Disposability study of the treated wastewater was performed by determining the toxicity of the effluent after the EO and EF treatment processes.

5.2 CHARACTERIZATION OF REAL TEXTILE EFFLUENT

The variation in the characteristics of textile effluents depends upon the type of textile manufactured and the chemicals used during textile processing. The textile wastewater contains high suspended and dissolved solids, pH, biological oxygen demand (BOD), chemical oxygen demand (COD), odour, color and toxic chemicals.

Collected real textile effluent was characterized for various water quality parameters, and the results are shown in Table 5.2.1. To precede the study on textile effluent, it was necessary to characterize the effluent to determine whether it is suitable for EO and EF treatment. The BOD/COD ratio of the collected real textile effluent was found to be 0.3, which implies that the textile wastewater is non-biodegradable/recalcitrant and toxic in nature. The high concentration of chloride, TDS, TSS makes it undesirable for the environment. The threshold acceptable level of the TSS is 500 mg/l and TDS is 2100 mg/l. The elevation in the TSS above 1000 mg/l and TDS above 7100 mg/l is toxic to the flora and fauna. The maximum color acceptability is 150 pt.co. The oil and grease concentration is also quite high (83 mg/l) in textile wastewater. Oil and Grease are very sensitive parameters in water. Its presence even in lower concentration may cause serious health problems. High oil and grease

concentration in water are very hazardous to the environment. The alkalinity of the textile wastewater is quite high as 812 mg/l. Most common dyes used in Mink blanket industry are Orcolan group of dyes. These dyes are very effective in alkaline medium**.** The pH of the wastewater is directly depended upon the alkalinity of the wastewater. So, higher alkalinity increases the pH of wastewater. If the high alkalinity wastewater is disposed into the environment without any treatment then it causes skin problem to the aquatic life. Therefore, it is necessary to treat the textile effluent for its safe disposal to the environment.

Table 5.2.1. Physicochemical characterization of textile effluent

PARAMETERS	VALUES
pH	9.84
BOD (mg/l)	200
COD (mg/l)	544
TDS (mg/l)	50800
TSS (mg/l)	59400
Color (pt.co)	936
Chloride (mg/l)	1182
Alkalinity (mg/l)	812
Oil/grease (mg/l)	83
Total Kjeldahl Nitrogen (mg/l)	**2.12**
Conductivity (mS/cm)	3.7
Turbidity (NTU)	276
Hardness (mg/l)	831

5.3 STUDY ON BATCH ELECTRO-OXIDATION (EO) TREATMENT PROCESS

5.3.1 Model Fitting and Statistical Analysis

The experiments for batch EO were designed using three-level BBD under RSM. The three independent variables were taken as input parameters for the batch EO process such as *pH*: 3-11; electrolysis time (*t*): 10-90 min and current (*i*): 0.25 - 3 A. % COD removal (X_1), % color removal (X_2) and energy consumed (X_3) were evaluated as responses of the process. Total 17 experiments as suggested by RSM were conducted, and the calculated responses values of X_1, X_2 and X_3 are shown in Table 5.3.1. Experimental data were then analyzed by multiple regression analysis of RSM. The quadratic model was suggested by exploiting sequential F-test and other adequacy measures. For the responses X_1, X_2 and X_3, the adequate precision indicated that the model is efficient and significant. Adequate precision expresses the signal to noise ratio, and adequate precision ratio above 4 shows that the model was efficient in navigating the design space. The model summary statistics for responses X_1, X_2 and X_3 showed a high value of the coefficient of determination. The values of R^2, Adjusted R^2 and predicted R^2 are shown in Table 5.3.2. It supports a satisfactory adjustment between the observed and predicted values for the selected responses as shown in Fig 5.3.1, 5.3.2 and 5.3.3 for X_1, X_2 and X_3, respectively. Quadratic model for batch EO was also supported by ANOVA with F- values of 32.84, 27.73 and 30.51 for the responses X_1, X_2, and X_3, respectively (Table 5.3.3a, b, c). The "Prob>F" smaller than 0.05 indicates, that the quadratic model and its terms are significant with a 95% confidence level. The significant terms of batch EO for X_1: *t, i, pH*, t^2, i^2, (*t* x *pH*) and (*i* x *pH*); X_2: *t, i, pH*, t^2, i^2, (*t* x *i*) and (*i* x *pH*); X_3= *t, i,* i^2 and (*t* x *i)* were observed from the ANOVA (Table 5.3.3a, b, c).The quadratic model equation obtained in terms of significant process parameters for batch EO process are given below.

$$1.0/(X_1)^{0.5} = 0.26471 - 0.00160t - 0.0433\, i - 0.0095\, pH + 6.95\text{x}10^{6}\, t^2 + 0.0085\, i^2 + 5.43\text{x}10^{5} \quad (t \text{ x } pH) + 0.00125(i \text{ x } pH) \qquad \textbf{(5.3.1)}$$

$$X_2 = 25.82510 + 1.40216\, t + 26.9836\, i - 2.2928\, pH - 0.0097\, t^2 - 5.95871\, i^2 + 0.07322\, (t \text{ x } i) - 0.8172\, (i \text{ x } pH) \qquad \textbf{(5.3.2)}$$

$$X_3 = 0.12942 - 0.0024\, t - 0.2792\, i + 0.086345\, i^2 + 0.0068\, (t \text{ x } i) \qquad \textbf{(5.3.3)}$$

Table 5.3.1. Experimental design for the batch EO process

Standard Order	t (min)	*i* (A)	pH	X_1		X_2		X_3	
				$X_{1\ exp}$	$X_{1\ pre}$	$X_{2\ exp}$	$X_{2\ pre}$	$X_{3\ exp}$	$X_{3\ pre}$
7	10.00	1.63	11.00	47.10	44.44	56.40	53.23	0.07	$4.3x10^{-3}$
17	50.00	1.63	7.00	64.20	69.44	89.90	89.86	0.35	0.35
12	50.00	3.00	11.00	56.30	59.17	78.30	81.88	0.99	0.99
15	50.00	1.63	7.00	64.20	69.44	89.90	89.86	0.35	0.35
8	90.00	1.63	11.00	79.80	82.64	96.10	95.48	0.62	0.68
10	50.00	3.00	3.00	57.60	59.17	97.40	97.22	0.99	0.99
1	10.00	0.25	7.00	27.70	27.70	35.00	37.99	0.01	0.077
4	90.00	3.00	7.00	86.80	82.64	98.90	95.97	1.78	1.71
2	90.00	0.25	7.00	47.00	51.02	72.20	72.64	0.07	$5.6x10^{-4}$
11	50.00	0.25	11.00	49.10	51.02	75.40	75.58	0.04	0.036
9	50.00	0.25	3.00	35.10	34.60	76.50	72.94	0.04	0.036
5	10.00	1.63	3.00	29.70	30.86	58.50	59.13	0.07	$3.8x10^{-3}$
6	90.00	1.63	3.00	75.60	82.64	99.10	100	0.62	0.68
13	50.00	1.63	7.00	64.20	69.44	89.90	89.86	0.35	0.35
3	10.00	3.00	7.00	36.50	34.60	45.60	45.22	0.20	0.27
16	50.00	1.63	7.00	64.20	69.44	89.90	89.86	0.35	0.35
14	50.00	1.63	7.00	64.20	69.44	89.90	89.86	0.35	0.35

% COD removal (X_1), % color removal (X_2) and energy consumption (X_3)

Table 5.3.2. Various R-squared values suggested by BBD for responses %COD removal (X_1), % Color removal (X_2) and energy consume (X_3)

Responses	R-Squared	Adj R-Squared	Pred R-Squared
X_1	0.99	0.98	0.89
X_2	0.99	0.98	0.83
X_3	0.99	0.98	0.83

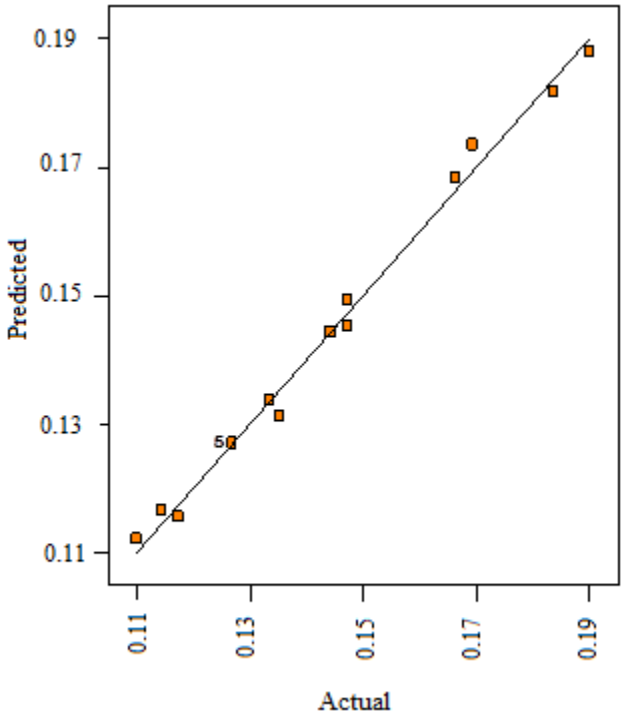

Fig 5.3.1. Predicted versus actual %COD removal for batch EO process

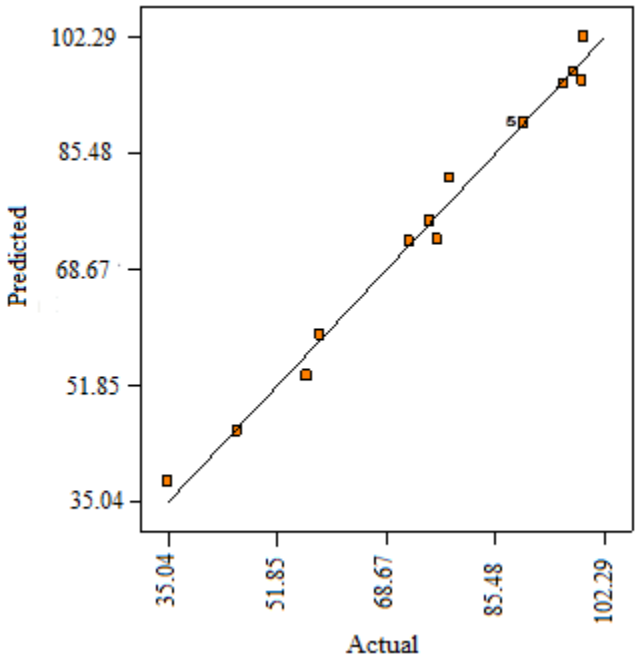

Fig 5.3.2. Predicted versus actual % color removal for batch EO process

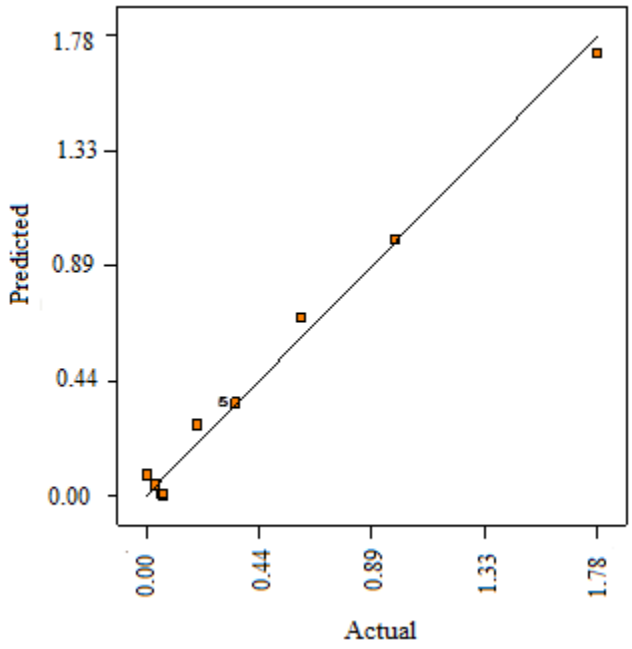

Fig 5.3.3. Predicted versus actual energy consume for batch EO process

Table 5.3.3a. ANOVA for the %COD removal of batch EO process

Source	Sum of Squares	DF	Mean Square	F-Value	Prob > F
Model	0.0095	9	0.0010	109.90	< 0.0001
T	0.0052	1	0.0052	539.10	< 0.0001
I	0.0014	1	0.0014	153.90	< 0.0001
pH	0.00053	1	0.00053	54.80	0.0001
t^2	0.0005	1	0.00051	53.70	0.0002
i^2	0.0011	1	0.0011	114.10	< 0.0001
pH^2	40×10^{-5}	1	4×10^{-5}	4.10	0.0804
t x *i*	50×10^{-5}	1	5×10^{-5}	5.10	0.0568
t x *pH*	30×10^{-5}	1	0.0030	31.10	0.0008
i x *pH*	0.00018	1	2×10^{-4}	19.50	0.0031
Residual	6.7×10^{-5}	7	9×10^{-6}		< 0.0001
Lack of Fit	6.7×10^{-5}	3	2×10^{-5}		< 0.0001
Pure Error	0	4	0		< 0.0001
Cor Total	0.0096	16			0.0001

Table 5.3.3b. ANOVA for the %Color removal of batch EO process

Source	Sum of Squares	DF	Mean Square	F-Value	Prob > F
Model	6001.20	9	666.80	72.90	< 0.0001
T	3646.50	1	3646.50	399.00	< 0.0001
I	467.20	1	467.20	51.10	0.0002
pH	80.70	1	80.70	8.83	0.0207
t^2	1029.70	1	1029.70	112.60	< 0.0001
i^2	534.30	1	534.30	58.40	0.0001
pH^2	46.10	1	46.10	5.00	0.0594
t x *i*	64.80	1	64.80	7.00	0.0323
t x *pH*	0.20	1	0.20	0.02	0.8844
i x *pH*	80.80	1	80.80	8.80	0.0207
Residual	63.90	7	9.10		
Lack of Fit	63.90	3	21.30		
Pure Error	0	4	0		
Cor Total	6065.1	16			

Table 5.3.3c. ANOVA for the energy consumed of batch EO process

Source	Sum of Squares	DF	Mean Square	F-Value	Prob > F
Model	3.40	9	0.30	71.20	< 0.0001
T	0.90	1	0.90	173.50	< 0.0001
I	1.80	1	1.80	339.10	< 0.0001
pH	5.2×10^{-8}	1	5.2×10^{-8}	9.9×10^{-6}	0.9976
t^2	7.1×10^{-5}	1	7×10^{-4}	0.01	0.9111
i^2	0.10	1	0.11	21.00	0.0025
pH^2	0.0015	1	0.0015	0.03	0.8682
t x *i*	0.57	1	0.50	107.6	< 0.0001
t x *pH*	1.0×10^{-7}	1	1.0×10^{-7}	1.98×10^{-5}	0.9966
i x *pH*	0	1	0	0	1.0000
Residual	0.04	7	0.0053		
Lack of Fit	0.04	3	0.012		
Pure Error	0	4	0		
Cor Total	3.40	16			

5.3.2. Effect of Batch EO Parameters and Optimization

Fig 5.3.4a & b shows the interaction of *pH* and *i* on the X_1 and X_2, respectively. The results showed decreasing the X_1 with increasing pH value at all *i* values. However, for $i < 1.7$ A increasing *i* ultimately increases X_1, while for $i > 1.7$ A change in X_1 is marginal. This trend was observed at all the *pH* values studied. On another side, for $i < 1.7$ A, X_2 always increases with increase in *pH*. However, at higher current ($i > 1.7$ A), X_2 was found to be 100% and being constant in highly acidic pH. But X_2 was found to decrease sharply in basic pH range. Also, at highly basic pH, increase in *i* value up to 1.7 A increased X_2, beyond 1.7 A X_2 decreased sharply. From Fig 5.3.5a & b, it is evident that the value of X_1 and X_2 increases with increasing *i* value up to ≈1.7 A at every value of *t*, thereafter, X_1 decreased, but X_2 remains nearly constant showing X_1=100 at higher electrolysis time (*t*).

Both direct and mediated EO claim for the removal of COD and color from textile wastewater. During the EO process, •OH radicals and chloro active species (Cl_2, HOCl and ClO^-) are formed. At highly acidic pH, oxidants such as Cl_2, HOCl and •OH radicals are generated (Pletcher *et al*. 1990; Deborde *et al*. 2008). The COD and color removal is due to direct oxidation by adsorbed •OH on the surface of Ti/RuO_2 anode and mediated oxidation by Cl_2 and HOCl. Adsorption rate of •OH radicals on the surface of Ti/RuO_2 decreases on increasing pH, and these generated •OH are transformed into lower oxidation potential oxidants H_2O_2 and HO_2• (equation 5.3.4 and 5.3.5). Furthermore, in highly basic pH chloro active species OCl^- are predominant over Cl_2 and HOCl. Therefore, in highly basic pH, COD removal is due to mediated oxidation by H_2O_2 and HO_2• and OCl^-, which ultimately decreases X_1, and due to bleaching effect, X_2 continues increasing. Increasing *i* value up to 1.7 A increases the generation rate of the oxidants, which in turn increases X_1 and X_2. Increasing current beyond 1.7 A, supports the O_2 evolution reaction from electrolysis of water via equation (5.3.6). This reduces the •OH, H_2O_2 and HO_2• radicals generation, which ultimately reduces the X_1.

$$2\ \bullet OH \rightarrow H_2O_2 \qquad \textbf{(5.3.4)}$$

$$\bullet OH + H_2O_2 \rightarrow HO_2\bullet + H_2O \qquad \textbf{(5.3.5)}$$

$$2H_2O \rightarrow O_2 + 4H^+ + 4e^- \qquad \textbf{(5.3.6)}$$

Fig. 5.3.6a & b shows the effect of pH, electrolysis time (*t*) and current *(i)* on Energy consumption (X_3). It was observed that X_3 value increases with increase in current (*i*) at all *pH* values, while the change in *pH* at any value of current (*i*) showed a marginal change in X_3 (Fig. 5.3.6 a). From Fig. 5.3.6b, it may be seen that increasing current (*i*) up to ≈2.3 A at the lower side of electrolysis time (*t*) marginally affect X_3. But, for all $i > 2.3$ A, X_3 found to be increased. At higher *t*, increasing *i* always increases X_3.

The optimization of operating parameters with the responses (X_1, X_2 and X_3) for the treatment of real textile wastewater using batch EO process, multi-response optimization technique with desirability function was carried out (Kushwaha et al., 2011) (equation 4.3.6). Optimization of the EO process was composed by the set of constraints as shown in Table 5.3.4.

Thus, the desirability for response X_1 is calculated by the equation 4.3.6 with acceptable $X_{1\text{-}min}$ and $X_{1\text{-}max}$ values as 27.73% and 100%, respectively (Table 5.3.4).

$$d_{1=}\begin{cases} 0 & if\ X_1 \le 27.73 \\ \left[\frac{X_1 - 27.73}{100 - 27.73}\right] & if\ 27.73 < X_1 < 100 \\ 1 & if\ X_1 \ge 100 \end{cases} \quad \textbf{(5.3.7)}$$

Similar to equation 5.3.7, **the** desirability for responses X_2 and X_3 were calculated by equation 5.3.8 and 5.3.9, respectively.

$$d_{2=}\begin{cases} 0 & if\ X_1 \le 35.04 \\ \left[\frac{X_2 - 35.04}{100 - 35.04}\right] & if\ 35.04 < X_1 < 100 \\ 1 & if\ X_1 \ge 100 \end{cases} \quad \textbf{(5.3.8)}$$

$$d_{3=}\begin{cases} 0 & if\ X_1 \le 0.01 \\ \left[\frac{X_3 - 0.01}{1.78 - 0.01}\right] & if\ 0.01 < X_1 < 1.78 \\ 1 & if\ X_1 \ge 1.78 \end{cases} \quad \textbf{(5.3.9)}$$

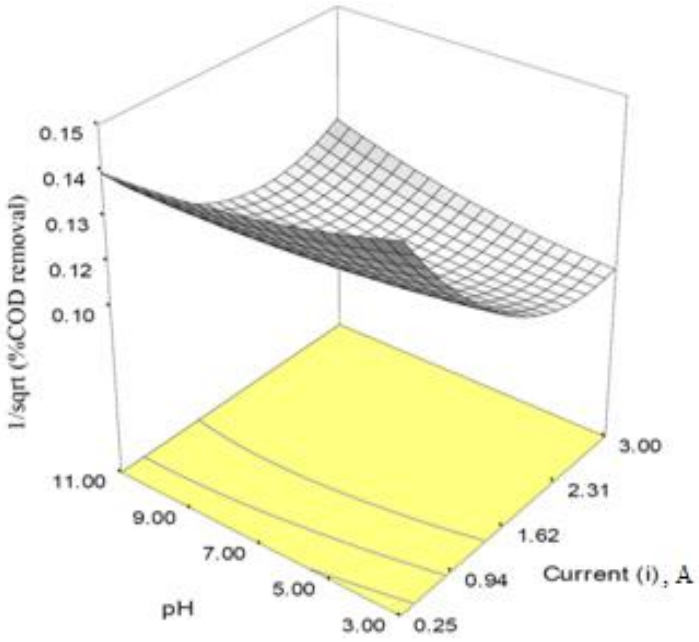

(a)

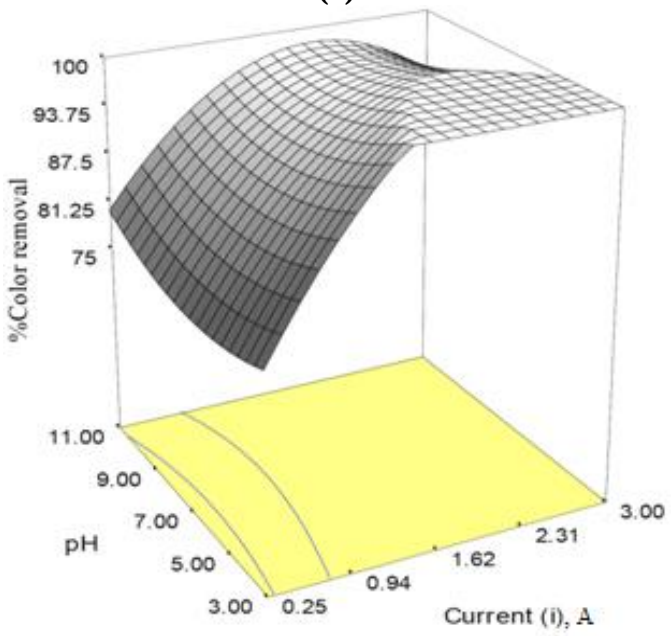

(b)

Fig 5.3.4. 3D response surface graph for the batch EO of textile wastewater (a) %COD removal versus *pH* and *i* (b) %Color removal versus *pH* and *i*

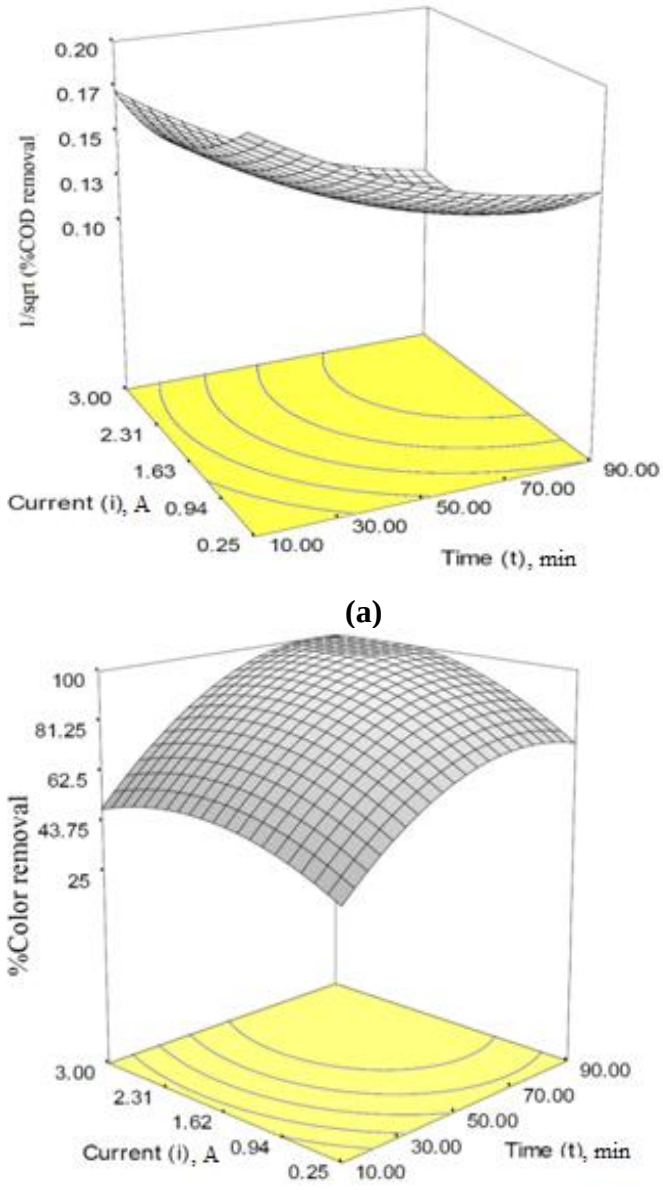

(a)

(b)

Fig 5.3.5. 3D response surface graph for the batch EO of textile wastewater (a) %COD removal versus *i* and *t* (b) %Color removal versus *i* and *t*

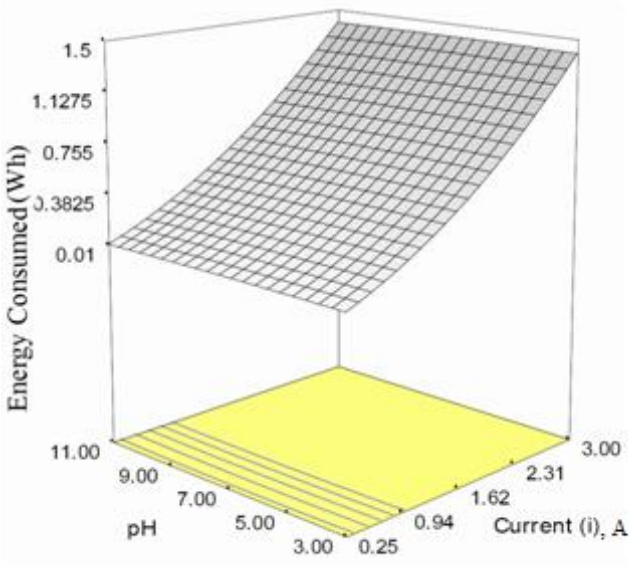

(a)

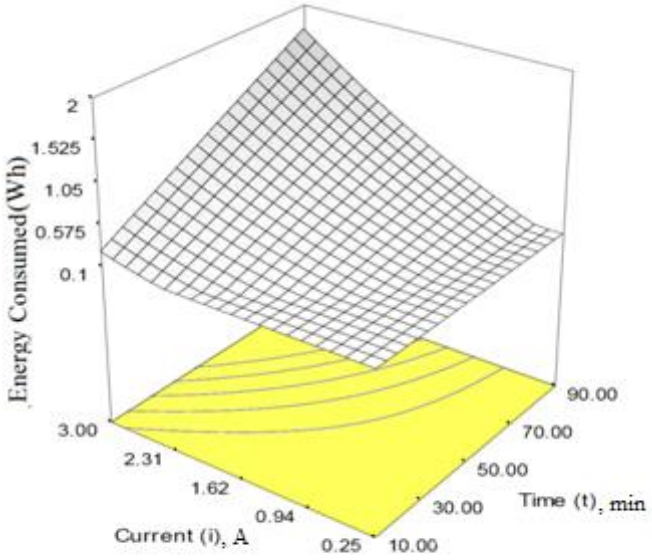

(b)

Fig 5.3.6. 3D response surface graph for the batch EO of textile wastewater (a) Energy Consumed versus *pH* and *i* (b) Energy consumed versus *i* and *t*

The most appropriate optimization condition was found to be *i*=1.66 A, t= 79.55 min and pH=5.49, which showed the highest overall desirability, D= 0.88. At this optimum condition, the X_1, X_2 and X_3 predicted by RSM was 78.80%, 99.10% and 14.00 kWh/kg COD removed, respectively (Table 5.3.5). In order to validate the responses suggested at the optimized condition, experiments were conducted in duplicate at the optimized condition. The average value of various responses X_1, X_2 and X_3 was observed to be 80.0%, 97.25% and 14.58 kWh/kg of COD removed, respectively, which can be observed closer to the predicted values as shown in Table 5.3.5. It also demonstrates that modelling and optimization using RSM under BBD was successfully performed.

Furthermore, during the EO treatment, the pH of the wastewater was found to be changed. In the present study, EO experiment for treatment of textile wastewater conducted at optimum condition (*i*=1.66 A, *t*= 79.55 min and *pH*=5.49) showed an increase in *pH* from 5.49 to a final pH_f =9.4 (Fig 5.3.7). Sharp and fast increase in pH_f can be seen from 5.49 to 9.12 within 45 min of EO treatment, and for all *t*> 45 min, pH_f stabilizes to ≈9.4. The shift of *pH* towards the alkaline side can be attributed to the HO^- production due to water reduction at the cathode. However, the pH_f was stabilized to ≈9.42 due to the buffer formation according to the following reaction (equation 5.3.10), from the produced CO_2 during EO of organics present in wastewater (Vlyssides *et al.* 1999).

$$CO_2 + H_2O \longrightarrow H^+ + HCO_3^- \qquad \textbf{(5.3.10)}$$

As the pH of the wastewater is increased from 5.49-9.4 in 79.55 min of electrolysis, COD and color removal was due to both of the mechanisms, direct and mediated EO. Furthermore, •OH radicals generated during the electrolysis were adsorbed on the surface of Ti/RuO_2 anode. But, due to the adsorption rate being low (because pH is not highly acidic side), •OH radicals were also involved in mediated EO with H_2O_2 and HO_2•. In addition to this, chloro-oxidant species HOCl and ClO^- (dominating among Cl_2, HOCl and ClO^-) oxidize the organics by mediated EO method. Since, chloro-oxidant species, HOCl and ClO^- were found to be partly participating in the dye oxidation. The chlorinated organic compounds have been reported very toxic, may be present in the treated textile wastewater. Therefore, from the safe disposal point of view of treated wastewater, it was necessary to verify/identify the presence of chlorinated organic compounds in treated wastewater.

Table 5.3.4. Constraints applied for optimization of batch EO of textile wastewater

Variables	Goal	Lower Limit	Upper Limit
t (min)	is in range	10	90
i (A)	is in range	0.25	3
pH	is in range	3	11
X_1	Maximize	27.73	100
X_2	Maximize	35.04	100
X_3	Minimize	0.01	1.78

Table 5.3.5. Individual and synchronised (simultaneous maximization of X_1 and X_2 and minimization of X_3) optimization

Individual response optimization				
Response	***pH***	***t* (min)**	***i* (A)**	**Desirability**
X_1=87.5%	7.12	85.63	2.15	1.00
X_2= 100%	4.43	82.66	1.68	1.00
X_3=9 kWh/kg of COD removed	10.50	10.92	1.05	1.00
Synchronised optimization of responses				
X_1=78.80% X_2= 99.10% X_3=14.58 kWh/kg of COD removed	5.49	79.55	1.66	0.89

Table 5.3.6. Comparison between predicted and experimental values of responses

Responses	Predicted value	Experimental value
% COD removal (X_1)	78.80%	80.00%
% Color removal (X_2)	99.10%,	97.25%,
Energy consumed (X_3)	14.00 kWh/kg of COD removed	14.58 kWh/kg of COD removed

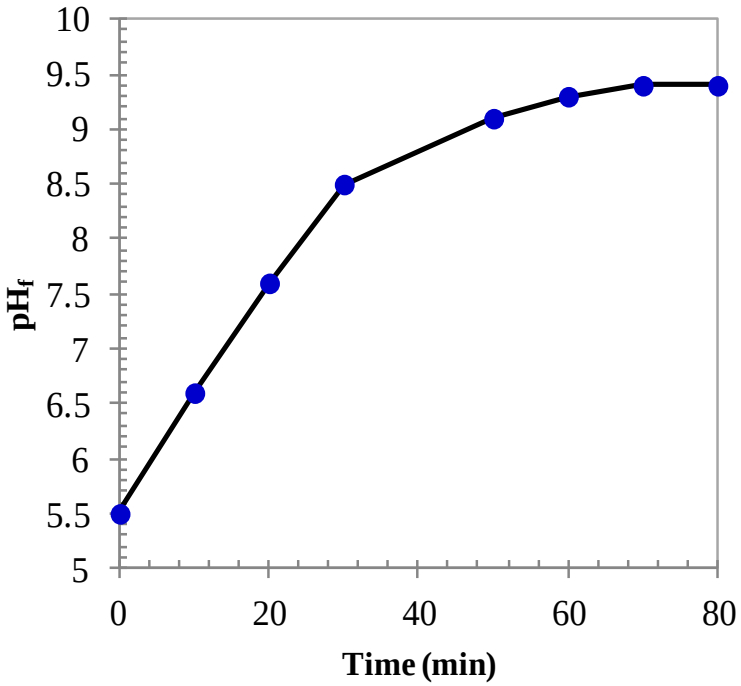

Fig 5.3.7. Graph of *t* versus pH_f for the batch EO treatment of Textile wastewater at optimum condition

5.3.3 Transformation Products and Treated Effluent Quality

In view of treated effluent quality for disposal, the samples of treated textile effluent by EO at the optimum condition were analyzed to identify the final electrolysis transformation products using spectrophotometer and GC-MS. Moreover, the untreated textile wastewater sample was also analyzed using the same method to compare the results.

Spectrophotometric analysis: This analysis was performed to gather the initial supporting information for treated wastewater disposability study. Treated and untreated wastewater samples were analysed in the wavelength range of 200-400nm and the results are shown in Fig 5.3.8. In case of the untreated textile effluent sample, two sharp peaks at λ value ~244 and ~250 nm having narrower band width with high absorption intensity. However, small intensity bands with λ, ~200-240 nm and λ, ~252-275 nm were seen. Further, the absorption spectra of EO treated textile effluent at the optimum time shows only a small intensity band with λ, ~200-240 nm. It has been reported that absorption band with λ above 200 nm, generally indicates the aromatic presence (Workman, 2001). (λ, 200-250 nm: primary band ketones, alkanes, acids, phthalates, aldehydes, esters, etc.); and λ, ~250-275 nm: secondary band ketones, alcohols, secondary band aldehydes etc.).

It was also seen that peaks at λ value ~244 and ~250 nm; and absorption band with λ, ~252-275 nm disappeared after EO treatment, and a small intensity band λ, ~200-230 nm only exist. It indicates that the organic compounds were degraded/oxidized during the electrolysis by the attack of various oxidants such as •OH, H_2O_2, HO_2• and HOCl produced during the EO process, and. The UV absorption band for the most of the identified compounds by GC-MS analysis of untreated wastewater was in the range of 200 to 275 nm, which was also supported by the spectrophotometric analysis of untreated textile wastewater.

GC-MS analysis: To explore the non-degraded and degraded compounds of textile effluent GC-MS analysis was conducted, and the identified compounds in untreated and treated textile wastewater are listed in Table 5.3.7 and 5.3.8. It was performed for untreated and treated textile effluent by EO process. It showed the presence of 3, 5-bis(ethoxycarbonyl) benzoic acid (coloring component of basic dye) and Tetracosamethyl-cyclododecasiloxane (a component of fluorescent dye) in untreated wastewater (Table 5.3.7). These compounds show UV light absorption in absorption band λ, 200-250 nm. The presence of these compounds was

observed in UV spectra of untreated textile effluent in absorption band λ, 200-250 nm (Fig. 5.3.8). However, these dye components were not detected in the treated textile wastewater GC-MS analysis (Table 5.3.8), due to degradation/oxidation during the EO treatment process.

Except these coloring compounds, other compounds such as Trimethyl-2-pentadecenyl, 3,5-bis(ethoxycarbonyl) benzoic acid, 5-ethoxycarbonyl-2-phenyl-1,3-dioxane-5-carboxylic acid, 2,4,4-trimethyl-3-(2-trimethylsilylethynyl)cyclohex-2en-1-ol, Tetracosamethylcyclododeca siloxane, Tetradecamethylhexasiloxane and Tetrakis(trimethylsilyl) orthosilicate were eliminated during the EO process (Table 5.3.7 & 5.3.8). The various organics such as dyes, coupling agents, polishing and coating agents, fabric softeners, anti-wrinkle agents, cleaning fluid etc. as identified by the GC-MS analysis (Table 5.3.7), contribute to the TDS of the textile wastewater.

During the EO process, various oxidants such as •OH, H_2O_2, HO_2• and HOCl and ClO^- are generated and oxidize/degrade the organics present in the textile wastewater. Most of the organics responsible for the TDS such as dyes, coupling agents, fabric softeners, anti-wrinkle agents etc. are oxidized/degraded during the EO process. Therefore, these compounds are absent in GC-MS analysis of treated wastewater (Table 5.3.8). Furthermore, comparative observation of Table 5.3.7 & 5.3.8 also elucidates that certain transformation/degradation compounds such as Butyl phthalate, 3,4-dihydro-4-(1,3-dioxolan-2-yl)-5,7-dimethoxy-1(2H)-benzopyran-2-one, dichloro acetaldehyde and 2-(7-chlorohept-2-ynyloxy) tetrahydro-2H-pyran were produced during the EO treatment process. This is also supported by the existence of small UV absorption band with λ, 200-230 nm (Fig. 5.3.8).

Textile wastewater bears high NaCl salt, therefore, in the course of the EO treatment, various chloro-compounds [dichloroacetaldehyde and 2-(7-chlorohept-2-ynyloxy) tetrahydro-2H-pyran] (Table 5.3.8) are produced due to mediated oxidation by generated chloro species. These compounds have been described as toxic/carcinogenic.

Further, toxicity bioassay test was performed to evaluate the toxicity of the treated and untreated textile wastewater, and the standard procedure IS: 6582 with test organism Aploclzeilus panchax was followed for the same. Aploclzeilus panchax is indicator micro-organism to environmental pollutants. This test showed 100% death of the indicator micro-organism within one minute for the untreated textile wastewater, while it was 55 min for the

treated wastewater. Therefore, untreated textile wastewater is highly toxic in nature, and the toxicity is considerably decreased after the EO treatment. However, the presence of chloro-compounds in the treated wastewater lethal to the aquatic life, therefore, before its disposal, some other polishing treatment must be applied to separate chloro-compounds.

5.3.4. Degradation Mechanism

The oxidation/degradation mechanism was predicted on the basis of GC-MS analysis and spectrophotometric analysis. The presence of high molecular weight compounds containing silicon, carbon, hydrogen, oxygen and certain metal ions were observed (Table 5.3.7 and 5.3.8). The degradation process and oxidation of organic matters in the EO process depend upon the anode material and electrolyte. From the spectrophotometric analysis and GC-MS analysis, two types of degradation/oxidation method were observed for the degradation of textile wastewater: direct anodic degradation (•OH mediated oxidation), and indirect anodic degradation (chloro-oxidants mediated oxidation). The probable mechanism of the EO treatment method of textile wastewater is shown in Fig 5.3.9. Direct anodic degradation or •OH mediated oxidation refers to the direct contact of degrading organic matter and transfer of electrons from anode to the degrading matter. On the other hand, indirect anodic degradation does not require direct contact of pollutants with anode material. The reactive oxygen species can be physisorbed and chemisorbed to degrade the pollutants.

Direct Oxidation: Real Textile wastewater was rich with chloride content, and the optimal pH for the process was found ≈ 5.5, therefore, Cl_2, ClO^- and HOCl species were actively participate in the degradation process. It was observed that some of the compounds of untreated wastewater like Trimethyl-2-pentadecenyl, 3,5-bis(ethoxycarbonyl) benzoic Acid, Dodecamethylcyclohexasiloxane, 3-Octanol 2-[(R)-(4-methylphenyl)sulfinyl]-1-(trimethylsilyl), 5-ethoxycarbonyl-2-phenyl-1,3-dioxane-5-carboxylic acid, 2,4,4 trimethyl-3-(2-trimethylsilylethynyl)cyclohex-2en-1-ol, Dibutyl phthalate, Tetracosamethyl-cyclododecasiloxane, Icosamethylcyclodecasiloxane, Tetradecamethylhexasiloxane, Tetrakis(trimethylsilyl) orthosilicate were oxidized with production of some transformation compounds such as 3,4-dihydro-4-(1,3-dioxolan-2-yl)-5,7-dimethoxy-1(2H)-benzopyran-2-one, Icosamethylcyclo decasiloxane, Butyl phthalate by partial oxidation via equation 5.3.12 and 5.3.13. There were certain compounds of the textile effluent, which were not undergoing any

kind oxidation i.e Dodecamethylcyclohexasiloxane, 3-Octanol 2-[(R)-(4-methylphenyl)sulfinyl]-1-(trimethylsilyl), Dibutyl phthalate, Icosamethyl cyclodecasiloxane.

Indirect Oxidation: Further, the transformed products produced by the direct oxidation mechanism, were attacked by chlorine species, and transformed to toxic chlorinated-compounds such as Neopentylchloride, Chlorinated cyclopentane and 1, 5-Dichlorinated pentane via indirect oxidation (equation 5.3.13 and 5.3.14). It was confirmed from the spectrophotometric analysis with λ in the absorption band of 200-275 nm, which represent the presence of phthalates, chlorinated -compounds in treated textile wastewater. Therefore, it can be claimed that complete mineralization didn't occur during the EO process. Further, transformation products are produced during the EO due to the deficiency of $^{\bullet}OH$ and mediated oxidation by various chlorine species.

$$RuO_2.(^{\bullet}OH)_{ads} + Cl_2/Cl^- \rightarrow RuO2.(^{\bullet}OCl) + H^+ + 2e^- \quad \textbf{(5.3.11)}$$

$$RuO_2.(^{\bullet}OH)_{ads} + Cl_2/Cl^- \rightarrow RuO2.(Cl^{\bullet}) + OH^- + 2e^- \quad \textbf{(5.3.12)}$$

$$RuO_2.(^{\bullet}OCl)_{ads} + R \rightarrow RO + \text{chlorinated -compounds} + RuO_2 \quad \textbf{(5.3.13)}$$

$$R + HOCl \rightarrow nCO_2 + mH_2O + \text{chlorinated –compounds} \quad \textbf{(5.3.14)}$$

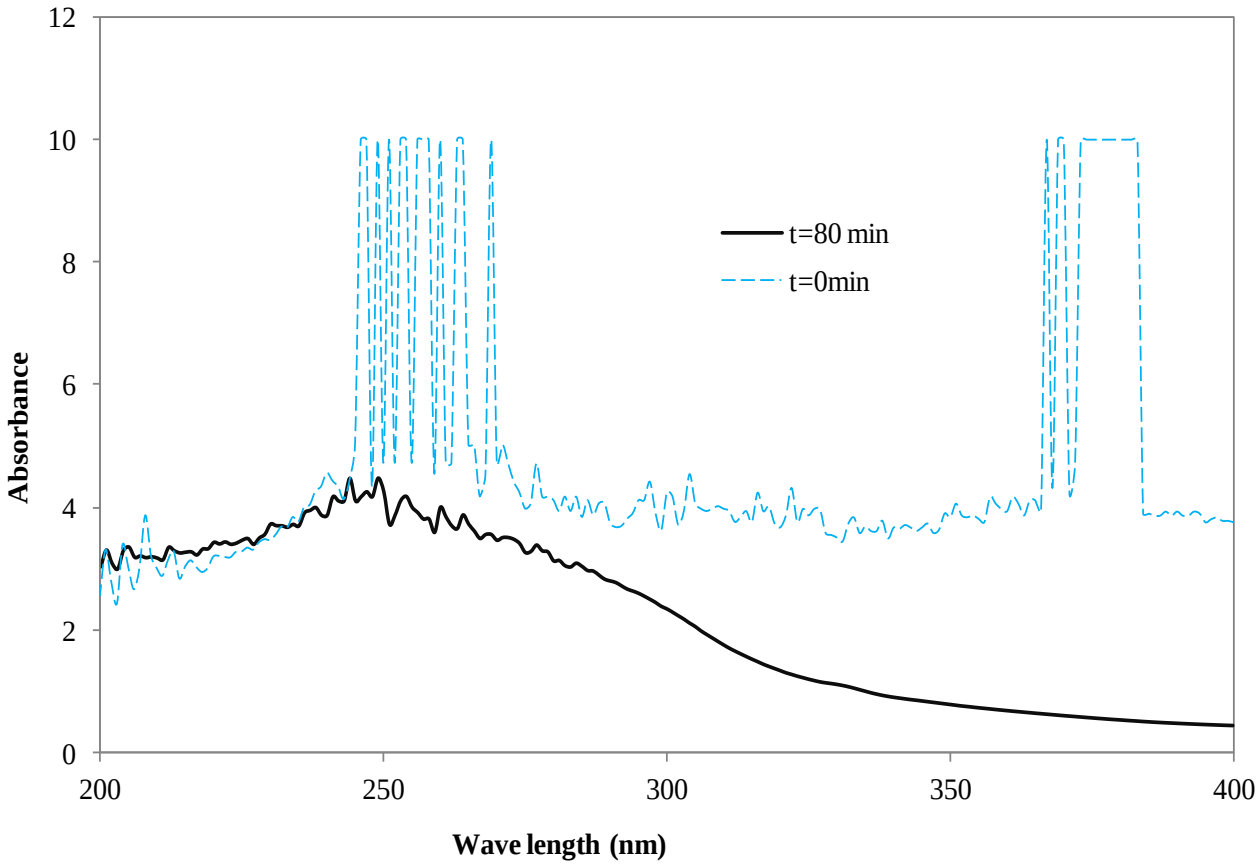

Fig 5.3.8. UV Visible spectra of untreated (*t*=0 min) and treated (*t*= 80 min) textile wastewater by batch EO at optimum condition

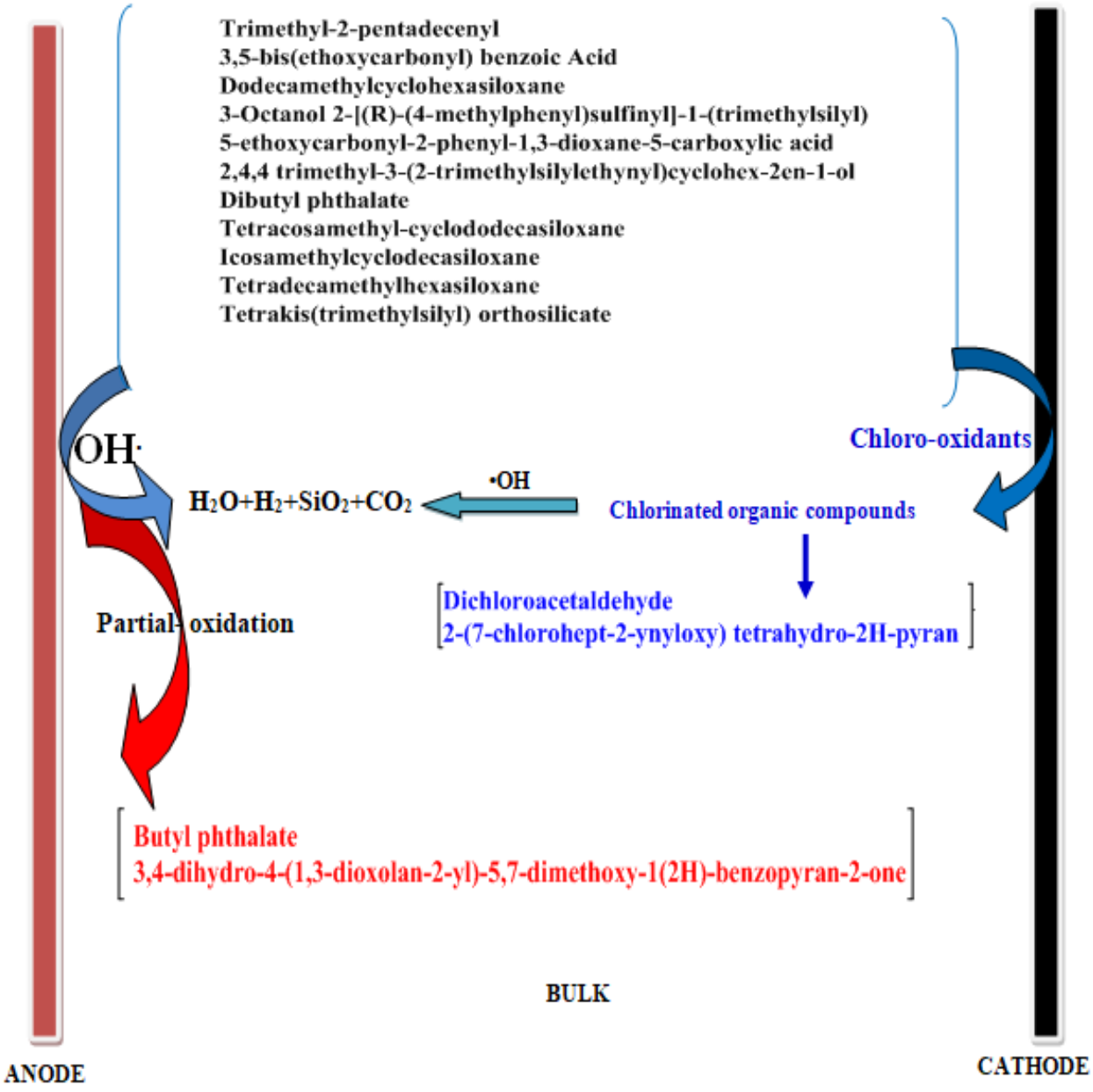

Fig 5.3.9. Persuasive mechanism for the degradation of textile wastewater by batch EO process

Table 5.3.7. GC-MS analysis of untreated Textile wastewater by batch EO process

Compounds	Retention Time (min)	Molecular Mass	Matching %	Comment
Trimethyl-2-pentadecenyl	10.35	282	91%	It is used in printing wax or ink in the textile industries.
3,5-bis(ethoxycarbonyl) benzoic Acid	10.35	266	90%	It is colorant compound comprising a basic dye component.
Dodecamethylcyclohexasiloxane	12.86	444	80.9%	Cleaning textiles and used as a cleaning fluid for removing spots
3-Octanol 2-[(R)-(4-methylphenyl)sulfinyl]-1-(trimethylsilyl)	12.86	340	80.5%	It is used as catalyst in the curing of exoxide resins and silane resins including highly fluorinated alkyl sulfonyl methane
5-ethoxycarbonyl-2-phenyl-1,3-dioxane-5-carboxylic acid	15.11	280	80.2%	It is used as pesticide or preservative for textile products
2,4,4 trimethyl-3-(2-trimethylsilylethynyl)cyclohex-2en-1-ol	18.8	236	95.6%	It is used as coupling agents in printing and coating
Dibutyl phthalate	20.01	278	90.5%	-
Tetracosamethyl-cyclododecasiloxane	22.27, 24.89 & 25.12	888	84.7% / 86.8% / 86.9%	It is a component of fluorescent dye
Icosamethylcyclodecasiloxane	24.89	740	82.1%	It is used as polishing and coating agents in textiles
Tetradecamethylhexasiloxane	24.89 & 25.12	458	80.7% / 80.7%	It is widely used in the textile industry as fiber lubricant and as fabric softeners and anti-wrinkle agents
Tetrakis(trimethylsilyl) orthosilicate	24.89	384	79.4%	It is used to remove oily and greasy stains from the textile stuff.

Table 5.3.8. GC-MS analysis of treated Textile wastewater by batch EO process

Compounds	Retention Time (min)	Molecular Mass	Matching %	Comment
Dodecamethyl Cyclohexasiloxane	12.87	444	82.9%	Already present
3-Octanol 2-[(R)-(4-methylphenyl)sulfinyl]-1-(trimethylsilyl)	12.87	340	79.7%	Already present
Dibutyl phthalate	20.02/20.51/ 21.16/ 21/ 24.77	278	81.2%/ 89.2% /92.2%	Already present
Icosamethyl Cyclodecasiloxane	25.13	740	81.2%	Already present
Dichloroacetaldehyde	3.61	112	78.9%	Transformation products (Toxic and carcinogenic)
2-(7-chlorohept-2-ynyloxy) tetrahydro-2H-pyran	65.6	230	65.9%	Transformation products (Toxic and carcinogenic)
Butyl phthalate	20.2/21.6/ 21	278	95.2% / 81.3%/92 %	Transformation products
3,4-dihydro-4-(1,3-dioxolan-2-yl)-5,7-dimethoxy-1(2H)-benzopyran-2-one	24.06/15.12	280	84%	Transformation products (non toxic, biodegradable)

5.3.5 Kinetic Study

The kinetics of the COD and color removal was studied for batch EO process at optimum parameters. The experimental data were tested for fitting to first and second order kinetic model. Kinetic data did not well fit to second order model. The first kinetic model fitted well to EO degradation process kinetic data according to the rate equation given below.

$$\frac{-dC}{dt} = k_1 C \quad \textbf{(5.3.15)}$$

On integrating:

$$-\left[ln\frac{C_s}{C_0}\right] = k_1 t \quad \textbf{(5.3.16)}$$

Where, C_o is COD/color intensity at t=0 and C_s are COD/color intensity at any degradation time t (min), k_1 rate constant. Fig 5.3.10 shows the fitting of experimental data to first order reaction kinetics (equation 5.3.16) for EO treatment process. Rate constant and R^2 values for X_1 and X_2 were observed to be 0.027 min^{-1} and 0.015 min^{-1}; and 0.998 and 0.986, respectively. The kinetic study shows that the rate of color removal was faster than COD removal. It was absorbed from the degradation mechanism that all the coloring components present in the real textile wastewater were eliminated after batch EO treatment process. But the other components contributing to COD were still observed remained in the treated wastewater. GC-MS analysis shows that there were certain compounds present in the treated textile effluent that was not oxidized during EO treatment process. The presence of these compounds affects the COD removal kinetic after 60 min of electrolysis time. Therefore, after 60 min of electrolysis time COD removal becomes constant. In case of coloring component, because color degradation was faster therefore, with in 40 min of electrolysis time most of the coloring components were eliminated. Hence, it was concluded that chloro-mediated oxidation/bleaching effect was dominant in the case of EO treatment and it was responsible for color removal during EO treatment process.

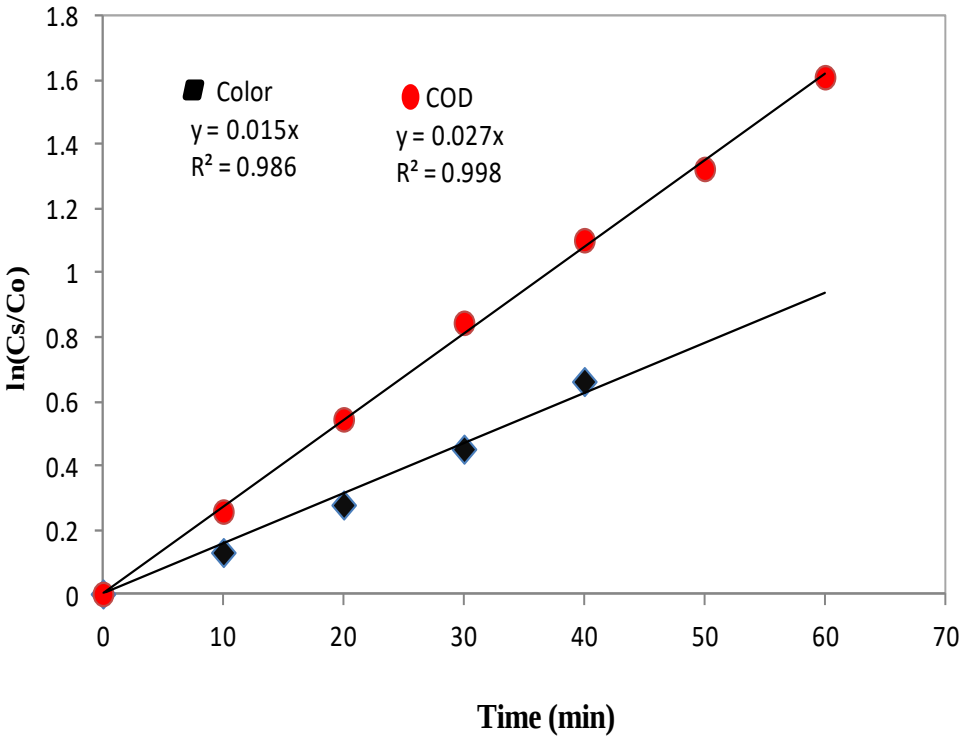

Fig 5.3.10. Fitting of first order kinetics for the COD removal and Color removal at optimum conditions of EO

5.3.6 Operating Cost Analysis

The total operational cost includes consumed electrical power cost, electrode cost, cost of wages, pumping cost, cost of stirring etc. However, the EO treatment process being energy intensive, the total operating cost is mainly due to consumed electrical power cost and electrode cost. Therefore, in the present study, the electrical power consumed and electrode cost was calculated as operating cost for batch EO treatment of textile wastewater.

The cost of specific electrical energy consumed and electrode required to remove one kg of COD from textile wastewater was calculated from the responses of EO experiment conducted (X_1 =80%, X_2=97.25% and X_3=14.58 kWh/kg of COD removed) at optimized parameters (*i*=1.66 A, t= 80 min and pH=5.49), and given below:

Specific electrical energy consumed = ~14.58 kWh/kg of COD removed

Electricity price in India, Punjab = ~ ₹ 5.00/kWh

Therefore, the cost of electrical energy consumed (C_E) = ₹ 72.9/kg of COD removed

In this study, two Ti/RuO_2 electrodes (dimension: 100 mm x 85 mm x 1.5 mm) of cost ₹ 2500.00 each were used. The manufacturer/supplier (Titanium Tantalum Products Limited, Chennai, India) specified the life of the electrodes 2.5 years at optimized condition (*i*=1.66 A, pH=5.49).

Since, at optimized condition 80% of COD is removed, therefore, the minimum cost of Ti/RuO_2 electrodes (C_{EL}) = ₹ 465.46/ kg of COD removed

Total operating cost (C_E + C_{EL}) = ₹ 538.36/ kg of COD removed

In the present study, the COD of collected wastewater (from a Mink Blanket manufacturing industry situated in Ludhiana, Punjab, India) was 544 mg/l. Therefore, to treat the textile wastewater by reducing the COD from 0.544 kg/m^3 to 0.108 kg/m^3 (as optimum %COD removal=80%) total operating cost (C_E + C_{EL}) in US$ is 8.97 $/ kg of COD removed.

5.4 STUDY OF BATCH ELECTRO-FENTON (EF) TREATMENT PROCESS

5.4.1 Model Fitting and Statistical Analysis

The experiments for batch EF were designed using three-level BBD under RSM. The three independent variables were taken as input parameters for batch EF process i.e current (0.25 to 1 A), time (10 to 90 min) and catalytic dose (0.20 to1 mM) and the % COD removal (X_1), % color removal (X_2) and energy consumed (X_3) were selected as responses. Total 17 experiments as suggested by RSM were conducted, and the calculated responses values of X_1, X_2 and X_3 are shown in Table 5.4.1. Experimental data were then analyzed by multiple regression analysis of RSM. The quadratic model was suggested by exploiting sequential F-test and other adequacy measures. For the responses X_1, X_2 and X_3, the adequate precision indicated that the model is efficient and significant. Adequate precision expresses the signal to noise ratio, and adequate precision ratio above 4 shows that the model was efficient in navigating the design space. The model summary statistics for responses X_1, X_2 and X_3 showed a high value of the coefficient of determination. The values of R^2, Adjusted R^2 and predicted R^2 are shown in Table 5.4.2. It supports a satisfactory adjustment between the observed and predicted values for the selected responses as shown in Fig 5.4.1, 5.4.2 and 5.4.3 for X_1, X_2 and X_3, respectively. Quadratic model for batch EF was also analyzed using ANOVA, which showed model F-values of the responses X_1, X_2, and X_3 to be 77.47, 72.10 and 1.1 x 10^4, respectively (Table 5.4.3a, b, c). The "Prob>F" smaller than 0.05 indicates, that the quadratic model and its terms are significant with a 95% confidence level. The significant terms of batch EF for X_1: i, t, i^2, t^2, C_{Fe}^2; X_2: t, i^2, t^2, C_{Fe}; X_3= i, t, C_{Fe}, i^2, t^2, C_{Fe}^2, and (i x C_{Fe}) were observed from the ANOVA (Table 5.4.3a, b, c). The quadratic model equation obtained in terms of significant process parameters for batch EF process is given below.

$$X_1 = 87.70 + 3.69\, i + 26.97 t - 17.29\, i^2 - 9.39\, t^2 - 8.87 C_{Fe}^2 \quad \textbf{(5.4.1)}$$

$$X_2 = 100 + 14.68\, t + 1.97 C_{Fe} - 5.36 i^2 - 12.19\, t^2 \quad \textbf{(5.4.2)}$$

$$X_3 = 2.59 + 1.66\, i + 0.046\, t + 0.020 C_{Fe} - 0.031\, i^2 - 0.035\, t^2 - 0.063 C_{Fe}^2 - 0.014\, (i \times C_{Fe}) \quad \textbf{(5.4.3)}$$

Table 5.4.1. Experimental design for the batch EF process

Standard Order	t (min)	*i* (A)	C_{Fe} (mM)	X_1		X_2		X_3	
				$X_{1\ exp}$	$X_{1\ pre}$	$X_{2\ exp}$	$X_{2\ pre}$	$X_{3\ exp}$	$X_{3\ pre}$
14	50	0.63	0.60	87.70	87.70	100.0	100.0	2.59	2.59
15	50	0.63	0.60	87.70	87.70	100.0	100.0	2.59	2.59
10	90	0.63	0.20	94.70	98.10	100.0	100.0	2.53	2.53
12	90	0.63	1.00	94.00	94.71	100.0	100.0	2.56	2.55
17	50	0.63	0.60	87.70	87.70	100.0	100.0	2.59	2.59
8	50	1.00	1.00	64.30	67.70	96.00	96.27	4.21	4.21
6	50	1.00	0.20	62.10	62.77	87.30	88.90	4.12	4.10
4	90	1.00	0.60	97.20	93.11	98.50	96.08	4.20	4.22
9	10	0.63	0.20	39.30	38.56	70.90	68.82	2.40	2.42
1	10	0.25	0.60	27.70	31.79	66.40	68.81	0.82	0.81
3	90	0.25	0.60	82.90	82.86	98.80	98.19	0.93	0.93
13	50	0.63	0.60	87.70	87.70	100.0	100.0	2.59	2.59
2	10	1.00	0.60	36.30	36.32	66.20	66.72	4.15	4.15
7	50	0.25	1.00	58.30	57.60	96.50	94.93	0.82	0.83
16	50	0.63	0.60	87.70	87.70	100.0	100.0	2.59	2.59
11	10	0.63	1.00	49.80	46.37	76.30	75.42	2.48	2.48
5	50	0.25	0.60	61.48	58.10	94.73	94.44	0.86	0.86

Table 5.4.2. Various R-squared values suggested by BBD for responses %COD removal (X_1), % Color removal (X_2) and energy consumed (X_3)

Responses	R-Squared	Adj R-Squared	Pred R-Squared
X_1	0.9901	0.9773	0.8410
X_2	0.9893	0.9756	0.8293
X_3	0.9999	0.9998	0.9989

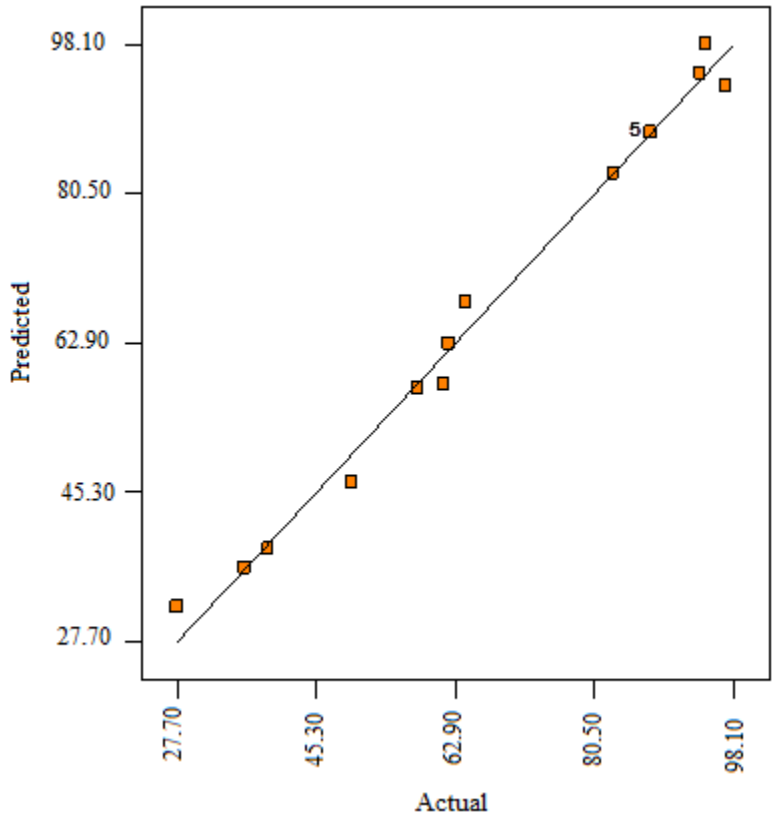

Fig 5.4.1. Predicted versus actual %COD removal for batch EF process

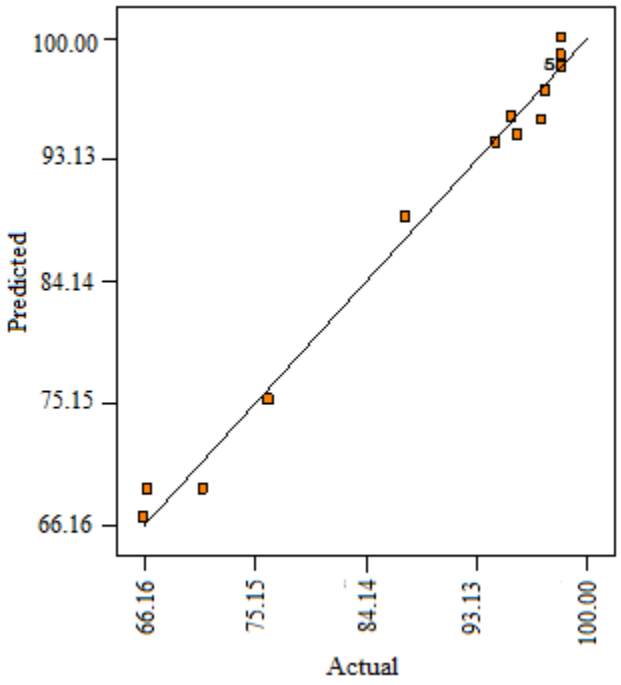

Fig 5.4.2. Predicted versus actual % color removal for batch EF process

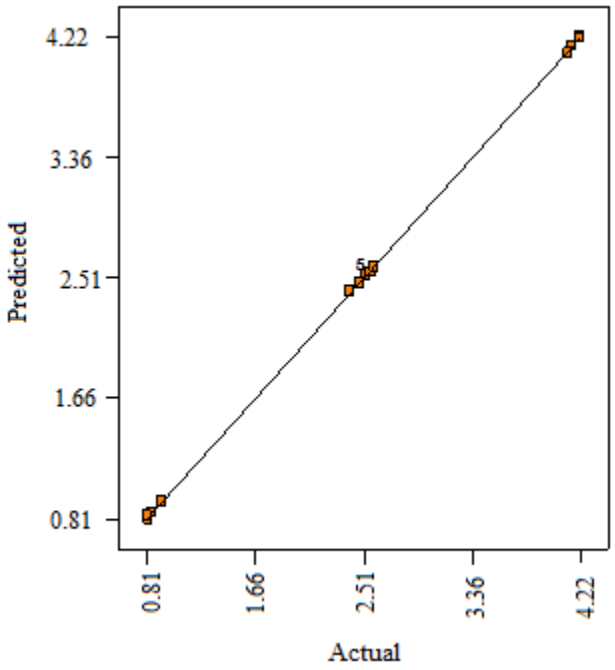

Fig 5.4.3. Predicted versus actual energy consumed for batch EF process

Table 5.4.3a. ANOVA for the %COD removal of batch EF process

Source	Sum of Squares	DF	Mean Square	F-Value	Prob > F
Model	8144.20	9	904.90	77.47	< 0.0001
i	109.10	1	109.10	9.34	0.0184
T	5817.90	1	5817.90	498.09	< 0.0001
C_{Fe}	9.70	1	9.73	0.83	0.3904
i^2	1258.10	1	1258.10	107.70	< 0.0001
t^2	371.50	1	371.50	31.80	0.0008
$(C_{Fe})^2$	331.30	1	331.30	28.36	0.0011
t x i	8.10	1	8.10	0.70	0.4303
t x C_{Fe}	7.30	1	7.30	0.63	0.4530
t x C_{Fe}	31.30	1	31.30	2.68	0.1453
Residual	81.70	7	11.60		
Lack of Fit	81.70	3	27.25		
Pure Error	0	4	0		
Cor Total	8225.90	16			

Table 5.4.3b. ANOVA for the % Color removal of batch EF process

Source	Sum of Squares	DF	Mean Square	F-Value	Prob > F
Model	2578.15	9	286.40	72.10	< 0.0001
I	8.79	1	8.70	2.20	< 0.0001
T	1724.90	1	1724.90	434.40	0.0002
C_{Fe}	30.96	1	30.96	7.70	0.0207
i^2	121.02	1	121.02	30.40	< 0.0001
t^2	625.79	1	625.70	157.60	0.0001
$(C_{Fe})^2$	4.24	1	4.20	1.06	0.0594
t x i	2.2×10^{-4}	1	2×10^{-4}	5.67×10^{-5}	0.0323
t x C_{Fe}	11.83	1	11.80	2.98	0.8844
t x C_{Fe}	7.12	1	7.10	1.79	0.0207
Residual	27.78	7	3.90		
Lack of Fit	27.70	3	9.20		
Pure Error	0	4	0		
Cor Total	2605.9	16			

Table 5.4.3c. ANOVA for the energy consumed of batch EF process

Source	Sum of Squares	DF	Mean Square	F-Value	Prob > F
Model	21.90	9	2.40	1.1×10^{4}	< 0.0001
i	21.90	1	21.90	10.5×10^{4}	< 0.0001
t	0.02	1	0.01	82.40	< 0.0001
C_{Fe}	0.003	1	3×10^{-3}	15.10	0.0060
i^2	0.004	1	4×10^{-3}	19.80	0.0030
t^2	0.005	1	5×10^{-3}	24.10	0.0017
$(C_{Fe})^2$	0.016	1	0.01	79.10	< 0.0001
t x i	0.0008	1	8×10^{-4}	4.02	0.0847
t x C_{Fe}	0.004	1	4×10^{-3}	20.2	0.0028
t x C_{Fe}	0.0003	1	3×10^{-4}	1.60	0.2412
Residual	0.001	7	2×10^{-4}		
Lack of Fit	0.001	3	4×10^{-4}		
Pure Error	0	4	0		
Cor Total	21.90	16			

5.4.2 Effect of Batch EF Parameters and Optimization

To explore the effects of EF parameters, 3-D response surface graph obtained from RSM were observed. Fig. 5.4.4a and b show the interaction of C_{Fe} and i on the X_1 and X_2 with time, t respectively. The 3-D plot shows that X_1 decreases at higher and lower C_{Fe} at all the i values. However, X_1 increases with the increase in i from 0.25 to ≈0.81 A, after it starts decreases. X_1 also increases with the increase C_{Fe} 0.20 to ≈0.53 Mm. This trend was also observed for X_1. On the other side, with increasing C_{Fe} along the increase in i value from 0.30 to ≈0.81 A increase X_2. 100% X_2 was observed, when C_{Fe} was up to 0.53 mM at i = 0.32 A.

Fig. 5.4.5a and b showed that X_1 and X_2, increases with the increase in t for every i value. However, the increase in t at the i between 0.50 to ≈0.81 A, showed 100% X_1 and X_2. X_3 value increases with the increase in C_{Fe}, t and i. It is asserted that Electro-Oxidation (EO) and Fenton •OH radicals mediated organics oxidation are responsible for the removal of COD and color from the real textile wastewater. It was well known that Fenton's reaction can be applied in acidic pH (Sun and Pignatello 1993) to efficiently produce •OH radicals, but EO at acidic pH, generate oxidants such as Cl_2, HOCl and •OH. It has been reported that Chloro-oxidants have lower oxidation potential and, are toxic/carcinogenic in nature (Deborde et al. 2008). However, oxidation of pollutant particles occur due to chloro-oxidants and •OH radicals. Due to lower oxidation potential chloro-oxidants transform pollutants into chloro-compounds. Furthermore, these chloro- compounds were mineralizing by Fenton •OH radicals mediated oxidation. Therefore, X_1 and X_2 were increased with an increase in C_{Fe} at all i values. But, it was also seen that after, C_{Fe} = 0.53 mM there was a sharp decrease in X_1 and X_2 along with electrolysis time (t) at particular i value. Because, the high generation of •OH radicals at the higher concentration of Fenton reagent, a competitive reaction occurs between the Fe^{2+} and hydroxyl radicals. It could reduce the concentration of hydroxyl radicals to the pollutant particles (Bouafia-Chergui et al. 2010). Therefore, above C_{Fe} = 0.53 mM, there was a sharp decrease in X_1 and X_2. Fig. 5.4.6a and b showed the effect of catalytic dose, electrolysis time (t) and current *(i)* on the energy consume(X_3). With an increase in time, it was found that X_3 value always increases with i up to ≈ 0.32 A. For i > 0.32 A, M_3 value was found to gradually decreased (Fig. 5.4.6a). X_3 value also marginally decreased with a decrease in catalytic dose. Energy consumed (X_3) was increasing with increase in time.

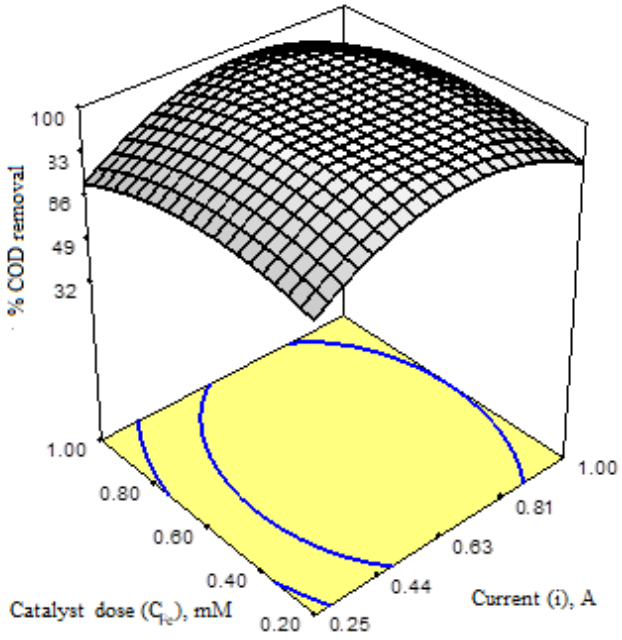

(a)

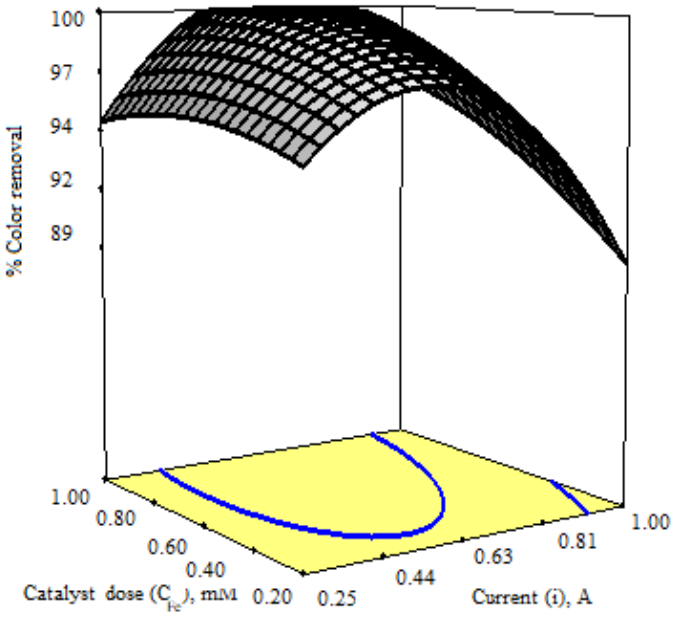

(b)

Fig 5.4.4. 3D response surface graph for the batch EF of textile wastewater (a) %COD removal versus C_{Fe} and *i* (b) %Color removal versus C_{Fe} and *i*

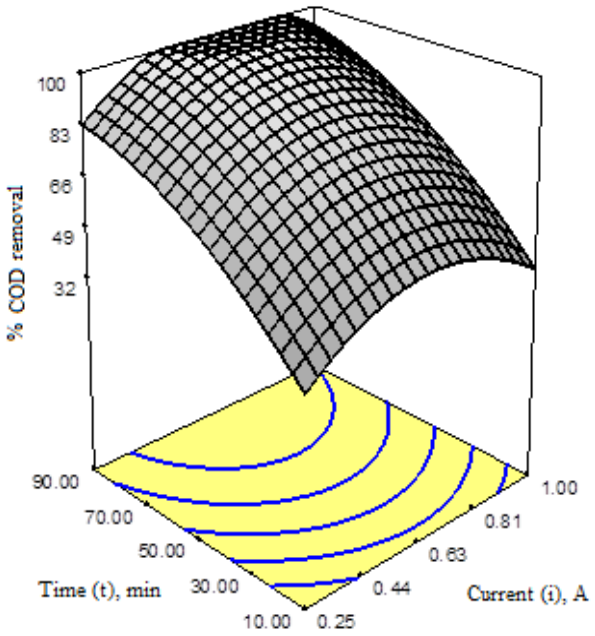

(a)

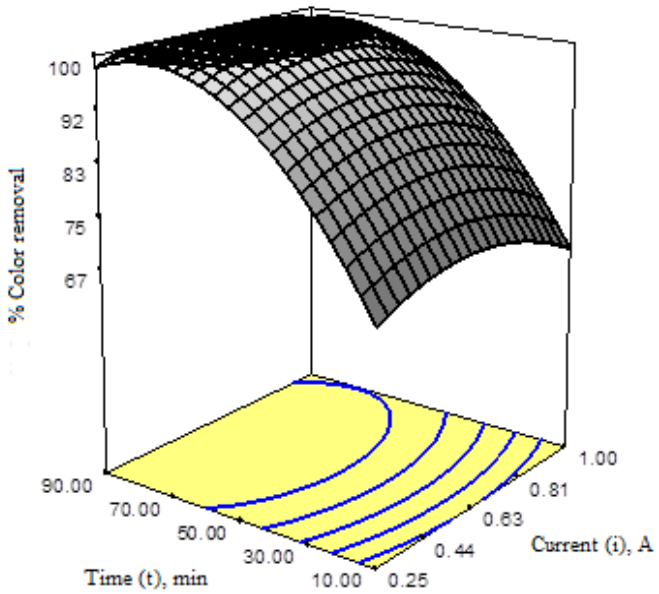

(b)

Fig 5.4.5. 3D response surface graph for the batch EF of textile wastewater (a) %COD removal versus *i* and *t* (b) %Color removal versus *i* and *t*

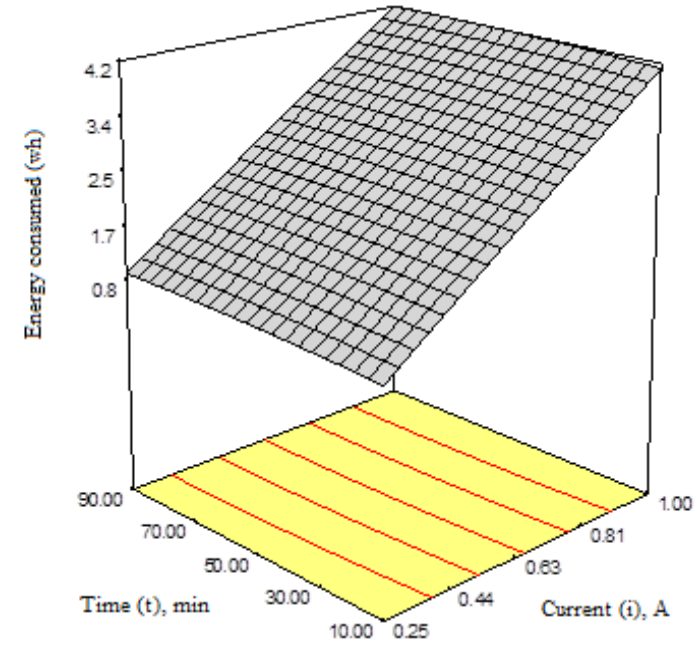

(a)

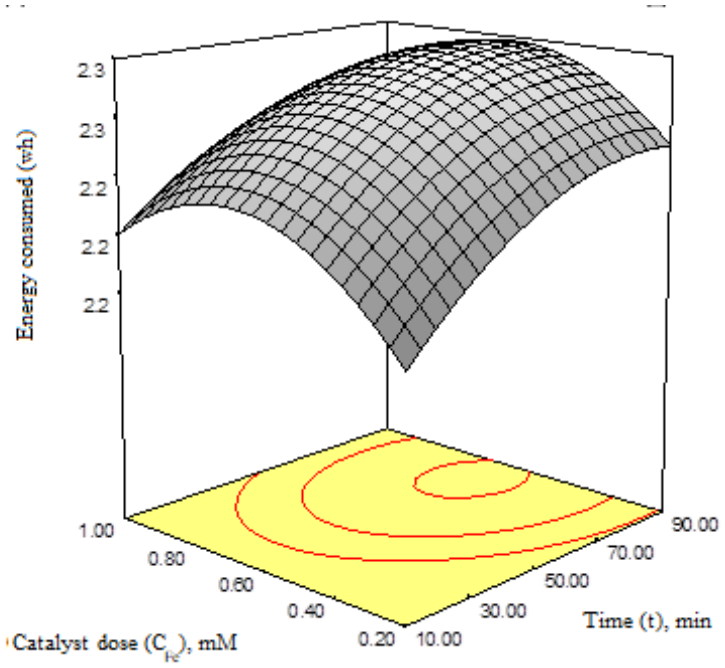

(b)

Fig 5.4.6. 3D response surface graph for the batch EF of textile wastewater (a) Energy Consumed versus *t* and *i* (b) Energy consumed versus C_{Fe} and *t*

The optimization of operating parameters with the responses (X_1, X_2 and X_3) for the treatment of real textile wastewater using batch EF process, multi-response optimization technique with desirability function was carried out (Equation 4.3.6). Optimization of the batch EF process was composed by the set of constraints as shown in Table 5.4.4.

Thus, the desirability for response X_1 is calculated by the Equation 4.3.6 with acceptable $X_{1\text{-}min}$ and $X_{1\text{-}max}$ values as 28% and 100%, respectively (Table 5.4.4).

$$d_{1=}\begin{cases} 0 & if\ X_1 \le 28 \\ \left[\frac{X_1 - 28}{100 - 28}\right] & if\ 28 < X_1 < 100 \\ 1 & if\ X_1 \ge 100 \end{cases} \quad \textbf{(5.4.4)}$$

Similar to equation 5.4.4, **the** desirability for responses X_2 and X_3 were calculated by equation 5.4.5 and 5.4.6, respectively.

$$d_{2=}\begin{cases} 0 & if\ X_1 \le 66.2 \\ \left[\frac{X_2 - 66.2}{100 - 66.2}\right] & if\ 66.2 < X_1 < 100 \\ 1 & if\ X_1 \ge 100 \end{cases} \quad \textbf{(5.4.5)}$$

$$d_{3=}\begin{cases} 0 & if\ X_1 \le 0.8 \\ \left[\frac{X_3 - 0.8}{4.2 - 0.8}\right] & if\ 0.8 < X_1 < 4.2 \\ 1 & if\ X_1 \ge 4.2 \end{cases} \quad \textbf{(5.4.6)}$$

The most appropriate optimization condition was found to be *i*= 0.32 A, *t*= 90 min and C_{Fe} =0.53 mM, which showed highest overall desirability, D = 0.92. At this optimum condition, the X_1, X_2 and X_3 suggested by RSM under BBD were 90.30%, 100% and 1.27 Wh respectively (Table 5.3.5). To verify the acceptability of the optimization analysis, actual experiments were performed in duplicate and average values of responses X_1, X_2 and X_3 at the optimum condition was found to be 90.30%, 100% and 1.27 Wh, respectively, which were closer to the predicted values as shown in Table 5.6.5. It also demonstrates that modelling and optimization using RSM under BBD was successfully performed.

Furthermore, the pH of the wastewater was found to be changed during the EF treatment. In the present study, EF experiment for treatment of textile wastewater conducted at optimum condition (*i*=1.66 A, *t*= 79.55 min and *pH*=5.49) showed an increase in *pH* from 3 to a final pH_f =4 (Fig 5.4.7). Sharp and fast increase in pH_f can be seen from 3 to 4 within 89 min of EF treatment, and for all *t*> 89 min, pH_f stabilizes to ≈4. The shift of *pH* towards the alkaline side can be attributed to the HO^- production due to water reduction at the cathode.

As the pH of the wastewater was increased from 3 to 4 in 90 min of electrolysis, COD and color removal was due to both of the mechanisms, Fenton mediated and EO. Furthermore, •OH radicals generated during the electrolysis were adsorbed on the surface of Ti/RuO_2 anode. As pH of the wastewater was acidic due to which adsorption rate become high. So, •OH radicals were actively involved in mediated EO with H_2O_2 and HO_2•. In addition to this, chloro-oxidant species oxidizes the organics by mediated EO method. Since, chloro-oxidant species, HOCl and Cl^- were found to be partly participating in the dye oxidation.

Table 5.4.4. Constraints applied for optimization of batch EF of textile wastewater

Variables	Goal	Lower Limit	Upper Limit
t	is in range	10	90
i	is in range	0.25	3
Catalytic dose (C_{Fe})	is in range	0.20	1
% COD removal	Maximize	27.70	100
% Color removal	Maximize	66.20	100
Energy consumed(wh)	minimize	0.82	4.21

Table 5.4.5. Individual and synchronized (maximization of X_1 and X_2 and minimization of X_3) optimization

Individual response optimization				
Response	**C_{Fe}**	***t* (min)**	***i* (A)**	**Desirability**
X_1=98.90%	0.57	83.85	0.47	1.00
X_2= 100%	0.25	62.75	0.34	1.00
X_3=1.24 kWh/kg of COD removed	0.95	16.22	0.25	1.00
Synchronized optimization of responses				
X_1=90.00% X_2= 100% X_3=1.3 kWh/kg of COD removed	0.54	89.63	0.32	0.92

Table 5.4.6. Comparison Between the predicted and experimental Results of responses

Responses	Predicted value	Experimental value
% COD removal (X_1)	90%	89.75%
% Color removal (X_2)	100%,	99.49%,
Energy consumed (X_3)	1.3 kWh/kg of COD removed	1.306 kWh/kg of COD removed

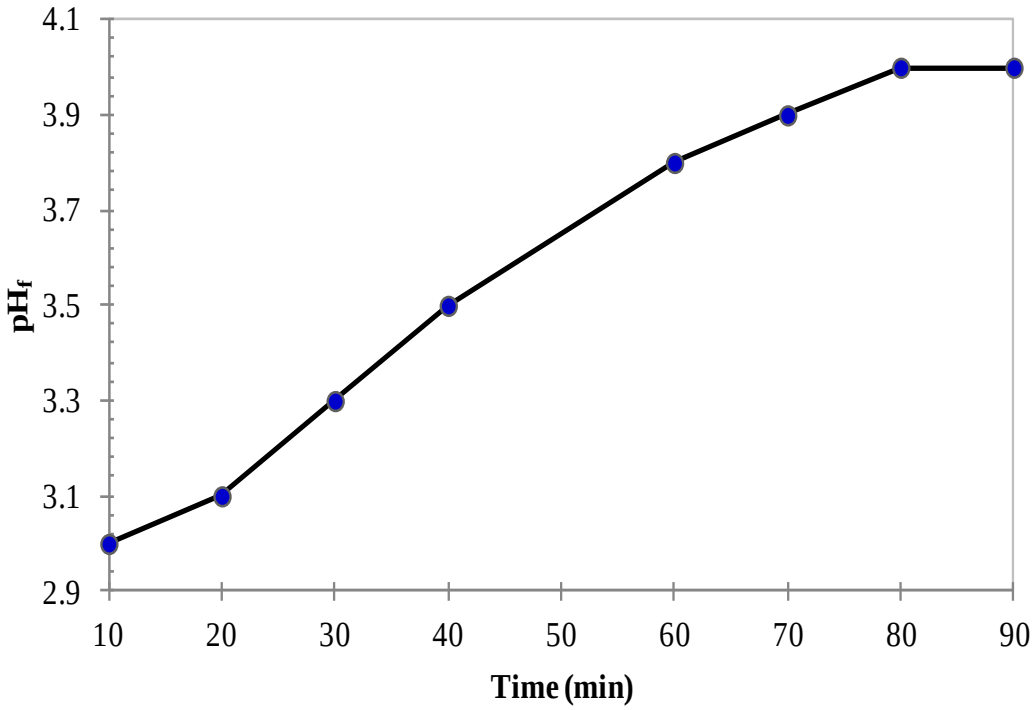

Fig 5.4.7. Graph of *t* versus pH_f for the batch EF treatment of Textile wastewater at optimum condition

5.4.3 Transformation Products and Treated Effluent Quality

Disposable study of the treated textile effluent by EF at the optimum conditions was performed. The comparison of the treated textile wastewater was analyzed with respect to untreated textile wastewater. Spectrophotometric analysis and GC-MS analysis was performed for disposal study of the treated sample by EF and untreated sample.

Spectrophotometric analysis: The analysis of untreated and treated textile effluent by EF was conducted between 200-400nm wavelengths by spectrophotometer. The spectra obtained from spectrophotometer for the untreated and treated samples by EF are shown in Fig 5.4.8. The spectrum of the untreated wastewater was discussed in disposal study of EO process. As it is discussed earlier, two sharp peaks at λ value ~244 and ~250 nm and small intensity bands with λ, ~200-240 nm and λ, ~252-275 nm were observed in the spectra of untreated textile wastewater (Workman, 2001).

It was also seen that, peaks at λ value ~244 and ~250 nm; and λ, ~252-275 nm have been completely disappeared after EF. It was observed that, small intensity peaks at λ value ~200 and ~225 nm in the spectra of EF treated wastewater. These peaks were of transformation products during the EF treatment process.

GC-MS analysis: During the GC-MS analysis of untreated wastewater, identified compounds are shown in Table 5.3.7**.** As it was discussed in batch EO study, the presence of 3, 5-bis(ethoxycarbonyl) benzoic acid (coloring component of basic dye) and Tetracosamethyl-cyclododecasiloxane (a component of fluorescent dye) in untreated wastewater was observed (Table 5.3.7). The GC-MS analysis of EF treated textile effluent shows that dye components were totally eliminated.

Furthermore, comparative observation of Table 5.3.7 and 5.4.7 also elucidate that certain transformation/degradation compounds such as Butyl phthalate, 3,4-dihydro-4-(1,3-dioxolan-2-yl)-5,7-dimethoxy-1(2H)-benzopyran-2-one etc. were generated during the EF treatment process, which show their existence in UV absorption band with λ, 200-250 nm (Fig. 5.3.8). Furthermore, textile wastewater contains high quantity of sodium chloride, therefore, during the EO process, various chlorinated compounds were generated during the indirect oxidation mediated by the chloro oxidant species (Cl_2, HOCl and Cl^-) as shown in

Table 5.3.8. These chlorinated compounds have been reported to be toxic and carcinogenic. It was clear from GCMS analysis that, there was no toxic compound generated after EF treatment real textile wastewater. It was concluded that the •OH mediated oxidation was dominant during EF treatment. Butyl phthalate was found in the treated sample with the highest matching % as shown in Table 5.4.7. It is biodegradable in nature.

To confirm the toxicity of the treated textile wastewater by EF process toxicity bioassay was performed using standard procedure IS: 6582. Test organism for the acute toxicity bioassay test was Aploclzeilus panchax. The toxicity of the EF treated textile effluent was determined by bioassay testing. A test result for the untreated textile wastewater showed 100% mortality rate within one minute and the treated wastewater by EF show 0% mortality rate within 96 hours. Bioassay testing proved that the untreated textile wastewater was highly toxic and lethal to the water bodies. Toxicity of textile wastewater was reduced after EF treatment so, treated wastewater was safe to dispose off in the environment.

5.4.4 Degradation Mechanism

The oxidation/degradation mechanism was predicted on the basis of GC-MS analysis and spectrophotometric analysis. The presence of high molecular weight compounds containing silicon, carbon, hydrogen, oxygen and certain metal ions were observed (Table 5.3.7 and 5.4.7). The degradation process and oxidation of organic matters in the EF process were due to three types of degradation/oxidation method. The degradation/oxidation method was observed for the degradation of textile wastewater: direct anodic degradation (•*OH mediated oxidation)*, indirect anodic degradation (chloro-oxidants mediated oxidation), and •*OH mediated oxidation* in bulk. The probable mechanism of the EF treatment method of textile wastewater is shown in Fig 5.4.9. Direct anodic degradation or •*OH mediated oxidation* refers to the direct contact of degrading organic matter and transfer of electrons from anode to the degrading matter. On the other hand, indirect anodic degradation did not require direct contact of pollutants with anode material. The reactive oxygen species can be physisorbed and chemisorbed to degrade the pollutants. •OH, mediated oxidation in bulk was due to the generation of H_2O_2 due to the hydrolysis of water.

Direct Oxidation: Real Textile wastewater was rich with chloride content, and the optimal pH for the EF process was ≈ 3.0, therefore, Cl_2, HOCl and Cl^- partially participated in the degradation process. It was observed that some of the compounds of untreated wastewater like Trimethyl-2-pentadecenyl, 3,5-bis(ethoxycarbonyl) benzoic Acid, Dodecamethylcyclohexasiloxane, 3-Octanol 2-[(R)-(4-methylphenyl)sulfinyl]-1-(trimethylsilyl), 5-ethoxycarbonyl-2-phenyl-1,3-dioxane-5-carboxylic acid, 2,4,4 trimethyl-3-(2-trimethylsilylethynyl)cyclohex-2en-1-ol, Dibutyl phthalate, Tetracosamethyl-cyclododecasiloxane, Icosamethylcyclodecasiloxane, Tetradecamethylhexasiloxane, Tetrakis(trimethylsilyl) orthosilicate were completely oxidized with production of some transformation compounds such as Dibutyl phthalate, Pyrrolidine and 2-Ethoxy-2-oxoethyl ethyl phthalate by partial oxidation via equation 5.3.11 and 5.3.12

Indirect Oxidation: Further, the transformed products produced via equation 8 and 9 were attacked by chlorine species, and transformed into toxic chlorinated -compounds via indirect oxidation (equation 5.3.12, and 5.3.13). It was further undergoing the $^{\bullet}OH$ *mediated oxidation* in bulk (equation 5.3.13). The partial degradation of the toxic transformed compounds converts them into non-toxic transform compounds. Further, transformation products are produced during the EO due to the deficiency of $^{\bullet}OH$ *and mediated oxidation by various chlorine species.* It represent the presence of 1-acetamidoadamantane, Butyl phthalate, 3,4-dihydro-4-(1,3-dioxolan-2-yl)-5,7-dimethoxy-1(2H)-benzopyran-2-one in treated textile wastewater.

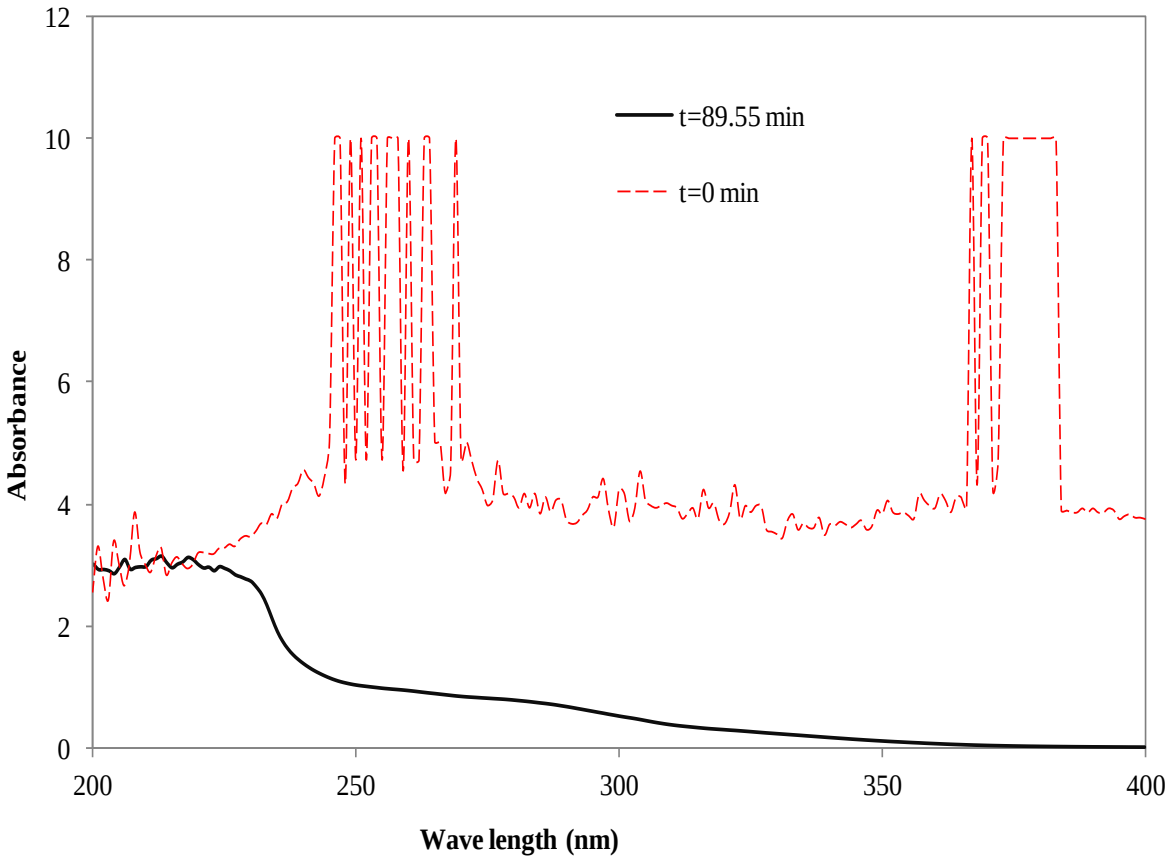

Fig 5.4.8. UV Visible spectra of untreated (*t*=0 min) and treated (*t*= 89.55 min) textile wastewater by EF at optimum condition

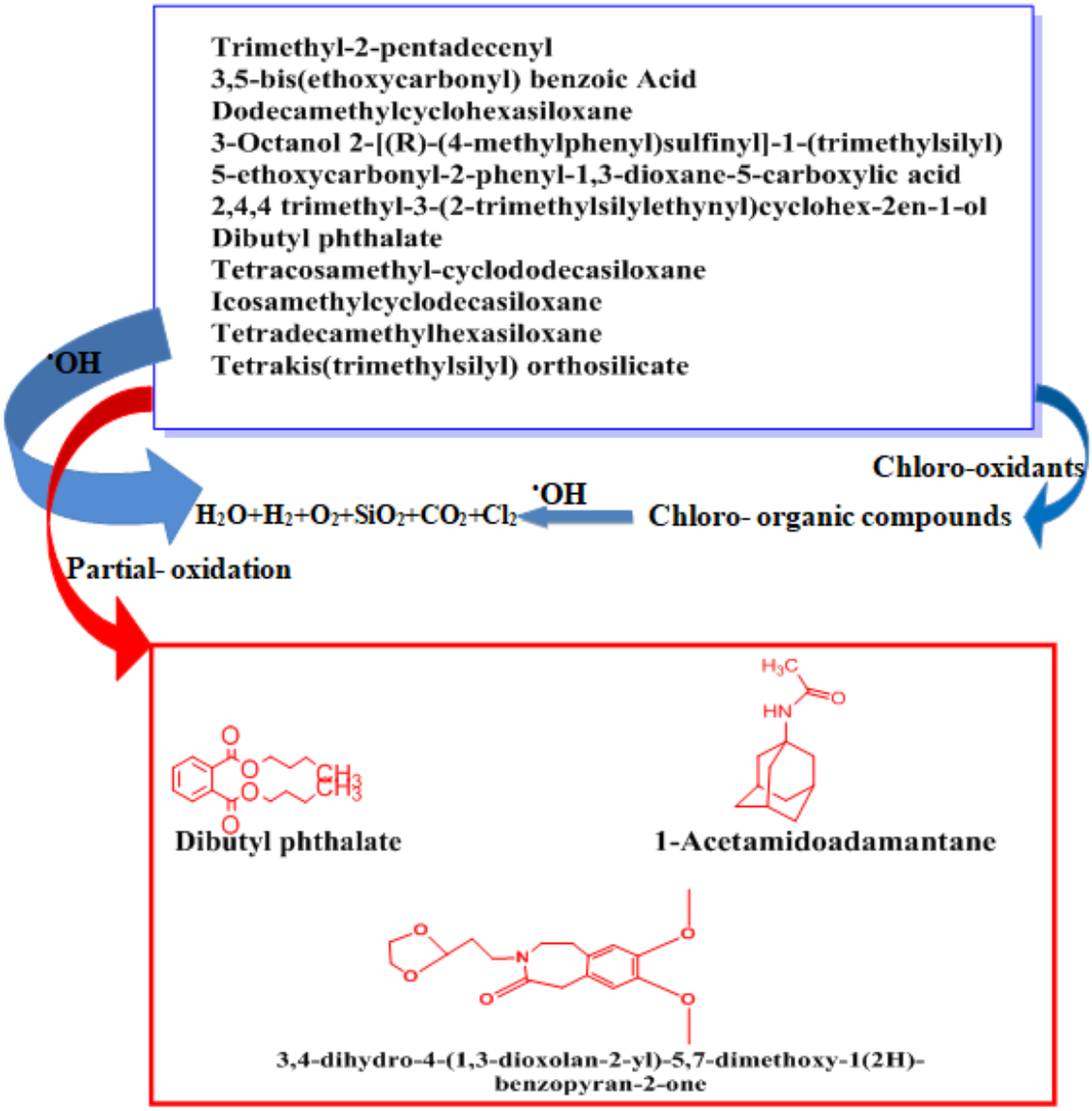

Fig 5.4.9. Persuasive mechanism for the degradation of textile wastewater by batch EF process

Table 5.4.7. GC-MS analysis of treated Textile wastewater by batch EF process

Compound	Retention Time	Molecular Mass	Matching %	Comment
Butyl phthalate	20.02/21.51/21.16/21	278	95.2% / 81.3%/92.9%	Biodegradable
3,4-dihydro-4-(1,3-dioxolan-2-yl)-5,7-dimethoxy-1(2H)-benzopyran-2-one	24.06/15.12	280	84%	-
1-acetamidoadamantane	21.91	193	90.7%	-

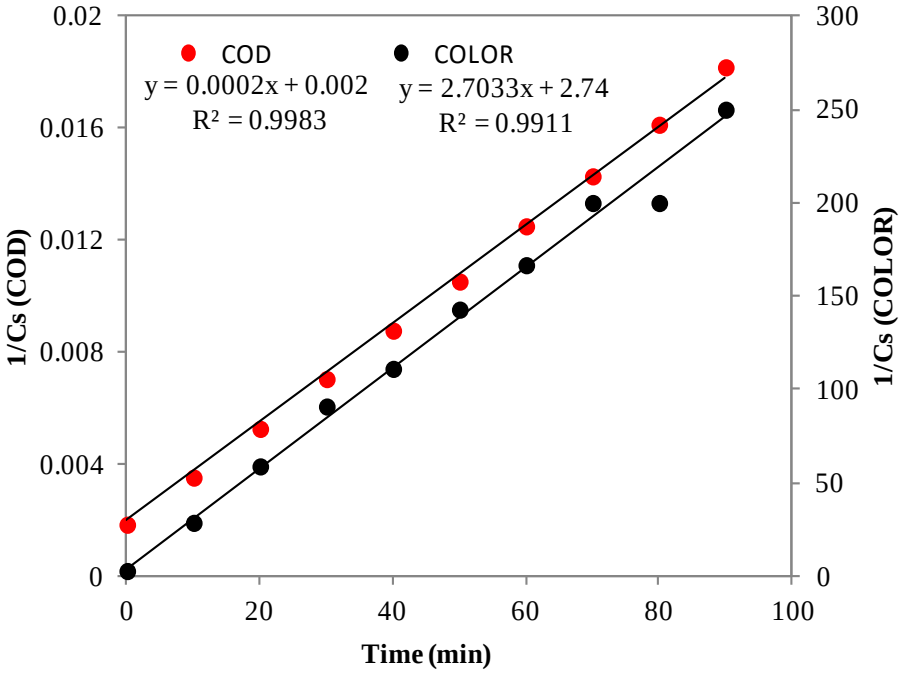

Fig 5.4.10. Fitting of second-order reaction kinetics to the COD removal and color removal at optimum conditions of EF

5.4.5 Kinetic Study

At optimum parameters of the EF process, kinetics of COD and color removal was studied. Second-order model was fitted to the experimental data at optimum conditions (i = 0.32 and C_{Fe} = 0.53 mM) for COD removal and Color removal according to the rate equation. According to the rate equation of the second order:

$$\frac{-dC_S}{dt} = k[C_S]^2 \quad \textbf{(5.4.7)}$$

On integrating between known limits and rearranging, the above model becomes

$$\frac{1}{[Cs]} = \frac{1}{[Co]} + Kt \quad \textbf{(5.4.8)}$$

Where, C_0 is initial color intensity or initial COD concentration, C_s is final color intensity or final COD concentration, t is degradation time (min) and K is second-order rate constant (*l*/mg min). Fig 5.4.10 shows the fitting of second-order reaction kinetics to the %Color removal and %COD removal for the treatment of textile effluent by EF process. The values of the rate constant of second-order reaction kinetics are 0.0002 *l*/mg min and 2.7033 *l*/mg min along with the R^2 value 0.998 and 0.991 for X_1 and X_2, respectively. The kinetic study of the COD and color showed that the COD and color from real textile effluent were concurrently removed with respect to elapsed time. Concurrent removal of COD and color can also be verified from its degradation mechanism. The compounds initially present in the textile effluent were eliminated after EF treatment.

5.4.6 Operational Cost analysis of Batch EF Process

The cost of specific electrical energy consumed and electrode required to remove one kg of COD from textile wastewater was calculated from the responses of EF experiment conducted (X_1 =89.75%, X_2=99.49% and X_3=1.306 kWh/kg of COD removed) at optimized parameters (i = 0.32 and C_{Fe} = 0.53 mM), and given below:

Specific electrical energy consumed = ~1.306 kWh/kg of COD removed

Electricity price in India, Punjab = ~ ₹ 5.00/kWh

Therefore, the cost of electrical energy consumed (C_E) = ₹ 6.5/kg of COD removed

In this study, two Ti/RuO_2 electrodes (dimension: 100 mm x 85 mm x 1.5 mm) of cost ₹ 2500.00 each were used. The manufacturer/supplier (Titanium Tantalum Products Limited, Chennai, India) specified the life of the electrodes 2.5 years at optimized condition (i = 0.32 and C_{Fe} = 0.53 mM).

Since at optimized condition 89.75% of COD is removed, therefore, the minimum cost of Ti/RuO_2 electrodes (C_{EL}) = ₹ 465.46/ kg of COD removed

Total operating cost (C_E + C_{EL}) = ₹ 471.96/ kg of COD removed

In the present study, the COD of collected wastewater (from a Mink Blanket manufacturing industry situated in Ludhiana, Punjab, India) was 544 mg/l. Therefore, to treat 1 m^3 of this wastewater by reducing the COD from 0.544 kg/m^3 to 0.108 kg/m^3 (as optimum %COD removal=80%) total operating cost (C_E + C_{EL}) in US$ is 7.866 $/ kg of COD removed.

5.5 STUDY ON CONTINUOUS EO TREATMENT PROCESS

5.5.1 Characterization of Real Textile Effluent

The textile effluent from the same industry (Mink Blanket manufacturing industry, situated in Ludhiana, Punjab) was collected again for the study of continuous EO and EF treatment process. Collected real textile effluent was again characterized by various water quality parameters, and the results are shown in Table 5.5.1. The BOD/COD ratio of the collected real textile effluent was found to be 0.169, which implies that the textile wastewater is toxic and non-biodegradable/recalcitrant in nature. The high concentration of chloride, TDS, TSS makes it undesirable for the environment. Therefore, the textile effluent is suitable for electrochemical treatment.

Table 5.5.1. Physicochemical characterization of textile effluent

PARAMETERS	VALUES
pH	10.0
BOD (mg/l)	196
COD (mg/l)	1156
TDS (mg/l)	9640
TSS (mg/l)	8430
Color (pt.co)	1410
Chloride (mg/l)	1682
Alkalinity (mg/l)	940
Oil/grease (mg/l)	90
Total Kjeldahl Nitrogen (mg/l)	2.24
Conductivity (mS/cm)	4.6
Turbidity (NTU)	182
Hardness (mg/l)	746

5.5.2 Model Fitting and Statistical analysis

The ranges of the selected parameters for experimental designing of continuous EO were selected from preliminary experiments. The four independent variables were taken as input parameters for continuous EO process i.e. *pH*: (3-11); elapsed time, *t*: (15-175 min),

retention time, R_T: (50-250) and current, i: (0.25 - 3 A), and the % COD removal (X_1), % color removal (X_2) and energy consume (X_3) were selected as responses.

Total 30 experimental runs suggested by CCD, were performed and the response (X_1), (X_2) and (X_3) were obtained (Table 5.5.2). Further, experimental data of continuous EO processes were analysed and the quadratic model was suggested by exploiting sequential F-test, model summary and subsequent ANOVA for EO process. The adequate precision for the responses X_1, X_2 and X_3 was 18.878, 24.564 and 58.633, respectively. The value of adequate precision above 4 indicates the suggested model was efficient to analyze the relationship between variables and the responses of the process. Comparison between the actual and predicted values of responses for continuous EO process shows a good correlation with the coefficient of determination R^2, Adjusted R^2 and predicted R^2 as shown in Table 5.5.3. The model's lack of fit F-values for continuous EO processes was insignificant for X_1, X_2 and X_3. The actual versus predicted values of responses shows a good correlation as shown in Fig 5.5.1, 5.5.2 and 5.5.3. The ANOVA for responses X_1, X_2 and X_3 showed model F- the value of 32.16, 40.80, 303.67, respectively (Table 5.5.4a, b, c.), advocating that the quadratic model was significant, and model terms were significant at the 95% confidence level. According to studentized residuals, normal probability and outlier-t residual plots the quadratic model well satisfied the ANOVA (Fig. 5.5.1, 5.5.2, 5.5.3) for X_1, X_2 and X_3, respectively. Values of "Prob>F" greater than 0.1 indicate that model terms were not significant. The significant terms for X_1: *t, i, pH,* t^2, i^2, pH^2, R_T^2, *t*x*pH, i*x*pH*; X_2: *t, i, pH,* t^2, pH^2, *i* x *pH*; and X_3: *t, i,* i^2, *t*x*i* were observed from the ANOVA (Table 5.5.4a, b, c). The quadratic model equation obtained in terms of significant process parameters and interaction parameters is given below.

$$X_1=76.22 + 10.24t + 7.19i - 11.11pH - 9.2t^2 - 4.70i^2 - 10.64pH^2 - 7.65R_T^2 - 7.34\,(t \text{ x } pH) - 3.11(i \text{ x } pH) \quad \textbf{(5.5.1)}$$

$$X_2 = 84.32 + 8.90t + 7.76i - 9.81pH - 4.12t^2 - 7.29\,pH^2 + 2.41\,(i \text{ x } pH) \quad \textbf{(5.5.2)}$$

$$X_3 = 7.72 + 3.28t + 3.98i + 0.47i^2 + 1.60(t \text{ x } i) \quad \textbf{(5.5.3)}$$

Table 5.5.2. Experimental design for the continuous EO process

Standard Order	*t (min)*	*i (A)*	*pH*	R_T *(min)*	X_1		X_2		X_3	
					$X_{1\ exp}$	$X_{1\ pre}$	$X_{2\ exp}$	$X_{2\ pre}$	$X_{3\ exp}$	$X_{3\ pre}$
29	95	1.25	7	140	76.22	76.22	84.32	84.32	7.72	7.72
27	95	1.25	7	140	76.22	76.22	84.32	84.32	7.72	7.72
12	135	1.75	5	185	86.22	83.27	99.65	99.48	16.59	16.87
20	95	2.25	7	140	80.22	71.79	99.98	95.78	18.52	17.54
5	55	0.75	9	95	21.22	24.45	47.11	44.41	2.34	2.32
15	55	1.75	9	185	35.11	33.14	67.65	65.77	6.73	7.06
7	55	1.75	9	95	28.99	33.26	65.12	67.98	6.74	7.06
23	95	1.25	7	50	45.66	43.89	84.64	85.90	7.72	7.44
17	15	1.25	7	140	19.17	18.68	47.55	50.03	1.22	0.87
25	95	1.25	7	140	76.22	76.22	84.32	84.32	7.72	7.72
8	135	1.75	9	95	38.72	42.07	80.44	79.57	16.54	16.83
4	135	1.75	5	95	83.66	84.30	95.42	95.07	16.54	16.84
14	135	0.75	9	185	33.42	31.77	66.42	62.27	5.74	5.68
30	95	1.25	7	140	76.22	76.22	84.32	84.32	7.72	7.72
13	55	0.75	9	185	26.47	28.96	44.04	44.26	2.34	2.31
2	135	0.75	5	95	57.45	59.71	86.52	85.53	5.74	5.68
22	95	1.25	11	140	18.95	11.43	36.54	35.53	7.72	7.44
6	135	0.75	9	95	31.48	29.92	59.96	60.39	5.74	5.68
16	135	1.75	9	185	28.98	39.28	74.32	79.40	16.54	16.84
10	135	0.75	5	185	64.44	63.31	94.98	91.99	5.74	5.69
3	55	1.75	5	95	44.22	46.15	76.2	77.48	6.74	7.07
26	95	1.25	7	140	76.22	76.22	84.32	84.32	7.72	7.72
9	55	0.75	5	185	34.22	31.15	69.98	67.98	2.34	2.31
24	95	1.25	7	230	49.02	47.37	88.43	90.15	7.72	7.45
28	95	1.25	7	140	76.22	76.22	84.32	84.32	7.72	7.72
11	55	1.75	5	140	76.22	47.78	84.32	79.86	7.72	7.08
19	95	1.25	7	185	86.22	43.02	99.65	64.75	16.59	1.62
1	95	1.25	7	140	80.22	24.88	99.98	63.56	18.53	2.31
18	135	1.75	5	95	21.22	59.64	47.11	85.63	2.34	14.01
21	95	2.25	7	185	35.11	55.86	67.65	74.76	6.74	7.45

Table 5.5.3. Various R-squared values suggested by CCD for responses %COD removal (X_1), % Color removal (X_2) and energy consume (X_3)

Responses	R-Squared	Adj R-Squared	Pred R-Squared
X_1	0.97	0.94	0.81
X_2	0.97	0.95	0.85
X_3	0.99	0.99	0.98

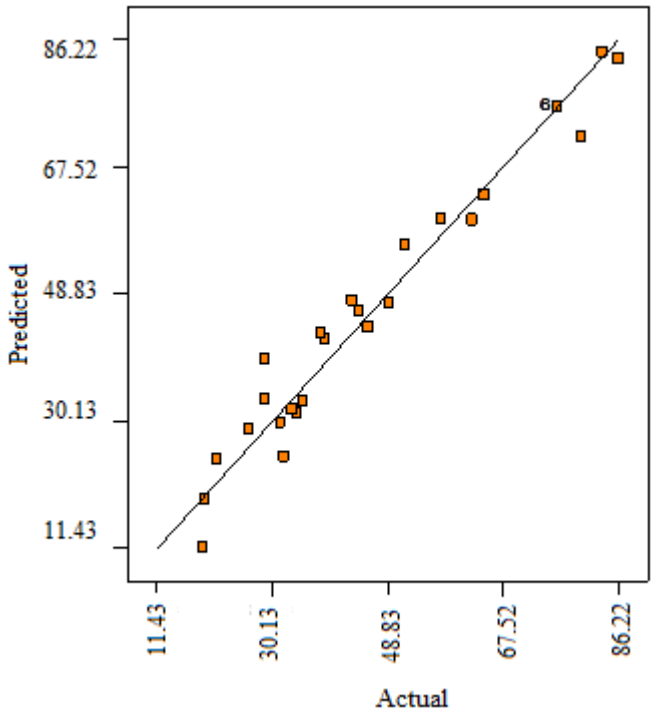

Fig 5.5.1. Predicted versus actual %COD removal for continuous EO process

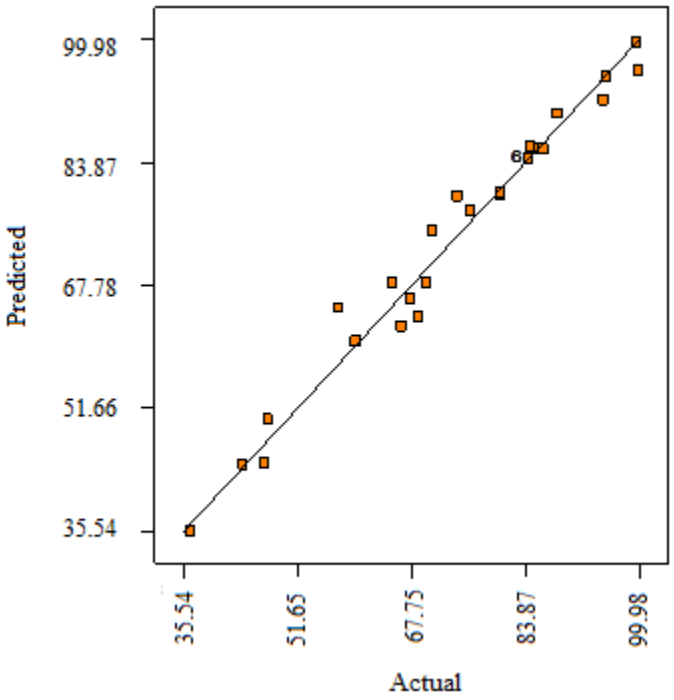

Fig 5.5.2. Predicted versus actual %Color removal for continuous EO process

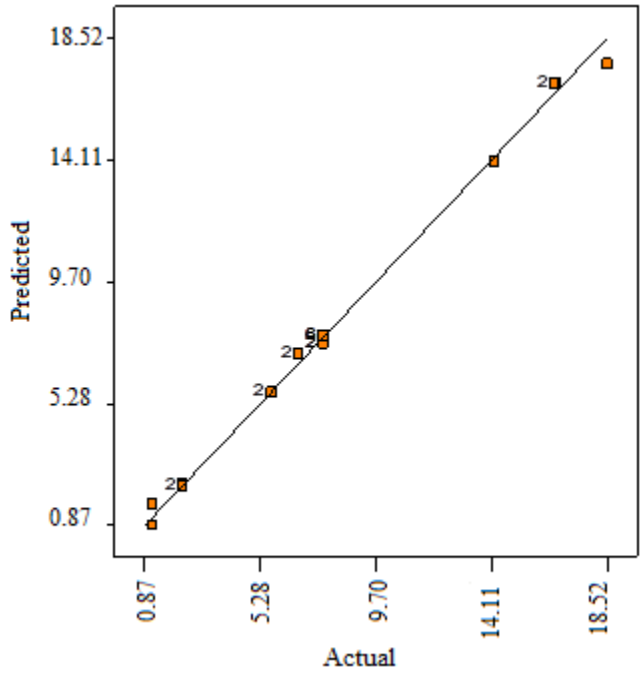

Fig 5.5.3. Predicted versus actual energy consume for continuous EO process

Table 5.5.4a. ANOVA for the %COD removal of continuous EO process

Source	Sum of Squares	DF	Mean Square	F-Value	Prob > F
Model	13418.08	14	958.43	32.16	< 0.0001
T	2516.99	1	2516.99	84.46	< 0.0001
I	1241.86	1	1241.85	41.67	< 0.0001
Ph	2961.04	1	2961.03	99.35	< 0.0001
R_T	18.17	1	18.16	0.61	0.4471
t^2	2354.79	1	2354.79	79.01	< 0.0001
i^2	606.38	1	606.38	20.34	0.0004
pH^2	3107	1	3107	104.2	< 0.0001
R_T^2	1603.88	1	1603.88	53.81	< 0.0001
t x i	11.12	1	11.12	0.37	0.5504
t x pH	861.13	1	861.13	28.89	< 0.0001
t x R_T	7.10	1	7.10	0.23	0.6325
t x pH	155.13	1	155.13	5.20	0.0375
i x pH	21.48	1	21.48	0.72	0.4092
pH x R_T	3.08	1	3.08	0.10	0.7523
Residual	447.03	15	29.80		
Lack of Fit	447.03	10	44.70		
Pure Error	0	5	0		
Cor Total	13865.11	29			

Table 5.5.4b. ANOVA for the %Color removal of continuous EO process

Source	Sum of Squares	DF	Mean Square	F-Value	Prob > F
Model	7742.12	14	553.01	40.80	< 0.0001
t	1900.50	1	1900.51	140.22	< 0.0001
i	1446.62	1	1446.62	106.73	< 0.0001
pH	2307.90	1	2307.90	170.28	< 0.0001
R_T	27.11	1	27.12	2.00	0.1777
t^2	465.93	1	465.94	34.38	< 0.0001
i^2	28.34	1	28.34	2.09	0.1687
pH^2	1458.79	1	1458.79	107.63	< 0.0001
R_T^2	23.57	1	23.58	1.74	0.2070
t x i	19.25	1	19.25	1.42	0.2519
t x pH	35.91	1	35.91	2.65	0.1244
t x R_T	4.13	1	4.13	0.30	0.5890
t x pH	92.88	1	92.88	6.85	0.0194
i x pH	4.19	1	4.19	0.31	0.5863
pH x R_T	20.99	1	20.99	1.55	0.2323
Residual	203.30	15	13.55		
Lack of Fit	203.30	10	20.33		
Pure Error	0	5	0		
Cor Total	7945.42	29			

Table 5.5.4c. ANOVA for the Energy consumed of continuous EO process

Source	Sum of Squares	DF	Mean Square	F-Value	Prob > F
Model	3.56×10^{-4}	14	2.54×10^{-5}	44.41	< 0.0001
T	7.81×10^{-5}	1	7.81×10^{-5}	136.61	< 0.0001
I	1.97×10^{-4}	1	1.97×10^{-4}	343.90	< 0.0001
pH	8.52×10^{-6}	1	8.52×10^{-6}	14.90	0.0015
R_T	1.65×10^{-5}	1	1.65×10^{-5}	28.86	< 0.0001
t^2	5.63×10^{-6}	1	5.63×10^{-6}	9.85	0.0068
i^2	5.42×10^{-7}	1	5.42×10^{-7}	0.95	0.3455
pH^2	3.67×10^{-7}	1	3.67×10^{-7}	0.64	0.4358
R_T^2	5.92×10^{-7}	1	5.92×10^{-7}	1.03	0.3252
t x i	3.28×10^{-5}	1	3.28×10^{-5}	57.32	< 0.0001
t x pH	4.1×10^{-6}	1	4.1×10^{-6}	7.17	0.0172
t x R_T	5.64×10^{-6}	1	5.64×10^{-6}	9.86	0.0067
t x pH	3.52×10^{-6}	1	3.52×10^{-6}	6.15	0.0255
i x pH	2.18×10^{-6}	1	2.18×10^{-6}	3.80	0.0701
pH x R_T	2.26×10^{-7}	1	2.26×10^{-7}	0.39	0.5394
Residual	8.58×10^{-6}	15	5.72×10^{-7}		
Lack of Fit	8.58×10^{-6}	10	8.58×10^{-7}		
Pure Error	0	5	0		
Cor Total	0.000364	29			

5.5.3 Effect of Continuous EO Parameters and Optimization

Fig 5.5.4 a, b & c show the interaction of pH, current (*i*), time (t) and retention time (R_T) on the X_1. It can be seen that X_1 increases up to t≈120 min at all *i* values. For all t> 120 min marginal change in the X_1 was observed. This change in X_1 value was also seen at all *i* values (Fig. 5.5.4a). Therefore, steady-state time is concluded to be ≈120 min, beyond which no significant change in X_1 was observed. Further, at lower *t* value, increasing *i* up to ≈0.75 A shows no COD removal. However, for i>0.75 A, X_1 were found increasing up to ≈1.4 A, then after becomes constant (Fig. 5.5.4a). At higher t values, increasing *i* increases X_1 up to ≈1.4 A, then after a marginal change in X_1 were seen.

pH is a highly significant parameter of the EO process. A sharp increase in X_1 was seen for increasing pH from highly acidic pH to ≈5.5 (Fig. 5.5.4b). Beyond pH>5.5, a sharp decrease in X_1 was observed, and X_1 becomes nearly zero at highly basic pH. Further, in highly acidic pH, increasing current increases X_1 value. However, no effect of increasing *i* was observed on X_1 at a highly basic pH (Fig. 5.5.4b). Fig. 5.5.4c explains the interaction of R_T with *t* on %COD removal. It was observed that there was no change in X_1 at very low R_T values and *t*. However, X_1 is sharply increased with increasing R_T value up to ≈150 min, and for R_T>150 min X_1 is decreased but marginally. This was found true at all the *t*. Further, at any R_T value, increasing *t* increases X_1, but marginally for *t* beyond ≈120 min. Therefore, the steady state of the continuous process was achieved after *t*~120 min. X_1 was maximum at the *t*~ 120 to125 min with the R_T values of 150 to 158 min. Fig. 5.5.5 a, b & c show the interaction of pH, current (*i*), time (t) and retention time (R_T) on the X_2. Like X_1, pH significantly affects the X_2 also. Increasing pH from high acidic side to ≈ 5.5 increases X_2, and beyond this, a sharp decrease in X_2 was observed. However, unlike to X_1, X_2 was found 70% at higher t values in highly basic pH (Fig. 5.5.5a & b). Further, at any pH increasing *i* values up to ≈1.4 A, increases X_2, and beyond 1.4 A marginal change was observed (Fig. 5.5.6b). Fig. 5.5.5c explains the interaction of R_T with *t* on %Color removal, X_2. The variation in X_2 with R_T and *t* was the same as it was for %COD removal concluding the steady state of the continuous process was *t*~120 min.

Fig 5.5.6a & b shows the effects of R_T, pH, i and t on energy consumption (X_3). Fig. 5.5.6a shows that at any R_T value, increased pH up to ≈5.5 increases X_3. However, beyond pH

>5.5, X_3 decreased sharply. The increase in X_3 at a lower value of current, *i* with increasing *t* was smaller than the increase in X_3 at a high value of *i* (Fig. 5.5.6b).

From the above study, it appeared that both direct and indirect EO is responsible for the COD and color removal from real textile wastewater. The steady state of a continuous EO process for textile wastewater was achieved at ≈120 min of elapsed time. This was further verified with optimized values of various process parameters studied. The increase in X_1 values from highly acidic pH to the pH ≈ 5.5. During the electrolysis, various oxidants such as •OH, H_2O_2 and chlorine species: Cl_2, ClO^- and HOCl (textile wastewater contains a high amount of NaCl salt) were generated in EO reactor. However, in highly acidic pH only •OH and chlorine species such as Cl_2 and HOCl exist (Deborde et al. 2008; Pletcher et al. 1999). The •OH was adsorbed on the surface of the anode (5.5.4) and mineralize the pollutants (P) at the surface of anode via direct oxidation mechanism (equation 5.5.5 and 5.5.6). However, Cl_2 and HOCl degrade the pollutant via indirect oxidation mechanism in the bulk of the solution.

$$Ti/RuO_2 + H_2O \rightarrow Ti/RuO_2(\bullet OH) + H^+ + e^- \quad \textbf{(5.5.4)}$$

$$P + Ti/RuO_2(\bullet OH) \rightarrow nCO_2 + zH^+ + e^- + Ti/RuO_2 + \text{transformation products} \quad \textbf{(5.5.5)}$$

$$Ti(\bullet OH)_{ads} + P \rightarrow nCO_2 + mH_2O + \text{transformation products} + Ti \quad \textbf{(5.5.6)}$$

In basic pH range, the generation, as well as adsorption rate of •OH radicals on the surface of Ti/RuO_2, is reduced (Enache et al. 2009; Kaur et al. 2017), and other lower potential oxidants like H_2O_2 and HO_2• are produced (equation 5.3.4, 5.3.5 and 5.5.7) (Sires et al. 2014).

$$H_2O \rightarrow \bullet OH + H^+ + e- \quad \textbf{(5.5.7)}$$

Therefore, lower potential oxidants like H_2O_2 and HO_2• generation in increasing pH in basic pH range reduced the X_1 and X_2. However, chlorine species, ClO^-, which dominates in highly basic pH degrade the pollutants via an indirect mechanism. Increasing *i* value increases the generations rate of the oxidants, which in turn increases X_1 and X_2. Higher current supports the side reaction of electrolysis of water to O_2 (equation 5.3.6), which reduces the •OH radicals generation and X_1 and X_2 is decreased.

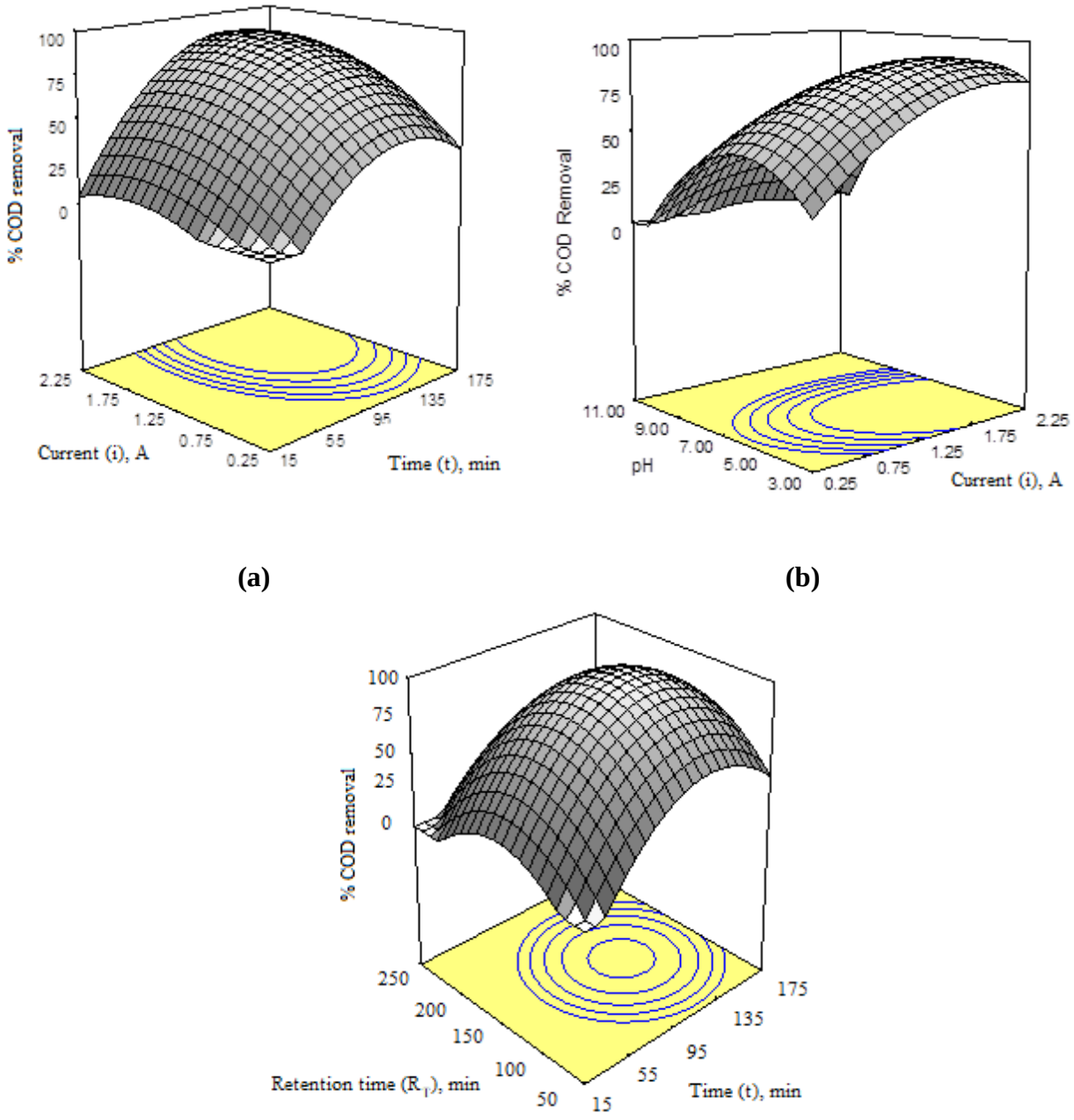

Fig. 5.5.4. 3D response surface for continuous EO of textile wastewater (a) %COD removal versus i and t (b) %COD removal versus pH and i (c) %COD removal versus t and R_T

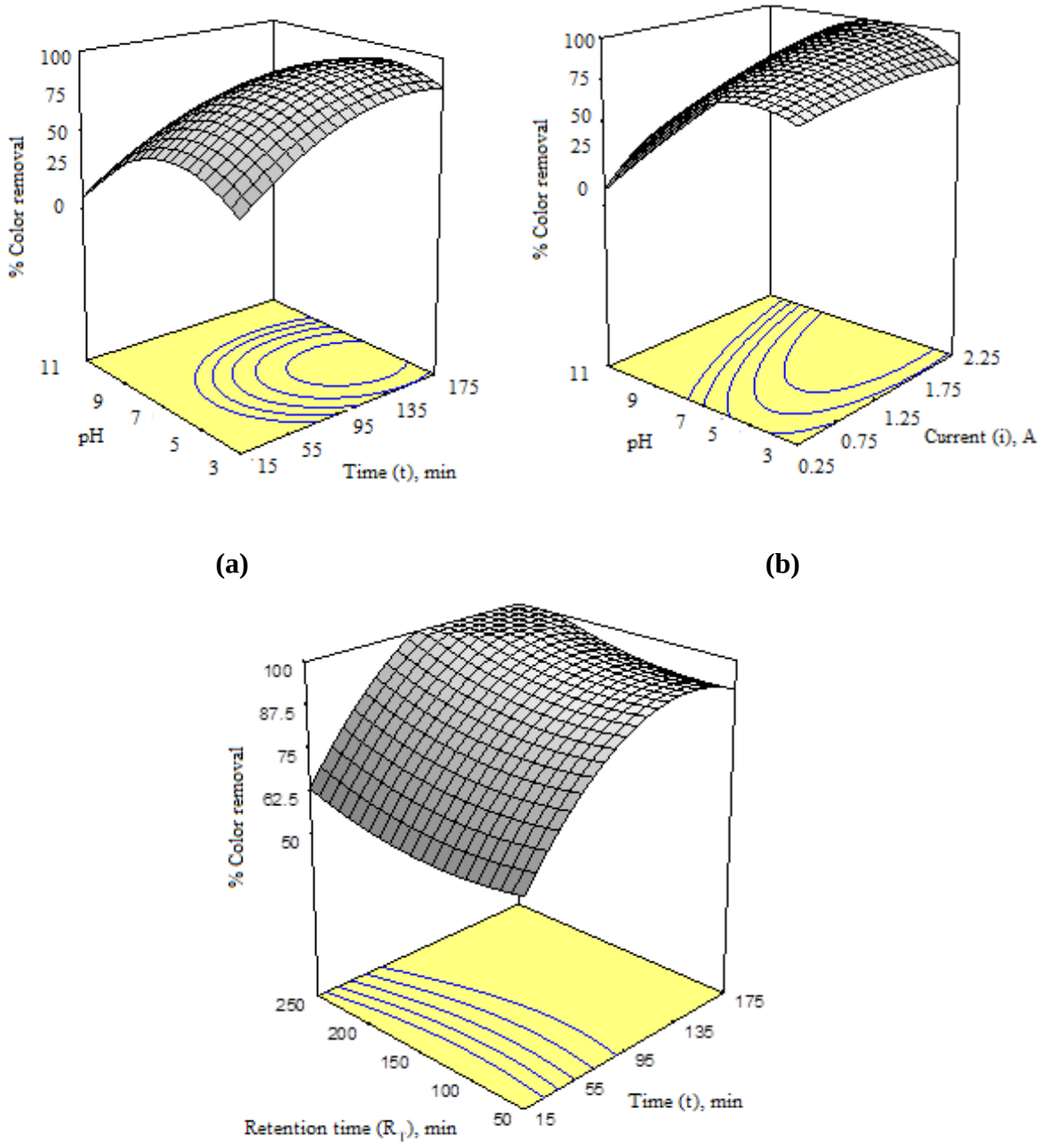

Fig 5.5.5. 3D response surface for continuous EO of textile wastewater (a) %Color removal versus t and pH (b) %Color removal versus pH and i (c) %Color removal versus t and R_T

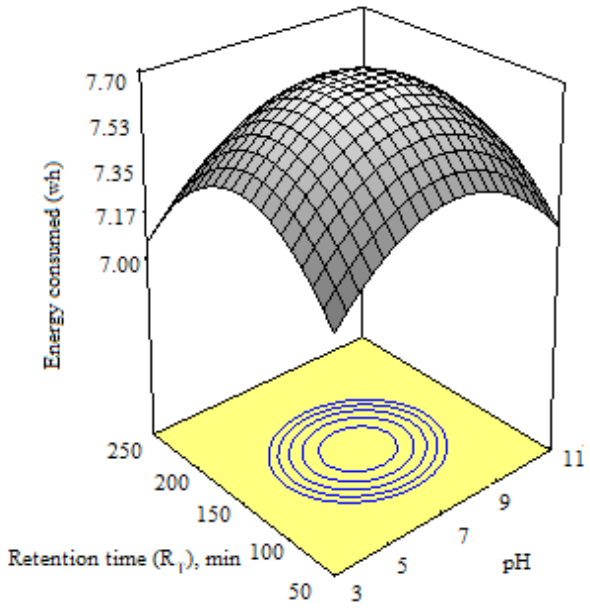

(a)

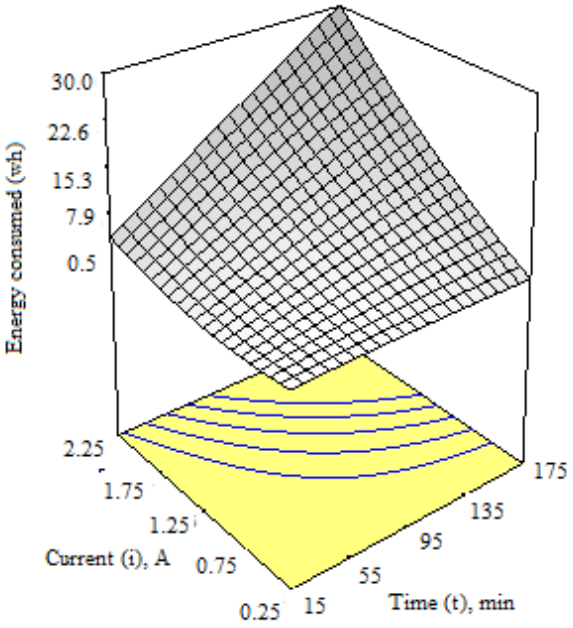

(b)

Fig. 5.5.6. 3D response surface for the continuous EO of textile wastewater (a) Energy consumed versus *pH* and R_T (b) Energy consume versus, *i* and *t*

The optimization of operating parameters with the responses (X_1, X_2 and X_3) for the treatment of real textile wastewater using continuous EO process, multi-response optimization technique with desirability function was carried out (Equation 4.3.7). Optimization of the continuous EF process was composed by the set of constraints as shown in Table 5.5.5.

$$d_{1=}\begin{cases} 0 & if\ X_1 \le 18.95 \\ \left[\frac{X_1 - 18.95}{100 - 18.95}\right] & if\ 18.95 < X_1 < 100 \\ 1 & if\ X_1 \ge 100 \end{cases} \quad \textbf{(5.5.8)}$$

Similar to equation 5.5.8, **the** desirability for responses X_2 and X_3 were calculated by equation 5.5.9 and 5.5.10, respectively.

$$d_{2=}\begin{cases} 0 & if\ X_1 \le 36.54 \\ \left[\frac{X_2 - 36.54}{100 - 36.54}\right] & if\ 36.54 < X_1 < 100 \\ 1 & if\ X_1 \ge 100 \end{cases} \quad \textbf{(5.5.9)}$$

$$d_{3=}\begin{cases} 0 & if\ X_1 \le 0.001 \\ \left[\frac{X_3 - 0.001}{0.0157 - 0.001}\right] & if\ 0.001 < X_1 < 0.0157 \\ 1 & if\ X_1 \ge 0.0157 \end{cases} \quad \textbf{(5.5.10)}$$

The most appropriate optimization condition was found to be *t*= 124 min, *i*=1.37 A, *pH*=5.54 and R_T=157.6 min which showed the highest overall desirability, D = 0.89. At this optimum condition, the X_1, X_2 and X_3 suggested by RSM under CCD were 86.22%, 94.74% and 9.42 KWh /Kg of COD removed respectively (Table 5.5.6). To verify the acceptability of the optimization analysis, actual experiments were performed in duplicate and average values of responses X_1, X_2 and X_3 at the optimum condition was found to be 81.00%, 92.25% and 10.88 kWh/Kg of COD removed, respectively, which were closer to the predicted values as shown in Table 5.5.7. It also demonstrates that modelling and optimization using RSM under CCD was successfully performed.

As it is discussed during batch EO study, the pH of the wastewater was found to be changed. During EO experiment for treatment of textile wastewater conducted at optimum condition (*t*= 124 min, *i*=1.37 A, *pH*=5.54 and R_T=157.6 min) showed an increase in *pH* from 5.54 to a final pH_f =9.2 (Fig 5.5.7). Sharp and fast increase in pH_f can be seen from 5.49 to 9.2 within 124 min of EO treatment at R_T=157.6 min, and for all *t*> 124 min, pH_f stabilizes to ≈9.2. It shows the establishment of steady state condition during the continuous EO process. The shift of *pH* towards the alkaline side is due to the reduction of water at the cathode.

However, the pH_f was stabilized to ≈9.42 due to the buffer formation according to the following reaction (equation 5.3.11).

Table 5.5.5. Constraints applied for optimization of continuous EO of textile wastewater

Variables	Goal	Lower Limit	Upper Limit
t (min)	is in range	15	175
i (A)	is in range	0.25	2.25
pH	is in range	3	11
X_1	Maximize	18.95	100
X_2	Maximize	36.54	100
X_3	Minimize	0.001	0.0157

Table 5.5.6. Individual and synchronised (maximization of X_1 and X_2 and minimization of X_3) optimization

Individual response optimization					
Response	***pH***	***t* (min)**	***i* (A)**	**R_T (min)**	**Desirability**
X_1=86.6%	4.39	116.93	1.94	119.83	1.00
X_2= 100%	5.43	133.21	2.16	203.86	1.00
X_3=7 kWh /kg of COD	9.38	15.92	1.35	57.44	1.00
Synchronised optimization of responses					
X_1=86.20% X_2= 94.70% X_3=9.42 kWh /kg of COD	5.45	124	1.37	157.6	0.89

Table 5.5.7. Correlation of experimental and predicted responses at optimized condition

Responses	Predicted value	Experimental value
% COD removal (X_1)	86.22%	81.00%
% Color removal (X_2)	94.74%,	92.25%
Energy consumed (X_3)	9.42 kWh/kg of COD removed	10.88 kWh/kg of COD removed

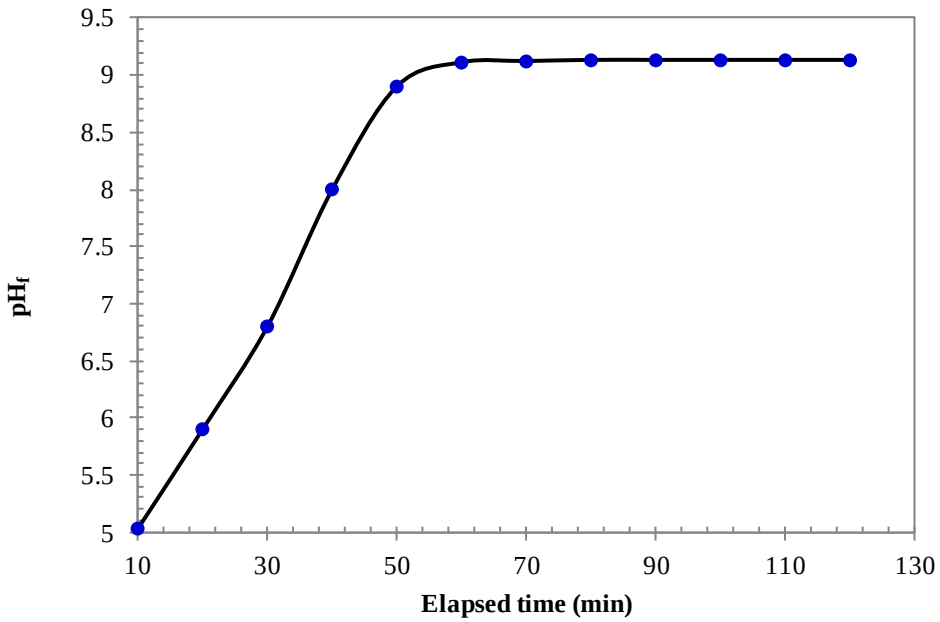

Fig 5.5.7. Graph of *t* versus pH_f for the continuous EO treatment of Textile wastewater at optimum condition

5.5.4 Transformation Products and Treated Effluent Quality

The disposal study of the treated textile effluent by continuous EO at the optimum condition was accessed by spectrophotometric analysis and GCMS analysis. The untreated textile wastewater was also analyzed with the same procedure for the comparison with treated textile effluentnt by continuous EO process.

Spectrophotometric analysis: The results obtained from spectrophotometer for the untreated and treated samples at optimal condition is shown in Fig. 5.5.8. In spectra of untreated textile wastewater, sharp peaks of high absorption intensity peaks with λ value ~200-210 nm, ~240-275 nm and in the range of ~365-380 nm can be seen. Low-intensity peaks can be seen with λ from ~200-245 nm and from ~275-370 nm. Further, a drastic change in the absorption spectra of treated textile wastewater can be seen. Spectra show high-intensity peaks with λ value 200 and in the range of ~255-280 nm. The absorption band with λ above 200 nm, indicates the presence of aromatic compounds.

Absorption band of 200-250 nm represents the presence of primary band ketones, acids, phthalates, aldehydes, esters, alkanes etc. and λ, ~250-275 nm represents secondary band aldehydes, alcohols, ketones etc. (Workman 2001). Bands of λ, ~250-275 nm are generated during the EO process exhibits degraded compounds confirming the degradation of compounds during the EO process. In treated wastewater spectra, small peaks at λ value ~205 - 257 nm; and absorption band with λ, ~275-305 nm have also been seen. Peaks at λ value ~305 - 400 nm have been completely disappeared. It shows some of the organic compounds were degraded/oxidized by the oxidant species (•OH, H_2O_2, and HOCl) generated during the EO process, and only large intensity band with λ, ~255-275 nm exist. From this study, it was concluded that there is no complete mineralization occurred and some new degraded compounds appeared during the continuous EO process.

GC- MS analysis: To explore the non-degraded and degraded compounds of textile effluent GC-MS analysis was performed. The list of identified compounds of untreated and treated textile wastewater is shown in Table 5.5.8 and 5.5.9. The identified compounds by GC-MS analysis of untreated wastewater are mostly aromatic in nature (Table 5.5.8). The wavelength range of these aromatic compounds is 200-275 nm, which supports the spectrophotometric analysis of untreated textile wastewater as shown in Fig. 5.5.8. The highest matching % and

maximum peak area were found for Dodecamethyl cyclohexasiloxane. It is used as a cleaning fluid for removing spots during textile processing (Table 5.5.8). GC-MS analysis of treated wastewater exhibited certain non-degradable compounds, which are produced during the EO process (Table 5.5.9). The presence of such compounds in treated textile wastewater has also been confirmed from the spectrophotometric analysis (Fig. 5.5.8). However, most of the dye components, which were detected in untreated textile wastewater were not detected in the treated textile wastewater GC-MS analysis (Table 5.5.9), confirming the oxidation/degradation of such compounds during the EO treatment process.

Except the coloring compounds, other compounds like Decamethyl cyclopentasiloxane, Trimethylsilyl 3,5-bis[(trimethylsilyl)oxy]benzoate, Adamantan-1-yl(phenyl)[(trimethylsilyl)oxy]acetonitrile, 3,3,5-Triethoxy-1,1,1,7,7,7-hexamethyl-5-(trimethylsilyloxy)tetrasiloxane, Tetra decamethyl cycloheptasiloxane, 1,1,1,3,5,7,9,11,11,11-Decamethyl-5-(trimethylsiloxy)hexasiloxane, Icosamethyl cyclodecasiloxane, Silicone oil are oxidize/degraded during EO treatment process (Table 5.5.8 and 5.5.9). These compounds contribute to TDS to the textile wastewater. The oxidation/degradation of these compounds can be confirmed from the reduction in TDS from 9640 to 1300 mg/*l* after the EO treatment.

Furthermore, comparative observation of Table 5.5.8 and 5.5.9 also elucidate that certain transformation/degradation compounds such as Butyl phthalate, Pyrrolidine etc. were produced during the EO treatment process, which show their existence in UV absorption band with λ, 250-275 nm (Fig. 5.5.8). Furthermore, textile wastewater contains high quantity of sodium chloride, therefore, during the EO process, various chlorinated compounds were generated during the indirect oxidation mediated by the chloro oxidant species (Cl_2, HOCl and ClO^-) as shown in Table 5.5.9. These chlorinated compounds have been reported to be toxic and carcinogenic.

Therefore, to confirm the acute toxicity of the treated textile wastewater due to the generation of such compounds, toxicity bioassay test was performed using standard procedure IS: 6582. Test organism for the acute toxicity bioassay test was *Aploclzeilus panchax*. These organisms are sensitive indicator species response to environmental contaminants. A test result showed 100% mortality rate within one-minute exposure of *Aploclzeilus panchax* with untreated wastewater, however, 100% mortality rate in one hour was observed for treated

textile effluent. Acute toxicity bioassay proves that the untreated textile wastewater is highly toxic and after treatment toxicity of textile wastewater is reduced. The EO treated wastewater is still lethal to the aquatic life, therefore, its disposal to the environment requires further treatments to further reduce the toxicity.

5.5.5 Degradation Mechanism

The oxidation/degradation mechanism was predicted on the basis of GC-MS analysis and spectrophotometric analysis. The presence of high molecular weight compounds containing silicon, carbon, hydrogen, oxygen and certain metal ions were observed (Table 5.5.8 and 5.5.9). The degradation process and oxidation of organic matters in the EO process depend upon the anode material and electrolyte. From the above study and GC-MS analysis, three types of degradation/oxidation method were observed for the degradation of textile wastewater: direct anodic degradation (*$^{\bullet}$OH mediated oxidation)*, indirect anodic degradation (chloro-oxidants mediated oxidation), and cathodic reduction. The probable mechanism of the EO treatment method of textile wastewater has been shown in Fig 5.5.9. Direct anodic degradation or *$^{\bullet}$OH mediated oxidation* refers to the direct contact of degrading organic matter and transfer of electrons from anode to the degrading matter. On the other hand, indirect anodic degradation does not require direct contact of pollutants with anode material. The reactive oxygen species can be physisorbed and chemisorbed to degrade the pollutants.

Direct Oxidation: Real Textile wastewater was rich with chloride content, and the optimal pH for the process was found ≈ 5.5, therefore, Cl_2, ClO^- and HOCl species were actively participate in the degradation process as discussed above. It was observed that some of the compounds of untreated wastewater like Decamethyl cyclopentasiloxane, Trimethylsilyl 3,5-bis[(trimethylsilyl)oxy]benzoate, Adamantan-1-yl(phenyl)[(trimethylsilyl)oxy]acetonitrile, (5R,7R,8E,10E)-2,2,3,3,5,15,15,16,16-Nonamethyl-4,14-dioxa -3,15-disilaheptadeca-8,10-dien-7-ol, 3,3,5-Triethoxy-1,1,1,7,7,7-hexamethyl-5-(trimethylsilyloxy)tetrasiloxane, 3-Isopropoxy-1,1,1,7,7,7-hexamethyl-3,5,5-tris(trimethylsiloxy)tetrasiloxane, 1,1,1,3,5,7,9,11,11,11-Decamethyl-5-(trimethylsiloxy)hexasiloxane, Octadecamethyl cyclononasiloxane, Icosamethylcyclodecasiloxane, Iron monocarbonyl 1,3 butadiene 1,4, dicarbonic acid diethyl ether, Silicone oil, Hexadecamethyl heptasiloxane were completely oxidized with production of some transformation compounds such as Dibutyl phthalate,

Pyrrolidine and 2-Ethoxy-2-oxoethyl ethyl phthalate by partial oxidation via equation 5.3.11 and 5.3.12.

Indirect Oxidation: Further, the transformed products produced via equation 8 and 9 were attacked by chlorine species, and transformed to toxic chlorinated -compounds such as Neopentylchloride, Chlorinated cyclopentane and 1, 5-Dichlorinated pentane via indirect oxidation (equation 5.5.11 and 5.5.12). It was confirmed from the spectrophotometric analysis with λ in the absorption band of 200-275 nm, which represent the presence of phthalates, chlorinated -compounds and alcohols in treated textile wastewater. Therefore, it can be claimed that complete mineralization didn't occur during the continuous EO process. Further, transformation products are produced during the EO due to the deficiency of ˙OH and mediated oxidation by various chlorine species.

$$RuO_2.(^{\bullet}OCl)_{ads} + R \rightarrow RO + \text{chlorinated -compounds} + RuO_2 \quad \textbf{(5.5.11)}$$

$$R + HOCl \rightarrow nCO_2 + mH_2O + \text{chlorinated -compounds} \quad \textbf{(5.5.12)}$$

At the cathode, chemisorbed hydrogen due to the hydrolysis of water reduces (Goyal et al. 2017) Adamantan-1-yl(phenyl)[(trimethylsilyl)oxy]acetonitrile, (5R,7R,8E,10E)-2,2,3,3,5,15,15,16,16-Nonamethyl-4,14-dioxa-3,15-disilaheptadeca-8,10-dien-7-ol, 3,3,5-Triethoxy-1,1,1,7,7,7-hexamethyl-5-(trimethylsilyloxy)tetrasiloxane and 3-Isopropoxy-1,1,1,7,7,7-hexamethyl-3,5,5-tris(trimethylsiloxy)tetrasiloxane into 3-Ethoxy-1,1,1,7,7,7-hexamethyl-3,5,5-tris(trimethylsiloxy)tetrasiloxane.

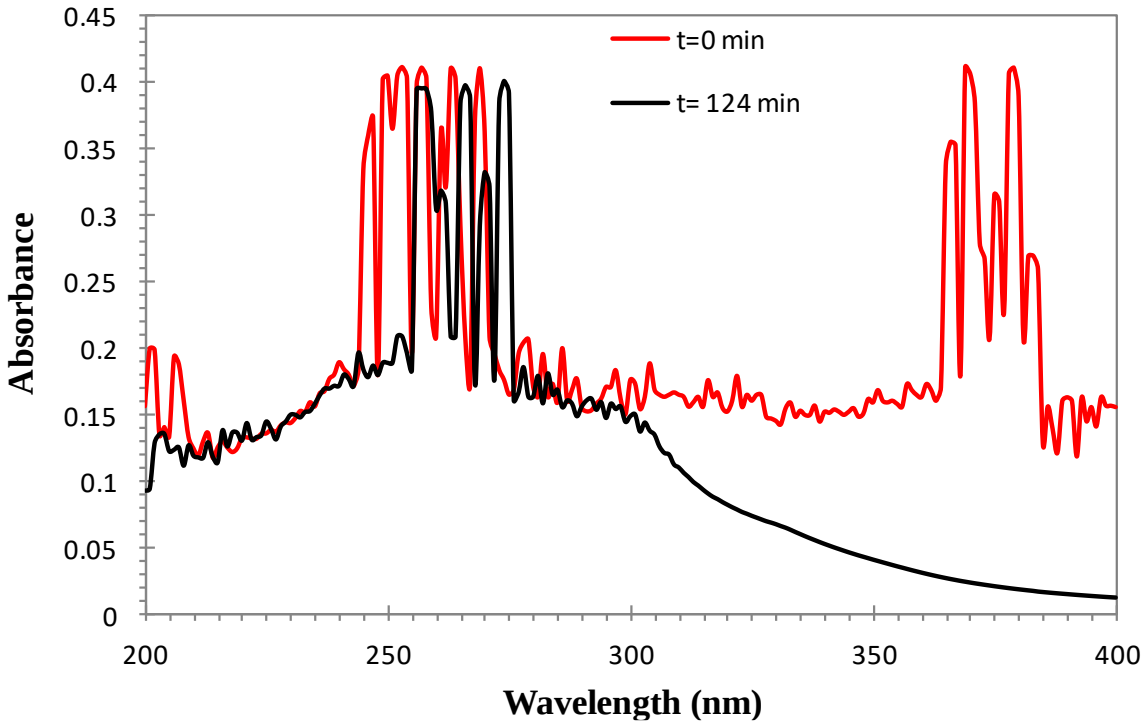

Fig 5.5.8. UV Visible spectra of untreated (*t*=0 min) and treated *(t*= 124 min) textile wastewater by continuous EO at optimum condition.

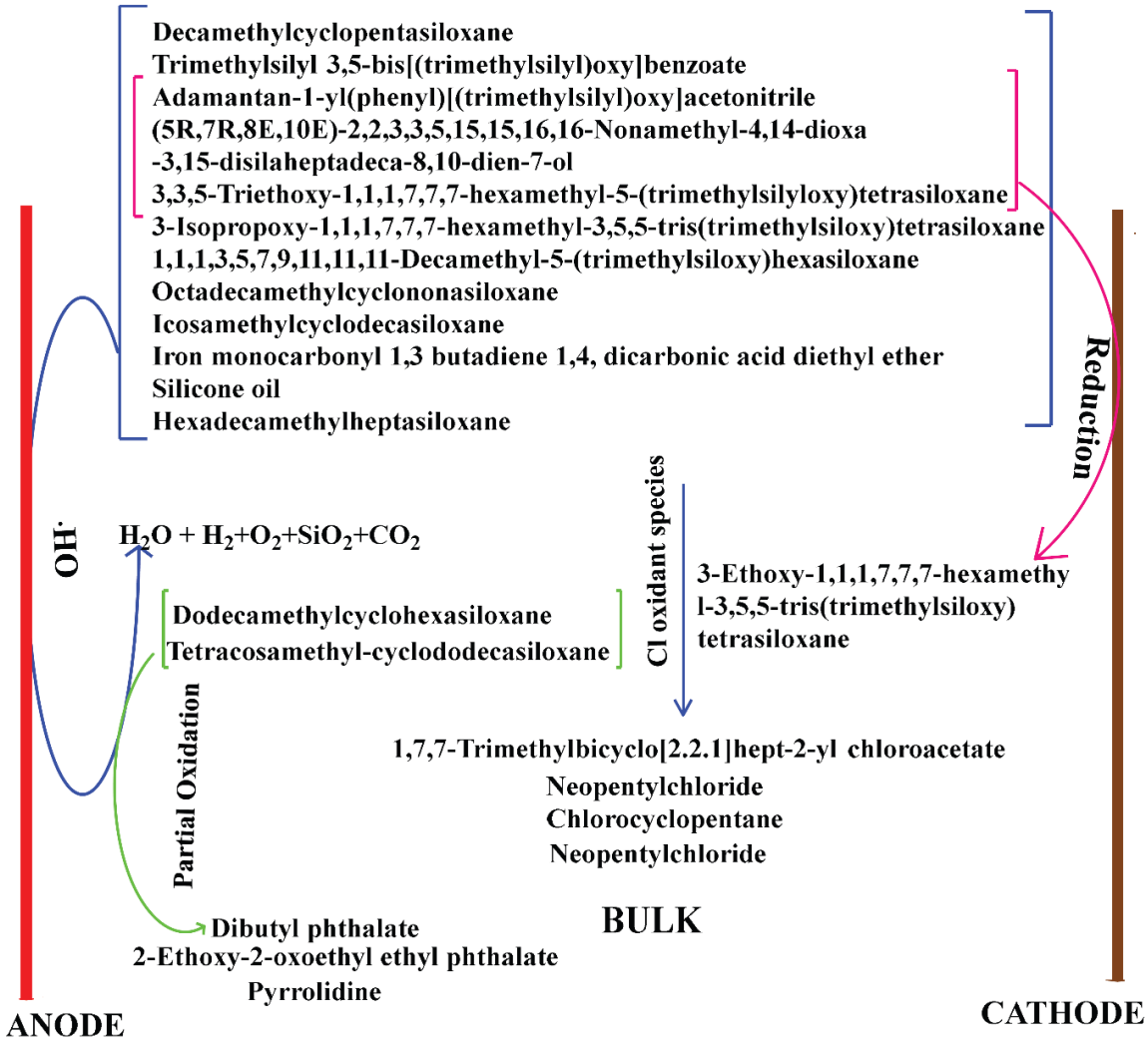

Fig 5.5.9. Persuasive mechanism for the degradation of textile wastewater by continuous EO process

Table 5.5.8. GC-MS analysis of untreated Textile wastewater by continuous EO process

Compound	Retention Time	Molecular Mass	Matching %	Remark
Decamethylcyclopentasiloxane	10.40/10.50	370	89.50%	Finishing of textiles
Trimethylsilyl 3,5-bis[(trimethylsilyl)oxy]benzoate	12.38	370	86.70%	Anti-microbial agent
Adamantan-1-yl(phenyl)[(trimethylsilyl)oxy]acetonitrile	12.41	339	89.50%	Tailored lubrication
(5R,7R,8E,10E)-2,2,3,3,5,15,15,16,16-Nonamethyl-4,14-dioxa-3,15-disilaheptadeca-8,10-dien-7-ol	13.12/13.2	414.77	78.70%	Dye component
3,3,5-Triethoxy-1,1,1,7,7,7-hexamethyl-5-(trimethylsilyloxy)tetrasiloxane	13.26	474.917	79.80%	Softeners
Dodecamethylcyclohexasiloxane	13.86	444	96.40%	Used for cleaning textiles and r removing spots
Tetradecamethylcycloheptasiloxane	15.61	519	92.90%	
3-Octanol 2-[(R)-(4-methylphenyl)sulfinyl]-1-(trimethylsilyl)	15.61	340	90.10%	used as catalyst in the curing of exoxide resins and silane resins including highly fluorinated alkyl sulfonyl methane
3-Isopropoxy-1,1,1,7,7,7-hexamethyl-3,5,5-tris(trimethylsiloxy)tetrasiloxane	15.61	577	80.80%	Dye component
1,1,1,3,5,7,9,11,11,11-Decamethyl-5-(trimethylsiloxy)hexasiloxane	15.61	490	76.90%	odor control

Compound	Retention Time	Molecular Mass	Matching %	Remark
Benzoic acid, 2,4bis [(trimethyl silyl)oxy]-, trimethylsilyl ester	17.01	370	88.10%	It is used as pesticide or preservative for textile products or coloring component of basic dye
Tetracosamethylcyclododecasiloxane	17.01/18.17/19.20/20.31/21/22.60	888	85.8%/80.77%/86.20/86.90%/94%/92%	It is a component of fluorescent dye
Octadecamethylcyclononasiloxane	20.31/21	667	79.4%/83%	used in washing and cleaning products
Icosamethylcyclodecasiloxane	18.17/20.31	740	90.4%/86.90%	It is used as polishing and coating agents in textiles
Iron monocarbonyl 1,3 butadiene 1,4, dicarbonic acid diethyl ether	19.2	438	92.22%	Antifungal activity
Silicone oil	21/22.60	9999	89.6%/92.22%	Used in pump
Hexadecamethylheptasiloxane	22.6	532	84.30%	Used in polymer preparation

Table 5.5.9. GC-MS analysis of treated Textile wastewater by continuous EO process

Compound	Retention Time	Molecular Mass	Matching %	Remark
Neopentylchloride	3.61	106	69.2	Transformed products, Acute toxic
1,7,7-Trimethylbicyclo[2.2.1]hept-2-yl chlorinated acetate	3.61	230	65.60%	Transformed products, Toxic
Pyrrolidine	3.61	70	69.80%	Transformed products, natural alkaloids
Chlorinated cyclopentane	3.91	104	66.50%	Transformed products, Toxic
1,5-Dichlorinated pentane	5.75	140	65.80%	Transformed products, Toxic
(2R,3R)-2-[(R)-(4-Methylphenyl)sulfinyl]-1-(trimethylsilyl)-3-octanol	12.87	340	79.70%	Not Degraded
Dodecamethylcyclohexasiloxane	12.87	444	82.90%	Not Degraded
2-Ethoxy-2-oxoethyl ethyl phthalate	15.12	280	84%	Transformed products, non-toxic
3-Ethoxy-1,1,1,7,7,7-hexamethyl-3,5,5-tris(trimethylsiloxy)tetrasiloxane	15.12	562	74.20%	Transformed products, Toxic
Tetracosamethyl-cyclododecasiloxane	15.12/25.13	888	71.6%/85.90%	Not Degraded
Benzoic acid, 2,4-bis[(trimethylsilyl)oxy]-, trimethylsilyl ester	17.11/25.13	370	69.2%/81.40%	Not Degraded
Dibutyl phthalate	20.2/21	278	95.2%/92%	Transformed products

5.5.6 Kinetic Study

The experimental data obtained at the optimal condition of continuous EO was used to determine the order of the reaction. The experimental data were fitted to first order kinetic model for continuous EO process according to the rate equations 5.3.16 and 5.3.17.

The experimental data of continuous EO obtained at the optimum process conditions was fitted to the first order reaction kinetics as shown in Fig 5.5.10. Rate constant and R^2 values for X_1 and X_2 were observed to be 0.0127 min^{-1} and 0.0168 min^{-1}; and 0.99 and 0.99, respectively. It is evident, that color removal is faster than the COD removal. GC-MS analysis exhibited absence of coloring compounds in the treated textile wastewater which was earlier detected in untreated textile wastewater. However, due to some degraded/transformed compounds generation COD reduction was lower than color. It was also concluded from the degradation mechanism study and GC-MS analysis that toxic choro- compounds were generated during EO treatment process. GCMS analysis shows that there were certain compounds present in the treated textile effluent that was not oxidized during EO treatment process. The presence of these compounds affects the COD removal kinetic after 130 min of elapsed time. So, after 130 min of elapsed time COD removal kinetic was not follow first order of kinetic. In case of coloring component, the kinetics of color removal was not followed, kinetic of first order after 60 min of electrolysis time. Because color degradation was fast so, with in 60 min of electrolysis time most of the coloring components were eliminated. So, it was concluded that chloro- mediated oxidation was dominant in the case of EO treatment.

5.5.7 Cost Analysis of Continuous EO Treatment of Textile Wastewater

Operating cost analysis is a necessary component of every treatment process. Electrochemical treatment methods are electrical energy-dependent processes, so it necessary to determine its operating cost. The total operational cost consists of a number of costs but in the case of electrochemical treatment methods, electrodes and energy cost is most important. For the application of EO treatment method, operational cost is calculated in terms of per Kg of COD removal. The cost of specific electrical energy consumed and electrode required to remove one kg of COD from textile wastewater was calculated from the responses of

continuous EO experiment conducted (X_1 =81%, X_2=92.25% and X_3=10.88 kWh/kg of COD removed) at optimized parameters (*i*=1.37 A, t= 124 min and pH=5.45), and given below:

Specific electrical energy consumed = ~10.88 kWh/kg of COD removed

Electricity price in India, Punjab = ~ ₹ 5.00/kWh

Therefore, the cost of electrical energy consumed (C_E) = ₹ 54.4/kg of COD removed

In this study, two Ti/RuO_2 electrodes (dimension: 100 mm x 85 mm x 1.5 mm) of cost ₹ 2500.00 each were used. The manufacturer/supplier (Titanium Tantalum Products Limited, Chennai, India) specified the life of the electrodes 2.5 years at optimized condition (*i*=1.37 A, pH=5.45).

Since, at optimized condition 81% of COD is removed, therefore, the minimum cost of Ti/RuO_2 electrodes (C_{EL}) = ₹ 465.46/ kg of COD removed

Total operating cost (C_E + C_{EL}) = ₹ 519.86/ kg of COD removed

In the present study, the COD of collected wastewater (from a Mink Blanket manufacturing industry situated in Ludhiana, Punjab, India) was 1156 mg/l. Therefore, to treat textile wastewater by reducing the COD from 1.156 kg/m^3 to 0.231 kg/m^3 (as optimum %COD removal=81%) total operating cost (C_E + C_{EL}) in US$ is 8.66 $/ kg of COD removed.

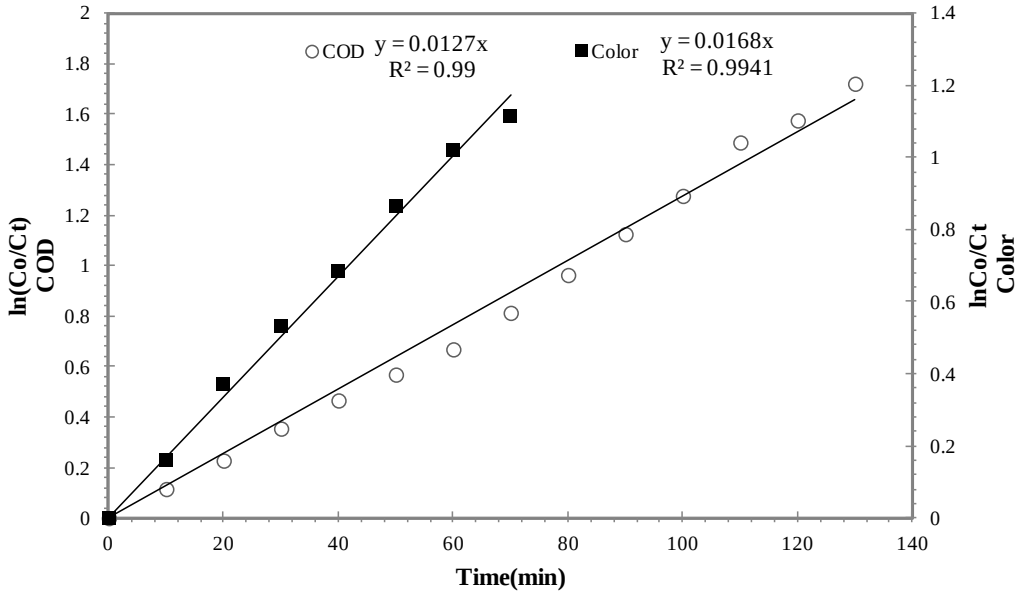

Fig 5.5.10. Kinetic of the COD and Color removal by Continuous EO process

5.6 STUDY OF CONTINUOUS EF TREATMENT PROCESS

5.6.1 Model Fitting and Statistical analysis

Experiments were designed using five level CCD under RSM. The four independent variables for continuous EF process such as elapsed time, *t* (15-175 min); retention time, R_T (50-230 min), current; *i* (0.25 - 3 A), and catalytic dose C_{Fe} (0.20 – 1.0 mM) were taken as input parameters, and % COD removal (X_1), % color removal (X_2) and energy consumed (X_3) as responses. Total 30 experiments suggested by RSM were conducted, and the calculated responses X_1, X_2 and X_3 are shown in Table 5.6.1. Further, experimental data were analyzed by multiple regression analysis of RSM. The quadratic model was suggested by exploiting sequential F-test and other adequacy measures. For the responses X_1, X_2 and X_3, the adequate precision indicated that the model is efficient and significant. Adequate precision expresses the signal to noise ratio, and adequate precision ratio above 4 shows that the model was efficient in navigating the design space. The model summary statistics for responses X_1, X_2 and X_3 showed a high value of the coefficient of determination. The values of R^2, Adjusted R^2 and predicted R^2 are shown in Table 5.6.2. It supports a satisfactory adjustment between the observed and predicted values for the selected responses as shown in Fig 5.6.1, 5.6.2 and 5.6.3 for X_1, X_2 and X_3, respectively. Quadratic model for continuous EF process was also supported by ANOVA with F- values of 36, 24 and 20.5 for the responses X_1, X_2, and X_3, respectively (Table 5.6.3a, b, c). The "Prob>F" smaller than 0.05 indicates, that the quadratic model and its terms are significant with a 95% confidence level. The significant terms of continuous EF for X_1: t, C_{Fe}, i, i^2, R_T^2, C_{Fe}^2, txR_T, and txi; X_2: t, R_T, i, t^2, $R_T{}^2$, i^2, C_{Fe}^2, R_T xC_{Fe},and ixC_{Fe}; X_3= t, i, t^2, i^2, txR_T, txC_{Fe}, R_T x C_{Fe},and ixC_{Fe} were observed from the ANOVA (Table 5.6.3a, b, c).The quadratic model equation obtained in terms of significant process parameters for continuous EF is given below.

$$X_1 = 71.82 + 11.69t + 5.65i - 5.2C_{Fe} - 2.72R_T^2 - 7.55i^2 - 4.97C_{Fe}^2 - 2.45(t \text{x} R_T) - 2.60(t \text{ x } i) \quad \textbf{(5.6.1)}$$

$$X_2 = 92.53 + 9.14t - 2.07R_T + 2.33i - 7.39t^2 - 5R_T^2 - 3.96i^2 - 3.2C_{Fe}^2 + 6.32(R_T \text{ x} C_{Fe}) + 3.77(i \text{ x } C_{Fe}) \quad \textbf{(5.6.2)}$$

$$X_3 = 0.017 + 0.003t + 0.0034\, i - 0.0021\, t^2 - 0.00152\, i^2 - 0.0016\, (t \text{ x } R_T) - 0.0026\, (t \text{ x } C_{Fe}) + 0.0013\, (R_T \text{ x } C_{Fe}) + 0.0012\, (i \text{ x } C_{Fe}) \quad \textbf{(5.6.3)}$$

Table 5.6.1. Experimental design for the continuous electro-Fenton process

Standard Order	*t (min)*	*i (A)*	C_{Fe}	R_T *(min)*	X_1		X_2		X_3	
					$X_{1\ exp}$	$X_{1\ pre}$	$X_{2\ exp}$	$X_{2\ pre}$	$X_{3\ exp}$	$X_{3\ pre}$
29	95	1.25	0.6	150	73.58	71.82	94.13	92.53	0.015	0.017
23	95	1.25	0.2	150	57.00	62.32	79.00	80.74	0.015	0.017
4	135	0.75	0.4	200	69.53	67.19	79.14	77.98	0.016	0.014
7	55	1.75	0.4	200	53.15	54.25	52.42	53.09	0.013	0.012
14	135	1.75	0.8	100	70.32	68.24	80.1	79.13	0.019	0.019
11	55	0.75	0.8	200	33.04	32.79	62.42	60.79	0.014	0.012
26	95	1.25	0.6	150	73.58	71.82	94.13	92.53	0.018	0.017
30	95	1.25	0.6	150	73.58	71.82	94.13	92.53	0.018	0.017
13	55	1.75	0.8	100	45.42	47.52	68.34	67.45	0.014	0.015
18	175	1.25	0.6	150	85.41	90.92	76.00	81.25	0.015	0.014
3	55	0.75	0.4	200	43.00	41.16	51.00	53.10	0.005	0.006
2	135	0.75	0.4	100	81.78	76.55	99.15	94.66	0.019	0.019
10	135	0.75	0.8	100	60.05	58.71	72.52	69.80	0.010	0.011
6	135	1.75	0.4	100	80.63	80.65	89.33	88.91	0.022	0.023
8	135	1.75	0.4	200	73.18	69.88	77.17	76.23	0.020	0.019
21	95	0.25	0.6	150	27.00	30.33	68.82	72.04	0.003	0.004
20	95	1.25	0.6	250	57.12	58.14	70.80	68.37	0.019	0.019
12	135	0.75	0.8	200	54.07	54.11	78.54	78.42	0.009	0.010
27	95	1.25	0.6	150	73.58	71.87	94.13	92.53	0.015	0.017
17	15	1.25	0.6	150	45.54	44.17	49.05	44.69	0.0009	0.002
22	95	2.25	0.6	150	52.14	52.95	83.67	81.35	0.018	0.018
19	95	1.25	0.6	50	60.61	63.72	73.34	76.66	0.018	0.017
16	135	1.75	0.8	200	63.19	62.23	92.36	91.74	0.019	0.020
9	55	0.75	0.8	100	28.22	27.60	54.32	56.39	0.006	0.006
25	95	1.25	0.6	150	70.58	71.82	94.13	92.53	0.018	0.017
24	95	1.25	1	150	42.72	41.54	79.49	78.64	0.019	0.019
5	55	1.75	0.4	100	59.19	55.23	68.74	69.99	0.010	0.009
28	95	1.25	0.6	150	66.03	71.82	84.54	92.53	0.019	0.017
1	55	0.75	0.4	100	40.00	40.73	75.42	73.99	0.007	0.005
15	55	1.75	0.8	200	50.00	51.31	70.22	75.84	0.023	0.023

Table 5.6.2. Various R-squared values for responses %COD removal (X_1), % Color removal (X_2) and energy consume (X_3) for continuous EF

Responses	R-Squared	Adj R-Squared	Pred R-Squared
X_1	0.97	0.95	0.95
X_2	0.94	0.92	0.90
X_3	0.86	0.81	0.79

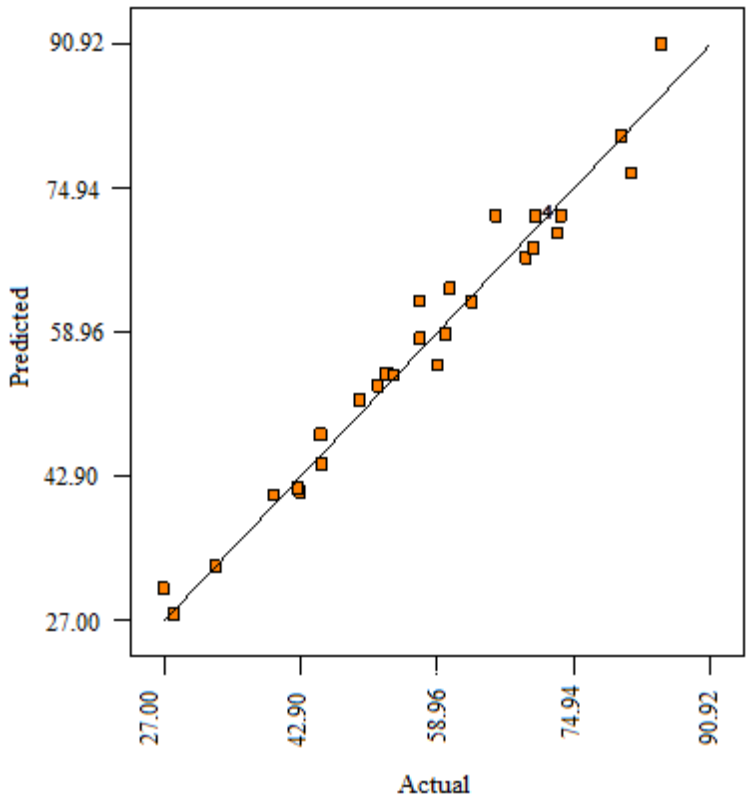

Fig 5.6.1. Predicted versus actual %COD removal (X_1) for continuous EF process

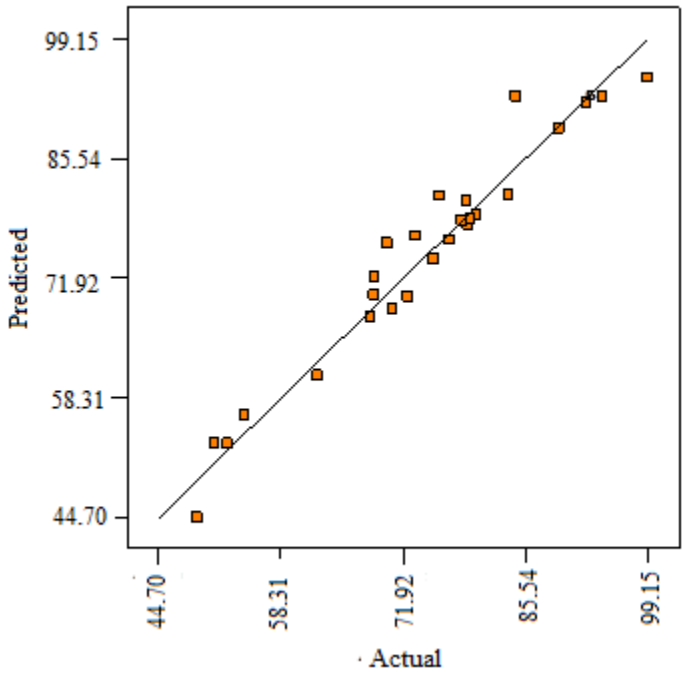

Fig 5.6.2. Predicted versus actual for %Color removal (X_2) of continuous EF process

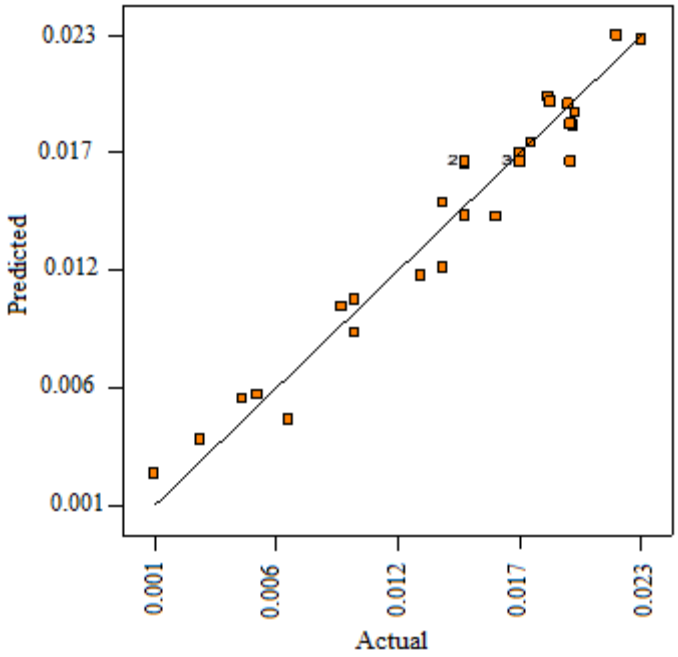

Fig 5.6.3. Predicted versus actual for energy consumed (X_3) of continuous EF process

Table 5.6.3a. ANOVA for the %COD removal of continuous EF process

Source	Sum of Squares	DF	Mean Square	F-Value	Prob > F
Model	7055.10	14	503.90	36	< 0.0001
T	3277.60	1	3277.60	234.20	< 0.0001
R_T	46.50	1	46.60	3.30	0.0881
I	766.90	1	766.90	54.80	< 0.0001
C_{Fe}	648.00	1	648.00	46.30	< 0.0001
t^2	31.30	1	31.30	2.20	0.1552
$R_T{}^2$	203.20	1	203.20	14.50	0.0017
i^2	1561.60	1	1561.50	111.50	< 0.0001
$C_{Fe}{}^2$	678.30	1	678.30	48.40	< 0.0001
t x R_T	95.80	1	95.90	6.90	0.0194
t x i	108.20	1	108.20	7.70	0.0140
t x C_{Fe}	22.20	1	22.20	1.60	0.2275
R_T x i	1.90	1	1.90	0.10	0.7120
R_T x C_{Fe}	22.60	1	22.60	1.60	0.2228
i x C_{Fe}	29.40	1	29.50	2.10	0.1674
Residual	209.90	15	13.90		
Lack of Fit	162.40	10	16.20	1.70	0.2875
Pure Error	47.50	5	9.50		
Cor Total	7265.00	29			

Table 5.6.3b. ANOVA for the % Color removal of continuous EF process

Source	Sum of Squares	DF	Mean Square	F-Value	Prob > F
Model	5354.60	14	382.50	24	< 0.0001
t	2004.40	1	2004.40	125.90	< 0.0001
R_T	103.00	1	103.00	6.50	0.0224
i	130.10	1	130.10	8.20	0.0119
C_{Fe}	6.60	1	6.60	0.40	0.5298
t^2	1497.40	1	1497.40	94.10	< 0.0001
$R_T{}^2$	686.40	1	686.40	43.10	< 0.0001
i^2	429.80	1	429.80	27	0.0001
$C_{Fe}{}^2$	282.40	1	282.40	17.70	0.0008
t x R_T	17.80	1	17.80	1.10	0.3071
t x i	3.00	1	3	0.20	0.6694
t x C_{Fe}	52.50	1	52.50	3.30	0.0893
R_T x i	15.90	1	15.90	1	0.3328
R_T x C_{Fe}	639.70	1	639.70	40.20	< 0.0001
i x C_{Fe}	227.00	1	227.00	14.30	0.0018
Residual	238.70	15	15.90		
Lack of Fit	162.10	10	16.20	1.10	0.5073
Pure Error	76.60	5	15.30		
Cor Total	5593.30	29			

Table 5.6.3c. ANOVA for the energy consumed of continuous EF process

Source	Sum of Squares	DF	Mean Square	F-Value	Prob > F
Model	9.3 $X10^{-4}$	14	6.6 $X10^{-5}$	20.50	< 0.0001
T	2.2 $X10^{-4}$	1	2.2 $X10^{-4}$	68.60	< 0.0001
R_T	8.4 $X10^{-6}$	1	8.4 $X10^{-6}$	2.60	0.1270
I	2.9$X10^{-4}$	1	2.9 $X10^{-4}$	90.50	< 0.0001
C_{Fe}	5.4 $X10^{-6}$	1	5.4 $X10^{-6}$	1.70	0.2142
t^2	1.3 $X10^{-6}$	1	1.3 $X10^{-4}$	39.60	< 0.0001
$R_T{}^2$	4.5 $X10^{-6}$	1	4.5 $X10^{-5}$	1.40	0.2541
i^2	6.3 $X10^{-5}$	1	6.3 $X10^{-5}$	19.70	0.0005
$C_{Fe}{}^2$	1.2 $X10^{-6}$	1	1.2 $X10^{-6}$	0.40	0.5561
t x R_T	3.9 $X10^{-5}$	1	3.9 $X10^{-7}$	12.30	0.0031
t x i	7.2 $X10^{-5}$	1	7.2 $X10^{-7}$	0.20	0.6424
t x C_{Fe}	1.1 $X10^{-4}$	1	1.1 $X10^{-4}$	33.60	< 0.0001
R_T x i	2.7 $X10^{-6}$	1	2.7 $X10^{-6}$	0.80	0.3722
R_T x C_{Fe}	2.5 $X10^{-5}$	1	2.5 $X10^{-5}$	7.80	0.0138
i x C_{Fe}	2.5 $X10^{-5}$	1	2.5 $X10^{-5}$	7.60	0.0146
Residual	4.8 $X10^{-5}$	15	3.2 $X10^{-6}$		
Lack of Fit	3.2 $X10^{-5}$	10	3.2 $X10^{-6}$	1	0.5571
Pure Error	1.7 $X10^{-5}$	5	3.3 $X10^{-6}$		
Cor Total	9.7 $X10^{-4}$	29			

5.6.2 Effect of Continuous EF Parameters and Optimization

The interactive effect of parameters *i*, *t*, R_T and C_{Fe} for the X_1 is represented in Fig. 5.6.4 a, b & c. It has been seen that at the higher and lower values of *i*, X_1 was found always decreasing. A sharp increase in X_1 with increasing t can be observed with the rise in i from 0.25 to ≈1.25 A. However, for i=1.25 A, at steady state (t=140 min), showed maximum X_1 (Fig. 5.6.4a). The effect of increasing C_{Fe} with increased *i* on the X_1 is shown in Fig 5.6.4b. Increasing C_{Fe} from 0.2 mM to 0.4 mM increases the X_1 at all *i* values, and decreased sharply for all C_{Fe} > 0.4 mM. Increasing i increases the X_1up to 1.25 A, and for i>1.25 A, X_1 decreased sharply. Fig. 5.6.4c illustrates that the X_1 increases with increasing R_T value, however, X_1 is marginally affected for higher R_T values. R_T and t were crucial parameters for continuous EF treatment process, it has been clearly seen that X_1 was increasing with the increase in R_T up to ≈140 min. Thereafter, X_1 was decreasing with the increase in R_T at all the t values. Therefore, a steady state can be achieved at t≈140 min.

The influences of parameters i, t, R_T and C_{Fe} on the X_2 are also illustrated in Fig. 5.6.5 a, b & c. A similar trend of effects of these parameters on X_2 was observed as on X_1. Fig. 5.6.5a shows the interaction of C_{Fe} and i on the X_2. It can be observed that X_2 is increasing for 0.2 mM<C_{Fe}< 0.4 mM, however, for all C_{Fe}> 0.4 mM, it is decreasing. This effect of increasing C_{Fe} on X_2 was found true for all i values. Further, increasing i up to i=1.25 A, X_2 was found increasing and was observed decreasing beyond 1.25 A. Fig. 5.6.5b shows the interaction of C_{Fe} and R_T on the X_2. Similar to X_1, X_2 was also observed increasing with the R_T values up to R_T≈140 min. Beyond R_T≈140 min, X_2 was observed decreasing sharply. This was found true at all C_{Fe} values. In Fig. 5.6.5c, it can be seen that the increasing t increases the X_2 up to t≈135 min, and beyond this the change in X_2 is marginal. This was true for all R_T values. However, at any t value, increasing R_T value first increases the X_2 up to ≈ 140 min and then starts decreasing beyond 140 min of R_T value.

Fig. 5.6.6a & b attributed that energy consumption is minimum at the steady state. In the higher range of R_T, X_3 was increasing with the increase in t. X_3 was also increased with the increase in *i* at all the t values as shown in Fig. 5.6.6b.

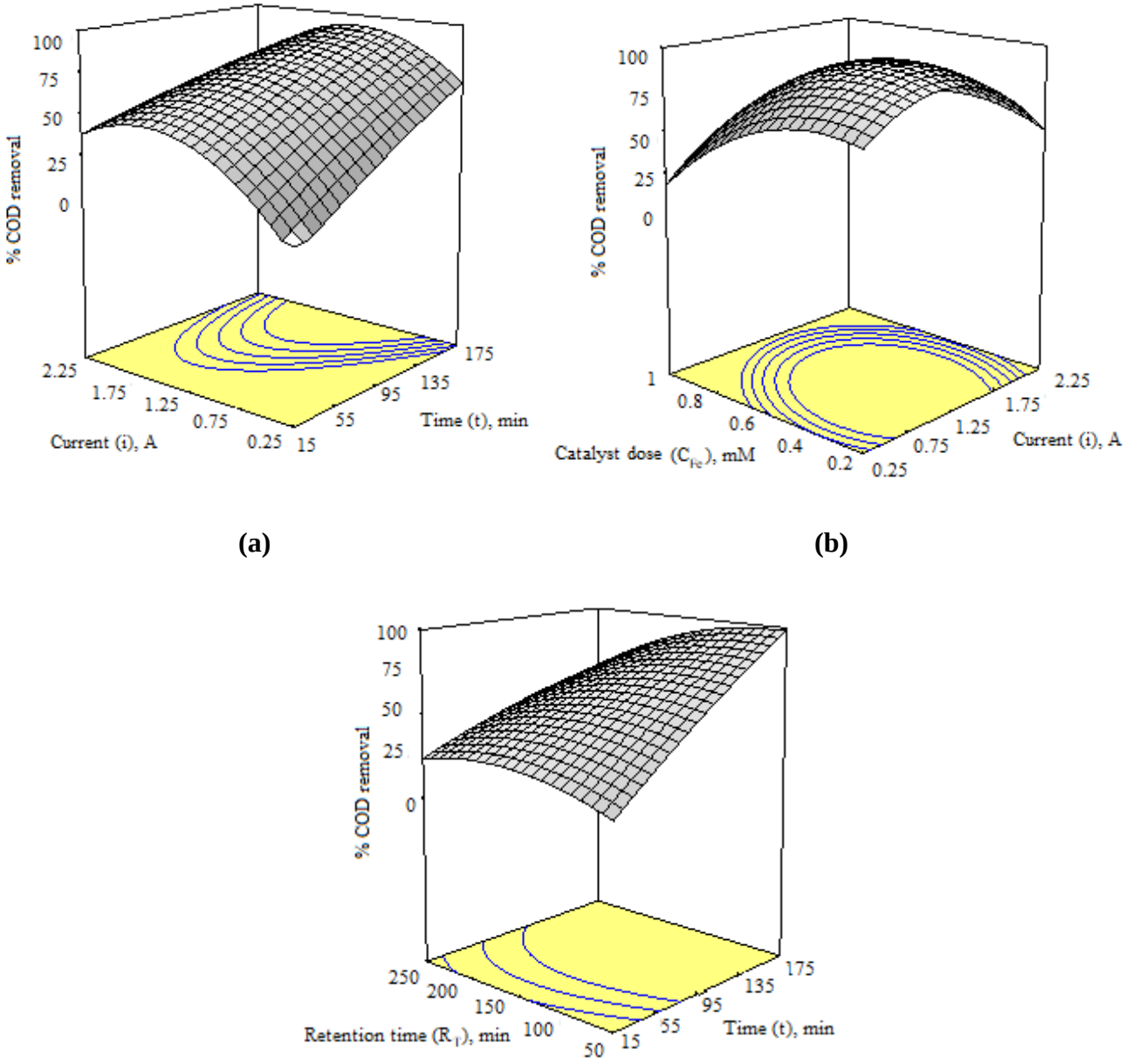

Fig 5.6.4. 3D response surface for the continuous EF of textile wastewater (a) %COD removal versus i and t (b) %COD removal versus C_{Fe} and i (c) %COD removal versus t and R_T

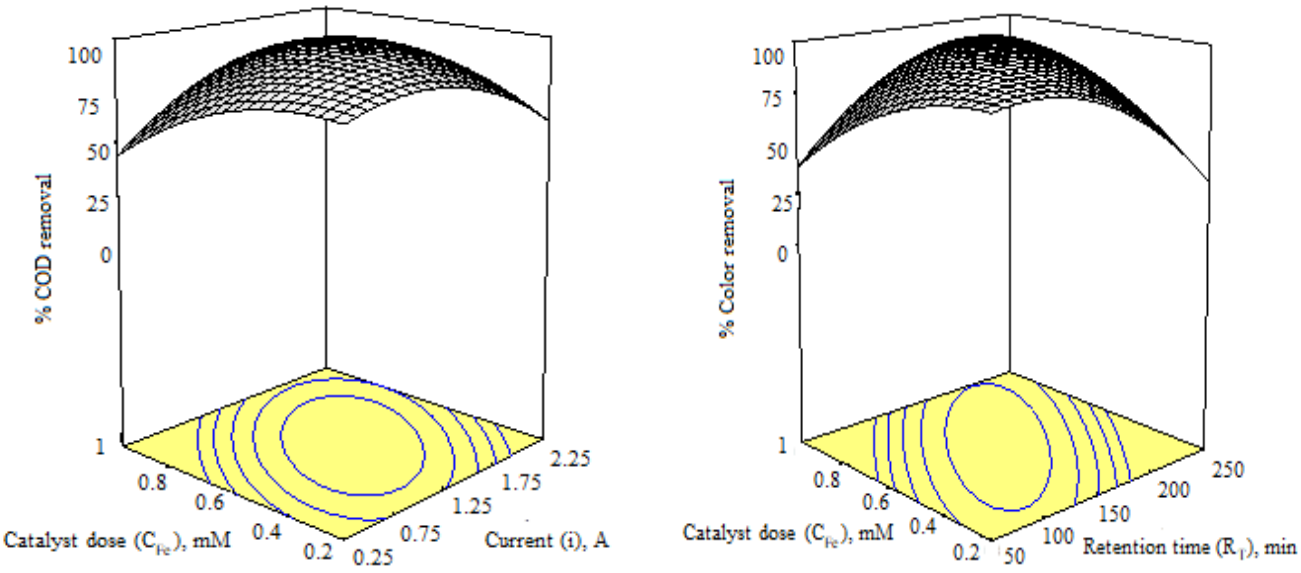

(a) **(b)**

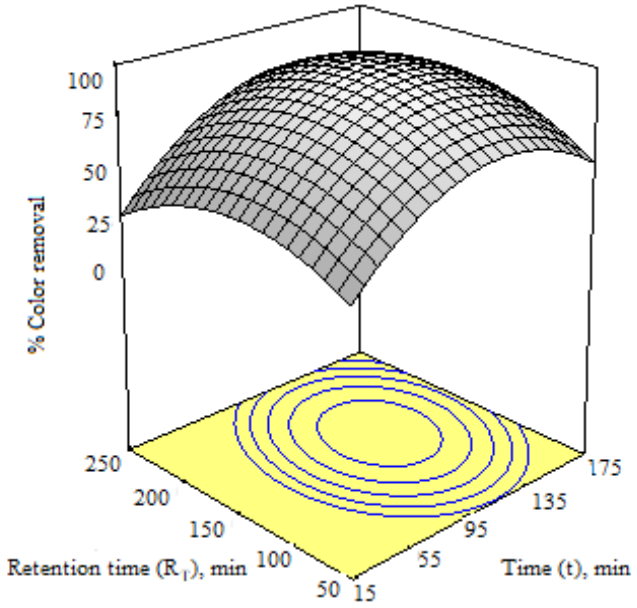

(C)

Fig 5.6.5. 3D response surface for the continuous EF of textile wastewater (a) %Color removal versus C_{Fe} and *i* (b) %Color removal versus C_{Fe} and R_T (c) %Color removal versus *t* and R_T

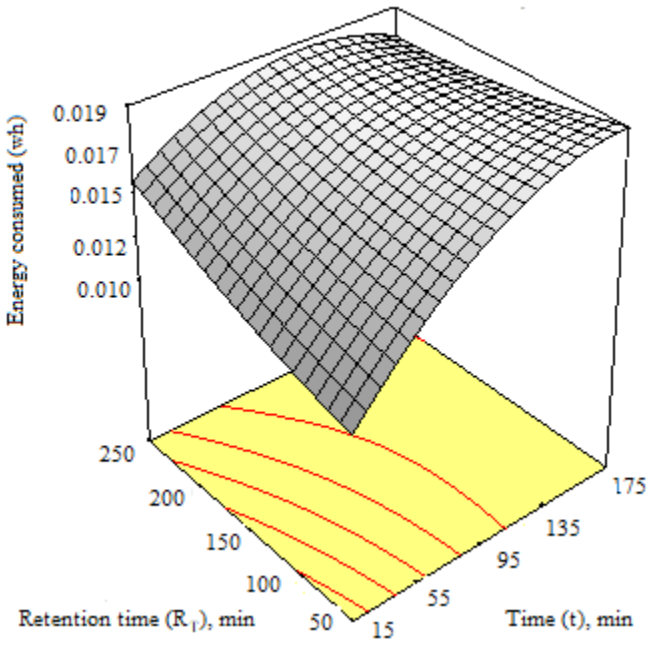

(a)

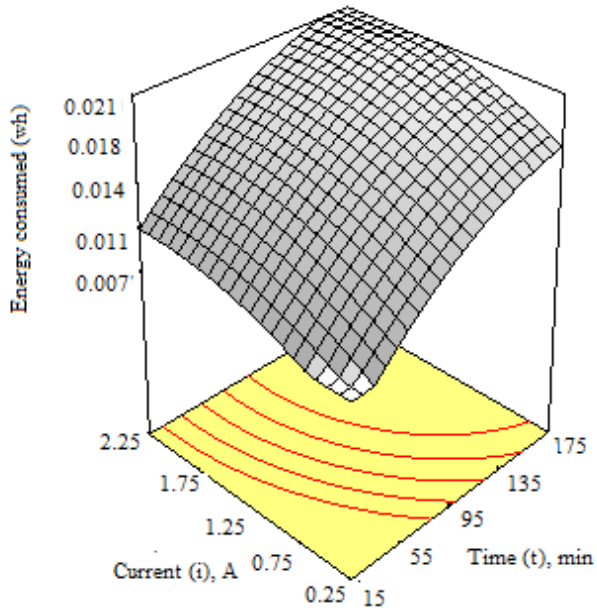

(b)

Fig 5.6.6. 3D response surface and contour plots for the EF of real textile wastewater (a) Energy consume versus *t* and R_T (b) Energy consumed versus *i* and *t*

Investigation of interaction parameters asserted that •*OH mediated direct oxidation* and chloro-oxidants (generated via equation 5.6.4-5.6.10) mediated indirect oxidation (Sirés et al., 2014; Brillas et al., 2004), since textile wastewater was rich of chloride ions, was responsible for the expulsion of COD and color at the steady state condition. The •OH generated at the anode is adsorbed on the surface of anode via equation 5.6.4, and the COD/color is reduced through oxidation via equation 5.6.5 and 5.6.6.

$$Ti/RuO_2 + H_2O \rightarrow Ti/RuO_2(\bullet OH) + H^+ + e^- \quad (\mathbf{5.6.4})$$

$$COD/color + Ti/RuO_{2+1} \rightarrow (COD/color) - O + Ti/RuO_2 \quad (\mathbf{5.6.5})$$

$$COD/color + Ti/RuO_2(\bullet OH) \rightarrow CO_2 + H^+ + e^- + Ti/RuO_2 \quad (\mathbf{5.6.6})$$

$$2Cl^- \rightarrow Cl_2 + 2e^- \quad (\mathbf{5.6.7})$$

$$Cl_2 + H_2O \rightarrow HOCl + H^+ + Cl^- \quad (\mathbf{5.6.8})$$

$$COD/Dye + HOCl/Cl_2 \rightarrow \text{chlorinated organic compounds (COC)} + H_2O \quad (\mathbf{5.6.9})$$

$$COC + Ti/RuO_2(\bullet OH) \rightarrow CO_2 + H^+ + e^- + Ti/RuO_2 + Cl^- \quad (\mathbf{5.6.10})$$

The steady state of a continuous EF reactor for textile wastewater was attained at ≈2.3 hr of elapsed time for COD removal and 2.1 hr for color removal. It implied that color removal was a rapid process, which indicates that coloring components of the dyes degraded into colorless organic and inorganic products, and further degradation was followed by •*OH mediated oxidation*. COD removal was lacking behind because of high bond dissociation energy of colorless organic and inorganic products. It was evident that, increasing R_T after ≈ 142, disturbs the steady state profile so, X_1 and X_2 decreases (Korbahti et al., 2009). It can also be concluded that due to the disturbance of steady-state steric hindrance between the reaction molecules increases. It ultimately affected the degradation process. C_{Fe} and i were a significant parameters in the EF process. C_{Fe} >5.5 at i>1.01, influences the negative impact on the electro-chemical reaction, because of scavenged hydroxyl radicals and generation of hydroperoxyl radicals (Equation 5.6.11) (Brillas et al., 2009), which have low oxidation power. Increase in i and at higher C_{Fe}, in the wastewater also enhanced the competitive reaction between the hydroxyl ions and the ferrous ion which could decline the X_1 & X_2 process. (Equation 5.6.11-5.6.12).

$$Fe^{2+} + {}^{\bullet}OH \rightarrow HO_2^{\bullet} + Fe^{2+} \quad \textbf{(5.6.11)}$$

$$Fe^{2+} + {}^{\bullet}OH \rightarrow Fe^{3+} + OH^{-} \quad \textbf{(5.6.12)}$$

It was proclaimed that COD and color removal were due to •*OH mediated oxidation* on the surface of Ti/RuO_2 anode and mediated oxidation by Cl_2 and HOCl. Chloro-mediated oxidation attributed chlorinated organic compounds, which further undergo •*OH mediated oxidation* in the bulk. The energy consumption (X_3) in continuous EF process was relatively increased at low R_T and the minimum X_3 was obtained for 2.3 hr of R_T. The EF reactor could be operated at optimum R_T for cost-driven purpose. Increase in i > 1.10 A disturbs steady state condition the X_3 increases.

The optimization of operating parameters with the responses (X_1, X_2 and X_3) for the treatment of real textile wastewater using EF process, multi-response optimization technique with desirability function was carried out (Equation 5.3.7). Optimization of the EF process was composed by the set of constraints as shown in Table 5.6.4.

$$d_{1=}\begin{cases} 0 & if\ X_1 \le 27 \\ [\frac{X_1 - 27}{100 - 27}] & if\ 27 < X_1 < 100 \\ 1 & if\ X_1 \ge 100 \end{cases} \quad \textbf{(5.6.13)}$$

Similar to equation 5.6.13, desirability for responses X_2 and X_3 were calculated by equation 5.6.14 and 5.6.15, respectively.

$$d_{2=}\begin{cases} 0 & if\ X_1 \le 49 \\ [\frac{X_2 - 49}{100 - 49}] & if\ 49 < X_1 < 100 \\ 1 & if\ X_1 \ge 100 \end{cases} \quad \textbf{(5.6.14)}$$

$$d_{3=}\begin{cases} 0 & if\ X_1 \le 0.0009 \\ [\frac{X_3 - 0.0009}{0.025 - 0.0009}] & if\ 0.0009 < X_1 < 0.025 \\ 1 & if\ X_1 \ge 0.025 \end{cases} \quad \textbf{(5.6.15)}$$

The most appropriate optimization condition was found to be t= 137 min *i*=1.10 A, R_T=142 min and C_{Fe}=0.55 mM, which showed the highest overall desirability, D = 0.8 as shown in Table 5.6.5. At this optimum condition, the X_1, X_2 and X_3 suggested by RSM under CCD were 85%, 94% and 17 kWh/kg of COD removed respectively. To verify the

acceptability of the optimization analysis, actual experiments were performed in duplicate and average values of responses X_1, X_2 and X_3 at the optimum condition was found to be 84.16%, 94% and 15 kWh/kg of COD removed, respectively, which were closer to the predicted values as shown in Table 5.6.6. It also demonstrates that modelling and optimization using RSM under CCD was successfully performed.

Furthermore, the pH of the textile wastewater was found to be increase with time. At the optimum condition of the EF treatment process (t= 137 min i=1.10 A, R_T=142 min and C_{Fe}=0.55 mM) pH of the textile effluent varies from 3 to 4.1 as shown in Fig 5.6.7. During the initial minutes of the treatment process, there was a sharp change in the pH. But after steady state equilibrium, it became constant at pH_f = 4.1. The shift of *pH* form more acidic towards less acidic pH can be attributed to the HO^- production due to water reduction at the cathode. The carboxylic acids were generated during the EF oxidation process (Oturan and Aaron, 2014). The sharp change in the pH is mainly due to the counterbalancing of proton consumed during the Fenton reaction by the protons produced via water oxidation at the anode (El-Desoky et al., 2010). Aeration during the EF treatment process can be contributed in the stabilization of acidic pH range. As textile wastewater was rich in chloride ions and favourable for the generation of chloro-oxidant species. The chloro-oxidant species did not dominate in case of EF. So, it is also supported that chloro- compounds generation is negligible during EF treatment. To the point of view of disposal, the verification of generated compounds is necessary.

Table 5.6.4. Constraints applied for optimization of continuous electro-Fenton of textile wastewater

Variables	Goal	Lower Limit	Upper Limit
t (min)	is in range	15	175
R_T (min)	is in range	15	250
i (A)	is in range	0.25	2.25
C_{Fe} (mM)	is in range	0.2	1
X_1	Maximize	27	100
X_2	Maximize	49.05	100
X_3	Minimize	0.0009	0.025

Table 5.6.5. Individual and synchronised (maximization of X_1 and X_2 and minimization of X_3) optimization

Individual response optimization					
Response	***C_{Fe}(mM)***	***t* (min)**	***i* (A)**	***R_T* (min)**	**Desirability**
X_1=89.2%	0.30	154.53	1.41	103.44	1.00
X_2= 99%	0.20	126.40	0.81	76.18	1.00
X_3= 12 kWh/kg of COD removed	0.71	146.13	0.26	222.67	1.00
Synchronised optimization of responses					
X_1=83.60% X_2= 94.00% X_3=17 kWh/kg of COD removed	0.55	137	1.10	141.70	0.8

Table 5.6.6. Correlation of experimental and predicted responses at optimized condition

Responses	Predicted value	Experimental value
% COD removal (X_1)	85.00%	84.16%
% Color removal (X_2)	94.00%,	94.00%
Energy consumed (X_3)	17 kWh/kg of COD removed	15 kWh/kg of COD removed

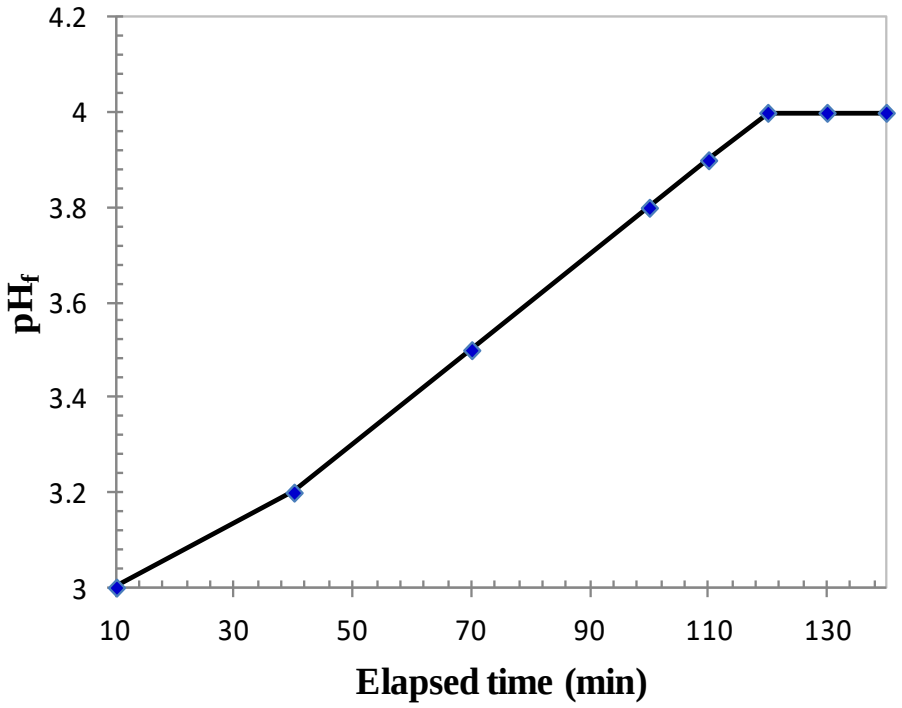

Fig 5.6.7. Graph of *t* versus pH_f for the EF treatment of Textile wastewater at optimum condition

5.6.3 Transformation Products and Treated Effluent Quality

Disposability study was performed by identifying the transformation products in treated wastewater and compounds/organics originally present in untreated textile wastewater through spectrophotometric and GC-MS analysis. Also, the bioassay test was performed to test the toxicity of treated wastewater.

Spectrophotometric analysis: Spectrophotometric analysis showed that all the compounds of the textile wastewater were degraded but certain new transformed compounds were observed in the range of λ, ~280-345 shown in Fig. 5.6.8. Low-intensity peaks can be seen with λ, ~280-310 nm and λ, ~330-345 nm. Sharp peaks of high absorption intensity with λ, ~310-330 nm can be seen. Further, there was a radicle change in the absorption spectra of treated textile wastewater at t=137 min showed there were no high-intensity peaks with λ, 200-280 nm and ~350-400 nm. After EF treatment all aromatic compounds were eliminated. Small intensity peaks were observed at λ, ~280-315 nm and were generated during the EF process indicating the degradation of compounds.

GC- MS analysis: To explore the non-degraded and degraded compounds of textile effluent GC-MS analysis was performed. The list of identified compounds of untreated and treated textile wastewater is shown in Table 5.5.8 and 5.6.7. The identified compounds by GC-MS analysis of untreated wastewater were mostly aromatic in nature (Table 5.6.7) and their range was of 200 to 275 nm, which supports the spectrophotometric analysis of untreated textile wastewater as shown in Fig. 5.6.8. The highest matching% was shown for 3,4-dihydro-4-(1,3-dioxolan-2-yl)-5,7-dimethoxy-1(2H)-benzopyran-2-one and its peak area was also maximum λ, ~308. The spectrophotometric range of polyaromatic compounds was 238-310 ranges (Fig. 5.6.8) and also identified in GC-MS analysis as shown in Table 5.6.7.

Since real textile wastewater bears high chloride concentration, therefore, toxic and carcinogenic chlorinated organic compounds may possibly be generated during the EF process via equation 5.6.7-5.6.9. GC-MS analysis of treated wastewater identifies four different types of non-chlorinated organic transformation compounds (Dibutyl phthalate, 5,7-Dimethoxy-2,3-dihydro-4H-chromen-4-one, 1-acetamidoadamantane, Tetradecamethylcycloheptasiloxane), which were not originally present in untreated textile

wastewater (Table 5.5.8). Therefore, the treated textile wastewater is free from the toxic and carcinogenic chlorinated organic compounds.

However, from the point of view of disposability, it is necessary to evaluate the toxicity of the treated textile wastewater bioassay for acute toxicity towards possible toxic transformation/degraded compounds (Table 5.6.7). For this purpose, standard procedure IS: 6582 with *Aploclzeilus panchax* organism was followed. *Aploclzeilus panchax* organisms are sensitive responders to the water contamination. A test result for the untreated textile wastewater showed 100% mortality within one minute, however, for treated wastewater 0% mortality was observed in 96 hours. Acute toxicity bioassay test proved that the untreated textile wastewater was highly toxic and lethal if disposed to water bodies. However, toxicity was sufficiently reduced for EF treated textile wastewater indicating transformation products in treated wastewater are not acutely toxic and can be safely disposed in the environment.

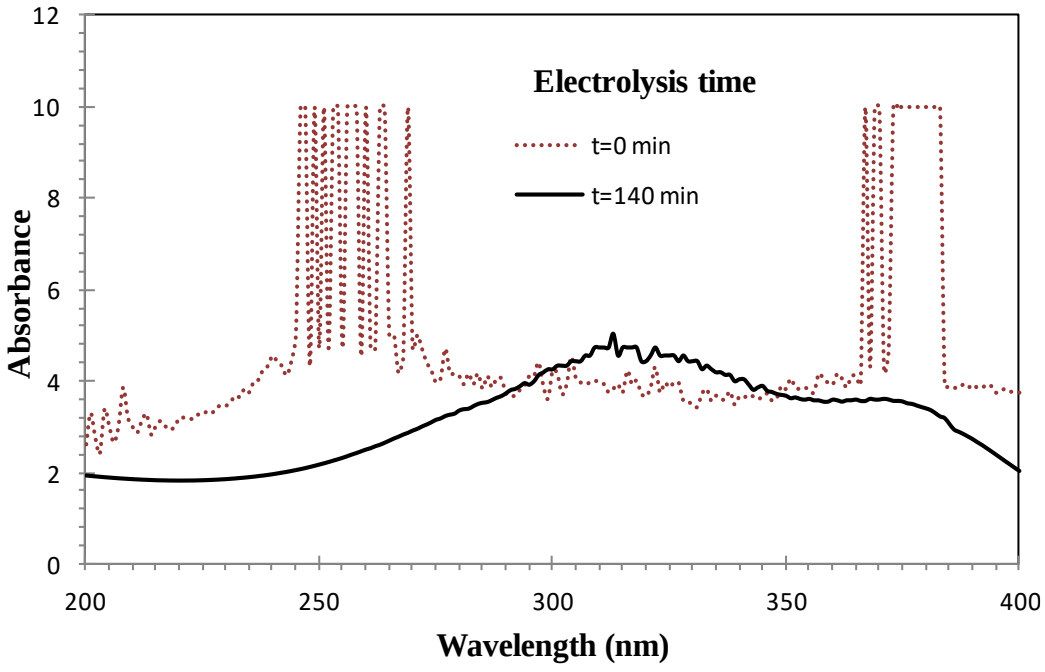

Fig 5.6.8. UV Visible spectra of untreated (*t*=0 min) and treated (*t*= 140 min) textile wastewater by Continuous EF at optimum condition

Table 5.6.7. GC-MS analysis of treated Textile wastewater by Continuous EF process

Compound	Retention Time	Molecular Mass	Matching %	Comments
Butyl phthalate	20.02/21.51/ 21.16/21	278	95.2% /81.3%/92. 9%	Transformation products
5,7-Dimethoxy-2,3-dihydro-4H-chromen-4-one	24.06/15.12	208	84%	Transformation products
1-acetamidoadamantane	21.91	193	90.7%	Transformation products
Tetradecamethylcyclohepta siloxane	15.65	519	84%	Transformation products

5.6.4 Degradation Mechanism

The spectrophotometric analysis and GC-MS analysis showed the presence of poly-aromatic compounds in the treated textile wastewater. The detected compounds contain low molecular weight elements such that silicon, carbon, hydrogen, oxygen and nitrogen. In the present study, two types of degradation processes were involved in the degradation of textile wastewater pollutants: *•OH mediated oxidation* and chlorine species-mediated oxidation. Transformation compounds generated during the EF treatment process were very few. The possible degradation mechanism of pollutants in textile wastewater is shown in Fig 5.6.9.

Direct Oxidation: It was observed that compounds of untreated wastewater like Decamethylcyclopentasiloxane, Trimethylsilyl 3,5-bis[(trimethylsilyl)oxy]benzoate, Adamantan-1-yl(phenyl)[(trimethylsilyl)oxy]acetonitrile, (5R,7R,8E,10E)-2,2,3,3,5,15,15,16,16-Nonamethyl-4,14-dioxa -3,15-disilaheptadeca-8,10-dien-7-ol, 3,3,5-Triethoxy-1,1,1,7,7,7-hexamethyl-5-(trimethylsilyloxy)tetrasiloxane, 3-Isopropoxy-1,1,1,7,7,7-hexamethyl-3,5,5-tris(trimethylsiloxy)tetrasiloxane, 1,1,1,3,5,7,9,11,11,11-Decamethyl-5-(trimethylsiloxy)hexasiloxane, Octadecamethylcyclononasiloxane, Icosamethylcyclodecasiloxane, Iron monocarbonyl 1,3 butadiene 1,4, dicarbonic acid diethyl

ether, Silicone oil, Hexadecamethylheptasiloxane undergo $^{\bullet}OH$ *mediated oxidation* via equation 5.3.11 and 5.3.12.

Indirect Oxidation: Real Textile wastewater was rich in chloride content, and the optimal pH for the EF process was ≈ 3.0. Therefore, Cl_2, HOCl and Cl^- were participated in the degradation process and transformed the textile pollutants into toxic chlorinated-compounds via indirect oxidation (equation 5.3.11 and 5.3.12). However, the final transformed compounds detected (Table 5.6.7) showed the absence of chlorinated-compounds. This may be due to the fact that the generated chlorinated-compounds are further oxidized by $^{\bullet}OH$ *mediated oxidation* in bulk (equation 5.3.13 and 5.6.16). It can also be verified from the absorption band of spectrophotometric analysis with λ, 200-280 nm (Fig. 5.6.8) that no chlorinated compound was present in the treated textile wastewater. Small spectrophotometric bands of transformed compounds were observed for λ, 280-340nm due to partial degradation. Small spectrophotometric bands are evident that compounds of the real textile wastewater were completely eliminated and some compounds undergo partial degradation and transformed into Dibutyl phthalate, 5,7-Dimethoxy-2,3-dihydro-4H-chromen-4-one, 1-acetamidoadamantane, Tetradecamethylcycloheptasiloxane**.**

$$\text{Chlorinated–compounds} + (^{\bullet}OH)_{bulk} \rightarrow nCO_2 + mH_2O + \text{transformed–compounds} \quad \textbf{(5.6.16)}$$

The comparison of the spectrophotometric analysis and GC-MS analysis of treated and untreated samples shows almost complete mineralization occurs during the EF process. Therefore, it can be concluded that, $^{\bullet}OH$ *mediated oxidation* was prominent in case of EF treatment process.

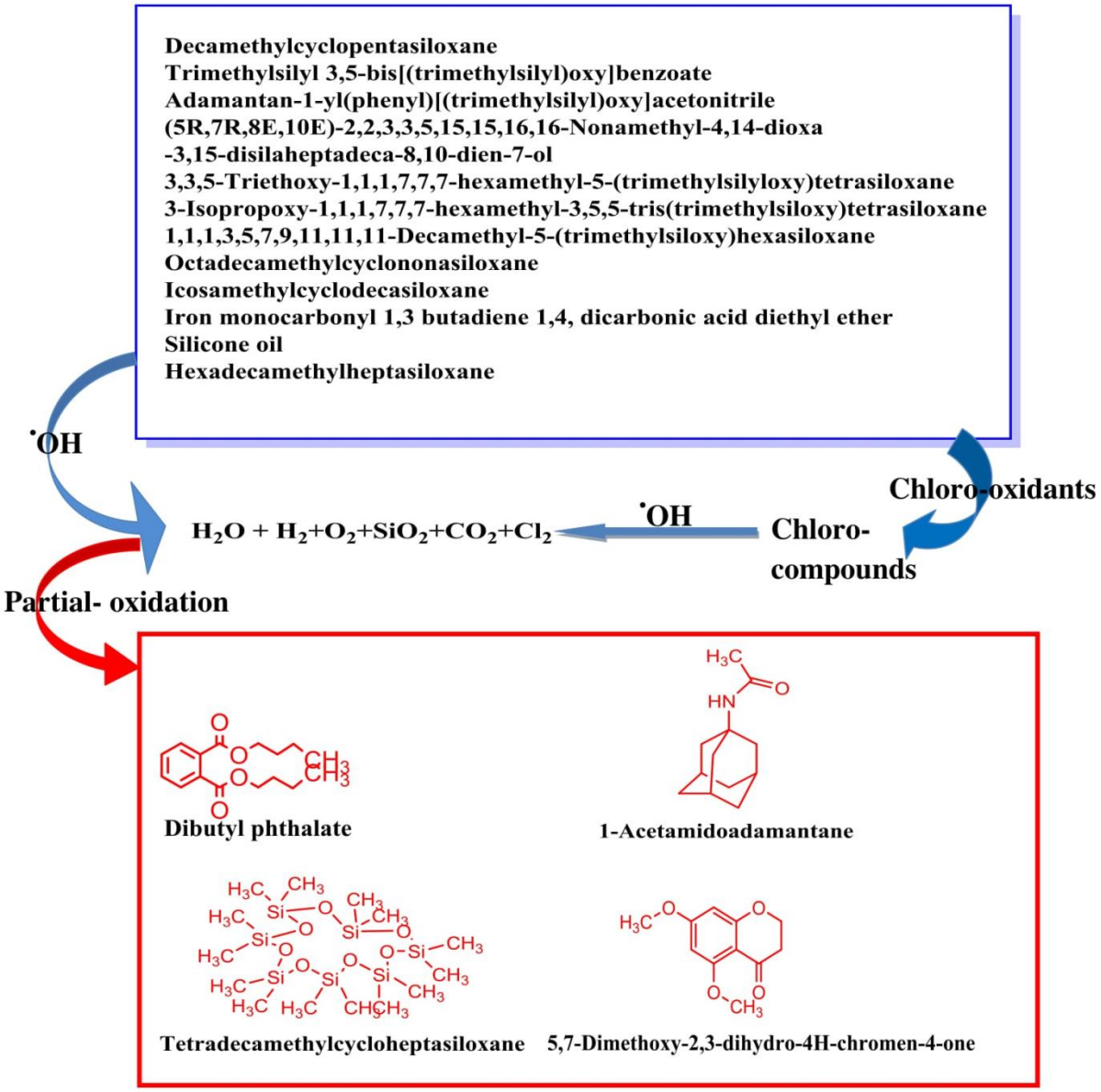

Fig 5.6.9. Persuasive mechanism of degradation of textile wastewater by EF process

5.6.5 Kinetic Study

The experimental data obtained at the optimal condition of continuous EF was used to determine the order of the reaction. At optimum parameters of the EF continuous process, kinetics of COD and Color removal was studied and Fig 5.6.10 shows the second-order kinetic model (equation 5.4.8.) fitting to the experimental data obtained from treatment of the textile effluent by continuous EF process at optimum condition (Bocos et al., 2016). Fig 5.6.11 shows the first order of the kinetic model fitting, which is incongruous.

The values of the rate constant of second-order reaction kinetics were found to be $2x10^{-5}$ *l*/mg min and 9.5 $x10^{-3}$ *l*/mg min along with the value of R^2 value 0.993 and 0.997 for X_1 (%COD removal) and X_2 (%Color removal). It was evident, that COD removal and Color removal was successfully described from the kinetic study but the kinetics of color removal was faster than COD removal. The study showed that, after 110 min and 120 min of elapsed time COD removal and Color removal, respectively, did not follow the second order kinetics. As discussed in the kinetic study of batch EO process, the COD and color of the real textile effluent were concurrently removed with respect to elapsed time. Concurrent removal of COD and color of the real textile effluent was described in the degradation mechanism section. The compounds initially present in the textile effluent were oxidized after EF treatment process. So, the oxidization of coloring compounds and other compounds of the textile effluent were simultaneously removed.

5.6.6 Operating Cost Analysis of EF Treatment of Textile Wastewater

Operational cost analysis is important within the criteria for the application of the EF process at the industrial scale. For the application of EF treatment method, operational cost is calculated in terms of per Kg of COD removal. The total operational cost consists of a number of costs but in the case of EF electrodes and energy cost is most important.

The cost of specific electrical energy consumed and electrode required to remove one kg of COD from textile wastewater was calculated from the responses of EF experiment conducted (X_1 =84.16%, X_2=94.00% and X_3=15 kWh/kg of COD removed) at optimized parameters (i = 1.10 A and C_{Fe} = 0.55 mM), and given below:

Specific electrical energy consumed = ~15 kWh/kg of COD removed

Electricity price in India, Punjab = ~ ₹ 5.00/kWh

Therefore, the cost of electrical energy consumed (C_E) = ₹ 75/kg of COD removed

In this study, two Ti/RuO_2 electrodes (dimension: 100 mm x 85 mm x 1.5 mm) of cost ₹ 2500.00 each were used. The manufacturer/supplier (Titanium Tantalum Products Limited, Chennai, India) specified the life of the electrodes 2.5 years at optimized condition (i = 1.10 and C_{Fe} = 0.55 mM).

Since, at optimized condition 84.16% of COD is removed, therefore, the minimum cost of Ti/RuO_2 electrodes (C_{EL}) = ₹ 465.46/ kg of COD removed

Total operating cost (C_E + C_{EL}) = ₹ 540.46/ kg of COD removed

In the present study, the COD of collected wastewater (from a Mink Blanket manufacturing industry situated in Ludhiana, Punjab, India) was 1156 mg/l. Therefore, to treat 1 m^3 of this wastewater by reducing the COD from 1.156 kg/m^3 to 0.231 kg/m^3 (as optimum %COD removal=84.16%) total operating cost (C_E + C_{EL}) in US$ is $ 9.00/ kg of COD removed.

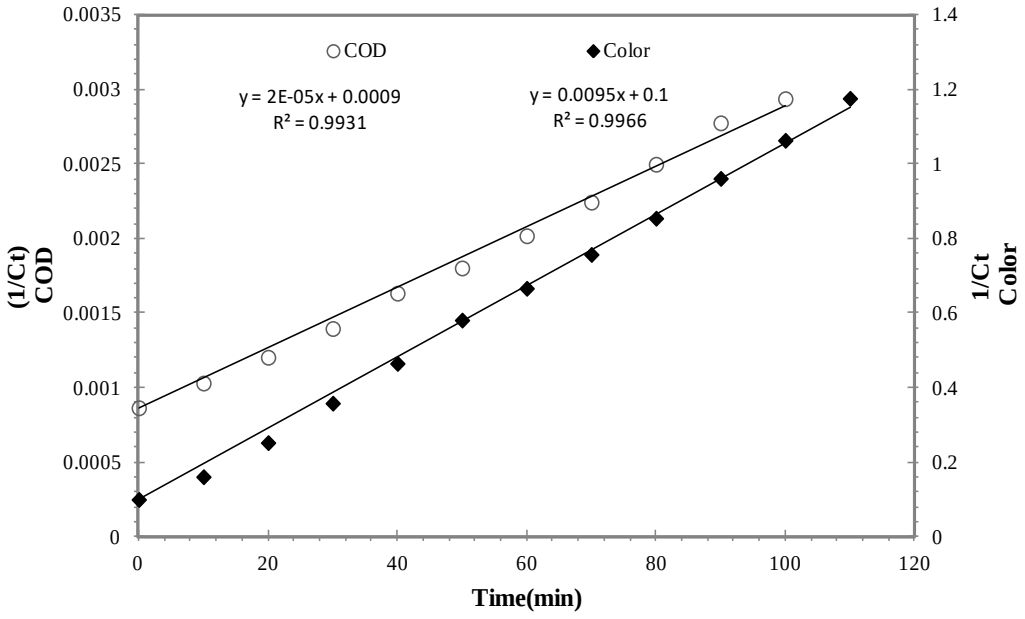

Fig 5.6.10. Degradation Kinetics in terms of COD and Color removal of textile wastewater by continuous EF process (Second order fitting)

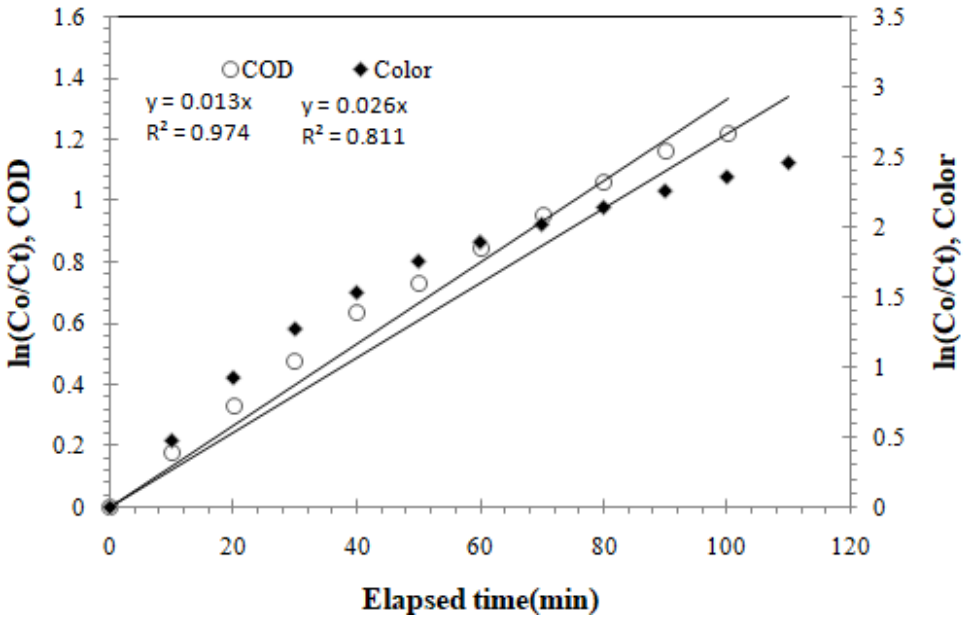

Fig 5.6.11. Degradation Kinetics in terms of COD and Color removal of textile wastewater by continuous EF process (First-order fitting)

5.7 PHYSICO-CHEMICAL ANALYSIS OF ELECTRODES

Since, the Ti/RuO_2 electrode is expensive, therefore, its durability needs to be studied. To study the degradation of electrode material after the EO and EF treatment, physico-chemical characterization of the electrodes, before treatment and after treatment, was performed. The SEM, EDX and X-ray diffraction (XRD) was performed and analysed for characterization of electrodes.

The SEM of fresh and used Ti/RuO_2 electrodes is shown in Fig 5.7.1. It can be seen clearly at the magnification of 50 µm that there is not much difference between the morphology of two electrodes, but used Ti/RuO_2 electrode show small wideness in the cracks after 256 runs of the electrochemical treatment process at different operational parameters. EDX was conducted to see the distribution of elements on the surface of fresh and used Ti/RuO_2 electrodes. EDX analysis showed the presence of Titanium (67.65%), oxygen (14.35%) and ruthenium (18.88%) elements on the surface of the fresh electrode. EDX analysis of used electrodes shows the presence of carbon (3.48%), oxygen (45.66%), titanium

(43.87%), and ruthenium (6.99%) on the surface as shown in Fig 5.7.2. The % weight and % atomic weight of identified elements on the surface of fresh and used electrodes have been shown in Table no. 5.7.1. The comparison of the EDX of the fresh electrode and used electrodes shows that there is a depletion of Ti and Ru elements from the surface of the electrode after the treatment. So, the depletion of elements from the surface of the electrode, limited the life of electrodes for 2.5 years. The presence of carbon on the surface of used electrodes shows that degradation of organic matter by electrochemical treatment process is prominent in the degradation process.

The micro structure and morphology of the $TiRuO_2$ electrodes were examined by X-ray diffraction. Fig 5.7.3 shows the XRD pattern of $TiRuO_2$ fresh and used electrodes (Zubavichus et al., 2002; Nan et al., 1994). A broad and symmetric RuO_2, Ti and TiO_2 rich peaks were obtained. It has been observed that there are very minute changes in the morphology of the electrodes after the degradation process. XRD pattern of $TiRuO_2$ on fresh and used electrodes shows that, the layer of RuO_2, on the Ti plate, is quite stable after 185 experimental runs of EO and EF.

Table 5.7.1. Elemental distribution of fresh and used electrodes

Elements	Fresh electrode		Used electrode	
	% Weight	% Atomic weight	% Weight	% Atomic weight
Titanium	67.65	45.67	43.87	46.33
Oxygen	14.35	51.33	45.66	44.54
Ruthenium	18.88	2.94	6.99	5.87
Carbon	-	-	3.48	3.26

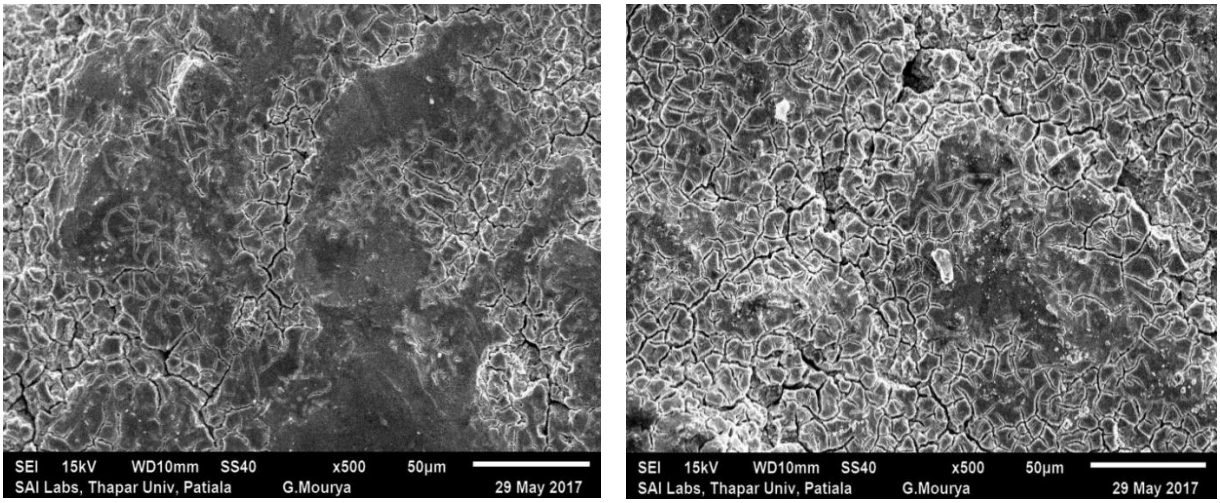

(a) **(b)**

Fig 5.7.1. SEM images of Ti/RuO_2 anode (a) Before treatment (b) After treatment

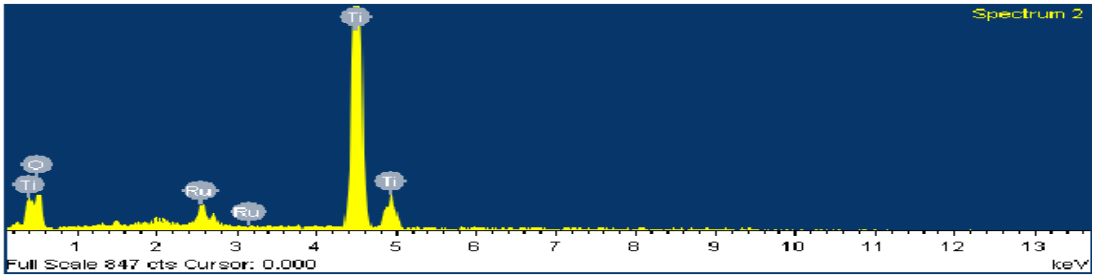

(a)

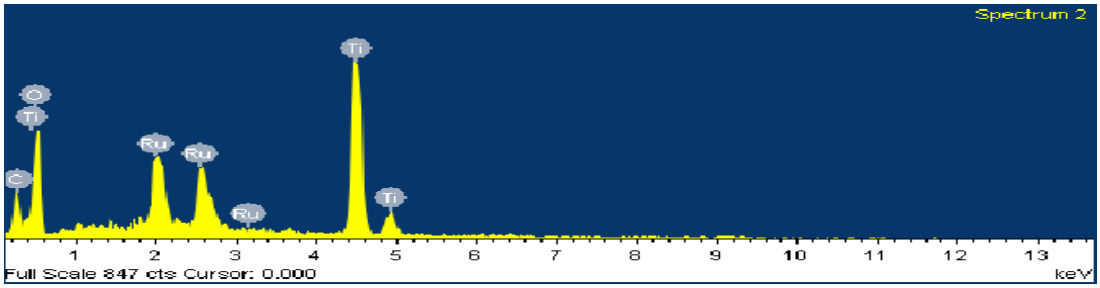

(b)

Fig 5.7.2. EDS of Ti/RuO_2 Anode (a) Before treatment (b) After treatment

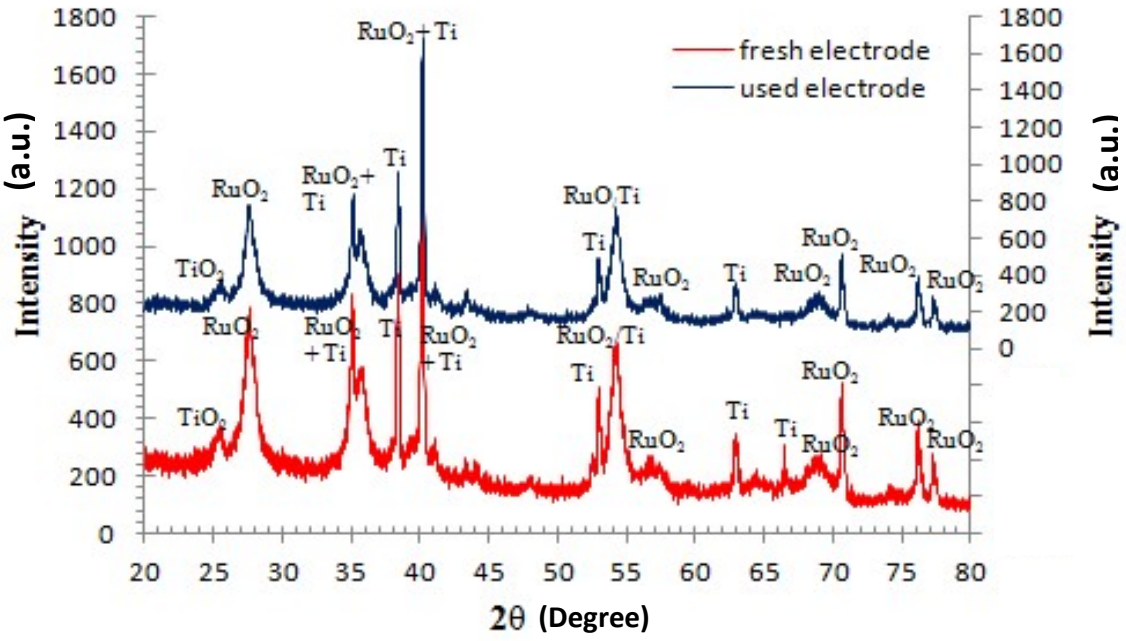

Fig 5.7.3. XRD plots of Ti/RuO_2, upper spectrum (used electrode) and lower spectrum (fresh electrode)

Chapter – 6

CONCLUSION

6.1GENERAL

On the basis of the present study for the treatment of textile effluent by EO and EF processes, following are the major conclusions are drawn.

6.1.1 Electro-Oxidation

- Optimization of textile wastewater treatment by EO method with Ti/RuO_2 anode using RSM in batch and continuous mode of operation was performed successfully.
- High R-squared values of the predicted models, suggested by the RSM, for various responses: % COD removal (X_1), %Color removal (X_2) and energy consumed (X_3) for the batch and continuous EO treatment of real textile wastewater using Ti/RuO_2 anode revealed high correlation between the predicted and experimental data.
- Maximum COD removal and color removal at the optimum conditions by the EO treatment in batch mode was found to be 80.00% and 97.25% respectively.
- Maximum COD removal and color removal at the optimum conditions by the EO treatment in continuous mode was found to be 81.00% and 92.25% respectively.
- The optimum retention time (R_T) was found to be 157.6 min, and the steady-state time at this R_T value was 124 min in case of continuous EO.
- At the optimum parameters, COD and color removal was found by both the mechanisms, direct and mediated EO. In highly acidic pH, adsorbed •OH on the Ti/RuO_2 surface directly oxidized the pollutants, however, Cl_2, and HOCl oxidized/degraded the pollutant via indirect oxidation. However, in highly basic pH ClO^- degraded the pollutants via an indirect mechanism.
- Chloro-oxidant species, HOCl and ClO^- was found to be partly participating in pollutants oxidation.

- GC-MS analysis showed that most of the compounds originally present in textile wastewater were eliminated after EO treatment. It was also found that organics were not oxidized completely, and present in treated effluent in degraded/transformed form.
- GC-MS analysis revealed that all the coloring compounds that were initially present in the textile wastewater, were eliminated after the EO treatment, however, some toxic chlorinated compounds were detected with other degraded compounds in treated effluent.
- Due to mediated EO by chloro-oxidant species, the chlorinated organic compounds such as dichloroacetaldehyde and 2-(7-chlorohept-2-ynyloxy) tetrahydro-2H-pyran were detected in treated wastewater and reported to be toxic and carcinogenic. Therefore, further tertiary treatment is necessary to remove these chlorinated organic compounds, before discharge.
- Acute toxicity bioassay test revealed that the untreated textile wastewater is highly toxic, and its toxicity is reduced after EO treatment.
- Kinetic study showed that the color degraded faster than the COD in case of EO. The % COD and % color removal follows the first order kinetics during EO treatment process.
- The EO operating cost was estimated for the treatment of real wastewater by batch EO and continuous EO. It was found to be 8.97 $/ kg of COD removed (batch EO) and 8.66 $/ kg of COD removed (continuous EO).

6.1.2 Electro-Fenton

- EF was successfully performed in batch and continuous mode for real textile wastewater. Statistical analysis advocates a good correlation between the observed and predicted values.
- 3-D response surface graph concluded that a very high concentration of the Fenton reagent hinders the degradation process during EF.
- Optimization of process parameters was successfully performed. EO and Fenton •OH radicals mediated oxidation were responsible for % COD removal and % Color removal.
- Maximum COD removal and color removal at the optimum conditions by the EF treatment in batch mode was found to be 89.75%% and 99.49%, respectively.

- Maximum COD removal and color removal at the optimum conditions by the EF treatment in continuous mode was found to be 84.16%and 94.00%, respectively.
- Spectrophotometric analysis and GC-MS analysis revealed that •OH mediated oxidation was prominent in the degradation process.
- Chloro-oxidant mediated oxidation also occur in EF process but chloro-compounds were mineralizing by Fenton •OH radicals mediated oxidation. It was clear by GCMS analysis that there was no generation of chloro-compounds.
- Bioassay analysis confirmed that treated real textile wastewater was not toxic. Therefore, it is concluded that textile wastewater after treatment by EF is safe to dispose of the environment. Since, $FeSO_4$ is added during the treatment, therefore, the recovery of Fe from the treated wastewater before disposal to the environment is necessary, and requires further treatment. However, bioassay analysis confirmed that the concentration of Fe in the treated wastewater is not lethal, but might have some chronic effects on the water-bodies.
- EF is a more effective electro-chemical method as compare to EO in terms of cost and degradation efficiency.
- The degradation kinetics follows second-order kinetic for EF treatment process.
- The EF operating cost was estimated for the treatment of real wastewater by batch EF and continuous EF. It was found to be 7.866 $/ kg of COD removed (batch EF) and 9.00 $/ kg of COD removed (continuous EF).

6.1.3 Comparison of EO and EF (Batch and Continuous) Treatment

Physico-chemical characterization of the real textile wastewater was performed before the treatment of real textile effluent. The physico-chemical characterization after EO and EF treatment (batch and continuous) of real textile effluent was performed to compare the effectiveness of the treatment processes. The characterization of real textile effluent was performed at the optimum process parameters of EO and EF treatment (batch and continuous). Table 6.1.1 and 6.1.2 shows the comparison of the characteristics of the real textile effluent before and after EO and EF treatment in batch and continuous mode respectively.

Table 6.1.1. Comparative table for real textile wastewater treatment in batch EO and EF at optimum conditions

Parameters		Untreated real textile effluent	EO (batch)	EF (batch)
Optimum parameters	**Current, i (A)**	-	1.66	0.32
	Time, t (min)	-	79.55	89.63
	Optimum pH	-	5.49	3
	Catalyst dose, C_{Fe} (mM)	-	-	0.54
pH		9.84	9.4	4.0
BOD (mg/l)		200	40	35
COD (mg/l)		544	108.8	55
TDS (mg/l)		50800	1300	800
TSS (mg/l)		59400	1000	3600
Color (pt.co)		936	27	26
Chloride (mg/l)		1182	1129	1130
Alkalinity (mg/l)		812	725	-
Oil/grease (mg/l)		83	2.76	1.54
Total Kjeldahl Nitrogen (mg/l)		2.12	2.07	1.62
Conductivity (mS/cm)		3.7	3.2	3.4
Turbidity (NTU)		276	92	113
Hardness (mg/l)		831	671	654

Table 6.1.2. Comparative table for real textile wastewater treatment in continuous EO and EF at optimum conditions

Parameters		Untreated real textile effluent	EO (continuous)	EF (continuous)
Optimum parameters	Current, i (A)	-	1.37	1.10
	Elapsed time, t (min)	-	124	137
	Optimum pH	-	5.45	3
	Retention time, R_T (min)	-	157.60	141.70
	Catalyst dose, C_{Fe} (mM)	-	-	0.55
pH		10.0	9.4	4.1
BOD (mg/l)		196	41.56	12.82
COD (mg/l)		1156	219.89	184.96
TDS (mg/l)		9640	3500	2112
TSS (mg/l)		8430	2200	1120
Color (pt.co)		1410	71	84.60
Chloride (mg/l)		1682	1659	1662
Alkalinity (mg/l)		940	932	-
Oil/grease (mg/l)		90	1.46	0.92
Total Kjeldahl Nitrogen (mg/l)		2.24	1.63	1.46
Conductivity (mS/cm)		4.6	4.2	4.1
Turbidity (NTU)		182	54	47
Hardness (mg/l)		746	724	717

REFERENCES

Akyol, A., Can, O. T., Demirbas, E., & Kobya, M. (2013). A comparative study of electrocoagulation and electro-Fenton for treatment of wastewater from liquid organic fertilizer plant. Separation & Purification Technology, 112, 11-19.

Anderson, P. W. (1961). Localized magnetic states in metals. Physical Review, 124(1), 41.

Andrade, L. S., Ruotolo, L. A. M., Rocha-Filho, R. C., Bocchi, N., Biaggio, S. R., Iniesta, J., & Montiel, V. (2007). On the performance of Fe and Fe, F doped Ti–Pt/PbO2 electrodes in the electrooxidation of the Blue Reactive 19 dye in simulated textile wastewater. Chemosphere, 66(11), 2035-2043.

Anglada, A., Urtiaga, A., & Ortiz, I. (2009). Contributions of electrochemical oxidation to waste-water treatment: fundamentals and review of applications. Journal of Chemical Technology & Biotechnology, 84(12), 1747-1755.

Aouni, A., Fersi, C., Ali, M. B. S., & Dhahbi, M. (2009). Treatment of textile wastewater by a hybrid electrocoagulation/nanofiltration process. Journal of Hazardous Materials, 168(2-3), 868-874.

Aravind, P., Subramanyan, V., Ferro, S., & Gopalakrishnan, R. (2016). Eco-friendly and facile integrated biological-cum-photo assisted electrooxidation process for degradation of textile wastewater. Water Research, 93, 230-241.

Asghar, A., Raman, A. A. A., & Daud, W. M. A. W. (2015). Advanced oxidation processes for in-situ production of hydrogen peroxide/hydroxyl radical for textile wastewater treatment: a review. Journal of Cleaner Production, 87, 826-838.

Balci, B., Oturan, M. A., Oturan, N., & *Sirés, I.* (2009). Decontamination of aqueous glyphosate, (aminomethyl) phosphonic acid, and glufosinate solutions by electro-Fenton-like process with Mn2+ as the catalyst. Journal of Agricultural & Food Chemistry, 57(11), 4888-4894.

Bansal, S., Kushwaha, J. P., & Sangal, V. K. (2013). Electrochemical treatment of reactive black 5 textile wastewater: optimization, kinetics, and disposal study. Water Environment Research, 85(12), 2294-2306.

Barredo-Damas, S., Iborra-Clar, M. I., Bes-Pia, A., Alcaina-Miranda, M. I., Mendoza-Roca, J. A., & Iborra-Clar, A. (2005). Study of preozonation influence on the physical-chemical treatment of textile wastewater. Desalination, 182(1-3), 267-274.

Benazzi, T. L., Di Luccio, M., Dallago, R. M., Steffens, J., Mores, R., Do Nascimento, M. S., & Ceni, G. (2016). Continuous flow electrocoagulation in the treatment of wastewater from dairy industries. Water Science & Technology, 73(6), 1418-1425.

Bhalla, N., Sidhu, T., & Kaur, R. (2017). Human resource practices and commitment of employees in india's textile industry in context of management levels. Journal on Management, 12(2).

Bidin, H., Basri, M., Radzi, S. M., Ariff, A., Rahman, R. N. Z. R. A., & Salleh, A. B. (2009). Optimization of lipase-catalyzed synthesis of palm amino acid surfactant using response surface methodology (RSM). Industrial Crops and Products, 30(2), 206-211.

Bisschops, I., & Spanjers, H. (2003). Literature review on textile wastewater characterisation. Environmental Technology, 24(11), 1399-1411.

Bocos, E., Pazos, M., & Sanromán, M. A. (2014). Electro-Fenton decolourization of dyes in batch mode by the use of catalytic activity of iron loaded hydrogels. Journal of Chemical Technology & Biotechnology, 89(8), 1235-1242.

Bocos, E., Pérez-Álvarez, D., Pazos, M., Rodríguez-Argüelles, M. C., & Sanromán, M. Á. (2016). Coated nickel foam electrode for the implementation of continuous electro-Fenton treatment. Journal of Chemical Technology & Biotechnology, 91(3), 685-692.

Bouafia-Chergui, S., Oturan, N., Khalaf, H., & Oturan, M. A. (2010). Parametric study on the effect of the ratios [H2O2]/[Fe3+] and [H2O2]/[substrate] on the photo-Fenton

degradation of cationic azo dye Basic Blue 41. Journal of Environmental Science & Health Part A, 45(5), 622-629.

Brillas, E., Baños, M. A., Camps, S., Arias, C., Cabot, P. L., Garrido, J. A., & Rodríguez, R. M. (2004). Catalytic effect of Fe 2+, Cu 2+ and UVA light on the electrochemical degradation of nitrobenzene using an oxygen-diffusion cathode. New Journal of Chemistry, 28(2), 314-322.

Brillas, E., Sirés, I., & Oturan, M. A. (2009). Electro-Fenton process and related electrochemical technologies based on Fenton's reaction chemistry. Chemical Reviews, 109(12), 6570-6631.

Britto-Costa, P. H., & Ruotolo, L. A. M. (2012). Phenol removal from wastewaters by electrochemical oxidation using boron doped diamond (BDD) and Ti/Ti0. 7Ru0. 3O2 dsa® electrodes. Brazilian Journal of Chemical Engineering, 29(4), 763-773.

Cañizares, P., Martínez, F., Jiménez, C., Lobato, J., & Rodrigo, M. A. (2006). Coagulation and electrocoagulation of wastes polluted with dyes. Environmental Science & Technology, 40(20), 6418-6424.

Canizares, P., Paz, R., Sáez, C., & Rodrigo, M. A. (2009). Costs of the electrochemical oxidation of wastewaters: a comparison with ozonation and Fenton oxidation processes. Journal of Environmental Management, 90(1), 410-420.

Central pollution control board, INDIA. http://cpcb.nic.in/Industry-Specific-Standards/Effluent/DyeandDye_Inter_Indus.pdf, 2017 (accessed on 2.04.16)

Chen, G. (2004). Electrochemical technologies in wastewater treatment. Separation & Purification Technology, 38(1), 11-41.

Chen, W., & Liu, J. (2012). The possibility and applicability of coagulation-MBR hybrid system in reclamation of dairy wastewater. Desalination, 285, 226-231.

Cho, S. H., Shim, J., & Moon, S. H. (2009). Detoxification of simulated textile wastewater using a membraneless electrochemical reactor with immobilized peroxidase. Journal of Hazardous Materials, 162(2-3), 1014-1018.

Chou, S., Huang, Y. H., Lee, S. N., Huang, G. H., & Huang, C. (1999). Treatment of high strength hexamine-containing wastewater by electro-Fenton method. Water Research, 33(3), 751-759.

Clark, M. (Ed.). (2011). Handbook of textile and industrial dyeing: principles, processes and types of dyes. Elsevier.

Comninellis, C. (1994). Electrocatalysis in the electrochemical conversion/combustion of organic pollutants for waste water treatment. ElectrochimicaActa, 39(11-12), 1857-1862.

Comninellis, C. (2006). Electrochemical oxidation of organic pollutants for wastewater treatment. In Meeting Abstracts (No. 39, pp. 1775-1775). The Electrochemical Society.

Correia, V. M., Stephenson, T., & Judd, S. J. (1994). Characterisation of textile wastewaters-a review. Environmental Technology, 15(10), 917-929.

Cossu, R., Polcaro, A. M., Lavagnolo, M. C., Mascia, M., Palmas, S., & Renoldi, F. (1998). Electrochemical treatment of landfill leachate: oxidation at Ti/PbO2 and Ti/SnO2 anodes. Environmental Science & Technology, 32(22), 3570-3573.

Davarnejad, R., & Hosseinitabar, P. (2016). Application of iron electrode in textile industry wastewater treatment using electro-fenton technique: Experimental and statistical study. International Journal of Engineering-Transactions A: Basics, 29(7), 887.

De Araújo, D. M., Sáez, C., Martínez-Huitle, C. A., Cañizares, P., & Rodrigo, M. A. (2015). Influence of mediated processes on the removal of Rhodamine with conductive-diamond electrochemical oxidation. Applied Catalysis B: Environmental, 166, 454-459.

Deborde, M., & Von Gunten, U. R. S. (2008). Reactions of chlorine with inorganic and organic compounds during water treatment—kinetics and mechanisms: a critical review. Water Research, 42(1-2), 13-51.

Del Río, A. I., Molina, J., Bonastre, J., & Cases, F. (2009). Influence of electrochemical reduction and oxidation processes on the decolourisation and degradation of CI Reactive Orange 4 solutions. Chemosphere, 75(10), 1329-1337.

Divya, N., Bansal, A., & Jana, A. K. (2009). Degradation of acidic Orange G dye using UV-H2O2 in batch photoreactor. International Journal of Biological and Chemical Sciences, 3(1).

Doğan, D., & Türkdemir, H. (2005). Electrochemical oxidation of textile dye indigo. Journal of Chemical Technology & Biotechnology, 80(8), 916-923.

Dos Santos, A. J., de Lima, M. D., da Silva, D. R., Garcia-Segura, S., & Martínez-Huitle, C. A. (2016). Influence of the water hardness on the performance of electro-Fenton approach: decolorization and mineralization of Eriochrome Black T. ElectrochimicaActa, 208, 156-163.

El-Desoky, H. S., Ghoneim, M. M., El-Sheikh, R., & Zidan, N. M. (2010). Oxidation of Levafix CA reactive azo-dyes in industrial wastewater of textile dyeing by electro-generated Fenton's reagent. Journal of Hazardous Materials, 175(1-3), 858-865.

Enache-Pommer, E., Liu, B., & Aydil, E. S. (2009). Electron transport and recombination in dye-sensitized solar cells made from single-crystal rutile TiO 2 nanowires. Physical Chemistry Chemical Physics, 11(42), 9648-9652.

EPA, E. (1997). Office of Compliance Sector Notebook Project: Profile of the Textile Industry. EPA310R97009, Washington.

Estrada, A. L., Li, Y. Y., & Wang, A. (2012). Biodegradability enhancement of wastewater containing cefalexin by means of the electro-Fenton oxidation process. Journal of Hazardous Materials, 227, 41-48.

Fernandes, A., Morao, A., Magrinho, M., Lopes, A., & Gonçalves, I. (2004). Electrochemical degradation of CI acid orange 7. Dyes & Pigments, 61(3), 287-296.

Ferreira, S. C., Bruns, R. E., Ferreira, H. S., Matos, G. D., David, J. M., Brandao, G. C., & Dos Santos, W. N. L. (2007). Box-Behnken design: an alternative for the optimization of analytical methods. AnalyticaChimicaActa, 597(2), 179-186.

Florenza, X., Solano, A. M. S., Centellas, F., Martínez-Huitle, C. A., Brillas, E., & Garcia-Segura, S. (2014). Degradation of the azo dye Acid Red 1 by anodic oxidation and

indirect electrochemical processes based on Fenton's reaction chemistry. Relationship between decolorization, mineralization and products. ElectrochimicaActa, 142, 276-288.

Fu, F., Wang, Q., & Tang, B. (2010). Effective degradation of CI Acid Red 73 by advanced Fenton process. Journal of Hazardous Materials, 174(1-3), 17-22.

Fu, L., You, S. J., Zhang, G. Q., Yang, F. L., & Fang, X. H. (2010). Degradation of azo dyes using in-situ Fenton reaction incorporated into H2O2-producing microbial fuel cell. Chemical Engineering Journal, 160(1), 164-169.

Garcia-Segura, S., & Brillas, E. (2016). Combustion of textile monoazo, diazo and triazo dyes by solar photoelectro-Fenton: decolorization, kinetics and degradation routes. Applied Catalysis B: Environmental, 181, 681-691.

Georgiou, D., Melidis, P., & Aivasidis, A. (2002). Use of a microbial sensor: inhibition effect of azo-reactive dyes on activated sludge. Bioprocess & Biosystems Engineering, 25(2), 79-83.

Ghanbari, F., & Moradi, M. (2015). A comparative study of electrocoagulation, electrochemical Fenton, electro-Fenton and peroxi-coagulation for decolorization of real textile wastewater: electrical energy consumption and biodegradability improvement. Journal of Environmental Chemical Engineering, 3(1), 499-506.

Ghoneim, M. M., El-Desoky, H. S., & Zidan, N. M. (2011). Electro-Fenton oxidation of Sunset Yellow FCF azo-dye in aqueous solutions. Desalination, 274(1-3), 22-30.

Gregory, P. (1986). Azo dyes: Structure-carcinogenicity relationships. Dyes and Pigments, 7(1), 45-56.

Gupta, A., & Garg, A. (2018). Degradation of ciprofloxacin using Fenton's oxidation: Effect of operating parameters, identification of oxidized by-products and toxicity assessment. Chemosphere, 193, 1181-1188.

Hanay, Ö., & Hasar, H. (2011). Effect of anions on removing Cu2+, Mn2+ and Zn2+ in electrocoagulation process using aluminum electrodes. Journal of Hazardous Materials, 189(1-2), 572-576.

Hanrahan, G., & Lu, K. (2006). Application of factorial and response surface methodology in modern experimental design and optimization. Critical Reviews in Analytical Chemistry, 36(3-4), 141-151.

Hendrickx, I. (1995). Pollution prevention studies in the textile wet processing industry (Doctoral Dissertation, Virginia Tech). http://www.alokind.com/Downloads/Indian%20Textile%20&%20Apparel%20Industry%20-%20Brightest%20Future%20ever-%20Arvind%20Singhal-20September%202010.pdf

Husain, Q. (2006). Potential applications of the oxidoreductive enzymes in the decolorization and detoxification of textile and other synthetic dyes from polluted water: a review. Critical Reviews in Biotechnology, 26(4), 201-221.

Iglesias, O., De Dios, M. F., Pazos, M., & Sanromán, M. A. (2013). Using iron-loaded sepiolite obtained by adsorption as a catalyst in the electro-Fenton oxidation of Reactive Black 5. Environmental Science & Pollution Research, 20(9), 5983-5993.

Jeirani, Z., Sadeghi, A., Soltan, J., Roshani, B., & Rindall, B. (2015). Effectiveness of advanced oxidation processes for the removal of manganese and organic compounds in membrane concentrate. Separation and Purification Technology, 149, 110-115.

Kaur, P., Kushwaha, J. P., & Sangal, V. K. (2017). Evaluation and disposability study of actual textile wastewater treatment by electro-oxidation method using Ti/RuO2 anode. Process Safety & Environmental Protection, 111, 13-22.

Kaur, P., Sangal, V. K., & Kushwaha, J. P. (2015). Modeling and evaluation of electro-oxidation of dye wastewater using artificial neural networks. RSC Advances, 5(44), 34663-34671

Khataee, A. R., Fathinia, M., Zarei, M., Izadkhah, B., & Joo, S. W. (2014). Modeling and optimization of photocatalytic/photoassisted-electro-Fenton like degradation of phenol using a neural network coupled with genetic algorithm. Journal of Industrial & Engineering Chemistry, 20(4), 1852-1860.

Kim, S., Park, C., Kim, T. H., Lee, J., & Kim, S. W. (2003). COD reduction and decolorization of textile effluent using a combined process. Journal of Bioscience & Bioengineering, 95(1), 102-105

Kobya, M., Can, O. T., & Bayramoglu, M. (2003). Treatment of textile wastewaters by electrocoagulation using iron and aluminum electrodes. Journal of Hazardous Materials, 100(1-3), 163-178.

Kobya, M., Gengec, E., & Demirbas, E. (2016). Operating parameters and costs assessments of a real dyehouse wastewater effluent treated by a continuous electrocoagulation process. Chemical Engineering & Processing: Process Intensification, 101, 87-100.

Kong, Y., Yuan, J., Wang, Z., Yao, S., & Chen, Z. (2009). Application of expanded graphite/attapulgite composite materials as electrode for treatment of textile wastewater. Applied Clay Science, 46(4), 358-362.

Kong, Y., Yuan, J., Wang, Z., Yao, S., & Chen, Z. (2009). Application of expanded graphite/attapulgite composite materials as electrode for treatment of textile wastewater. Applied Clay Science, 46(4), 358-362.

Koparal, A. S., Yavuz, Y., Gürel, C., & Öğütveren, Ü. B. (2007). Electrochemical degradation and toxicity reduction of CI Basic Red 29 solution and textile wastewater by using diamond anode. Journal of Hazardous Materials, 145(1-2), 100-108.

Körbahti, B. K., & Tanyolaç, A. (2008). Electrochemical treatment of simulated textile wastewater with industrial components and Levafix Blue CA reactive dye: Optimization through response surface methodology. Journal of Hazardous Materials, 151(2-3), 422-431.

Körbahti, B. K., & Tanyolac, A. (2009). Continuous electrochemical treatment of simulated industrial textile wastewater from industrial components in a tubular reactor. Journal of Hazardous Materials, 170(2-3), 771-778.

Körbahti, B. K., & Tanyolaç, A. (2009). Electrochemical treatment of simulated industrial paint wastewater in a continuous tubular reactor. Chemical Engineering Journal, 148(2-3), 444-451.

Kulkarni, S. V., Blackwell, C. D., Blackard, A. L., Stackhouse, C. W., & Alexandar, M. W. (1985). Textile dyes and dyeing equipment: classification, properties and environmental aspects. US Government Printing Office.

Kushwaha, J. P., Srivastava, V. C., & Mall, I. D. (2010). Organics removal from dairy wastewater by electrochemical treatment and residue disposal. Separation and Purification Technology, 76(2), 198-205.

Le, T. X. H., Van Nguyen, T., Yacouba, Z. A., Zoungrana, L., Avril, F., Petit, E., & Lesage, G. (2016). Toxicity removal assessments related to degradation pathways of azo dyes: Toward an optimization of Electro-Fenton treatment. Chemosphere, 161, 308-318.

Lei, Y., Liu, H., Shen, Z., & Wang, W. (2013). Development of a trickle bed reactor of electro-Fenton process for wastewater treatment. Journal of Hazardous Materials, 261, 570-576.

Li, X., Jin, X., Zhao, N., Angelidaki, I., & Zhang, Y. (2017). Novel bio-electro-Fenton technology for azo dye wastewater treatment using microbial reverse-electrodialysis electrolysis cell. Bioresource Technology, 228, 322-329.

Lin, H., Zhang, H., Wang, X., Wang, L., & Wu, J. (2014). Electro-Fenton removal of Orange II in a divided cell: Reaction mechanism, degradation pathway and toxicity evolution. Separation and Purification Technology, 122, 533-540.

Lin, S. H., & Chen, M. L. (1997). Treatment of textile wastewater by chemical methods for reuse. Water Research, 31(4), 868-876.

Lin, S. H., & Peng, C. F. (1996). Continuous treatment of textile wastewater by combined coagulation, electrochemical oxidation and activated sludge. Water Research, 30(3), 587-592.

Linares-Hernández, I., Barrera-Díaz, C., Roa-Morales, G., Bilyeu, B., & Ureña-Núñez, F. (2009). Influence of the anodic material on electrocoagulation performance. Chemical Engineering Journal, 148(1), 97-105.

Liu, H., Li, X. Z., Leng, Y. J., & Wang, C. (2007). Kinetic modeling of electro-Fenton reaction in aqueous solution. Water Research, 41(5), 1161-1167.

Maljaei, A., Arami, M., & Mahmoodi, N. M. (2009). Decolorization and aromatic ring degradation of colored textile wastewater using indirect electrochemical oxidation method. Desalination, 249(3), 1074-1078.

Manoli, K., Ghosh, M., Nakhla, G., & Ray, A. K. (2017). A Review on Ferrate (VI) and Photocatalysis as Oxidation Processes for the Removal of Organic Pollutants in Water and Wastewater. Advanced Materials for Wastewater Treatment, 331-390.

Mansour, D., Fourcade, F., Huguet, S., Soutrel, I., Bellakhal, N., Dachraoui, M., & Amrane, A. (2014). Improvement of the activated sludge treatment by its combination with electro Fenton for the mineralization of sulfamethazine. International Biodeterioration & Biodegradation, 88, 29-36.

Martinez-Huitle, C. A., & Brillas, E. (2009). Decontamination of wastewaters containing synthetic organic dyes by electrochemical methods: a general review. ApplCatal B Environ 87(3): 105–145

McMullan, G., Meehan, C., Conneely, A., Kirby, N., Robinson, T., Nigam, P., & Smyth, W. F. (2001). Microbial decolourisation and degradation of textile dyes. Applied Microbiology and Biotechnology, 56(1-2), 81-87.

Meriç, S., Kaptan, D., & Ölmez, T. (2004). Color and COD removal from wastewater containing Reactive Black 5 using Fenton's oxidation process. Chemosphere, 54(3), 435-441.

Michael, W., & Jaspen, N., 1959. Book Reviews: Experimental Designs (Second Edition) by William G. Cochran and Gertrude M. Cox. New York: John Wiley & Sons. Educ. Psychol. Meas. 19, 259-261

Miled, W., Said, A. H., & Roudesli, S. (2010). Decolorization of high polluted textile wastewater by indirect electrochemical oxidation process. Journal of Textile and Apparel, Technology and Management, 6(3).

Módenes, A. N., Espinoza-Quiñones, F. R., Borba, F. H., & Manenti, D. R. (2012). Performance evaluation of an integrated photo-Fenton–Electrocoagulation process applied to pollutant removal from tannery effluent in batch system. Chemical Engineering Journal, 197, 1-9.

Moghaddam, S. S., Moghaddam, M. A., & Arami, M. (2010). Coagulation/flocculation process for dye removal using sludge from water treatment plant: optimization through response surface methodology. Journal of Hazardous Materials, 175(1-3), 651-657.

Mohan, N., Balasubramanian, N., & Basha, C. A. (2007). Electrochemical oxidation of textile wastewater and its reuse. Journal of Hazardous Materials, 147(1-2), 644-651.

Moussavi, G., Bagheri, A., & Khavanin, A. (2012). The investigation of degradation and mineralization of high concentrations of formaldehyde in an electro-Fenton process combined with the biodegradation. Journal of Hazardous Materials, 237, 147-152.

Nan, H., Chen, Y. R., Luo, J. M., Jin, Y., Rong, L., Jing, X., & Liu, X. H. (1994). In vitro investigation of blood compatibility of Ti with oxide layers of rutile structure. Journal of Biomaterials Applications, 8(4), 404-412.

Nasr, B., Abdellatif, G., Canizares, P., Sáez, C., Lobato, J., & Rodrigo, M. A. (2005). Electrochemical oxidation of hydroquinone, resorcinol, and catechol on boron-doped diamond anodes. Environmental Science & Technology, 39(18), 7234-7239.

Naumczyk, J., Szpyrkowicz, L., De Faveri, M. D., & Zilio-Grandi, F. (1996). Electrochemical treatment of tannery wastewater containing high strength pollutants. Process Safety and Environmental Protection, 74(1).

Naveed, S., Bhatti, I., & Ali, K. (2006). Membrane technology and its suitability for treatment of textile waste water in Pakistan. Journal of Research (Science), 17(3), 155-164.

Nidheesh, P. V., & Gandhimathi, R. (2012). Trends in electro-Fenton process for water and wastewater treatment: an overview. Desalination, 299, 1-15.

Nidheesh, P. V., & Gandhimathi, R. (2014). Removal of Rhodamine B from aqueous solution using graphite–graphite electro-Fenton system. Desalination and Water Treatment, 52(10-12), 1872-1877.

Nidheesh, P. V., & Gandhimathi, R. (2014). Textile wastewater treatment by electro-Fenton process in batch and continuous modes. Journal of Hazardous, Toxic, and Radioactive Waste, 19(3), 04014038.

Nidheesh, P. V., & Gandhimathi, R. (2015). Electro Fenton oxidation for the removal of Rhodamine B from aqueous solution in a bubble column reactor under continuous mode. Desalination and Water Treatment, 55(1), 263-271.

Nidheesh, P. V., Gandhimathi, R., & Ramesh, S. T. (2013). Degradation of dyes from aqueous solution by Fenton processes: a review. Environmental Science and Pollution Research, 20(4), 2099-2132.

O'Neill, C., Hawkes, F. R., Hawkes, D. L., Lourenço, N. D., Pinheiro, H. M., & Delée, W. (1999). Colour in textile effluents–sources, measurement, discharge consents and simulation: a review. Journal of Chemical Technology and Biotechnology, 74(11), 1009-1018.

Ölmez, T., Kabdaşlı, I., & Tünay, O. (2007). The effect of the textile industry dye bath additive EDTMPA on colour removal characteristics by ozone oxidation. Water Science and Technology, 55(10), 145-153.

Oturan, M. A, & Brillas, E. (2007). Electrochemical advanced oxidation processes (EAOPs) for environmental applications. Portugaliae Electrochimica Acta, 25(1), 1-18.

Oturan, M. A., & Aaron, J. J. (2014). Advanced oxidation processes in water/wastewater treatment: principles and applications. A review. Critical Reviews in Environmental Science and Technology, 44(23), 2577-2641.

Oturan, M. A., Peiroten, J., Chartrin, P., & Acher, A. J. (2000). Complete destruction of p-nitrophenol in aqueous medium by electro-Fenton method. Environmental Science & Technology, 34(16), 3474-3479.

Oturan, M. A., Oturan, N., & Aaron, J. J. (2004). Treatment of organic micropollutants in water by advanced oxidation processes. Chemical News, 277, 57-64.

Oturan, N., Brillas, E., & Oturan, M. A. (2012). Unprecedented total mineralization of atrazine and cyanuric acid by anodic oxidation and electro-Fenton with a boron-doped diamond anode. Environmental Chemistry Letters, 10(2), 165-170.

Pajootan, E., Arami, M., & Rahimdokht, M. (2014). Discoloration of wastewater in a continuous electro-Fenton process using modified graphite electrode with multi-walled carbon nanotubes/surfactant. Separation and Purification Technology, 130, 34-44.

Panizza, M., & Cerisola, G. (2009). Direct and mediated anodic oxidation of organic pollutants. Chemical Reviews, 109(12), 6541-6569.

Phalakornkule, C., Polgumhang, S., Tongdaung, W., Karakat, B., & Nuyut, T. (2010). Electrocoagulation of blue reactive, red disperse and mixed dyes, and application in treating textile effluent. Journal of Environmental Management, 91(4), 918-926.

Pillai, I. M. S., & Gupta, A. K. (2017). Performance analysis of a continuous serpentine flow reactor for electrochemical oxidation of synthetic and real textile wastewater: Energy consumption, mass transfer coefficient and economic analysis. Journal of Environmental Management, 193, 524-531.

Pimentel, M., Oturan, N., Dezotti, M., & Oturan, M. A. (2008). Phenol degradation by advanced electrochemical oxidation process electro-Fenton using a carbon felt cathode. Applied Catalysis B: Environmental, 83(1-2), 140-149.

Pletcher, D., & Walsh, F. C. (1999). Industrial Electrochemistry, Chapman and Hall, London XII, 325

Kushwaha, J. P., Srivastava, V. C., & Mall I. D. (2011). Studies on electrochemical treatment of dairy wastewater using aluminum electrode. *AIChE Journal*, *57*(9), 2589-2598.

Pulgarin, C., Adler, N., Peringer, P., & Comninellis, C. (1994). Electrochemical detoxification of a 1, 4-benzoquinone solution in wastewater treatment. Water Research, 28(4), 887-893.

Raghu, S., & Basha, C. A. (2007). Electrochemical treatment of Procion Black 5B using cylindrical flow reactor—a pilot plant study. Journal of Hazardous Materials, 139(2), 381-390.

Raghu, S., Lee, C. W., Chellammal, S., Palanichamy, S., & Basha, C. A. (2009). Evaluation of electrochemical oxidation techniques for degradation of dye effluents—a comparative approach. Journal of Hazardous Materials, 171(1-3), 748-754.

Rajkumar, D., & Kim, J. G. (2006). Oxidation of various reactive dyes with in situ electro-generated active chlorine for textile dyeing industry wastewater treatment. Journal of Hazardous Materials, 136(2), 203-212.

Rajkumar, D., Song, B. J., & Kim, J. G. (2007). Electrochemical degradation of Reactive Blue 19 in chloride medium for the treatment of textile dyeing wastewater with identification of intermediate compounds. Dyes and Pigments, 72(1), 1-7.

Rajkumar, K., & Muthukumar, M. (2012). Optimization of electro-oxidation process for the treatment of Reactive Orange 107 using response surface methodology. Environmental Science and Pollution Research, 19(1), 148-160.

Rajkumar, K., & Muthukumar, M. (2017). Statistical Optimization of Electro Oxidation Process for Removal of Textile Dye CI Reactive Blue 198. *International Journal of Environmental* Sciences & Natural *Resources*, 1(4), 555570.

Raju, G. B., Karuppiah, M. T., Latha, S. S., Priya, D. L., Parvathy, S., & Prabhakar, S. (2009). Electrochemical pretreatment of textile effluents and effect of electrode materials on the removal of organics. Desalination, 249(1), 167-174.

Ramesh B, Parande A K, Raghu S, Kumar P T (2007) Textile Technology- Cotton Textile Processing: Waste Generation and Effluent Treatment. The Journal of Cotton Science 11: 141–153.

Ranganathan, K., Jeyapaul, S., & Sharma, D. C. (2007). Assessment of water pollution in different bleaching based paper manufacturing and textile dyeing industries in India. Environmental Monitoring & Assessment, 134(1-3), 363.

Ren, G., Zhou, M., Liu, M., Ma, L., & Yang, H. (2016). A novel vertical-flow electro-Fenton reactor for organic wastewater treatment. Chemical Engineering Journal, 298, 55-67.

Rodgers, J. D., Jedral, W., & Bunce, N. J. (1999). Electrochemical oxidation of chlorinated phenols. Environmental science & technology, 33(9), 1453-1457.

Rosales, E., Pazos, M., Longo, M. A., &Sanromán, M. A. (2009). Electro-Fenton decoloration of dyes in a continuous reactor: a promising technology in colored wastewater treatment. Chemical Engineering Journal, 155(1-2), 62-67.

Roshini, P. S., Gandhimathi, R., Ramesh, S. T., & Nidheesh, P. V. (2017). Combined electro-Fenton and biological processes for the treatment of industrial textile effluent: mineralization and toxicity analysis. Journal of Hazardous, Toxic, and Radioactive Waste, 21(4), 04017016.

Sahu, O. P., Gupta, V., Chaudhari, P. K., & Srivastava, V. C. (2015). Electrochemical treatment of actual sugar industry wastewater using aluminum electrode. International Journal of Environmental Science and Technology, 12(11), 3519-3530.

Sakalis, A., Mpoulmpasakos, K., Nickel, U., Fytianos, K., &Voulgaropoulos, A. (2005). Evaluation of a novel electrochemical pilot plant process for azodyes removal from textile wastewater. Chemical Engineering Journal, 111(1), 63-70.

Salazar, R., & Ureta-Zañartu, M. S. (2012). Degradation of acid violet 7 and reactive black 5 in water by electro-fenton and photo electro-fenton by. Journal of the Chilean Chemical Society, 57(1), 999-1003.

Salazar, R., Brillas, E., & Sirés, I. (2012). Finding the best $Fe^{2+/}Cu^{2+}$ combination for the solar photoelectro-Fenton treatment of simulated wastewater containing the industrial textile dye Disperse Blue 3. Applied Catalysis B: Environmental, 115, 107-116.

Sandhwar, V. K., & Prasad, B. (2017). Comparative study of electrochemical oxidation and electrochemical Fenton processes for simultaneous degradation of phthalic and para-toluic acids from aqueous medium. Journal of Molecular Liquids, *243*, 519-532.

Sandhwar, V. K., & Prasad, B. (2017). Terephthalic acid removal from aqueous solution by electrocoagulation and electro-Fenton methods: Process optimization through response surface methodology. Process Safety and Environmental Protection, 107, 269-280.

Sangal, V. K., Kumar, V., & Mishra, M. I. (2013). Optimization of a divided wall column for the separation of C4-C6 normal paraffin mixture using Box-Behnken design. Chemical Industry and Chemical Engineering Quarterly/CICEQ, 19(1), 107-119.

Santos, I. D. D., Afonso, J. C., & Dutra, A. J. (2011). Electrooxidation of phenol on a Ti/RuO2 anode: effect of some electrolysis parameters. Journal of the Brazilian Chemical Society, 22(5), 875-883.

Santos, I. D., Afonso, J. C., & Dutra, A. J. B. (2010). Behavior of a Ti/RuO2 anode in concentrated chloride medium for phenol and their chlorinated intermediates electrooxidation. Separation and Purification Technology, 76(2), 151-157.

Särkkä, H., Bhatnagar, A., & Sillanpää, M. (2015). Recent developments of electro-oxidation in water treatment-a review. Journal of Electroanalytical Chemistry, 754, 46-56.

Selcuk, H. (2005). Decolorization and detoxification of textile wastewater by ozonation and coagulation processes. Dyes and Pigments, 64(3), 217-222.

Şengil, İ. A., Kulac, S., & Özacar, M. (2009). Treatment of tannery liming drum wastewater by electrocoagulation. Journal of Hazardous Materials, 167(1-3), 940-946.

Senthilkumar, S., Basha, C. A., Perumalsamy, M., & Prabhu, H. J. (2012). Electrochemical oxidation and aerobic biodegradation with isolated bacterial strains for dye wastewater: combined and integrated approach. ElectrochimicaActa, 77, 171-178.

Sharma, K., Dalai, A. K., & Vyas, R. K. (2017). Removal of synthetic dyes from multicomponent industrial wastewaters. Reviews in Chemical Engineering, *34*(1), 107-134.

Simond, O., Schaller, V., & Comninellis, C. (1997). Theoretical model for the anodic oxidation of organics on metal oxide electrodes. ElectrochimicaActa, 42(13-14), 2009-2012.

Singhal, A. (2010). Indian textile & Apparel industry: Brightest Future.

Sirés, I., & Brillas, E. (2012). Remediation of water pollution caused by pharmaceutical residues based on electrochemical separation and degradation technologies: a review. Environment International, 40, 212-229.

Sirés, I., Brillas, E., Oturan, M. A., Rodrigo, M. A., & Panizza, M. (2014). Electrochemical advanced oxidation processes: today and tomorrow. A review. Environmental Science and Pollution Research, 21(14), 8336-8367.

Sun, J. H., Sun, S. P., Wang, G. L., & Qiao, L. P. (2007). Degradation of azo dye Amido black 10B in aqueous solution by Fenton oxidation process. Dyes & Pigments, 74(3), 647-652.

Sun, Y., & Pignatello, J. J. (1993). Photochemical reactions involved in the total mineralization of 2, 4-D by iron (3+)/hydrogen peroxide/UV. Environmental Science & Technology, 27(2), 304-310.

Szpyrkowicz, L., Juzzolino, C., Kaul, S. N., Daniele, S., & De Faveri, M. D. (2000). Electrochemical oxidation of dyeing baths bearing disperse dyes. Industrial & Engineering Chemistry Research, 39(9), 3241-3248.

Szpyrkowicz, L., Kaul, S. N., Neti, R. N., & Satyanarayan, S. (2005). Influence of anode material on electrochemical oxidation for the treatment of tannery wastewater. Water Research, 39(8), 1601-1613.

Thiam, A., Zhou, M., Brillas, E., & Sirés, I. (2014). Two-step mineralization of Tartrazine solutions: study of parameters and by-products during the coupling of electrocoagulation with electrochemical advanced oxidation processes. Applied Catalysis B: Environmental, 150, 116-125.

Ting, W. P., Lu, M. C., & Huang, Y. H. (2009). Kinetics of 2, 6-dimethylaniline degradation by electro-Fenton process. Journal of Hazardous Materials, 161(2-3), 1484-1490.

U.S. Environmental Protection Agency (1996) Best management practices for pollution prevention in the textile industry, EPA625R96004, USA

U.S. Environmental Protection Agency, (1996), Guidance on Use of Modeled Results to Demonstrate Attainment of the Ozone NAAQS, EPA-454/B-95-007.

Van der Bruggen, B., De Vreese, I., & Vandecasteele, C. (2001). Water reclamation in the textile industry: nanofiltration of dye baths for wool dyeing. Industrial & Engineering Chemistry Research, 40(18), 3973-3978.

Vlyssides, A. G., & Israilides, C. J. (1997). Detoxification of tannery waste liquors with an electrolysis system. Environmental Pollution, 97(1-2), 147-152.

Vlyssides, A. G., Karlis, P. K., Rori, N., & Zorpas, A. A. (2002). Electrochemical treatment in relation to pH of domestic wastewater using Ti/Pt electrodes. Journal of Hazardous Materials, 95(1-2), 215-226.

Vlyssides, A. G., Loizidou, M., Karlis, P. K., Zorpas, A. A., & Papaioannou, D. (1999). Electrochemical oxidation of a textile dye wastewater using a Pt/Ti electrode. Journal of Hazardous Materials, 70(1-2), 41-52.

Vlyssides, A. G., Loizidou, M., Karlis, P. K., Zorpas, A. A., & Papaioannou, D. (1999). Electrochemical oxidation of a textile dye wastewater using a Pt/Ti electrode. Journal of Hazardous Materials, 70(1-2), 41-52.

Wang, A., Qu, J., Ru, J., Liu, H., & Ge, J. (2005). Mineralization of an azo dye Acid Red 14 by electro-Fenton's reagent using an activated carbon fiber cathode. Dyes and Pigments, 65(3), 227-233.

Wang, C. T., Hu, J. L., Chou, W. L., & Kuo, Y. M. (2008). Removal of color from real dyeing wastewater by Electro-Fenton technology using a three-dimensional graphite cathode. Journal of Hazardous Materials, 152(2), 601-606.

Wang, Y., Liu, Y., Li, X. Z., Zeng, F., & Liu, H. (2013). A highly-ordered porous carbon material based cathode for energy-efficient electro-Fenton process. Separation and Purification Technology, 106, 32-37.

Weng, C. H., Lin, Y. T., Chang, C. K., & Liu, N. (2013). Decolourization of direct blue 15 by Fenton/ultrasonic process using a zero-valent iron aggregate catalyst. UltrasonicsSonochemistry, 20(3), 970-977.

Workman, J. Jr., (2001). The handbook of organic compounds, I edition, Academic press, USA.

Xu, X., Chen, J., Zhang, G., Song, Y., & Yang, F. (2014). Homogeneous electro-Fenton oxidative degradation of reactive brilliant blue using a graphene doped gas-diffusion cathode. *International Journal* of *Electrochemical Science*, 9, 569-579.

Xu, X., Liao, P., Yuan, S., Tong, M., Luo, M., & Xie, W. (2013). Cu-catalytic generation of reactive oxidizing species from H_2 and O_2 produced by water electrolysis for electro-fenton degradation of organic contaminants. Chemical Engineering Journal, 233, 117-123.

Yavuz, Y., Shahbazi, R., Koparal, A. S., & Öğütveren, Ü. B. (2014). Treatment of Basic Red 29 dye solution using iron-aluminum electrode pairs by electrocoagulation and electro-Fenton methods. Environmental Science and Pollution Research, 21(14), 8603-8609.

Yigit, N. O., Uzal, N., Koseoglu, H., Harman, I., Yukseler, H., Yetis, U., & Kitis, M. (2009). Treatment of a denim producing textile industry wastewater using pilot-scale membrane bioreactor. Desalination, 240(1-3), 143-150.

Yu, R. F., Lin, C. H., Chen, H. W., Cheng, W. P., & Kao, M. C. (2013). Possible control approaches of the Electro-Fenton process for textile wastewater treatment using on-line monitoring of DO and ORP. Chemical Engineering Journal, 218, 341-349.

Yuan, S., Gou, N., Alshawabkeh, A. N., & Gu, A. Z. (2013). Efficient degradation of contaminants of emerging concerns by a new electro-Fenton process with Ti/MMO cathode. Chemosphere, 93(11), 2796-2804.

Zheng, Y. M., Yunus, R. F., Nanayakkara, K. N., & Chen, J. P. (2012). Electrochemical decoloration of synthetic wastewater containing rhodamine 6G: behaviors and mechanism. Industrial & Engineering Chemistry Research, 51(17), 5953-5960.

Zhou, M., & He, J. (2007). Degradation of azo dye by three clean advanced oxidation processes: wet oxidation, electrochemical oxidation and wet electrochemical oxidation—a comparative study. ElectrochimicaActa, 53(4), 1902-1910.

Zollinger, H. (2003). Color chemistry: syntheses, properties, and applications of organic dyes and pigments. John Wiley & Sons.

Zubavichus, Y. V., Slovokhotov, Y. L., Nazeeruddin, M. K., Zakeeruddin, S. M., Grätzel, M., & Shklover, V. (2002). Structural characterization of solar cell prototypes based on nanocrystalline TiO_2anatase sensitized with Ru complexes. X-ray diffraction, XPS, and XAFS spectroscopy study. Chemistry of Materials, 14(8), 3556-3563.

PUBLICATIONS

Papers Published in SCI Journals

1. Kaur P, Kushwaha J P and Sangal V K, Evaluation and disposability study of actual textile wastewater treatment by electro-oxidation method using Ti/RuO_2 anode. *Process Safety and Environmental Protection,* 2017, (111) 13-22. (**Impact factor: 3.441**)

2. Kaur P, Kushwaha J P and Sangal V K, Electrocatalytic oxidative treatment of real textile wastewater in continuous reactor: degradation pathway and disposability study. *Journal of Hazardous Materials, 2018, (346)* 242–252. (**Impact factor: 6.434**)

3. Kaur P, Kushwaha J P and Sangal V K, Transformation products and degradation pathway of textile industry wastewater pollutants in Electro-Fenton process. *Chemosphere*, 2018, (207) 690-698. (**Impact factor: 4.427**)

4. Kaur P, Sangal V K and Kushwaha J P, Parametric study of electro-Fenton treatment for real textile wastewater, disposal study and its cost analysis. *International Journal of Environmental Science and Technology*, 2019, (16-2) 801-810. (**Impact factor: 2.037**)